Order, Disorder and Criticality

Advanced Problems of Phase Transition Theory

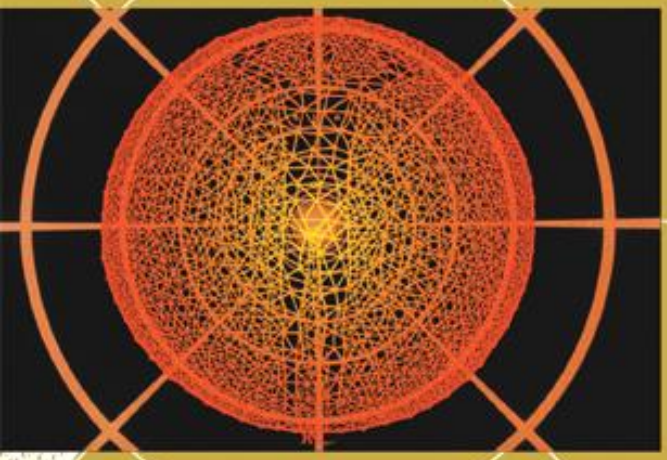

Editor

Yurij Holovatch

World Scientific

Order, Disorder and Criticality

Advanced Problems of Phase Transition Theory

This page intentionally left blank

Order, Disorder and Criticality

Advanced Problems of Phase Transition Theory

Editor

Yurij Holovatch

National Academy of Sciences, Ukraine

World Scientific

NEW JERSEY • LONDON • SINGAPORE • SHANGHAI • HONG KONG • TAIPEI • BANGALORE

Published by

World Scientific Publishing Co. Pte. Ltd.

5 Toh Tuck Link, Singapore 596224

USA office: 27 Warren Street, Suite 401-402, Hackensack, NJ 07601

UK office: 57 Shelton Street, Covent Garden, London WC2H 9HE

British Library Cataloguing-in-Publication Data
A catalogue record for this book is available from the British Library.

The design of the cover incorporates the artwork of Jacques Hnizdovsky (Constructor, Woodcut, 1967).

ORDER, DISORDER AND CRITICALITY
Advanced Problems of Phase Transition Theory

Copyright © 2004 by World Scientific Publishing Co. Pte. Ltd.

All rights reserved. This book, or parts thereof, may not be reproduced in any form or by any means, electronic or mechanical, including photocopying, recording or any information storage and retrieval system now known or to be invented, without written permission from the Publisher.

For photocopying of material in this volume, please pay a copying fee through the Copyright Clearance Center, Inc., 222 Rosewood Drive, Danvers, MA 01923, USA. In this case permission to photocopy is not required from the publisher.

ISBN 981-238-583-5

Typeset by Stallion Press
Email: enquiries@stallionpress.com

Printed in Singapore.

PREFACE

It is hard to name another branch of physics more essentially changed in the last few decades than the theory of phase transitions. One can go further: having appeared in different variants of a mean field theory for the description of equilibrium phase transitions in problems of statistical physics and thermodynamics, the theory of phase transitions now appears to be an interdisciplinary science such as, say, the theory of oscillations. Also the concepts contained in the term "phase transition" has been substantially broadened. In condensed matter physics, besides traditional equilibrium thermodynamic phase transitions, this term includes quantum phase transitions, non-equilibrium dissipative phase transitions, percolation phenomena, *etc.*

During the last several decades we have witnessed intensive studies of the above phenomena in condensed matter physics, and of similar phenomena in different branches of physics (on a larger scale, of similar phenomena in chemistry, biology, ecology, economy). In particular, a breakthrough in understanding and precise quantitative description of the long-range properties of different systems in the vicinity of a second-order phase transition occured due to the applications of renormalization group ideas. Such an intensive and fruitful activity in the field sometimes leads to the opinion that all principal work in phase transitions theory had already been completed by the middle of the 80's and no new physics remains to be explained. On the other hand, there exists an opposite opinion, stating that it is a fascinating part of physics still actively developing and there is a lot of work to be done in both the fundamental and the applied areas.

The purpose of this book is to support the latter opinion and, in doing so, to give a review of some current topics in phase transitions theory. The book contains six chapters reviewing state-of-the-art studies in various areas of phase transitions theory: rigorous results for the classical and

quantum lattice models, dynamics and statics of quantum phase transitions in regular and disordered one-dimensional systems, phase transitions in two-dimensional systems with weak quenched disorder, field theoretical analysis of critical behavior in polymer physics and of the superconducting phase transition.

The above list of advanced topics in the theory of phase transitions is far from being complete, but it reflects some of the main trends in the development of the subject. The book opens with a review of Yuri Kozitsky giving an introduction to the rigorous theory of the Ising model and its generalizations. It may serve as a bridge for those physicists who do not work in the field of mathematical physics but are interested both in the modern methods and in the recent results.

The articles of Dragi Karevski and Oleg Derzhko are devoted to the study of quantum phase transitions in quantum spin chains. These simple quantum mechanical many-particle systems are of current interest for several reasons. On the one hand nowadays it is possible to perform an experimental study of a phase transition driven by quantum fluctuations, on the other hand the theoretical analysis of one-dimensional quantum systems is far from being trivial, as the above reviews will convince the reader. Moreover, new phenomena of interest appear when one introduces structural disorder to such systems. The influence of structural disorder is also the subject of the paper by Bertrand Berche and Christophe Chatelain who give a comprehensive review of experimental and theoretical studies of the two-dimensional random Potts model. The reviewed methods include perturbative expansions, MC simulations, transfer matrix technique, and short-time dynamic scaling.

The review by Christian von Ferber concerns scaling properties of star polymers. Since the early 70's, thanks to the work of P.-G. de Gennes, it has been understood that properties of long flexible polymer chains in good solvents may be described in terms of critical phenomena. The review shows modern state-of-the-art insight in studies of the scaling properties of (co-)polymer stars and networks, including possible applications of the theory for describing the interaction of star polymers in a solvent and for the analysis of the multifractal properties of diffusion in the vicinity of polymer absorber. The paper by Flavio S. Nogueira and Hagen Kleinert aims to answer the question concerning the order of a normal-to-superconducting phase transition. This question becomes nontrivial when one considers also the fluctuating magnetic field. The paper reviews different field-theoretical

approaches to the problem, emphasizing the renormalization group and the duality approach.

The selection of the contributors to this review volume stems from the presentations of their review lectures in March 2002 in Lviv (Ukraine) in the setting of the "Ising lectures" – a traditional annual workshop on phase transitions and critical phenomena. The workshop is organized by the Institute for Condensed Matter Physics of the National Academy of Sciences of Ukraine and the Ivan Franko National University of Lviv, and aims to bring together scientists working in the field of phase transitions with university students and those who are interested in the subject. On this occasion, it is my pleasure to express my cordial thanks to the lecturers for coming to Lviv and presenting their lectures. Special thanks are due to Professor Ivan Vakarchuk, Dr. Ihor Mryglod, and Dr. Mykhailo Kozlovskii for their support in the organization of the workshop and to Dr. Kyrylo Tabunshchyk, Mr. Maksym Dudka, and Mrs. Viktoria Blavats'ka for their help, before, during, and after the workshop. I am very much oblidged to World Scientific Publishers for the interest in getting these lectures published and to Dr. Kok-Kean Yim for the fruitful collaboration in the preparation of this book.

Yurij Holovatch
Institute for Condensed Matter Physics &
Ivan Franko National University of Lviv
Lviv, Ukraine, May 2003

This page intentionally left blank

CONTENTS

This page intentionally left blank

CHAPTER 1

MATHEMATICAL THEORY OF THE ISING MODEL AND ITS GENERALIZATIONS: AN INTRODUCTION

Yuri Kozitsky

Institute of Mathematics, Maria Curie-Skłodowska University, 20-031 Lublin, Poland
E-mail: jkozi@golem.umcs.lublin.pl

An introduction into the rigorous theory of equilibrium states of a number of lattice models of classical and quantum statistical physics is given. Generalized Ising models with discrete, continuous, bounded and unbounded spins, translation invariant and with a hierarchical structure, quantum spin models, models of interacting quantum anharmonic oscillators are considered. For the classical models, certain properties of local Gibbs states, such as the Lee–Yang theorem, correlation inequalities, phase transitions and self-similarity, are discussed. The Gibbs states of such models are defined by means of the Dobrushin–Lanford–Ruelle equation. The problem of uniqueness of such states is also discussed. For the quantum models, an approach based on functional integration is presented on an introductory level. Within this approach phase transitions and the critical point convergence in models of interacting quantum oscillators are discussed.

1. Introduction

This article is addressed to those physicists working in statistical physics who would want to learn modern mathematical methods and concepts used by mathematicians who are also working in this area. Although both communities study the same object, there exists a serious gap between the ways of getting and expressing knowledge, which quite often impedes substantially the exchange of this knowledge between them. The intention of the article is to help making just the first steps towards treating equilibrium states, phase transitions, critical points, etc. as mathematical objects. As a continuation, a serious work on such classical sources as Refs. 1–14

is recommended. The article is more or less self-contained, nevertheless the reader is supposed to possess certain knowledge in functional analysis (linear operators on Banach and Hilbert spaces, see Ref. 15), analytic functions (holomorphic functions of one and several complex variables, entire functions, see Refs. 16 and 17), measure theory (see Refs. 18–20), probability and stochastic processes (see Ref. 21). The article is mainly a review, although certain results and approaches are new. Among them – a new approach to the description of the critical point in one-dimensional models (classical and quantum) with long-range interactions.

The Ising model was introduced in 1925. Ising solved the model in the one-dimensional case[22] (see also Refs. 23 and 24) and came to the conclusion that it has no phase transitions in all dimensions. Later, due to Onsager's solution,[25] it had become clear that the two-dimensional version of the model does have a phase transition and a critical point. Since that time, the Ising model has become one of the most popular models of statistical physics. A very important conclusion, which one can come up to by analyzing Onsager's solution, is that the phase transition singularities of thermodynamic functions, such as the free energy density, magnetization, etc., occur only in the infinite-volume (thermodynamic) limit. Another important peculiarity of Onsager's solution is that it cannot be extended to the three-dimensional case.[a] This fact stimulated a more serious mathematical approach to the description of lattice models of this kind. The state of the art account in this area may be found in the monographs Refs. 13 and 14.

Originally the Ising model was considered as a quantum model described in terms of spin operators. Later, it was understood[29] that there exists a deep connection between the Ising model, the φ^4-models of the Euclidean quantum field theory and classical lattice models. Moreover, due to its diagonality, the Ising model may be considered as a classical model as well. In accordance with this duality the main body of the article consists of two parts dedicated to classical and quantum models respectively. In the first part (Section 2), we consider a number of generalizations of the Ising model, which may be described in terms of systems of dependent random variables (spins) indexed by the elements of a d-dimensional simple cubic lattice

[a]It is believed[26] that the three-dimensional and two-dimensional Ising models have different types of time complexity. The $3D$-model has a non-polynomial time complexity; whereas the $2D$-model, polynomial. More about complexity – a very popular conception of modern science – see Refs. 27 and 28.

of unit spacing $\mathbb{Z}^d$. In this context the Ising model describes a system of interacting spins taking values ± 1. In its generalizations the spins take values: (a) from a finite sets $s_1, \ldots, s_n$ (discrete spins); (b) from intervals like $[a, b]$ (bounded continuous spins); (c) from the whole real line (unbounded spins). These values are taken with certain probability (in the Ising model both ± 1 are taken with probability $1/2$). Different types of probability laws, which prescribe these probabilities are discussed. Local Gibbs states are introduced as probability measures, which are constructed by means of local Hamiltonians and the probability laws discussed above. Here and below *local* means related to a finite subset of the lattice $\mathbb{Z}^d$. The central notion of this part is the infinite-volume Gibbs state, which is defined by means of local Gibbs states as a probability measure. As has been pointed out above, the only possibility to describe phase transitions in such models is to construct these infinite-volume states, or at least to get information about their properties. Such information may be obtained by studying local Gibbs states, in particular the analytic properties of local partition functions. Valuable information may be obtained with the help of correlation inequalities, which we discuss in Subsection 2.3. In Subsection 2.6 we show how to prove that the infinite-volume Gibbs state of the Ising model with a nonzero external field is unique at all temperatures. This uniqueness means that only one phase may exist hence no phase transitions are possible. The proof is based on the correlation inequalities and analytic properties of the model partition function as a function of the external field. Among the main problems of statistical physics a special place belongs to the problem of criticality. At a critical point the infinite-volume Gibbs state possesses unusual properties. In particular, it is characterized by large fluctuations due to which the usual central limit theorem fails to hold whereas the law of large numbers is still valid. Such a phenomenon is interesting not only for physicists – the appearance of the strong dependence between random patterns is studied in population genetics, mathematical finance, etc. In Subsection 2.7 we consider some new aspects of the theory of critical points in a number of models discussed in this section.

In Section 2 we have restricted ourselves to real-valued spin models. Therefore, we do not consider classical models with vector spins, taking values in $\mathbb{R}^n$ with $n > 1$. We also leave without consideration models like the Potts model, the clock model, etc. Finally, we do not consider a very interesting class of spin models on graphs (like the Bethe lattices), which now are getting more and more popular [see e.g., Refs. 30 and 31, and pp. 170–173 in Ref. 13].

In the second part (Section 3) we discuss how to construct local Gibbs states of quantum lattice models, which can be considered as generalizations of the Ising model. We consider two types of such models: (a) non-diagonal spin models (like the Heisenberg spin model), which may be described by means of finite complex matrices; (b) models of interacting localized quantum particles, described by unbounded momentum and position operators. A typical example of the latter models is the model of quantum anharmonic oscillators, which is now extensively employed in the theory of structural phase transitions.[32] The local Gibbs states of quantum models are constructed as positive linear normalized functionals on noncommutative algebras of observables. Such functionals are defined by means of density matrices, which in turn are defined in terms of local Hamiltonians. All these objects, i.e. local Hamiltonians, density matrices and observables, may be realized as operators acting on certain Hilbert spaces. In Subsection 3.1 we give a brief introduction and some examples on this matter, including a number of facts from the theory of such operators. In Subsection 3.2 we discuss the main technical tool in quantum statistical physics which provides a possibility to describe local Gibbs states by means of Matsubara functions constructed for observables taken from a commutative subalgebra of the algebra of all observables. In the approach to the description of the models of quantum anharmonic oscillators initiated in Ref. 33, the Matsubara functions are written as integrals on function spaces, which makes this description similar to the description of models of classical statistical physics, in particular the models considered in Section 2. The only difference is that now the spins are infinite-dimensional. This approach is called *Euclidean* because of its similarity to the corresponding approach in quantum field theory. Within this approach it is possible to construct infinite-volume Gibbs states on the same base as in the case of classical models. We present here certain aspects of this approach, a full description of which may be found in Ref. 34. In Subsection 3.3 we make some statements regarding phase transitions and critical phenomena in the models of quantum anharmonic oscillators obtained in the Euclidean approach.

2. Classical models

2.1. *Local Hamiltonians and Gibbs States*

We denote by $\mathbb{N}$, $\mathbb{N}_0$, $\mathbb{Z}$, $\mathbb{R}$, $\mathbb{C}$ the sets of positive integers, nonnegative integers, integers, real and complex numbers, respectively. For simplicity, we consider a simple cubic lattice of unit spacing, i.e., our lattice is $\mathbb{Z}^d$, $d \in \mathbb{N}$.

Let Δ be a finite subset of the lattice $\mathbb{Z}^d$. Among such subsets we will distinguish boxes

$$\Lambda = (-L, L]^d \cap \mathbb{Z}^d, \quad L \in \mathbb{N}. \tag{1}$$

Below, unless otherwise explicitly stated, Δ and Λ will always stand, respectively, for an arbitrary finite subset of $\mathbb{Z}^d$ and a box (1). The number of lattice points in Δ, Λ, will be denoted by $|\Delta|$, $|\Lambda|$. Since Λ is a special case of Δ, everything stated for subsets Δ will be valid also for boxes Λ.

We start the description of the models we consider by introducing the measure ϱ on $\mathbb{R}$ which describes *a priori* the probability distribution of a random variable corresponding to a "particle". The measure which would describe a system of such non-interacting particles, each of which is labelled by an element of a subset Δ, should be the product of this ϱ taken over Δ. If the particles interact with each other, the measure which describes this system is obtained[6] as a "Gibbsian reconstruction" of the product measure performed by means of the energy functional. In the simplest case this is a quadratic form on the Euclidean space $\mathbb{R}^{|\Delta|}$ consisting of vectors $\sigma_\Delta = (\sigma_{\boldsymbol{l}})_{\boldsymbol{l}\in\Delta}$ with components $\sigma_{\boldsymbol{l}}$, $\boldsymbol{l} \in \Delta$, which reads

$$H_\Delta = -\frac{1}{2} \sum_{\boldsymbol{l},\boldsymbol{l}'\in\Delta} J_{\boldsymbol{l}\boldsymbol{l}'}\sigma_{\boldsymbol{l}}\sigma_{\boldsymbol{l}'} - \sum_{\boldsymbol{l}\in\Delta} h_{\boldsymbol{l}}\sigma_{\boldsymbol{l}}, \tag{2}$$

where $J_{\boldsymbol{l}\boldsymbol{l}'} = J_{\boldsymbol{l}'\boldsymbol{l}}$, $h_{\boldsymbol{l}}$ are real parameters of the model defined for all $\boldsymbol{l}, \boldsymbol{l}' \in \mathbb{Z}^d$. By means of these objects, we introduce the following probability measure on the space $\mathbb{R}^{|\Delta|}$:

$$d\nu_\Delta(\sigma_\Delta) = Z^{-1}_{\beta,\Delta} \exp\left(-\beta H_\Delta\right) \prod_{\boldsymbol{l}\in\Delta} d\varrho(\sigma_{\boldsymbol{l}}), \tag{3}$$

$$Z_{\beta,\Delta} = \int_{\mathbb{R}^{|\Delta|}} \exp\left(-\beta H_\Delta\right) \prod_{\boldsymbol{l}\in\Delta} d\varrho(\sigma_{\boldsymbol{l}}),$$

where β is the inverse temperature measured in energy units. This measure is called *the local Gibbs measure*, or equivalently *the local Gibbs state*, corresponding to the zero condition on the boundary (i.e., outside) of Δ. The mentioned reconstruction was performed by multiplying the product measure in (3) by the corresponding factor, which turns out to be equal to unity for $\beta = 0$ when the particles become non-interacting. The normalization constant $Z_{\beta,\Delta}$, which *ensures* that $\int d\nu_\Delta = 1$, is called *the partition function* in the subset Δ and

$$F_{\beta,\Delta} = -\frac{1}{\beta|\Delta|} \ln Z_{\beta,\Delta}, \tag{4}$$

is called *the free energy density.*

A particular case of the above model, where the reference measure ϱ is

$$d\varrho(\sigma_{\boldsymbol{l}}) = \delta(\sigma_{\boldsymbol{l}}^2 - 1)\, d\sigma_{\boldsymbol{l}} = \frac{1}{2}\left[\delta(\sigma_{\boldsymbol{l}} - 1) + \delta(\sigma_{\boldsymbol{l}} + 1)\right] d\sigma_{\boldsymbol{l}}, \tag{5}$$

is nothing else but the Ising model with the interaction potential $J_{\boldsymbol{l}\boldsymbol{l}'}$ in the external field $h_{\boldsymbol{l}}$. This field is called *homogeneous* if $h_{\boldsymbol{l}} = h$ for all $\boldsymbol{l} \in \mathbb{Z}^d$. In (5) δ is the Dirac δ-function, thus the above measure is symmetric and concentrated at ± 1.

Due to the fact that the Ising model is a particular case of the model described by (2), the random variables in a general situation are called "spins", the energy functional (2) is called "Hamiltonian", and the measure ϱ is called "single-spin measure". The models for which the measure ϱ is concentrated at points $s_1,\ s_2, \ldots, s_n \in \mathbb{R}$, as is the case for the Ising model, are called models with discrete spin. Such a model with $s_1 = -1$, $s_2 = 0, s_3 = 1$ and with the single-spin measure

$$d\varrho(\sigma_{\boldsymbol{l}}) = c[\delta(\sigma_{\boldsymbol{l}} + 1) + \delta(\sigma_{\boldsymbol{l}} - 1)]d\sigma_{\boldsymbol{l}} + (1 - 2c)\delta(\sigma_{\boldsymbol{l}})d\sigma_{\boldsymbol{l}}, \quad c \in (0, 1/2),$$

was studied in Ref. 35. The models for which the measure ϱ is not concentrated at any points are called models with continuous spin. As an example here one may take the model with the single-spin measure

$$d\varrho(\sigma_{\boldsymbol{l}}) = \frac{1}{2}\varpi_{[-1,1]}(\sigma_{\boldsymbol{l}})\, d\sigma_{\boldsymbol{l}}, \tag{6}$$

where $\varpi_{[-1,1]}(t) = 1$ if $t \in [-1, 1]$ and $\varpi_{[-1,1]}(t) = 0$ otherwise. The models for which there exists $a > 0$ such that

$$\int_{[-a,a]} d\varrho \stackrel{\text{def}}{=} \int_{-a}^{a} d\varrho = 1,$$

are called models with bounded (compact) spins. Thus, discrete spins are always bounded. The models for which the measure ϱ is not concentrated on a bounded interval are called models with unbounded spins. Among such models, a significant role is played by the polynomial models, for which

$$d\varrho(\sigma_{\boldsymbol{l}}) = C^{-1} \exp\left(-P(\sigma_{\boldsymbol{l}})\right) d\sigma_{\boldsymbol{l}}, \quad C = \int_{\mathbb{R}} \exp\left(-P(\sigma_{\boldsymbol{l}})\right) d\sigma_{\boldsymbol{l}}, \tag{7}$$

where P is a polynomial, i.e.,

$$P(\sigma_{\boldsymbol{l}}) = b_1\sigma_{\boldsymbol{l}} + \cdots + b_{2r}\sigma_{\boldsymbol{l}}^{2r}, \quad b_{2r} > 0. \tag{8}$$

Such a polynomial is semi-bounded, which means that for all its arguments $P(\sigma_{\boldsymbol{l}}) \geq b_0$ for some real b_0. A measure ϱ on $\mathbb{R}$ is called symmetric if for

every $0 \le a < b$,

$$\int_a^b d\varrho = \int_{-b}^{-a} d\varrho.$$

The measure (7) is symmetric if P is even, i.e., if only even powers appear in (8). A typical example of such a measure is the symmetric Gaussian measure, for which $P(\sigma_{\boldsymbol{l}}) = (b/2)\sigma_{\boldsymbol{l}}^2$. Another typical example is obtained by setting $r = 2$,

$$d\varrho(\sigma_{\boldsymbol{l}}) = C^{-1} \exp\left(-a\sigma_{\boldsymbol{l}}^2 - b\sigma_{\boldsymbol{l}}^4\right) d\sigma_{\boldsymbol{l}}, \quad a \in \mathbb{R}, \quad b > 0; \tag{9}$$
$$C = \int_{\mathbb{R}} \exp\left(-P(\sigma_{\boldsymbol{l}})\right) d\sigma_{\boldsymbol{l}},$$

which is known as the φ^4 measure.

Such polynomial models have another interpretation. For the above P and the Hamiltonian (1), set

$$E_\Delta = -\frac{1}{2} \sum_{\boldsymbol{l},\boldsymbol{l}' \in \Delta} J_{\boldsymbol{l}\boldsymbol{l}'} \sigma_{\boldsymbol{l}} \sigma_{\boldsymbol{l}'} - \sum_{\boldsymbol{l} \in \Delta} h_{\boldsymbol{l}} \sigma_{\boldsymbol{l}} + \sum_{\boldsymbol{l} \in \Delta} P(\sigma_{\boldsymbol{l}}). \tag{10}$$

This functional may be considered as the potential energy of a system of interacting classical (non-quantum) oscillators, in which the first term is responsible for the inter-particle interaction whereas the second and the third ones represent the single-particle potential energy. In case $P(\sigma_{\boldsymbol{l}}) = (b/2)\sigma_{\boldsymbol{l}}^2$, $b > 0$, for all $\boldsymbol{l} \in \mathbb{Z}^d$, these oscillators are harmonic. A generalization of (7) and (10) may be made by replacing the polynomial P by a differentiable semi-bounded function. With the help of the potential energy (10) the measure (3) may be written in the form

$$d\nu_\Delta(\sigma_\Delta) = Z_{\beta,\Delta}^{-1} \exp\left(-\beta E_\Delta\right) \prod_{\boldsymbol{l} \in \Delta} d\sigma_{\boldsymbol{l}}, \tag{11}$$

which is the Gibbs measure of a system of classical oscillators; it is Gaussian if they are harmonic. Let us describe the latter case in more detail. For $P(\sigma_{\boldsymbol{l}}) = (b/2)\sigma_{\boldsymbol{l}}^2$, we set

$$S_{\boldsymbol{l}\boldsymbol{l}'} = b\delta_{\boldsymbol{l}\boldsymbol{l}'} - J_{\boldsymbol{l}\boldsymbol{l}'}, \quad \boldsymbol{l}, \boldsymbol{l}' \in \Delta, \tag{12}$$

where $\delta_{\boldsymbol{l}\boldsymbol{l}'}$ is the Kronecker delta. Let S be the $|\Delta| \times |\Delta|$ symmetric matrix, the elements of which are given by (12). It may be diagonalized and all its eigenvalues have to be real. The measure (11) will exist for all $d \in \mathbb{N}$ if all

these eigenvalues are strictly positive. In this case the inverse matrix S^{-1} exists and the partition function may be written explicitly

$$Z_{\beta,\Delta} = (2\pi)^{|\Delta|/2} \left[\det S\right]^{-1/2} \exp\left(\frac{1}{2} \sum_{\boldsymbol{l},\boldsymbol{l}' \in \Delta} (S^{-1})_{\boldsymbol{l}\boldsymbol{l}'} h_{\boldsymbol{l}} h_{\boldsymbol{l}'}\right). \tag{13}$$

If $J_{\boldsymbol{l}\boldsymbol{l}'} \geq 0$ for all $\boldsymbol{l}, \boldsymbol{l}' \in \mathbb{Z}^d$, the necessary and sufficient condition for the mentioned eigenvalues to be positive is

$$b > \max_{\boldsymbol{l} \in \Delta} \sum_{\boldsymbol{l}' \in \Delta} J_{\boldsymbol{l}\boldsymbol{l}'}. \tag{14}$$

It is sensible to consider the thermodynamic properties of the model only if the relation

$$\sum_{\boldsymbol{l}' \in \mathbb{Z}^d} J_{\boldsymbol{l}\boldsymbol{l}'} < \infty, \tag{15}$$

holds for all $\boldsymbol{l} \in \mathbb{Z}^d$. In this case condition (14) will be satisfied for any Δ if

$$b > \sup_{\boldsymbol{l} \in \mathbb{Z}^d} \sum_{\boldsymbol{l}' \in \mathbb{Z}^d} J_{\boldsymbol{l}\boldsymbol{l}'}. \tag{16}$$

If the latter condition fails to hold, the same will be the case with (14) for sufficiently large subsets Δ. In this case the infinite-volume Gibbs measure does not exist.

By means of the local Gibbs measure (3), one obtains physical quantities as the integrals

$$\int_{\Omega_\Delta} f(\sigma_\Delta)\, d\nu_\Delta(\sigma_\Delta) \stackrel{\text{def}}{=} \langle f \rangle_{\nu_\Delta}, \tag{17}$$

where we have set $\Omega_\Delta = \mathbb{R}^{|\Delta|}$. Such integrals are called expectation values of the functions f with respect to the measure ν_Δ. In particular, the mean magnetization in the set Δ, the two-point correlation function and the susceptibility of the model read, respectively,

$$M_\Delta = \frac{1}{|\Delta|} \sum_{\boldsymbol{l} \in \Delta} \langle \sigma_{\boldsymbol{l}} \rangle_{\nu_\Delta}, \quad K^\Delta_{\boldsymbol{l}\boldsymbol{l}'} = \langle \sigma_{\boldsymbol{l}} \sigma_{\boldsymbol{l}'} \rangle_{\nu_\Delta} - \langle \sigma_{\boldsymbol{l}} \rangle_{\nu_\Delta} \langle \sigma_{\boldsymbol{l}'} \rangle_{\nu_\Delta}, \tag{18}$$

$$\chi_\Delta = \frac{1}{|\Delta|} \sum_{\boldsymbol{l},\boldsymbol{l}' \in \Delta} K^\Delta_{\boldsymbol{l}\boldsymbol{l}'}. \tag{19}$$

The infinite-volume limit of such quantities, if it exists, will describe the thermodynamic properties of the model. In general, the integrals (17) exist not for all functions $f : \Omega_\Delta \to \mathbb{R}$. If such a function is continuous and

polynomially bounded, its expectation value $\langle f\rangle_{\nu_\Delta}$ exists for all measures ϱ of the type of (7). A polynomially bounded function by definition is a function $f:\Omega_\Delta\to\mathbb{R}$, which satisfies the condition

$$|f(\sigma_\Delta)|\le f_0+\left[\sum_{\boldsymbol{l}\in\Delta}\sigma_{\boldsymbol{l}}^2\right]^n, \tag{20}$$

with certain $f_0>0$ and $n\in\mathbb{N}$. In the case of compact spins, the integrals (17) exist for all continuous functions. It should be pointed out here that the integrals (17) exist not only for continuous functions, but their extension to wider classes of functions will complicate mathematics, which complications we are going to avoid in this article. Moreover, all functions for which the expectations $\langle f\rangle_{\nu_\Delta}$ have a physical meaning are continuous, hence we may restrict ourselves to considering such functions only. Thereby, we denote by $\mathcal{F}_\Delta$ the set of all polynomially bounded continuous functions $f:\Omega_\Delta\to\mathbb{R}$. All the single-spin measures we consider in this article are supposed to satisfy the condition

$$\int_{\mathbb{R}}\exp\left(as^2\right)d\varrho(s)<\infty, \tag{21}$$

with a certain $a>0$. In this case all functions from $\mathcal{F}_\Delta$ will be integrable with respect to the local Gibbs measures (3).

2.2. *Analytic Properties of Local Gibbs States*

In this Subsection we study the dependence of the partition function $Z_{\beta,\Delta}$, and hence of the free energy density $F_{\beta,\Delta}$, on the parameters $J_{\boldsymbol{ll}'}$ and $h_{\boldsymbol{l}}$. Here we extensively use notions and facts from the theory of entire functions, which may be found in the books of Refs. 16 and 17.

For discrete spins, the partition function $Z_{\beta,\Delta}$, as a sum of exponents, may be extended to an exponential type entire function of $h_\Delta=(h_{\boldsymbol{l}})_{\boldsymbol{l}\in\Delta}\in\mathbb{C}^{|\Delta|}$. The same remains true for all types of bounded spins – a fact which follows from the Paley–Wiener theorem (see e.g., Ref. 17). For the model of classical harmonic oscillators, i.e., for Gaussian ν_Δ, it may be extended to an entire function of h_Δ of order two (see (13)). For unbounded spins with the measure ϱ in the form (7), $Z_{\beta,\Delta}$ may be extended to an entire function of order between one and two, depending on the degree of the polynomial P (see below). Since for real $h_{\boldsymbol{l}}$, the function $\exp\left(-\beta H_\Delta\right)$ takes positive values only, the partition function $Z_{\beta,\Delta}$ is also positive, which means that the free energy density $F_{\beta,\Delta}$ is an analytic function on a domain in $\mathbb{C}^{|\Delta|}$, which contains $\mathbb{R}^{|\Delta|}$. This shows one more time that no phase transitions can arise

unless the volume (i.e., the subset Δ) remains finite since these phenomena are connected with the singularities of the free energy density (see Refs. 8, 10 and 14). On the other hand, by (4), the singularities of the free energy density may be connected with the zero points of the partition function. A classical result in this domain, known as the Lee–Yang theorem[36] (see also Refs. 10 and 11), states that for the Ising model, the only point of the real line which such zeros may reach in the infinite-volume limit is the origin. Here we present a generalization of this statement proven in Ref. 37. To this end we introduce the following notion.

Definition 1: A symmetric probability measure ϱ on the real line $\mathbb{R}$ is said to possess the Lee–Yang property if

$$\varphi_\varrho(z) = \int_{\mathbb{R}} e^{zt}\, d\varrho(t), \quad z \in \mathbb{C}, \tag{22}$$

is an entire function which has either imaginary zeros or none at all.

Then the Lee–Yang theorem in the version of E.H. Lieb and A.D. Sokal may be formulated as follows.

Proposition 2: *Let the spin model defined by the Hamiltonian (2) and the single-spin measure ϱ possess the properties: (a) $J_{\boldsymbol{l}\boldsymbol{l}'} \geq 0$ for all $\boldsymbol{l}, \boldsymbol{l}' \in \mathbb{Z}^d$; (b) the measure ϱ has the Lee–Yang property. Then, for every finite subset $\Delta \subset \mathbb{Z}^d$ and every $\beta > 0$, the partition function (3), as a function of h_Δ, can be extended to an entire function, which has nonzero values whenever $\Re(h_{\boldsymbol{l}}) > 0$ for all $\boldsymbol{l} \in \Delta$.*

Here $\Re(z)$ stands for the real part of $z \in \mathbb{C}$. The spin model for which $J_{\boldsymbol{l}\boldsymbol{l}'} \geq 0$ is called *ferromagnetic*. A corollary of the above statement, a particular case of which is equivalent to the original theorem proved by T.D. Lee and C.N. Yang (see below), is formulated as follows.

Proposition 3: *Let the conditions of the above proposition be satisfied and let $h_{\boldsymbol{l}} = z$ for all $\boldsymbol{l} \in \Delta$. Then, for every $\beta > 0$, the partition function (3), as a function of $z \in \mathbb{C}$, can be extended to an entire function, which has nonzero values whenever $\Re(z) \neq 0$.*

Let us analyze this statement in more detail. For $h_{\boldsymbol{l}} = z$, one has from (2) and (3) the following expression

$$Z_{\beta,\Delta}(z) = \int_{\Omega_\Delta} \exp\left(\beta z \sum_{\boldsymbol{l}\in\Delta} \sigma_{\boldsymbol{l}} + \frac{1}{2}\beta \sum_{\boldsymbol{l},\boldsymbol{l}'\in\Delta} J_{\boldsymbol{l}\boldsymbol{l}'}\sigma_{\boldsymbol{l}}\sigma_{\boldsymbol{l}'}\right) \prod_{\boldsymbol{l}\in\Delta} d\varrho(\sigma_{\boldsymbol{l}}). \tag{23}$$

As has been mentioned, the order ρ of $Z_{\beta,\Delta}$, as an entire function of z, belongs to the interval $\rho \in [1,2]$. Since the measure ϱ is supposed to be symmetric, this function ought to be even. Thus, it can be written as the following infinite product (see e.g., Ref. 17)

$$Z_{\beta,\Delta}(z) = Z_{\beta,\Delta}(0) \exp(\gamma_0(\beta,\Delta)z^2) \prod_{j=1}^{\infty} (1 + \gamma_j(\beta,\Delta)z^2), \tag{24}$$

where $Z_{\beta,\Delta}(0) > 0$, $\gamma_j(\beta,\Delta) \geq 0$, for all $j = 0,1,2,\ldots$. The case of all $\gamma_j(\beta,\Delta) = 0$ is degenerate, it holds if and only if the single-spin measure is concentrated at zero, i.e., $d\varrho(s) = \delta(s)\,ds$. The case $\gamma_0(\beta,\Delta) > 0$ and $\gamma_j(\beta,\Delta) = 0$ for $j \in \mathbb{N}$, corresponds to the model of harmonic oscillators, for which the single-spin measure is Gaussian. In this case the function (24) may be written (see (13))

$$Z_{\beta,\Delta}(z) = Z_{\beta,\Delta}(0) \exp\left\{ \left(\frac{1}{2}\beta^2 \sum_{\boldsymbol{\imath},\boldsymbol{\imath}' \in \Delta} (S^{-1})_{\boldsymbol{\imath}\boldsymbol{\imath}'} \right) z^2 \right\}.$$

It has no zeros at all and the corresponding infinite-volume free energy density exists and has no singularities. For polynomial models with even polynomials, for which the single-spin measure has the form (7) and (8) with $r \geq 2$, one has $\gamma_0(\beta,\Delta) = 0$ and $\gamma_j(\beta,\Delta) > 0$ for all $j \in \mathbb{N}$. In this case the order of growth of the function (24) is $\rho = 2r/(2r-1)$. This function has imaginary zeros at the points $z = \pm i/\sqrt{\gamma_j(\beta,\Delta)}$, $j \in \mathbb{N}$. An immediate consequence of the above analysis is that the only value of the homogeneous external field $h_{\boldsymbol{\imath}} = z$ at which the infinite-volume free energy density may have a singularity is $z = 0$. This occurs when the zeros of $Z_{\beta,\Delta}(z)$ reach the origin as $\Delta \to \mathbb{Z}^d$. Further analysis of measures with the Lee–Yang property may be found in Refs. 38 and 39. So far, we have had no examples of measures ϱ possessing the Lee–Yang property. Two such measures are well-known. These are the measure (5) and the symmetric Gaussian measure, i.e., a polynomial measure (7) with $P(\sigma_{\boldsymbol{\imath}}) = (b/2)\sigma_{\boldsymbol{\imath}}^2$:

$$d\varrho(s) = [b/2\pi]^{1/2} \exp(-(b/2)s^2)\,ds, \quad b > 0. \tag{25}$$

In fact, for the former measure, one has $\varphi_\varrho(z) = \cosh(z)$, whereas for the latter one, $\varphi_\varrho(z) = \exp(z^2/2b)$. The original Lee–Yang theorem is equivalent to Proposition 3 with the single-spin measure (5) and with the nearest-neighbor interaction potential $J_{\boldsymbol{\imath}\boldsymbol{\imath}'} = J\delta_{1,|\boldsymbol{\imath}-\boldsymbol{\imath}'|}$, $J > 0$.

Another example of measures possessing the Lee–Yang property are described by the following statement, which was proven in Ref. 40 (see also

Refs. 41 and 42). Let $\mathbb{L}$ stand for the class of entire functions of a single complex variable, which are the polynomials possessing real nonpositive zeros only or the limits of sequences of such polynomials, taken in the topology of uniform convergence on compact subsets of $\mathbb{C}$. Such functions are called *Laguerre entire functions*, their theory may be found in Ref. 16.

Proposition 4: *Given an entire function $g : \mathbb{C} \to \mathbb{C}$ let: (a) for every real $z \in [0, +\infty)$, this function have real positive values; (b) there exist $b > 0$ such that the function $\phi(z) = b + g'(z)$, where $g' = dg/dz$, belongs to the class $\mathbb{L}$. Then the measure*

$$d\varrho(s) = C \exp(-g(s^2))\, ds, \quad C = \int_{\mathbb{R}} \exp(-g(s^2))\, ds, \tag{26}$$

possesses the Lee–Yang property. For this measure, φ_ϱ is of order $\rho = 2r/(2r-1)$ if g is a polynomial of degree $r \in \mathbb{N}$, and $\rho = 1$, if g is a transcendental function.

An immediate consequence of this statement is that the φ^4 measure (9) possesses this property (see also Theorem IX.15 in Ref. 11).

2.3. *Correlation Inequalities*

As mentioned in the Introduction, correlation inequalities constitute the basis of a number of powerful methods in the theory of models we consider. Here we describe the most important of them, a more detailed description of such inequalities and their applications may be found in Ref. 3. Mostly these inequalities hold for ferromagnetic spin models only, i.e., for the models with $J_{\boldsymbol{l}\boldsymbol{l}'} \geq 0$, though some of them may be extended to more general interaction potentials. Therefore, in the statements presented below all inequalities hold for the ferromagnetic spin models described by the Hamiltonian (2) and a single-spin measure ϱ, which satisfies (21). In some cases we impose more specific conditions on the measure ϱ. The model with $h_{\boldsymbol{l}} \geq 0$ ($h_{\boldsymbol{l}} = 0$) will be called a model with a nonnegative (with a zero) external field.

The first example is known as the Fortuin–Kastelyn–Ginibre (FKG) inequality.[43] To formulate it we will need the following notion. For $\sigma_\Delta = (\sigma_{\boldsymbol{l}})_{\boldsymbol{l}\in\Delta}$ and $\sigma'_\Delta = (\sigma'_{\boldsymbol{l}})_{\boldsymbol{l}\in\Delta}$, we write $\sigma_\Delta \leq \sigma'_\Delta$ if $\sigma_{\boldsymbol{l}} \leq \sigma_{\boldsymbol{l}'}$ for all $\boldsymbol{l} \in \Delta$. A function $f \in \mathcal{F}_\Delta$ is said to be monotone on Ω_Δ if $f(\sigma_\Delta) \leq f(\sigma'_\Delta)$, whenever $\sigma_\Delta \leq \sigma'_\Delta$.

Proposition 5: *For any two monotone functions* $f, g \in \mathcal{F}_\Delta$

$$\langle fg \rangle_{\nu_\Delta} \geq \langle f \rangle_{\nu_\Delta} \langle g \rangle_{\nu_\Delta}. \tag{27}$$

The next correlation inequalities are known mostly due to R.B. Griffiths,[44] and they are called Griffiths–Kelly–Sherman (GKS) inequalities.

Proposition 6: *Let the functions* $f_1, \ldots, f_n, g_1, \ldots, g_n \in \mathcal{F}_\Delta$ *be given. Suppose that each of them satisfies the following conditions: (a) it depends on one component* $\sigma_{\boldsymbol{l}}$ *of the vector* σ_Δ *only; (b) as a function of this* $\sigma_{\boldsymbol{l}}$*, it is either odd and monotone or even and monotone as a function of* $|\sigma_{\boldsymbol{l}}|$*. Then for any ferromagnetic spin model with the zero external field,*

$$\langle f_1 \ldots f_n \rangle_{\nu_\Delta} \geq 0; \tag{28}$$

$$\langle f_1 \ldots f_n g_1 \ldots g_n \rangle_{\nu_\Delta} \geq \langle f_1 \ldots f_n \rangle_{\nu_\Delta} \langle g_1 \ldots g_n \rangle_{\nu_\Delta}. \tag{29}$$

Definition 7: A probability measure ϱ on the real line $\mathbb{R}$ is said to be a Bridges–Fröhlich–Spencer (BFS) measure if it is of the form

$$d\varrho(s) = C^{-1} \exp(-v(s^2))\, ds, \quad C = \int_{\mathbb{R}} \exp(-v(s^2))\, ds, \tag{30}$$

where the function $v : [0, +\infty) \to \mathbb{R}$ has the following properties: (a) there exist $v_0 \in \mathbb{R}$, $v_1 > 0$ such that $v(s^2) \geq v_0 + v_1 s^2$ for all $s \in \mathbb{R}$; (b) it is convex on $[0, +\infty)$, i.e., for any $\tau_1, \tau_2 \geq 0$ and $\theta \in [0, 1]$, it obeys $v(\theta\tau_1 + (1-\theta)\tau_2) \leq \theta v(\tau_1) + (1-\theta) v(\tau_2)$.

Definition 8: A probability measure ϱ on the real line $\mathbb{R}$ is said to be a Ellis–Monroe (EM) measure if it has the form (7) with an even polynomial (8), in which $b_2 \in \mathbb{R}$, $b_4, \ldots, b_{2r-2} \geq 0$, $b_{2r} > 0$.

The Gaussian measure (25), the φ^4-measure (9), the measures (26) are both BFS- and EM-measures. Moreover, every EM-measure is a BFS-measure.

Now we introduce the Griffiths–Hurst–Sherman (GHS) inequality, its proof may be found in Ref. 45.

Proposition 9: *For any ferromagnetic model with a nonnegative external field and a EM single-spin measure* ϱ*, the following inequality*

$$\begin{aligned} \langle \sigma_{\boldsymbol{l}_1} \sigma_{\boldsymbol{l}_2} \sigma_{\boldsymbol{l}_3} \rangle_{\nu_\Delta} \leq\ & \langle \sigma_{\boldsymbol{l}_1} \rangle_{\nu_\Delta} \langle \sigma_{\boldsymbol{l}_2} \sigma_{\boldsymbol{l}_3} \rangle_{\nu_\Delta} + \langle \sigma_{\boldsymbol{l}_2} \rangle_{\nu_\Delta} \langle \sigma_{\boldsymbol{l}_1} \sigma_{\boldsymbol{l}_3} \rangle_{\nu_\Delta} \\ & + \langle \sigma_{\boldsymbol{l}_3} \rangle_{\nu_\Delta} \langle \sigma_{\boldsymbol{l}_1} \sigma_{\boldsymbol{l}_2} \rangle_{\nu_\Delta} - 2 \langle \sigma_{\boldsymbol{l}_1} \rangle_{\nu_\Delta} \langle \sigma_{\boldsymbol{l}_2} \rangle_{\nu_\Delta} \langle \sigma_{\boldsymbol{l}_3} \rangle_{\nu_\Delta}, \end{aligned} \tag{31}$$

holds for any $\boldsymbol{l}_1, \boldsymbol{l}_2, \boldsymbol{l}_3 \in \Delta$.

The proof of the Lebowitz inequality, which we formulate below, may be found in Ref. 3.

Proposition 10: *For any ferromagnetic model with the zero external field and a BFS single-spin measure ϱ, the inequality*

$$\langle\sigma_{\boldsymbol{l}_1}\sigma_{\boldsymbol{l}_2}\sigma_{\boldsymbol{l}_3}\sigma_{\boldsymbol{l}_4}\rangle_{\nu_\Delta} \le \langle\sigma_{\boldsymbol{l}_1}\sigma_{\boldsymbol{l}_2}\rangle_{\nu_\Delta}\langle\sigma_{\boldsymbol{l}_3}\sigma_{\boldsymbol{l}_4}\rangle_{\nu_\Delta} + \langle\sigma_{\boldsymbol{l}_1}\sigma_{\boldsymbol{l}_3}\rangle_{\nu_\Delta}\langle\sigma_{\boldsymbol{l}_2}\sigma_{\boldsymbol{l}_4}\rangle_{\nu_\Delta} + \langle\sigma_{\boldsymbol{l}_1}\sigma_{\boldsymbol{l}_4}\rangle_{\nu_\Delta}\langle\sigma_{\boldsymbol{l}_2}\sigma_{\boldsymbol{l}_3}\rangle_{\nu_\Delta}, \tag{32}$$

holds for any $\boldsymbol{l}_1, \boldsymbol{l}_2, \boldsymbol{l}_3, \boldsymbol{l}_4 \in \Delta$.

Remark 11: All the above correlation inequalities hold for the ferromagnetic Ising model with the corresponding external field.

The proof of this statement follows from the fact that the Ising model can be approximated by the model with the single-spin measure of the form (9), for which all these inequalities hold. Let us provide some more details. The measure

$$d\varrho_\lambda(\sigma_{\boldsymbol{l}}) = C_\lambda^{-1}\exp(-\lambda(\sigma_{\boldsymbol{l}}^2-1)^2)\,d\sigma_{\boldsymbol{l}},\;\; C_\lambda = \int_{\mathbb{R}}\exp(-\lambda(\sigma_{\boldsymbol{l}}^2-1)^2)\,d\sigma_{\boldsymbol{l}}, \tag{33}$$

with $\lambda > 0$, is evidently of the type of (9). By means of the Laplace method,[46] one may prove the following statement. For any continuous polynomially bounded function $f : \mathbb{R} \to \mathbb{R}$,

$$\lim_{\lambda\to+\infty}\int_{\mathbb{R}} f(\sigma_{\boldsymbol{l}})\,d\varrho_\lambda(\sigma_{\boldsymbol{l}}) = \int_{\mathbb{R}} f(\sigma_{\boldsymbol{l}})\,d\varrho^{\mathrm{I}}(\sigma_{\boldsymbol{l}}) = \frac{1}{2}[f(1)+f(-1)], \tag{34}$$

where ϱ^{I} is the measure (5). This statement has the following important corollary. Let ν_Δ^{I} or ν_Δ^λ denote the local Gibbs measure (3) corresponding, respectively, to the Ising mode, i.e., the model with the single-spin measure (5), or to the model with the single-spin measure (33). Then for any continuous polynomially bounded function $f : \mathbb{R}^{|\Delta|} \to \mathbb{R}$, the following holds

$$\lim_{\lambda\to+\infty}\int_{\Omega_\Delta} f(\sigma_\Delta)\,d\nu_\Delta^\lambda(\sigma_\Delta) = \int_{\Omega_\Delta} f(\sigma_\Delta)\,d\nu_\Delta^{\mathrm{I}}(\sigma_\Delta), \tag{35}$$

which proves Remark 11. On the other hand, for any $\lambda > 0$ the measure ν_Δ^λ may be approximated by ν_Δ^{I}.[29]

For the measure ν_Δ^{I} with the zero external field, the function

$$\psi_\Delta(z) = \int_{\Omega_\Delta}\exp\left(z\sum_{\boldsymbol{l}\in\Delta}\sigma_{\boldsymbol{l}}\right)d\nu_\Delta^{\mathrm{I}}(\sigma_\Delta), \tag{36}$$

may be written also as $\psi_\Delta(z) = Z_{\beta,\Delta}(\beta^{-1}z)/Z_{\beta,\Delta}(0)$, where $Z_{\beta,\Delta}(\beta^{-1}z)$ is defined by (23) with the single-spin measure ϱ^{I}. By the Bochner theorem,[18]

there exists a unique probability measure ϱ_Δ on $\mathbb{R}$, such that this ψ_Δ may be written (cf., Eq. (22))

$$\psi_\Delta(z) = \int_{\mathbb{R}} \exp(zt)\, d\varrho_\Delta(t).$$

The measure ϱ_Δ defines the probability distribution of the total spin

$$S_\Delta = \sum_{\boldsymbol{l}\in\Delta} s_{\boldsymbol{l}}.$$

By (24) and Definition 1, this measure has the Lee–Yang property.

Let $\mathcal{D}$ be a sequence of subsets $\Delta \subset \mathbb{Z}^d$, such that for any two of its elements Δ, Δ', one of them is contained in the other one. We also suppose that this sequence exhausts the lattice $\mathbb{Z}^d$, which means that any finite subset $A \subset \mathbb{Z}^d$ is contained in a certain $\Delta \in \mathcal{D}$. As a countable set, the sequence $\mathcal{D}$ can be enumerated in such a way that for any two of its elements Δ_n, Δ_m, their numbers satisfy $n < m$ if and only if $\Delta_n \subset \Delta_m$. Then we may write $\mathcal{D} = \{\Delta_n\}_{n\in\mathbb{N}}$. For a sequence $\{c_\Delta\}_{\Delta\in\mathcal{D}}$ indexed by the elements of such $\mathcal{D}$, we write $\lim_{\mathcal{D}} c_\Delta$ or, if the sequence $\mathcal{D}$ has been specified, $\lim_{\Delta\to\mathbb{Z}^d} c_\Delta$ meaning $\lim_{n\to+\infty} c_{\Delta_n}$.

Definition 12: A sequence of probability measures $\{\mu_n\}_{n\in\mathbb{N}}$ is said to converge weakly to the measure μ if for any bounded continuous function $f : \mathbb{R} \to \mathbb{R}$,

$$\lim_{n\to+\infty} \int_{\mathbb{R}} f(t)\, d\mu_n(t) = \int_{\mathbb{R}} f(t)\, d\mu(t). \tag{37}$$

Definition 13: A probability measure ϱ on $\mathbb{R}$ is called a Griffiths-Simon (GS) measure if it may be written as the ϱ_Δ defined above with the corresponding Δ and nonnegative $J_{\boldsymbol{ll}'}$, or if it is the weak limit of a sequence $\{\varrho_\Delta\}_{\Delta\in\mathcal{D}}$ of such measures.

Thus by Ref. 29, the φ^4-measure is a GS-measure. Another example is

$$d\varrho(t) = \frac{1}{3}[\delta(t-1) + \delta(t) + \delta(t+1)]\, dt.$$

One may show that the sequence of φ_{μ_n}, defined by (22) for the above measures μ_n converges uniformly on bounded closed (i.e., compact) subsets of the complex plane $\mathbb{C}$ to the function φ_μ, which means that φ_μ has the representation (24) and hence the measure μ possesses the Lee–Yang property. It should be pointed out that not all of the EM- and BFS-measures possess this property (cf., Proposition 4).

The Lebowitz inequality (32) may be generalized to the case of a nonzero external field, but for another type of single-spin measures. The result presented below was proven in Ref. 45.

Proposition 14: *For any ferromagnetic model with a nonnegative external field and a single-spin measure ϱ, which is either of EM or of GS type, the following inequality*

$$\begin{aligned}\langle\sigma_{\boldsymbol{l}_1}\sigma_{\boldsymbol{l}_2}\sigma_{\boldsymbol{l}_3}\sigma_{\boldsymbol{l}_4}\rangle_{\nu_\Delta} \le \langle\sigma_{\boldsymbol{l}_1}\sigma_{\boldsymbol{l}_2}\rangle_{\nu_\Delta}\langle\sigma_{\boldsymbol{l}_3}\sigma_{\boldsymbol{l}_4}\rangle_{\nu_\Delta} + \langle\sigma_{\boldsymbol{l}_1}\sigma_{\boldsymbol{l}_3}\rangle_{\nu_\Delta}\langle\sigma_{\boldsymbol{l}_2}\sigma_{\boldsymbol{l}_4}\rangle_{\nu_\Delta} \\ +\langle\sigma_{\boldsymbol{l}_1}\sigma_{\boldsymbol{l}_4}\rangle_{\nu_\Delta}\langle\sigma_{\boldsymbol{l}_2}\sigma_{\boldsymbol{l}_3}\rangle_{\nu_\Delta} - 2\langle\sigma_{\boldsymbol{l}_1}\rangle_{\nu_\Delta}\langle\sigma_{\boldsymbol{l}_2}\rangle_{\nu_\Delta}\langle\sigma_{\boldsymbol{l}_3}\rangle_{\nu_\Delta}\langle\sigma_{\boldsymbol{l}_4}\rangle_{\nu_\Delta},\end{aligned} \tag{38}$$

holds for any $\boldsymbol{l}_1, \boldsymbol{l}_2, \boldsymbol{l}_3, \boldsymbol{l}_4 \in \Delta$.

Yet another result connected with the Lebowitz inequality (32) was proven in Ref. 47, it is called the Aizenman–Fröhlich inequality (see also Ref. 3).

Proposition 15: *For any ferromagnetic model with the zero external field and a GS single-spin measure ϱ, the following inequality*

$$\begin{aligned}&\langle\sigma_{\boldsymbol{l}_1}\sigma_{\boldsymbol{l}_2}\sigma_{\boldsymbol{l}_3}\sigma_{\boldsymbol{l}_4}\rangle_{\nu_\Delta} - \langle\sigma_{\boldsymbol{l}_1}\sigma_{\boldsymbol{l}_2}\rangle_{\nu_\Delta}\langle\sigma_{\boldsymbol{l}_3}\sigma_{\boldsymbol{l}_4}\rangle_{\nu_\Delta} \\ &\quad -\langle\sigma_{\boldsymbol{l}_1}\sigma_{\boldsymbol{l}_3}\rangle_{\nu_\Delta}\langle\sigma_{\boldsymbol{l}_2}\sigma_{\boldsymbol{l}_4}\rangle_{\nu_\Delta} - \langle\sigma_{\boldsymbol{l}_1}\sigma_{\boldsymbol{l}_4}\rangle_{\nu_\Delta}\langle\sigma_{\boldsymbol{l}_2}\sigma_{\boldsymbol{l}_3}\rangle_{\nu_\Delta} \\ &\ge -2\sum_{\boldsymbol{l}\in\Delta}\langle\sigma_{\boldsymbol{l}_1}\sigma_{\boldsymbol{l}}\rangle_{\nu_\Delta}\langle\sigma_{\boldsymbol{l}_2}\sigma_{\boldsymbol{l}}\rangle_{\nu_\Delta}\langle\sigma_{\boldsymbol{l}_3}\sigma_{\boldsymbol{l}}\rangle_{\nu_\Delta}\langle\sigma_{\boldsymbol{l}_4}\sigma_{\boldsymbol{l}}\rangle_{\nu_\Delta},\end{aligned} \tag{39}$$

holds for any $\boldsymbol{l}_1, \boldsymbol{l}_2, \boldsymbol{l}_3, \boldsymbol{l}_4 \in \Delta$.

It is worth noting that the Lebowitz inequality (32) gives an upper bound (it is zero) for the left-hand side of (39), whereas the above inequality gives its lower bound.

By Proposition 2, the partition function of the Ising model $Z_{\beta,\Delta}(h_\Delta)$ can be extended to an entire function of complex h_Δ, which does not vanish in the vicinity of the point $h_\Delta = 0$. Therefore, in this vicinity its logarithm will be holomorphic and hence may be written

$$\begin{aligned}\Phi_{\beta,\Delta}(h_\Delta) &\stackrel{\text{def}}{=} \ln Z_{\beta,\Delta}(h_\Delta) \\ &= \ln Z_{\beta,\Delta}(0) + \sum_{n=1}^{\infty}\frac{1}{(2n)!}\sum_{\boldsymbol{l}_1,\ldots,\boldsymbol{l}_{2n}\in\Delta} U^{(2n)}_{\beta,\Delta}(\boldsymbol{l}_1,\ldots,\boldsymbol{l}_{2n})h_{\boldsymbol{l}_1}\cdots h_{\boldsymbol{l}_{2n}},\end{aligned} \tag{40}$$

where the

$$U^{(2n)}_{\beta,\Delta}(\boldsymbol{l}_1,\ldots,\boldsymbol{l}_{2n}) = \left(\frac{\partial^{2n}}{\partial h_{\boldsymbol{l}_1}\cdots\partial h_{\boldsymbol{l}_{2n}}}\Phi_{\beta,\Delta}\right)(0), \quad n\in\mathbb{N}, \tag{41}$$

are called *Ursell functions*. They are also called *cumulants* or *semi-invariants*. By direct calculation,

$$U^{(2)}_{\beta,\Delta}(\boldsymbol{l}_1,\boldsymbol{l}_2) = K^{\Delta}_{\boldsymbol{l}_1\boldsymbol{l}_2}(0),$$

which is the correlation function for this model with the zero external field (see (18)). By Remark 11 and Propositions 10 and 15

$$-2\sum_{\boldsymbol{l}\in\Delta} U^{(2)}_{\beta,\Delta}(\boldsymbol{l}_1,\boldsymbol{l})\, U^{(2)}_{\beta,\Delta}(\boldsymbol{l}_2,\boldsymbol{l})\, U^{(2)}_{\beta,\Delta}(\boldsymbol{l}_3,\boldsymbol{l}) U^{(2)}_{\beta,\Delta}(\boldsymbol{l}_4,\boldsymbol{l})$$
$$\leq U^{(4)}_{\beta,\Delta}(\boldsymbol{l}_1,\ldots,\boldsymbol{l}_4) \leq 0. \tag{42}$$

For certain models, $U^{(2n)}_{\beta,\Delta}(\boldsymbol{l}_1,\ldots,\boldsymbol{l}_{2n})$, $n \in \mathbb{N}$ satisfy the following sign rule.[48]

Proposition 16: *For all $\beta > 0$ and any finite subset Δ, the Ursell functions (41) for the ferromagnetic model with the zero external field and a GS single-spin measure, satisfy the sign rule*

$$(-1)^{n-1} U^{(2n)}_{\beta,\Delta}(\boldsymbol{l}_1,\ldots,\boldsymbol{l}_{2n}) \geq 0, \quad n \in \mathbb{N}. \tag{43}$$

Moreover, the equality in (43) occurs either if the single-spin measure ϱ is Gaussian, or if and only if among the indices $\boldsymbol{l}_1,\ldots,\boldsymbol{l}_{2n}$ one finds the pair $\boldsymbol{l}_i,\boldsymbol{l}_j$ such that Δ may be divided onto disjoint Δ_1,Δ_2, $\boldsymbol{l}_i \in \Delta_1$ and $\boldsymbol{l}_j \in \Delta_2$, such that for any $\boldsymbol{l} \in \Delta_1$ and $\boldsymbol{l}' \in \Delta_2$, one has $J_{\boldsymbol{l}\boldsymbol{l}'} = 0$.

The following statements are important corollaries of the inequalities presented above. First, we obtain a property of the correlation functions $K^{\Delta}_{\boldsymbol{l}\boldsymbol{l}'}(h_\Delta)$ defined by (18).

Corollary 17: *For any ferromagnetic model with a nonnegative external field*

$$K^{\Delta}_{\boldsymbol{l}\boldsymbol{l}'}(h_\Delta) \geq 0. \tag{44}$$

Proof: By (18),

$$K^{\Delta}_{\boldsymbol{l}\boldsymbol{l}'}(h_\Delta) = \langle fg\rangle_{\nu_\Delta} - \langle f\rangle_{\nu_\Delta}\langle g\rangle_{\nu_\Delta} \geq 0,$$

where we have set $f(\sigma_\Delta) = \sigma_{\boldsymbol{l}}$, $g(\sigma_\Delta) = \sigma_{\boldsymbol{l}'}$ and employed the FKG inequality (27). □

Recall that $h_\Delta \leq h'_\Delta$ means $h_{\boldsymbol{l}} \leq h'_{\boldsymbol{l}}$ for all $\boldsymbol{l} \in \Delta$, moreover, 0_Δ stands for such a vector h_Δ with all $h_{\boldsymbol{l}} = 0$.

Corollary 18: *For any ferromagnetic model with an EM single-spin measure ϱ, the correlation function has the property*

$$K^{\Delta}_{\boldsymbol{l}\boldsymbol{l}'}(h'_{\Delta}) \leq K^{\Delta}_{\boldsymbol{l}\boldsymbol{l}'}(h_{\Delta}) \leq K^{\Delta}_{\boldsymbol{l}\boldsymbol{l}'}(0_{\Delta}), \tag{45}$$

for any h_{Δ}, h'_{Δ} such that $0_{\Delta} \leq h_{\Delta} \leq h'_{\Delta}$.

Proof: By (18) and (2), (3), one has

$$\begin{aligned}\frac{\partial}{\partial h_{\boldsymbol{l}''}} K^{\Delta}_{\boldsymbol{l}\boldsymbol{l}'}(h_{\Delta}) = {} & \langle \sigma_{\boldsymbol{l}}\sigma_{\boldsymbol{l}'}\sigma_{\boldsymbol{l}''}\rangle_{\nu_{\Delta}} - \langle \sigma_{\boldsymbol{l}}\sigma_{\boldsymbol{l}'}\rangle_{\nu_{\Delta}}\langle \sigma_{\boldsymbol{l}''}\rangle_{\nu_{\Delta}} - \langle \sigma_{\boldsymbol{l}}\sigma_{\boldsymbol{l}''}\rangle_{\nu_{\Delta}}\langle \sigma_{\boldsymbol{l}'}\rangle_{\nu_{\Delta}} \\ & - \langle \sigma_{\boldsymbol{l}'}\sigma_{\boldsymbol{l}''}\rangle_{\nu_{\Delta}}\langle \sigma_{\boldsymbol{l}}\rangle_{\nu_{\Delta}} + 2\langle \sigma_{\boldsymbol{l}}\rangle_{\nu_{\Delta}}\langle \sigma_{\boldsymbol{l}'}\rangle_{\nu_{\Delta}}\langle \sigma_{\boldsymbol{l}''}\rangle_{\nu_{\Delta}} \leq 0,\end{aligned}$$

where we have used the GHS-inequality (31). Thus, as a function of h_{Δ}, $K^{\Delta}_{\boldsymbol{l}\boldsymbol{l}'}(h_{\Delta})$ is monotone decreasing for all h_{Δ}, for which (31) is valid, i.e., for $h_{\Delta} \geq 0$. □

Corollary 19: *For every monotone function $f \in \mathcal{F}_{\Delta}$, the expectation value $\langle f\rangle_{\nu_{\Delta}}$ is a monotone function of the external field h_{Δ}. This means that for any h_{Δ}, h'_{Δ}, such that $h_{\Delta} \leq h'_{\Delta}$, the following holds*

$$\langle f\rangle_{\nu_{\Delta}} \leq \langle f\rangle_{\nu'_{\Delta}}, \tag{46}$$

where ν_{Δ} and ν'_{Δ} are respectively, the local Gibbs measure (3) corresponding to the local Hamiltonian (2) with the external field h_{Δ} and h'_{Δ}.

Proof: For $t \in [0,1]$ and the mentioned h_{Δ}, h'_{Δ}, we set $x_{\Delta}(t) = h_{\Delta} + t(h'_{\Delta} - h_{\Delta})$ and let $\nu_{\Delta}(t)$ be the measure (3) corresponding to the external field $x_{\Delta}(t)$, which obviously satisfies the "boundary condition" $\nu_{\Delta}(0) = \nu_{\Delta}$ and $\nu_{\Delta}(1) = \nu'_{\Delta}$. Then

$$\begin{aligned}&\langle f\rangle_{\nu_{\Delta}(t)} \\ &= \frac{1}{Z_{\beta,\Delta}(t)} \int_{\Omega_{\Delta}} f(\sigma_{\Delta}) \exp\left(\frac{1}{2}\beta \sum_{\boldsymbol{l},\boldsymbol{l}'\in\Delta} J_{\boldsymbol{l}\boldsymbol{l}'}\sigma_{\boldsymbol{l}}\sigma_{\boldsymbol{l}'} + \beta \sum_{\boldsymbol{l}\in\Delta} x_{\boldsymbol{l}}(t)\sigma_{\boldsymbol{l}}\right) \prod_{\boldsymbol{l}\in\Delta} d\varrho(\sigma_{\boldsymbol{l}}),\end{aligned} \tag{47}$$

where

$$Z_{\beta,\Delta}(t) = \int_{\Omega_{\Delta}} \exp\left(\frac{1}{2}\beta \sum_{\boldsymbol{l},\boldsymbol{l}'\in\Delta} J_{\boldsymbol{l}\boldsymbol{l}'}\sigma_{\boldsymbol{l}}\sigma_{\boldsymbol{l}'} + \beta \sum_{\boldsymbol{l}\in\Delta} x_{\boldsymbol{l}}(t)\sigma_{\boldsymbol{l}}\right) \prod_{\boldsymbol{l}\in\Delta} d\varrho(\sigma_{\boldsymbol{l}}). \tag{48}$$

Differentiating both parts of (47) and taking into account (48) one obtains

$$\frac{\partial}{\partial t}\langle f\rangle_{\nu_{\Delta}(t)} = \langle fg\rangle_{\nu_{\Delta}(t)} - \langle f\rangle_{\nu_{\Delta}(t)}\langle g\rangle_{\nu_{\Delta}(t)}, \tag{49}$$

where

$$g(\sigma_\Delta) \stackrel{\text{def}}{=} \beta \sum_{\boldsymbol{l}\in\Delta} (h'_{\boldsymbol{l}} - h_{\boldsymbol{l}})\sigma_{\boldsymbol{l}},$$

which is a monotone function since $h_\Delta \le h'_\Delta$. Now we apply in (49) the FKG-inequality, which obviously holds for the measure $\nu_\Delta(t)$ with any $t \in [0,1]$, and obtain

$$\frac{\partial}{\partial t}\langle f\rangle_{\nu_\Delta(t)} \ge 0,$$

for all $t \in [0,1]$. Therefore, $\langle f\rangle_{\nu_\Delta(t)}$ is a monotone function of t, which yields (46). □

Corollary 20: *For every monotone function $f \in \mathcal{F}_\Delta$ and for any ferromagnetic model with the zero external field, the expectation value $\langle f\rangle_{\nu_\Delta}$ is a monotone function of the interaction parameter $J_{\boldsymbol{ll}'}$. This means that for $0 \le J_{\boldsymbol{ll}'} \le J'_{\boldsymbol{ll}'}$ for all $\boldsymbol{l},\boldsymbol{l}' \in \Delta$, the following holds*

$$\langle f\rangle_{\nu_\Delta} \le \langle f\rangle_{\nu'_\Delta}, \tag{50}$$

where ν_Δ and ν'_Δ are respectively, the local Gibbs measure (3) corresponding to the local Hamiltonian (2) with the interaction potential $J_{\boldsymbol{ll}'}$ and $J'_{\boldsymbol{ll}'}$.

The proof of this statement is almost the same as the proof of the previous one and is based on the GKS-inequalities. Below we give another applications of the above inequalities.

A wide variety of correlation inequalities and examples of their applications are presented in Ref. 3 (see also Ref. 49).

2.4. *Infinite-Volume Gibbs States*

As has been pointed out above, phase transitions are possible only in the infinite-volume limit $\Delta \to \mathbb{Z}^d$. In order to pass to such a limit, we have to relate with each other functions belonging to $\mathcal{F}_\Delta$ and $\mathcal{F}_{\Delta'}$ with $\Delta \subset \Delta'$. Thus, each $f \in \mathcal{F}_\Delta$ will be considered also as an element of $\mathcal{F}_{\Delta'}$, which is independent of $\sigma_{\boldsymbol{l}}$ with $\boldsymbol{l} \in \Delta' \setminus \Delta$. This defines an embedding $\mathcal{F}_\Delta \subset \mathcal{F}_{\Delta'}$ for $\Delta \subset \Delta'$. We recall that a sequence $\mathcal{D}$ of subsets Δ is called increasing if, for every two of its elements, one of them is a subset of the other one. It exhausts the lattice $\mathbb{Z}^d$ if every finite subset of the latter is contained in an element of $\mathcal{D}$. For such a sequence $\mathcal{D}$, we set

$$\mathcal{F} = \bigcup_{\Delta\in\mathcal{D}} \mathcal{F}_\Delta. \tag{51}$$

Therefore, for every $f \in \mathcal{F}$, one may find Δ_1, such that $f \in \mathcal{F}_{\Delta_1}$, and a sequence $\mathcal{D}$ in which this Δ_1 is the first element. Then the infinite-volume limit $\lim_{\mathcal{D}} \langle f \rangle_{\nu_\Delta}$ will make sense. By $\lim_{\mathcal{D}}$ we mean the limit in which $\Delta \to \mathbb{Z}^d$ along the sequence $\mathcal{D}$. At first glance, this setting is sufficient to describe possible phase transitions in our model. But a more detailed consideration immediately yields that it is not. For example, in the case of symmetric ϱ and all $h_{\boldsymbol{l}} = 0$ there is no way to break the symmetry $\sigma_{\boldsymbol{l}} \to -\sigma_{\boldsymbol{l}}$ of the model in such a limit. This means that certain thermodynamic properties of the model, especially those related to phase transitions, are described by quantities, which cannot be obtained as infinite-volume limits of expectations (averages) with respect to the measures (3). To obtain such quantities N.N. Bogolyubov[50] introduced a notion of quasi-averages. They are obtained by adding to the Hamiltonian (2) corresponding infinitesimal fields, which are to be removed after passing to the infinite-volume limit. At the same time, an approach to the construction of "all possible" infinite-volume Gibbs measures[b] on the basis of conditional probabilities was elaborated by R.L. Dobrushin[51,52] and by O.E. Lanford and D. Ruelle.[53] In this approach such measures are obtained as solutions of a certain equation, now known as *the Dobrushin–Lanford–Ruelle (DLR) equation*. A detailed description of this approach is given in Ref. 4. Here we present a short introduction into this theory.

First of all we will need the space on which such infinite-volume measures are defined. Set

$$\Omega = \{\sigma = (\sigma_{\boldsymbol{l}})_{\boldsymbol{l} \in \mathbb{Z}^d} \mid \sigma_{\boldsymbol{l}} \in \mathbb{R}\}. \tag{52}$$

This set consists of vectors σ, which have infinitely many real components $\sigma_{\boldsymbol{l}}$ indexed by the points of the lattice. Such vectors are called *configurations*. This set can be metrized by introducing the following "distance" between any two of its elements σ, σ'

$$\boldsymbol{d}(\sigma, \sigma') = \sum_{\boldsymbol{l} \in \mathbb{Z}^d} \frac{1}{2^{|\boldsymbol{l}|}} \frac{|\sigma_{\boldsymbol{l}} - \sigma'_{\boldsymbol{l}}|}{1 + |\sigma_{\boldsymbol{l}} - \sigma'_{\boldsymbol{l}}|}, \tag{53}$$

where $|\boldsymbol{l}| = \sqrt{|l_1|^2 + \cdots + |l_d|^2}$. This enables us to introduce the set of all probability measures on Ω , which will be denoted by $\mathcal{P}(\Omega)$. It appears, see Ref. 4 (p. 59), that the above introduced set of functions $\mathcal{F}$ separates the

[b]More details on the relation between infinite-volume Gibbs states and phase transitions are given in the next subsection.

points of $\mathcal{P}(\Omega)$. This means that if the measures $\mu_1, \mu_2 \in \mathcal{P}(\Omega)$ have the property $\langle f \rangle_{\mu_1} = \langle f \rangle_{\mu_2}$ for all $f \in \mathcal{F}$, then they coincide. Here we write

$$\langle f \rangle_\mu = \int_\Omega f \, d\mu. \tag{54}$$

In order to have the things we deal with as simple as possible, we suppose in this subsection that the interaction potential $J_{\boldsymbol{l}\boldsymbol{l}'}$ in the Hamiltonian (2) has a finite range, which means that this potential takes zero values whenever the distance $|\boldsymbol{l} - \boldsymbol{l}'|$ exceeds a certain $R > 0$. Given a subset Δ and a configuration $\xi \in \Omega$, we define the following probability measures

$$d\nu_\Delta(\sigma_\Delta|\xi) = Z^{-1}_{\beta,\Delta}(\xi) \exp(-\beta H_\Delta(\xi)) \prod_{\boldsymbol{l}\in\Delta} d\varrho(\sigma_{\boldsymbol{l}}), \tag{55}$$

$$d\pi_\Delta(\sigma|\xi) = d\nu_\Delta(\sigma_\Delta|\xi) \prod_{\boldsymbol{l}\in\Delta^c} \left[\delta(\sigma_{\boldsymbol{l}} - \xi_{\boldsymbol{l}}) \, d\sigma_{\boldsymbol{l}}\right], \tag{56}$$

where

$$H_\Delta(\xi) = -\frac{1}{2} \sum_{\boldsymbol{l},\boldsymbol{l}'\in\Delta} J_{\boldsymbol{l}\boldsymbol{l}'}\sigma_{\boldsymbol{l}}\sigma_{\boldsymbol{l}'} - \sum_{\boldsymbol{l}\in\Delta} h_{\boldsymbol{l}}\sigma_{\boldsymbol{l}} - \sum_{\boldsymbol{l}\in\Delta,\boldsymbol{l}'\in\Delta^c} J_{\boldsymbol{l}\boldsymbol{l}'}\sigma_{\boldsymbol{l}}\xi_{\boldsymbol{l}'}, \tag{57}$$

$$Z_{\beta,\Delta}(\xi) = \int_{\Omega_\Delta} \exp(-\beta H_\Delta(\xi)) \prod_{\boldsymbol{l}\in\Delta} d\varrho(\sigma_{\boldsymbol{l}}), \tag{58}$$

and $\Delta^c = \mathbb{Z}^d \setminus \Delta$. The first two terms of the last Hamiltonian describe the energy of the self-interaction of the spins located in Δ whereas the third term corresponds to the interaction of these spins with the fixed configuration ξ outside Δ. Due to our assumption regarding the range of $J_{\boldsymbol{l}\boldsymbol{l}'}$, the sum in this term is finite hence no convergence problems appear. The essential difference between the above introduced measures is that $\nu_\Delta(\cdot|\xi)$[c] is defined on the space Ω_Δ consisting of vectors σ_Δ of finitely many components. The measure $\pi_\Delta(\cdot|\xi)$ is defined on the space Ω, but due to the presence of the δ-functions on the right-hand side of (56), the components of σ labelled by $\boldsymbol{l} \in \Delta^c$ are "frozen", i.e., they should coincide with the corresponding components of the configuration ξ. The partition function $Z_{\beta,\Delta}(\xi)$ is defined in the same way as in (3). In what follows, the measure (3) is a particular case of (55), which corresponds to the zero configuration $\xi = 0$. Hence ν_Δ is called the local Gibbs measure with the zero boundary condition, whereas $\nu_\Delta(\cdot|\xi)$ is the local Gibbs measure with the boundary condition defined

[c]In this way we indicate the dependence of ν_Δ, π_Δ on ξ.

by the configuration ξ, or simply, with the boundary condition ξ. For a function $f \in \mathcal{F}_\Delta$, one readily has

$$\int_{\Omega_\Delta} f(\sigma_\Delta)\, d\nu_{\beta,\Delta}(\sigma_\Delta|\xi) = \int_\Omega f(\sigma)\, d\pi_{\beta,\Delta}(\sigma|\xi),$$

where the function under the integral on the right-hand side is the same f but considered as a function defined on the whole Ω, which is independent of the components of σ labelled by $\boldsymbol{l} \in \Delta^c$. The measure $\pi_{\beta,\Delta}$ has the following property. For every $\mu \in \mathcal{P}(\Omega)$, the integral

$$\int_\Omega d\pi_{\beta,\Delta}(\sigma|\xi)\, d\mu(\xi),$$

is again a probability measure on Ω. We will denote this new measure by $\pi_{\beta,\Delta} \circ \mu$, that is we set

$$d(\pi_{\beta,\Delta} \circ \mu)(\sigma) = \int_\Omega d\pi_{\beta,\Delta}(\sigma|\xi)\, d\mu(\xi). \tag{59}$$

The above integration has the following interpretation. Given a configuration $\xi \in \Omega$, the measure $\pi_{\beta,\Delta}(\cdot|\xi)$ defines a probability distribution of configurations $\sigma \in \Omega$ which ought to coincide with this ξ outside Δ. In the course of the integration (59) the boundary conditions are averaged, i.e., they are taken with their weights which are prescribed by the measure μ. Suppose now that this new measure (59) coincides with the averaging measure μ and this takes place for every finite subset Δ. Then for any $f \in \mathcal{F}$, one finds Δ such that $f \in \mathcal{F}_\Delta$ and then

$$\int_\Omega f\, d\mu = \int_\Omega \left(\int_\Omega f(\sigma)\, d\pi_{\beta,\Delta}(\sigma|\xi) \right) d\mu(\xi) = \int_\Omega f\, d(\pi_{\beta,\Lambda} \circ \mu),$$

which means that the expectation value of f with respect to the local Gibbs measure with averaged boundary conditions is the same as its expectation taken directly with respect to the measure μ. In other words, a kind of equilibrium between configurations inside and outside each such a Δ holds.

Definition 21: A probability measure $\mu \in \mathcal{P}(\Omega)$ is called an equilibrium (Gibbs) measure if, for any finite $\Delta \subset \mathbb{Z}^d$, the following equilibrium condition holds

$$\pi_{\beta,\Delta} \circ \mu = \mu. \tag{60}$$

The set of all Gibbs measures existing at a given β will be denoted by $\mathcal{G}_\beta$. It is defined by the family of all local Hamiltonians (2). The equality (60) may be considered as an equation, in which the unknown is μ. It is called the

Dobrushin–Lanford–Ruelle equation. On can show (see e.g., Ref. 4) that under the assumptions (21) made regarding the single-spin measure ϱ the set $\mathcal{G}_\beta$ in nonempty for all $\beta > 0$. If for a given β, it contains more than one element, the system considered may exists in more than one phases in the same conditions. And alternatively, if this set consists of exactly one element at all temperatures, no phase transitions are possible for this system. Suppose now that μ_1, μ_2 are two different elements of $\mathcal{G}_\beta$. Then, for every $\theta \in [0, 1]$, the combination

$$\mu = \theta\mu_1 + (1 - \theta)\mu_2, \tag{61}$$

which is called *a mixture* of the measures μ_1 and μ_2, is a probability measure (it is normalized since $\theta + (1 - \theta) = 1$). It solves the DLR equation (60) hence belongs to $\mathcal{G}_\beta$. This means that the last set may contain either one or infinitely many elements. If an element $\mu \in \mathcal{G}_\beta$ cannot be written as a convex combination (61) with $\theta \neq 1, 0$ of any other elements of this set, it is called *a pure state*. In the case of the Ising model such pure states $\mu_\pm$ may be obtained as infinite-volume limits of the measures (55) corresponding to the boundary conditions $\xi_\pm$, all elements of which are equal to ± 1. For $d \geq 2$ and large enough β, $\mu_+ \neq \mu_-$.

Now let us discuss how, for a given model, one may get its Gibbs states or at least how to get information regarding such states. Another question of this kind is whether one can get such states as infinite volume limits of local states, which would be very natural. The direct construction of Gibbs states may be made only for simple models, for example in the case of the Gaussian single-spin measure ϱ. In more nontrivial situations such states are studied by means of the DLR equation without their explicit construction. As for the second question, the answer is yes. It was obtained recently[54] and even for much more general objects than those we consider. In order to formulate the corresponding statement we have to make precise the notion of convergence. Recall that the set $\mathcal{F}$ consists of local polynomially bounded continuous functions $f : \Omega \to \mathbb{R}$, where "local" means that there exists a finite subset Δ, depending on f, such that f depends on $\sigma_{\boldsymbol{l}}$, $\boldsymbol{l} \in \Delta$ only. By $\mathcal{F}^{(0)}$ we denote the subset of $\mathcal{F}$ consisting of bounded functions. Let again $\mathcal{D}$ be an increasing sequence of subsets Δ, which exhausts the lattice $\mathbb{Z}^d$ and for which we write $\lim_{\mathcal{D}}$ meaning the limit $\Delta \to \mathbb{Z}^d$ taken along this sequence.

Definition 22: A sequence of probability measures $\{\mu_\Delta\}_{\Delta \in \mathcal{D}}$, defined on the configuration space Ω is said to converge locally weakly to a probability

measure μ if for every $f \in \mathcal{F}^{(0)}$,

$$\lim_{\mathcal{D}} \left(\int_\Omega f \, d\mu_\Delta \right) = \int_\Omega f \, d\mu. \tag{62}$$

Then we have the following result.[54]

Proposition 23: *For every $\xi \in \Omega$ and any sequence $\mathcal{D}$, the locally weak limit of the sequence of $\{\pi_{\beta,\Delta}(\cdot|\xi)\}_{\Delta\in\mathcal{D}}$, if it exists, is a Gibbs measure.*

Another result of this kind is taken from Ref. 4. Pure states, i.e., the Gibbs measures which cannot be written as nontrivial convex combinations (61), are called extreme elements[d] of $\mathcal{G}_\beta$. Theorem 7.26 of Ref. 4 (p. 13) has the following corollary.

Proposition 24: *The set of extreme elements $\mathcal{G}_\beta^{\rm ex} \subset \mathcal{G}_\beta$ is nonempty. If $|\mathcal{G}_\beta^{\rm ex}| = 1$, then $|\mathcal{G}_\beta| = 1$.*

Another result of this book (Ref. 4, Theorem 7.12 on p. 122) reads as follows.

Proposition 25: *For every $\mu \in \mathcal{G}_\beta^{\rm ex}$ and any sequence $\mathcal{D}$, the sequence $\{\pi_{\beta,\Delta}(\cdot|\xi)\}_{\Delta\in\mathcal{D}}$ locally weakly converges to μ for almost all ξ. The latter means that this convergence may fail to hold only for boundary conditions ξ, which belong to a subset $A \subset \Omega$, such that $\mu(A) = 0$.*

Given $\boldsymbol{l}_0 \in \mathbb{Z}^d$ and a configuration $\sigma = (\sigma_{\boldsymbol{l}})_{\boldsymbol{l}\in\mathbb{Z}^d}$, we set $\vartheta_{\boldsymbol{l}_0}\sigma = (\sigma_{\boldsymbol{l}+\boldsymbol{l}_0})_{\boldsymbol{l}\in\mathbb{Z}^d}$. Now for a function $f \in \mathcal{F}$, we set

$$t_{\boldsymbol{l}_0}(f)(\sigma) = f(\vartheta_{\boldsymbol{l}_0}\sigma), \tag{63}$$

i.e., $\vartheta_{\boldsymbol{l}_0}$ and $t_{\boldsymbol{l}_0}$ are translations defined on the set of configurations and real valued functions of configurations respectively.

Definition 26: The model, described by the family of Hamiltonians (2) with all possible finite $\Delta \subset \mathbb{Z}^d$, is called translation invariant if, for every $\boldsymbol{l}_0 \in \mathbb{Z}^d$, its parameters satisfy the following conditions

$$\forall \boldsymbol{l}, \boldsymbol{l}' \in \mathbb{Z}^d: \quad J_{\boldsymbol{l}\boldsymbol{l}'} = J_{(\boldsymbol{l}+\boldsymbol{l}_0)(\boldsymbol{l}'+\boldsymbol{l}_0)}; \qquad \forall \boldsymbol{l} \in \mathbb{Z}^d: \quad h_{\boldsymbol{l}} = h_{\boldsymbol{l}+\boldsymbol{l}_0}.$$

The external field $h_{\boldsymbol{l}}$ which satisfies the above condition is homogeneous, i.e., it is constant $h_{\boldsymbol{l}} = h$. A particular case of the translation invariant

[d] The extreme elements of a plane triangle are its vertices.

interaction potentials is $J_{\boldsymbol{l}\boldsymbol{l}'} = \phi(|\boldsymbol{l} - \boldsymbol{l}'|)$, where ϕ is a real valued function. One has to remark here that the Hamiltonians (2) are not translation invariant, but for a translation invariant model, in accordance with (63),

$$t_{\boldsymbol{l}_0} H_\Delta = H_{\Delta'},$$

where Δ' is obtained as a translation of Δ on the vector $\boldsymbol{l}_0$.

Definition 27: A Gibbs measure μ is called translation invariant if, for every $f \in \mathcal{F}$ and $\boldsymbol{l}_0 \in \mathbb{Z}^d$,

$$\langle f \rangle_\mu = \langle t_{\boldsymbol{l}_0}(f) \rangle_\mu.$$

One can show that, for any $\boldsymbol{l}_0 \in \mathbb{Z}^d$ and every $\mu \in \mathcal{P}(\Omega)$, there exists a $\tilde{\mu} \in \mathcal{P}(\Omega)$ such that, for every $f \in \mathcal{F}$,

$$\langle f \rangle_{\tilde{\mu}} = \langle t_{\boldsymbol{l}_0}(f) \rangle_\mu.$$

If this μ is translation invariant, then $\tilde{\mu} = \mu$. On the other hand, since $\mathcal{F}$ separates the points of $\mathcal{P}(\Omega)$, there exists exactly one such $\tilde{\mu}$. By Definition 21, for every $\mu \in \mathcal{G}_\beta$ and every $\boldsymbol{l}_0 \in \mathbb{Z}^d$, its $\tilde{\mu}$ will also belong to $\mathcal{G}_\beta$ provided the model is translation invariant. Therefore if, for a translation invariant model, the set of all Gibbs measures consists of one μ, this element should be a translation invariant measure. R.L. Dobrushin proved in Ref. 55 that, for the three-dimensional Ising model with the zero external field, below its critical point there exist infinitely many non-translation invariant phases. This is a consequence of the fact, also proved by R.L. Dobrushin,[56] that in the Ising model on the lattice $\mathbb{Z}^d$ with $d \geq 3$, below T_C different phases may coexist separated by stable surfaces, which is impossible in the case $d = 2$ (see also Refs. 57 and 58).

Now we present some facts about the infinite volume convergence of thermodynamic functions. By means of estimates proven by D. Ruelle,[59] J.L. Lebowitz and E. Presutti[60] proved the existence of the infinite-volume free energy density, which is independent of the boundary conditions. Below we present this result in a simplified version, for more details and generalizations we refer the reader to the original work in Ref. 60. Given $N \in \mathbb{N}$ and a finite $\Delta \subset \mathbb{Z}^d$, we set

$$\Omega(N, \Delta) = \left\{ \sigma \in \Omega \;\middle|\; \sum_{\boldsymbol{l} \in \Delta} \sigma_{\boldsymbol{l}}^2 \leq N^2 |\Delta| \right\}. \tag{64}$$

The set of *tempered configurations* Ω^{t} by definition consists of those $\sigma \in \Omega$ for which there exists $N \in \mathbb{N}$ such that, for any finite Δ, $\sigma \in \Omega(N, \Delta)$.

Of course, the zero configuration, for which all $\sigma_{\boldsymbol{l}} = 0$, is tempered. Let $\mathcal{L}$ be the sequence of cubes (1) defined by a sequence $\{L_n\}_{n\in\mathbb{N}}$ such that $L_{n+1} > L_n$, henceforth $L_n \to +\infty$. We say that the external field is bounded if there exists a constant a such that for all $\boldsymbol{l} \in \mathbb{Z}^d$, $|h_{\boldsymbol{l}}| \le a$.

Proposition 28: *For the spin model described by the Hamiltonian (2) with a bounded external field and with the single-spin measure ϱ which has the form (7), (8) with $r \ge 2$ or (5), the free energy density*

$$F_{\beta,\Lambda}(\xi) = -\frac{1}{\beta|\Lambda|} \ln Z_{\beta,\Lambda}(\xi), \tag{65}$$

with $\xi \in \Omega^{\mathrm{t}}$ converges, as $\Lambda \to \mathbb{Z}^d$ along any sequence $\mathcal{L}$, to a limit, which does not depend on the choice of $\mathcal{L}$ and on ξ, hence it is the same as for the zero boundary condition.

We complete this subsection by describing a special kind of translation invariant Gibbs measures. Of course, they may be constructed for translation invariant models only. We suppose that the interaction potential has the form $J_{\boldsymbol{ll}'} = \phi(|\boldsymbol{l} - \boldsymbol{l}'|)$. These measures are built by means of cubes (1). Given such a cube Λ, we define

$$|\boldsymbol{l} - \boldsymbol{l}'|_\Lambda = \sqrt{|l_1 - l_1'|_\Lambda^2 + \cdots + |l_d - l_d'|_\Lambda^2},$$

where $|l_j - l_j'|_\Lambda = \min\{|l_j - l_j'|; 2L - |l_j - l_j'|\}$, $j = 1, \ldots, d$. The above introduced function gives a periodic distance between the points $\boldsymbol{l}, \boldsymbol{l}' \in \Lambda$, it may be interpreted as a distance on the torus which one obtains by identifying the opposite walls of the cube Λ. Thereby, we set $J^\Lambda_{\boldsymbol{ll}'} = \phi(|\boldsymbol{l} - \boldsymbol{l}'|_\Lambda)$ with the same ϕ. The Hamiltonian

$$H_\Lambda = -\frac{1}{2} \sum_{\boldsymbol{l},\boldsymbol{l}' \in \Lambda} J^\Lambda_{\boldsymbol{ll}'} \sigma_{\boldsymbol{l}} \sigma_{\boldsymbol{l}'} - \sum_{\boldsymbol{l} \in \Lambda} h \sigma_{\boldsymbol{l}}, \tag{66}$$

is invariant with respect to translations on the mentioned torus. Such Hamiltonians are said to satisfy the Born–von Karman boundary condition. By means of this Hamiltonian, one may construct the corresponding (periodic) local Gibbs state $\nu^{(p)}_\Lambda$ exactly as was done in (3) for the zero boundary condition. The only difference is that such periodic local Gibbs states may be defined only for boxes like (1) or their translates. The following statement may be proven on the basis of the results of Refs. 54 and 61.

Proposition 29: *There exists a tending to $+\infty$ sequence $\{L_n\}_{n\in\mathbb{N}} \subset \mathbb{N}$, which defines by (1) the sequence of boxes $\{\Lambda_n\}_{n\in\mathbb{N}}$, such that the sequence*

of periodic local Gibbs states $\{\nu^{(p)}_{\beta,\Lambda_n}\}_{n\in\mathbb{N}}$ *locally weakly converges to an element of* $\mathcal{G}_\beta$*, which is a translation invariant Gibbs state.*

2.5. *Phase Transitions and Critical Points*

As has been pointed out in the preceding subsection, phase transitions are associated with the fact that the set $\mathcal{G}_\beta$ contains more than one element, i.e., more than one phase. There exist several methods to prove that $|\mathcal{G}_\beta| > 1$, depending on the model considered. A profound and extensive description of this problem is given in Part IV of Ref. 4. We recommend also Refs. 8 and 62–66 for further information on this subject.

In the case of the Ising model, the best known result, which inspired many of the approaches developed in the sequel, is due to R. Peierls[67] who proposed his famous contour method. One of its offsprings is now known as the Pirogov–Sinai theory, first publications of which are due to S.A. Pirogov and Ya.G. Sinai.[68] Its further development was due to several mathematicians, a complete description of this theory may be found in Ref. 69.

If the model possesses a symmetry, this symmetry should be preserved in the case $|\mathcal{G}_\beta| = 1$, i.e., a phase should possess this symmetry if it is unique. A typical example here is translation invariance, which was discussed in the preceding subsection. If $|\mathcal{G}_\beta| > 1$, the symmetry may be "distributed" among the different phases, whereas each of them lacks this symmetry. Then the phase transition is connected with the loss of symmetry and is often called "spontaneous symmetry breaking". Another example, appropriate for our model (2), is the Z_2-symmetry, i.e., the symmetry with respect to the transformation $\sigma_{\boldsymbol{l}} \to -\sigma_{\boldsymbol{l}}$ for all $\boldsymbol{l} \in \mathbb{Z}^d$. Of course, to have this symmetry one has to take $h_{\boldsymbol{l}} = 0$ for all $\boldsymbol{l} \in \mathbb{Z}^d$. In the following section we show that in the case of the Ising model $|\mathcal{G}_\beta| = 1$ for all temperatures for a nonzero external field. Therefore, the only possibility to get a phase transition in this model is connected with the Z_2-symmetry breaking.

Here one has to point out that phase transitions may occur without symmetry breaking (see Chapter 19 in Ref. 4 and references therein). An example here is model (2) with $d \geq 3$, a nearest neighbor interaction, zero external field and with the polynomial single-spin measure (7) for which the polynomial P has two asymmetric wells. If one well is deep and steep and the other one is wide and shallow, and if the barrier which separates the wells is high enough, there exist phases in which the particles are located mostly near the deep wells (one phase) and near the shallow wells (the other phase). This result was proven by R.L. Dobrushin and S.B. Shlosman.[70]

Now let us discuss how to demonstrate that $|\mathcal{G}_\beta| > 1$, i.e., how to prove a phase transition. One way may be described as follows. For model (2) with a homogeneous external field which takes two values $h_{\boldsymbol{l}} = \pm h$ and with a symmetric single-spin measure ϱ, one calculates the mean magnetization $M_\Delta^\pm(h)$, corresponding to these values [see (18)]. Then one has to show that there exists β_C such that, for $\beta > \beta_C$

$$\lim_{h\to 0+} \lim_{\Delta\to\mathbb{Z}^d} M_\Delta^+(h) \neq \lim_{h\to 0+} \lim_{\Delta\to\mathbb{Z}^d} M_\Delta^-(h),$$

which obviously contradicts uniqueness of Gibbs states. In fact, if the phase is unique, both limits ought to coincide with the mean magnetization calculated for this phase. This method is very natural from the physical point of view but its mathematical realization may be technically impossible. Of course, instead of calculating $M_\Delta^\pm(h)$ and then the above limits, it may suffice to just show that the difference $M_\Delta^+(h) - M_\Delta^-(h)$ is separated from zero for all $h > 0$ and Δ, but this task may be very difficult as well.

Another way to show that $|\mathcal{G}_\beta| > 1$ is based on the following important notion. For a probability measure μ on the set Ω, defined by (52), and a subset $A \subset \Omega$, we write

$$\mu(A) = \int_A d\mu, \tag{67}$$

if the above integral exists.[e] Given such a subset A and $\boldsymbol{l}_0 \in \mathbb{Z}^d$, we set $\vartheta_{\boldsymbol{l}_0} A = \{\vartheta_{\boldsymbol{l}_0}\sigma \mid \sigma \in A\}$, i.e., this set is obtained by translating on $\boldsymbol{l}_0$ every configuration which belongs to A. For $A, B \subset \Omega$, we denote by $A \triangle B = (A \cup B) \setminus (A \cap B)$ their symmetric difference, i.e., the new set consists of those configurations which belong to exactly one of these sets.

Definition 30: A translation invariant probability measure μ on the set of all configurations Ω is said to be ergodic, if it has the following property. For every subset A such that, for all $\boldsymbol{l}_0 \in \mathbb{Z}^d$

$$\mu((\vartheta_{\boldsymbol{l}_0} A) \triangle A) = 0, \tag{68}$$

one has $\mu(A) = 0$ or $\mu(A) = 1$.

Below we present a number of statements, proven in Ref. 13, which describe the properties of such ergodic measures.

[e]Such integrals exist for *measurable* subsets, which form a σ-algebra – a family of subsets of Ω, which contains Ω and is closed with respect to taking complements and countable unions. In our case this is the Borel σ-algebra – the smallest σ-algebra which contains all open subsets of Ω. To define which subsets are open one uses the metric (53).

Proposition 31: *A translation invariant Gibbs state $\mu \in \mathcal{G}_\beta$ is ergodic if and only if it is a pure state. If $|\mathcal{G}_\beta| = 1$, then its unique element is ergodic.*

Thus, in order to prove that $|\mathcal{G}_\beta| > 1$ it is enough to show that there exists a nonergodic Gibbs state. This may be done on the base of the following von Neumann ergodic theorem (see Theorem III.1.8 in Ref. 13).

Proposition 32: *A translation invariant state $\mu \in \mathcal{G}_\beta$ is ergodic if and only if, for every $f, g \in \mathcal{F}$,*

$$\lim_{\Lambda \to \mathbb{Z}^d} \frac{1}{|\Lambda|} \left(\sum_{\boldsymbol{l}_0 \in \Lambda} [\langle (t_{\boldsymbol{l}_0} f) g \rangle_\mu - \langle f \rangle_\mu \langle g \rangle_\mu] \right) = 0, \tag{69}$$

where Λ is defined by (1) and the above limit is taken in the sense $L \to +\infty$.

Now let $\mu \in \mathcal{G}_\beta$ be the periodic Gibbs measure to which a sequence of periodic local Gibbs states converges by Proposition 29. Let us take in (69) $f(\sigma) = g(\sigma) = \sigma_{\mathbf{0}}$. Set in (66) $h = 0$, then the state μ is Z_2-invariant, hence $\langle f \rangle_\mu = \langle g \rangle_\mu = 0$. By Proposition 29, one has

$$\langle \sigma_{\boldsymbol{l}_0} \sigma_{\mathbf{0}} \rangle_\mu = \lim_{n \to +\infty} \langle \sigma_{\boldsymbol{l}_0} \sigma_{\mathbf{0}} \rangle_{\nu^{(p)}_{\beta, \Lambda_n}}. \tag{70}$$

In view of the von Neumann ergodic theorem this immediately yields that the state μ is nonergodic if

$$\lim_{n \to +\infty} \frac{1}{|\Lambda_n|} \sum_{\boldsymbol{l}_0 \in \Lambda_n} \langle \sigma_{\boldsymbol{l}_0} \sigma_{\mathbf{0}} \rangle_{\nu^{(p)}_{\beta, \Lambda_n}} > 0, \tag{71}$$

for a certain sequence of boxes $\{\Lambda_n\}_{n \in \mathbb{N}}$. Since the local Gibbs state $\nu^{(p)}_{\beta, \Lambda}$ is invariant with respect to the translations on the corresponding torus, the above condition is equivalent to

$$P(\beta) \stackrel{\text{def}}{=} \lim_{n \to +\infty} \frac{1}{|\Lambda_n|^2} \sum_{\boldsymbol{l}, \boldsymbol{l}' \in \Lambda_n} \langle \sigma_{\boldsymbol{l}} \sigma_{\boldsymbol{l}'} \rangle_{\nu^{(p)}_{\beta, \Lambda_n}} > 0. \tag{72}$$

This $P(\beta)$ is called *an order parameter*. By (28), $P(\beta) \geq 0$. If $P(\beta) > 0$, there exists a periodic nonergodic Gibbs state, which contradicts $|\mathcal{G}_\beta| = 1$ since if $\mathcal{G}_\beta$ is a singleton, its unique element has to be ergodic. Therefore, $P(\beta) > 0$ implies nonuniqueness of phases, i.e., a phase transition. On the other hand, by (18),

$$\chi = \lim_{\Lambda \to \mathbb{Z}^d} \chi_\Lambda = \lim_{\Lambda \to \mathbb{Z}^d} \frac{1}{|\Lambda|} \sum_{\boldsymbol{l}, \boldsymbol{l}' \in \Lambda} \langle \sigma_{\boldsymbol{l}} \sigma_{\boldsymbol{l}'} \rangle_{\nu^{(p)}_{\beta, \Lambda}}, \tag{73}$$

is the infinite-volume susceptibility if the above order parameter $P(\beta)$ is zero, i.e., above the Curie temperature $T_C = \beta_C^{-1}$. The Curie temperature is defined as the supremum of the values of β^{-1} for which $P(\beta) > 0$. Comparing (72) and (73) one comes to the following conclusion:

- If $\chi < \infty$, then certainly $P(\beta) = 0$ and $T > T_C$.
- If $P(\beta) > 0$, then certainly the right-hand side of (73) is equal to $+\infty$, then there exist many phases, i.e., $T < T_C$ and one has to calculate the susceptibility taking into account this fact.
- If $\chi = \infty$ but $P(\beta) = 0$, then $T = T_C$?

The answer to the above question depends on the model. It may be negative if one has a first order phase transition at $T = T_C$. In this case the third possibility does not occur. If it occurs, one has a second order phase transition at $T = T_C$, or T_C is also called *a critical point*. At this point one may find $\lambda \in (0, 1)$ such that

$$0 < \lim_{\Lambda \to \mathbb{Z}^d} \frac{1}{|\Lambda|^{1+\lambda}} \sum_{\boldsymbol{l}, \boldsymbol{l}' \in \Lambda} \langle \sigma_{\boldsymbol{l}} \sigma_{\boldsymbol{l}'} \rangle_{\nu_{\beta,\Lambda}^{(p)}} < \infty. \tag{74}$$

Such a λ is known as *a critical exponent*. The calculation of such exponents for a given model is the main goal of many works in this field. Finally, let us remark that for the model described by (2) with $h_{\boldsymbol{l}} = h \neq 0$ and with the single-spin measure possessing the Lee–Yang property, $\chi < \infty$ for all temperatures. This fact was proven in Ref. 71.

2.6. *Uniqueness of Gibbs States for the Ising Model*

In this subsection we prove that the set of Gibbs states $\mathcal{G}_\beta$ of the ferromagnetic Ising model with a homogeneous external field h is unique at all temperatures and all dimensions of the lattice if $h \neq 0$. Our proof will be an extended version of the proof given by J.L. Lebowitz and A. Martin-Löf.[72] On the other hand, it is a simplified version of the proof given for quantum Gibbs states in Refs. 73 and 74.

We consider a ferromagnetic Ising model with the homogeneous external field, i.e., $h_{\boldsymbol{l}} = h$ for all $\boldsymbol{l} \in \mathbb{Z}^d$, with the interaction $J_{\boldsymbol{l}\boldsymbol{l}'} \geq 0$, which satisfies condition (15).

Theorem 33: For every $\beta > 0$ and $d \in \mathbb{N}$, the set of Gibbs measures $\mathcal{G}_\beta$ of the Ising model with a homogeneous external field h consists of exactly one element if $h \neq 0$.

To prove this statement we will need a number of new notions and auxiliary facts. For the Ising model, the set of local continuous functions $\mathcal{F}$ defined on the space of all configurations Ω is measure defining, i.e., it has the following property. If for given measures $\mu_1, \mu_2 \in \mathcal{G}_\beta$, the expectations $\langle f \rangle_{\mu_1}$, $\langle f \rangle_{\mu_2}$ coincide for all $f \in \mathcal{F}$, then $\mu_1 = \mu_2$. One could use this property in proving our theorem but the set $\mathcal{F}$ is too big and it would be natural to look for a smaller set possessing the same property. Before formulating a statement, which describes the properties of such sets, we remark that $\mathcal{F}$ is closed under pointwise multiplication, i.e., if one defines that for $f, g \in \mathcal{F}$, their product fg has the value $(fg)(\sigma) = f(\sigma)g(\sigma)$ at every $\sigma \in \Omega$, then $fg \in \mathcal{F}$. The following statement is a corollary of the monotone class theorems (see e.g., Ref. 21, p. 6).

Proposition 34: *A subset $\Phi \subset \mathcal{F}$ is measure defining if it has the following properties: (a) it is countable; (b) it is closed under pointwise multiplication; (c) for any $\sigma \in \Omega, \sigma' \in \Omega$ one finds $f \in \Phi$ such that $f(\sigma) \neq f(\sigma')$ if $\sigma \neq \sigma'$.*

Given $n \in \mathbb{N}$ and $\boldsymbol{l}_1, \ldots, \boldsymbol{l}_n \in \mathbb{Z}^d$, we set

$$f(\sigma) = \sigma_{\boldsymbol{l}_1} \ldots \sigma_{\boldsymbol{l}_n}. \tag{75}$$

Every such function is continuous and local, the set Φ of all such functions (all possible choices of $n \in \mathbb{N}$ and $\boldsymbol{l}_1, \ldots, \boldsymbol{l}_n \in \mathbb{Z}^d$) is a subset of $\mathcal{F}$. This set is countable since the set of all finite subsets of the countable set $\mathbb{Z}^d$ is countable. For every $f, g \in \Phi$, $fg \in \Phi$. Finally, it separates the points of Ω. In fact, if $\sigma \neq \sigma'$, then one finds $\boldsymbol{l} \in \mathbb{Z}^d$ such that $\sigma_{\boldsymbol{l}} \neq \sigma'_{\boldsymbol{l}}$. The function $f(\sigma) = \sigma_{\boldsymbol{l}}$ takes different values on such σ, σ'.

Now we introduce two specific configurations of spins, i.e., two specific elements of Ω. Recall that for the Ising model, all spins take values ± 1, thus the set Ω consists of vectors $\sigma = (\sigma_{\boldsymbol{l}})_{\boldsymbol{l} \in \mathbb{Z}^d}$, $\sigma_{\boldsymbol{l}} = \pm 1$. We set $\xi_+ = (\sigma_{\boldsymbol{l}})_{\boldsymbol{l} \in \mathbb{Z}^d}$, with all $\sigma_{\boldsymbol{l}} = 1$ and $\xi_- = (\sigma_{\boldsymbol{l}})_{\boldsymbol{l} \in \mathbb{Z}^d}$, with all $\sigma_{\boldsymbol{l}} = -1$.

Let $\mathcal{L}$ be a sequence of boxes Λ defined by (1). The following lemma plays a key role in the proof of our uniqueness theorem.

Lemma 35: *Suppose that for any $\boldsymbol{l} \in \mathbb{Z}^d$ and for a sequence of boxes $\mathcal{L}$, each of which contains this $\boldsymbol{l}$, the convergence*

$$\langle \sigma_{\boldsymbol{l}} \rangle_{\nu_{\beta,\Delta}(\cdot|\xi_+)} - \langle \sigma_{\boldsymbol{l}} \rangle_{\nu_{\beta,\Delta}(\cdot|\xi_-)} \to 0 \quad \textit{as} \quad \Lambda \to \mathbb{Z}^d, \tag{76}$$

holds. Then the set of all Gibbs measures $\mathcal{G}_\beta$ contains exactly one element.

Here the expectations are taken with respect to the conditional Gibbs measures (55) with the corresponding boundary conditions $\xi_\pm$.

Proof: We prove this lemma by showing that for any $f \in \Phi$ and two arbitrarily chosen Gibbs measures μ_1 and μ_2, one has $\langle f \rangle_{\mu_1} = \langle f \rangle_{\mu_2}$ if condition (76) holds. This should yield $\mu_1 = \mu_2$ since Φ is measure defining. Hence all elements of $\mathcal{G}_\beta$ coincide, which means $|\mathcal{G}_\beta| = 1$.

Take an arbitrary $f \in \Phi$ and write it in the form (75) with certain $\boldsymbol{l}_1, \ldots, \boldsymbol{l}_n$. For this f, one may pick up $\lambda > 0$ such that the function

$$\phi(\sigma) = \lambda \sum_{j=1}^{n} \sigma_{\boldsymbol{l}_j} + \theta f(\sigma), \tag{77}$$

will be monotone for both values $\theta = \pm 1$. Indeed, for any $\sigma, \sigma' \in \Omega$, such that $\sigma' \geq \sigma$, one has $\sigma'_{\boldsymbol{l}_j} \geq \sigma_{\boldsymbol{l}_j}$ with $j = 1, 2, \ldots, n$. Then by means of the identity

$$a'_1 a'_2 \cdots a'_n - a_1 a_2 \cdots a_n = \sum_{j=1}^{n} a'_1 a'_2 \cdots a'_{j-1} [a'_j - a_j] a_{j+1} \cdots a_n,$$

which holds for any n and any sets of numbers $a_1, \ldots, a_n$, $a'_1, \ldots, a'_n$, we get

$$\phi(\sigma') - \phi(\sigma) = \sum_{j=1}^{n} (\sigma'_{\boldsymbol{l}_j} - \sigma_{\boldsymbol{l}_j}) [\lambda + \theta \sigma'_{\boldsymbol{l}_1} \cdots \sigma'_{\boldsymbol{l}_{j-1}} \sigma_{\boldsymbol{l}_{j+1}} \cdots \sigma_{\boldsymbol{l}_n}]. \tag{78}$$

Obviously, the latter sum is nonnegative if $\lambda > 1$.

We recall that $\mathcal{G}_\beta^{\rm ex}$ denotes the set of extreme elements of $\mathcal{G}_\beta$, i.e., the elements which cannot be written as nontrivial convex combinations (61) of other elements of $\mathcal{G}_\beta$. By Proposition 25, $|\mathcal{G}_\beta| = 1$ if $|\mathcal{G}_\beta^{\rm ex}| = 1$.[f] Thus, the lemma may be proven by showing that for any $f \in \Phi$ and any two $\mu_1, \mu_2 \in \mathcal{G}_\beta^{\rm ex}$, one has $\langle f \rangle_{\mu_1} = \langle f \rangle_{\mu_2}$ if (76) holds. By (55) and (56),

$$\langle f \rangle_{\nu_\Lambda(\cdot|\xi_\pm)} = \langle f \rangle_{\pi_\Lambda(\cdot|\xi_\pm)}, \tag{79}$$

which holds for any Λ such that $\boldsymbol{l}_1, \boldsymbol{l}_2, \ldots, \boldsymbol{l}_n \in \Lambda$. Then by Proposition 25,

$$\langle f \rangle_{\mu_1} = \langle f \rangle_{\mu_2} \tag{80}$$

provided

$$\langle f \rangle_{\nu_\Delta(\cdot|\xi_+)} - \langle f \rangle_{\nu_\Delta(\cdot|\xi_-)} \to 0 \quad \text{as} \quad \Lambda \to \mathbb{Z}^d, \tag{81}$$

along a sequence $\mathcal{L}$ each element of which contains $\boldsymbol{l}_1, \boldsymbol{l}_2, \ldots, \boldsymbol{l}_n$. Thus, it remains to show that (76) implies (81). To this end we employ Corollary 19. Recall that for the case considered, the Hamiltonian which determines

[f] Like a triangle with just one vertex.

$\nu_\Lambda(\cdot|\xi)$ has the form (57), see also (55), with the external field $h_{\boldsymbol{l}} = h$ for all $\boldsymbol{l} \in \mathbb{Z}^d$. Then for $\xi = \xi_\pm$, it can be rewritten as

$$\begin{aligned} H_\Lambda &= -\frac{1}{2} \sum_{\boldsymbol{l},\boldsymbol{l}' \in \Lambda} J_{\boldsymbol{l}\boldsymbol{l}'} \sigma_{\boldsymbol{l}} \sigma_{\boldsymbol{l}'} - \sum_{\boldsymbol{l} \in \Lambda} \left(h \pm \sum_{\boldsymbol{l}' \in \Lambda^c} J_{\boldsymbol{l}\boldsymbol{l}'} \right) \sigma_{\boldsymbol{l}} \\ &= -\frac{1}{2} \sum_{\boldsymbol{l},\boldsymbol{l}' \in \Lambda} J_{\boldsymbol{l}\boldsymbol{l}'} \sigma_{\boldsymbol{l}} \sigma_{\boldsymbol{l}'} - \sum_{\boldsymbol{l} \in \Lambda} h_{\boldsymbol{l}}^{\pm}(\Lambda) \sigma_{\boldsymbol{l}}, \end{aligned} \tag{82}$$

where $h_{\boldsymbol{l}}^{\pm}(\Lambda) = h \pm \sum_{\boldsymbol{l}' \in \Lambda^c} J_{\boldsymbol{l}\boldsymbol{l}'}$. Our model is ferromagnetic, i.e., all $J_{\boldsymbol{l}\boldsymbol{l}'}$ are nonnegative, which yields $h_{\boldsymbol{l}}^{+}(\Lambda) \geq h_{\boldsymbol{l}}^{-}(\Lambda)$. Then by Corollary 19,

$$\langle \phi \rangle_{\nu_\Lambda(\cdot|\xi_+)} \geq \langle \phi \rangle_{\nu_\Lambda(\cdot|\xi_-)}, \tag{83}$$

since the function ϕ defined by (77) is monotone. Then by (77), one gets

$$\lambda \sum_{j=1}^{n} (\langle \sigma_{\boldsymbol{l}_j} \rangle_{\nu_\Lambda(\cdot|\xi_+)} - \langle \sigma_{\boldsymbol{l}_j} \rangle_{\nu_\Lambda(\cdot|\xi_-)}) \geq \theta (\langle f \rangle_{\nu_\Lambda(\cdot|\xi_+)} - \langle f \rangle_{\nu_\Lambda(\cdot|\xi_-)}).$$

Since the latter estimate holds for both $\theta = \pm 1$, it may be rewritten as

$$\lambda \sum_{j=1}^{n} (\langle \sigma_{\boldsymbol{l}_j} \rangle_{\nu_\Lambda(\cdot|\xi_+)} - \langle \sigma_{\boldsymbol{l}_j} \rangle_{\nu_\Lambda(\cdot|\xi_-)}) \geq |\langle f \rangle_{\nu_\Lambda(\cdot|\xi_+)} - \langle f \rangle_{\nu_\Lambda(\cdot|\xi_-)}|, \tag{84}$$

which yields (81) if (76) holds. □

The next step in proving Theorem 33 is to show that (76) always holds if $h \neq 0$. To this end we employ the infinite-volume free energy density and its properties as a function of the external field h. We recall that a function $f : \mathbb{R} \to \mathbb{R}$ is called *convex* if for every $\theta \in [0, 1]$ and any $s, t \in \mathbb{R}$, one has

$$f(\theta t + (1 - \theta)s) \leq \theta f(t) + (1 - \theta) f(s).$$

A wide variety of the properties of convex functions and their applications in the theory of lattice models may be found in Refs. 5 and 13. In particular, they have the following property (see Ref. 13, pp. 35–39).

Proposition 36: *Let a sequence of convex functions* $\{f_n\}_{n \in \mathbb{N}}$ *converge pointwise on* $\mathbb{R}$ *to a function* f*. Then this function is also convex, it is differentiable for all but countable values of its argument. If all* f_n *and* f *are differentiable at a given* $x_0 \in \mathbb{R}$*, then* $f_n'(x_0) \to f'(x_0)$*.*

For the model considered, the partition function in a box Λ with the external field $h = z$ and with the zero boundary condition is given by (23) with the single-spin measure (5), it also may be written in the form (24). We set

$$p_\Lambda(z) = \frac{1}{|\Lambda|} \ln Z_{\beta,\Lambda}(z). \tag{85}$$

In the lattice gas terminology,[13] such a function is called *pressure*. Its connection with the free energy density $F_{\beta,\Lambda}(0)$, where 0 means the zero boundary conditions, may be established by means of (65). Taking into account Proposition 28, we can state the following.

Proposition 37: *For every $z \in \mathbb{R}$ and $\beta > 0$, the sequence $\{p_\Lambda(z)\}_{\Lambda\in\mathcal{L}}$ converges as $\Lambda \to \mathbb{Z}^d$. Its limit $p(z)$ is a convex function of z. Moreover, for any $\xi \in \Omega$,*

$$p(z) = -\beta \lim_{\Lambda\to\mathbb{Z}^d} F_{\beta,\Lambda}(\xi), \tag{86}$$

where $F_{\beta,\Lambda}(\xi)$ is the free energy density of the model with the homogeneous external field $h_{\boldsymbol{l}} = z$.

Let us prove that the only point at which $p(z)$ may fail to be differentiable is $z = 0$. To this end we employ the Lee–Yang theorem in the form of Proposition 3, which yields (24), as well as the following well-known theorem of complex analysis (Vitali's theorem, see e.g., Theorem VIII.19 in Ref. 11).

Proposition 38: *Given a domain $D \subset \mathbb{C}$, let a sequence of functions $f_n : D \to \mathbb{C}$, $n \in \mathbb{N}$ have the following properties: (a) each f_n is holomorphic on D; (b) for every bounded closed subset $K \subset D$, there exists $C_K > 0$ such that $|f_n(z)| \le C_K$ for all $n \in \mathbb{N}$ and $z \in K$; (c) there exists a subset $F \subset D$, which has an accumulation point, such that, for every $z \in F$, the sequence $\{f_n(z)\}_{n\in\mathbb{N}}$ converges to a function $f : D \to \mathbb{C}$. Then this function is also holomorphic on D.*

This theorem has the following interpretation. Let a sequence of functions that are holomorphic on D have the properties: (a) it is uniformly bounded on compact subsets of D; and (b) it converges pointwise on D to a function, which is just defined on D. Then this sequence converges to the latter function uniformly on compact subsets of D, hence the limiting function is holomorphic on D.

Now we may prove the following result.

Lemma 39: *For every $\beta > 0$, the limit of the sequence $\{p_\Lambda(z)\}_{\Lambda\in\mathcal{L}}$ is an infinitely differentiable function at any $z \in \mathbb{R} \setminus \{0\}$.*

Proof: For the Ising model, one has in (24) $\gamma_0(\beta,\Lambda)=0$ [see the analysis following Eq. (24)], which yields

$$p_\Lambda(z)=\ln Z_{\beta,\Lambda}(0)+\sum_{j=1}^{\infty}\ln\left[1+\gamma_j(\beta,\Lambda)z^2\right],$$

and hence

$$\frac{p'_\Lambda(z)}{z}=\sum_{j=1}^{\infty}\frac{2\gamma_j(\beta,\Lambda)}{1+\gamma_j(\beta,\Lambda)z^2}. \tag{87}$$

This means that all the functions p_Λ are holomorphic in the domain $\mathbb{C}\setminus A$, where $A=A_+\cup A_-$, $A_\pm=\{z=\pm it \mid t\in[(\gamma_1(\beta,\Lambda))^{-1/2},+\infty)\}$, which includes the whole real line $\mathbb{R}$. Then, for $z=x+iy\in\mathbb{C}\setminus A$, one has

$$\begin{aligned}\left|\frac{2\gamma_j(\beta,\Lambda)}{1+\gamma_j(\beta,\Lambda)z^2}\right|^2&=\frac{4\gamma_j^2(\beta,\Lambda)}{[1+\gamma_j(\beta,\Lambda)(x^2-y^2)]^2+4\gamma_j^2(\beta,\Lambda)x^2y^2}\\&\le\frac{4\gamma_j^2(\beta,\Lambda)}{[1+\gamma_j(\beta,\Lambda)(x^2-y^2)]^2}.\end{aligned}$$

Given $\theta>0$, we set

$$B_\theta=\{z=x+iy\in\mathbb{C}\mid x\ge 0,\quad x^2-y^2\ge\theta^2\}.$$

Applying the above estimate in (87) we get for $z\in B_\theta$

$$\left|\frac{p'_\Lambda(z)}{z}\right|\le\sum_{j=1}^{\infty}\frac{2\gamma_j(\beta,\Lambda)}{1+\gamma_j(\beta,\Lambda)\theta^2}=\frac{p'_\Lambda(\theta)}{\theta}. \tag{88}$$

By Proposition 37, the limiting function $p(z)$ is convex on $\mathbb{R}$ hence it is not differentiable on a subset $E\subset\mathbb{R}$, which is at most countable. This means that for any $\varepsilon>0$, the interval $(0,\varepsilon)$ contains points at which $p'(z)$ exists. Moreover, by the same statement, $p'_\Lambda(z)\to p'(z)$, as $\Lambda\to\mathbb{Z}^d$, at each such point. Thus, we take an arbitrary ε and select $\theta\in(0,\varepsilon)$ such that $p'(\theta)$ exists. Then the sequence $\{p'_\Lambda(\theta)\}$ converges to $p'(\theta)$, hence this sequence is bounded. Now we take $t>\theta$ and set

$$B_{\theta,t}=\{z=x+iy\in\mathbb{C}\mid x^2-y^2\ge\theta^2,\quad x\in[0,t]\}. \tag{89}$$

This set contains $[\theta,t]\subset\mathbb{R}$. Then, for $z\in B_{\theta,t}$, one has

$$|z|=\sqrt{x^2+y^2}\le\sqrt{2x^2-\theta^2}\le\sqrt{2t^2-\theta^2},$$

and, by the estimate (88),

$$|p'_\Lambda(z)|\le(\sqrt{2(t/\theta)^2-1})p'_\Lambda(\theta).$$

Since the sequence $\{p'_\Lambda(\theta)\}_{\Lambda\in\mathcal{L}}$ is bounded, the sequence of functions $\{p'_\Lambda\}_{\Lambda\in\mathcal{L}}$ holomorphic in $B_{\theta,t}$ is uniformly bounded on $B_{\theta,t}$. Moreover, one

has $p'_\Lambda(z) \to p'(z)$ for all $z \in [\theta, t]$ except possibly for a countable subset of this interval. Thus, the subset of $[\theta, t]$ on which $p'_\Lambda(z) \to p'(z)$ has an accumulation point, which yields by Proposition 38 that p' is holomorphic on $B_{\theta,t}$; hence p is infinitely differentiable on (θ, t). Since this is true for any $t > \theta$ and θ may be chosen arbitrarily close to zero [recall that $\theta \in (0, \varepsilon)$ with any $\varepsilon > 0$], this is true for all $z \in (0, +\infty)$. Since all the functions p_Λ and p are even, the same is also true for $z \in (-\infty, 0)$. Thus, the only point where this may fail to hold is $z = 0$. □

The next step is based on the following simple result.

Lemma 40: *The Ising model with the homogeneous external field h and the zero boundary condition has the following property. For any Δ and $f \in \mathcal{F}_\Delta$,*

$$\lim_{h \to +\infty} \langle f \rangle_{\nu_\Delta(h)} = f(\sigma^+_\Delta), \tag{90}$$

where σ^+_Δ is the configuration $\sigma_\Delta = (\sigma_{\boldsymbol{l}})_{\boldsymbol{l} \in \Delta}$ for which $\sigma_{\boldsymbol{l}} = 1$ for all $\boldsymbol{l} \in \Delta$.

Proof: Set $S_\Delta = \sum_{\boldsymbol{l} \in \Delta} \sigma_{\boldsymbol{l}}$. The values of this total spin variable constitute the set $\mathcal{S}_\Delta = \{-|\Delta|, -(|\Delta| - 2), \ldots, |\Delta| - 2, |\Delta|\}$. Furthermore, let $\mathcal{S}'_\Delta = \mathcal{S}_\Delta \setminus \{|\Delta|\}$ (i.e., the latter set coincides with the former one up to the element $|\Delta|$). Then

$$\begin{aligned} \langle f \rangle_{\nu_\Delta(h)} = \frac{1}{Z_{\beta,\Delta}(h)} \sum_{S \in \mathcal{S}_\Delta} \sum_{\sigma_\Delta :\ S_\Delta = S} f(\sigma_\Delta) \\ \times \exp\left(\beta h S_\Delta + \frac{1}{2} \beta \sum_{\boldsymbol{l}, \boldsymbol{l}' \in \Delta} J_{\boldsymbol{l}\boldsymbol{l}'} \sigma_{\boldsymbol{l}} \sigma_{\boldsymbol{l}'} \right). \end{aligned} \tag{91}$$

When dealing with the Ising model, for which spin variables take discrete values, it is more convenient to use a notation in which expectations with respect to the corresponding local Gibbs measures are written as sums over the values of spins instead of integrals. Thus, for a given Δ, the sum $\sum_{\sigma_\Delta}$ is taken over all values of $\sigma_{\boldsymbol{l}}$ with $\boldsymbol{l} \in \Delta$. The second sum in the above expression is taken over all such values but with the restriction $\sum_{\boldsymbol{l} \in \Delta} \sigma_{\boldsymbol{l}} = S_\Delta = S$. Employing such notation the partition function becomes

$$Z_{\beta,\Delta}(h) = \sum_{S \in \mathcal{S}_\Delta} \sum_{\sigma_\Delta :\ S_\Delta = S} \exp\left(\beta h S_\Delta + \frac{1}{2} \beta \sum_{\boldsymbol{l}, \boldsymbol{l}' \in \Delta} J_{\boldsymbol{l}\boldsymbol{l}'} \sigma_{\boldsymbol{l}} \sigma_{\boldsymbol{l}'} \right),$$

which may be written in the form

$$Z_{\beta,\Delta}(h) = \exp\left(\beta h|\Delta| + \frac{1}{2}\beta \sum_{\boldsymbol{\iota},\boldsymbol{\iota}'\in\Delta} J_{\boldsymbol{\iota}\boldsymbol{\iota}'}\right) \times \left[1 + \sum_{S\in\mathcal{S}'_\Delta} \exp\left(\beta h(S-|\Delta|)\right) \times \sum_{\sigma_\Delta:\ S_\Delta=S} \exp\left(\frac{1}{2}\beta \sum_{\boldsymbol{\iota},\boldsymbol{\iota}'\in\Delta} J_{\boldsymbol{\iota}\boldsymbol{\iota}'}[\sigma_{\boldsymbol{\iota}}\sigma_{\boldsymbol{\iota}'}-1]\right)\right]. \quad (92)$$

Similarly (91) may be written as

$$\langle f\rangle_{\nu_\Delta} = f(\sigma^+_\Delta) + \frac{1}{1+A_\Delta(h)} \sum_{S\in\mathcal{S}'_\Delta} \exp\left(\beta h(S-|\Delta|)\right) \times \sum_{\sigma_\Delta:\ S_\Delta=S} f(\sigma_\Delta) \exp\left(\frac{1}{2}\beta \sum_{\boldsymbol{\iota},\boldsymbol{\iota}'\in\Delta} J_{\boldsymbol{\iota}\boldsymbol{\iota}'}[\sigma_{\boldsymbol{\iota}}\sigma_{\boldsymbol{\iota}'}-1]\right), \quad (93)$$

where $A_\Delta(h)$ stands for the second term in the square brackets in (92). For all $S \in \mathcal{S}'_\Delta$, one has $S < |\Delta|$, which yields $\exp\left(\beta h(S-|\Delta|)\right) \to 0$ as $h \to +\infty$. Furthermore, the sums over $\mathcal{S}'_\Delta$ are finite, hence both $A_\Delta(h)$ and the second term in (93) tend to zero as $h \to +\infty$, which completes the proof. □

Another result which we use to prove our theorem describes the expectations $\langle f\rangle_{\nu_\Delta(\cdot|\xi_+)}$.

Lemma 41: *The ferromagnetic Ising model with an arbitrary external field $h_\Delta = (h_{\boldsymbol{\iota}})_{\boldsymbol{\iota}\in\Delta}$ has the following property. For every $\beta > 0$, any finite subsets Δ, Δ', such that $\Delta' \subset \Delta$, and for any monotone function $f \in \mathcal{F}_{\Delta'}$,*

$$\langle f\rangle_{\nu_\Delta(\cdot|\xi_+)} \le \langle f\rangle_{\nu_{\Delta'}(\cdot|\xi_+)}. \quad (94)$$

Proof: For $\Delta' \subset \Delta$, we write $\Delta'' = \Delta \setminus \Delta'$. By $\xi_{\Delta'} \times \eta_{\Delta''}$ we denote the configuration ζ_Δ such that $\zeta_{\boldsymbol{\iota}} = \xi_{\boldsymbol{\iota}}$ for $\boldsymbol{\iota} \in \Delta'$, and $\zeta_{\boldsymbol{\iota}} = \eta_{\boldsymbol{\iota}}$ for $\boldsymbol{\iota} \in \Delta''$. Then for the mentioned Δ, Δ', we may write $\sigma_\Delta = \sigma_{\Delta'} \times \sigma_{\Delta''}$. Obviously, for appropriate functions,

$$\sum_{\sigma_\Delta} f(\sigma_\Delta) = \sum_{\sigma'_\Delta} \sum_{\sigma''_\Delta} f(\sigma_{\Delta'} \times \sigma_{\Delta''}).$$

Then the Hamiltonian H_Δ (2) may be written

$$H_\Delta = H_{\Delta'} + H_{\Delta''} - \sum_{\boldsymbol{l}_1\in\Delta',\boldsymbol{l}_2\in\Delta''} J_{\boldsymbol{l}_1\boldsymbol{l}_2}\sigma_{\boldsymbol{l}_1}\sigma_{\boldsymbol{l}_2}. \tag{95}$$

For $t \in [0, +\infty)$, we set

$$\phi(t) = \frac{1}{Z_{\beta,\Delta}(t)} \sum_{\sigma_\Delta} f(\sigma_\Delta) \times \exp\left(-\beta H_\Delta + \beta \sum_{\boldsymbol{l}\in\Delta} \sigma_{\boldsymbol{l}} \sum_{\boldsymbol{l}'\in\Delta^c} J_{\boldsymbol{l}\boldsymbol{l}'} + t \sum_{\boldsymbol{l}\in\Delta''} \sigma_{\boldsymbol{l}}\right), \tag{96}$$

where

$$Z_{\beta,\Delta}(t) = \sum_{\sigma_\Delta} \exp\left(-\beta H_\Delta + \beta \sum_{\boldsymbol{l}\in\Delta} \sigma_{\boldsymbol{l}} \sum_{\boldsymbol{l}'\in\Delta^c} J_{\boldsymbol{l}\boldsymbol{l}'} + t \sum_{\boldsymbol{l}\in\Delta''} \sigma_{\boldsymbol{l}}\right). \tag{97}$$

Here the terms $\sum_{\boldsymbol{l}\in\Delta} \sigma_{\boldsymbol{l}} \sum_{\boldsymbol{l}'\in\Delta^c} J_{\boldsymbol{l}\boldsymbol{l}'}$ describe interaction with the external spins ξ, fixed at $\xi = \xi_+$ (recall that $\Delta^c = \mathbb{Z}^d \setminus \Delta$). Thus, we have

$$\phi(0) = \langle f \rangle_{\nu_\Delta(\cdot|\xi_+)}. \tag{98}$$

Taking into account (95) and the fact that $f \in \mathcal{F}_{\Delta'}$ [which means f is independent of the components of σ_Δ with $\boldsymbol{l} \in \Delta''$, i.e., $f(\sigma_\Delta) = f(\sigma_{\Delta'})$], one can rewrite the above expressions as follows:

$$\begin{aligned}\phi(t) = \frac{1}{Z_{\beta,\Delta}(t)} \sum_{\sigma_{\Delta'}} f(\sigma_{\Delta'}) \exp\left(-\beta H_{\Delta'} + \beta \sum_{\boldsymbol{l}\in\Delta'} \sigma_{\boldsymbol{l}} \sum_{\boldsymbol{l}'\in\Delta^c} J_{\boldsymbol{l}\boldsymbol{l}'}\right) \\ \times \sum_{\sigma_{\Delta''}} \exp\Bigg(- \beta H_{\Delta''} + \beta \sum_{\boldsymbol{l}\in\Delta''} \sigma_{\boldsymbol{l}} \sum_{\boldsymbol{l}'\in\Delta^c} J_{\boldsymbol{l}\boldsymbol{l}'} \\ + \beta \sum_{\boldsymbol{l}_1\in\Delta',\boldsymbol{l}_2\in\Delta''} J_{\boldsymbol{l}\boldsymbol{l}'}\sigma_{\boldsymbol{l}_1}\sigma_{\boldsymbol{l}_2} + t \sum_{\boldsymbol{l}\in\Delta''} \sigma_{\boldsymbol{l}}\Bigg),\end{aligned} \tag{99}$$

$$\begin{aligned}Z_{\beta,\Delta}(t) = \sum_{\sigma_{\Delta'}} \exp\left(-\beta H_{\Delta'} + \beta \sum_{\boldsymbol{l}\in\Delta'} \sigma_{\boldsymbol{l}} \sum_{\boldsymbol{l}'\in\Delta^c} J_{\boldsymbol{l}\boldsymbol{l}'}\right) \\ \times \sum_{\sigma_{\Delta''}} \exp\Bigg(- \beta H_{\Delta''} + \beta \sum_{\boldsymbol{l}\in\Delta''} \sigma_{\boldsymbol{l}} \sum_{\boldsymbol{l}'\in\Delta^c} J_{\boldsymbol{l}\boldsymbol{l}'} \\ + \beta \sum_{\boldsymbol{l}_1\in\Delta',\boldsymbol{l}_2\in\Delta''} J_{\boldsymbol{l}\boldsymbol{l}'}\sigma_{\boldsymbol{l}_1}\sigma_{\boldsymbol{l}_2} + t \sum_{\boldsymbol{l}\in\Delta''} \sigma_{\boldsymbol{l}}\Bigg).\end{aligned} \tag{100}$$

The external field in $\exp(\cdot)$ in (96) is $h'_\Delta = (h_{\boldsymbol{l}} + t)_{\boldsymbol{l}\in\Delta}$, where $h_{\boldsymbol{l}}$, $\boldsymbol{l} \in \Delta$ is the external field in H_Δ. Since $t \geq 0$, $h'_\Delta \geq h_\Delta$, which by Corollary 19

yields

$$\phi(t) \geq \phi(0) = \langle f \rangle_{\nu_\Delta(\cdot|\xi_+)}. \tag{101}$$

We recall that f is monotone. Set

$$F(\sigma_{\Delta''}) = \frac{1}{Z_{\beta,\Delta'}(\sigma_{\Delta''})} \sum_{\sigma_{\Delta'}} f(\sigma_{\Delta'}) \times \exp\left(\beta \sum_{\boldsymbol{l}_1 \in \Delta', \boldsymbol{l}_2 \in \Delta''} J_{\boldsymbol{l}_1 \boldsymbol{l}_2} \sigma_{\boldsymbol{l}_1} \sigma_{\boldsymbol{l}_2} - \beta H_{\Delta'} + \beta \sum_{\boldsymbol{l} \in \Delta'} \sigma_{\boldsymbol{l}} \sum_{\boldsymbol{l}' \in \Delta^c} J_{\boldsymbol{l}\boldsymbol{l}'}\right), \tag{102}$$

$$Z_{\beta,\Delta'}(\sigma_{\Delta''}) = \sum_{\sigma_{\Delta'}} \exp\left(\beta \sum_{\boldsymbol{l}_1 \in \Delta', \boldsymbol{l}_2 \in \Delta''} J_{\boldsymbol{l}_1 \boldsymbol{l}_2} \sigma_{\boldsymbol{l}_1} \sigma_{\boldsymbol{l}_2} - \beta H_{\Delta'} + \beta \sum_{\boldsymbol{l} \in \Delta'} \sigma_{\boldsymbol{l}} \sum_{\boldsymbol{l}' \in \Delta^c} J_{\boldsymbol{l}\boldsymbol{l}'}\right). \tag{103}$$

Let $\nu_{\Delta''}(t)$ be the local Gibbs measure of the Ising model in the set Δ'' corresponding to the Hamiltonian $H_{\Delta''} - \beta^{-1} t \sum_{\boldsymbol{l} \in \Delta''} \sigma_{\boldsymbol{l}}$ (we have fixed β which, by the end of this proof, is just a parameter) and to the zero boundary condition. Its partition function is

$$Z_{\beta,\Delta''}(t) = \sum_{\sigma_{\Delta''}} \exp\left(-\beta H_{\Delta''} + t \sum_{\boldsymbol{l} \in \Delta''} \sigma_{\boldsymbol{l}}\right).$$

By means of this measure, the above expectations may be rewritten as

$$\begin{aligned} Z_{\beta,\Delta'}(t) &= \sum_{\sigma_{\Delta''}} \left[Z_{\beta,\Delta'}(\sigma_{\Delta''}) \exp\left(\beta \sum_{\boldsymbol{l} \in \Delta''} \sigma_{\boldsymbol{l}} \sum_{\boldsymbol{l}' \in \Delta^c} J_{\boldsymbol{l}\boldsymbol{l}'}\right)\right] \\ &\quad \times \exp\left(-\beta H_{\Delta''} + t \sum_{\boldsymbol{l} \in \Delta''} \sigma_{\boldsymbol{l}}\right) \\ &= Z_{\beta,\Delta''}(t) \left\langle Z_{\beta,\Delta'}(\sigma_{\Delta''}) \exp\left(\beta \sum_{\boldsymbol{l} \in \Delta''} \sigma_{\boldsymbol{l}} \sum_{\boldsymbol{l}' \in \Delta^c} J_{\boldsymbol{l}\boldsymbol{l}'}\right)\right\rangle \nu_{\Delta''}(t). \end{aligned} \tag{104}$$

Similarly

$$\begin{aligned}\phi(t) &= \left[Z_{\beta,\Delta''}(t) \left\langle Z_{\beta,\Delta'}(\sigma_{\Delta''}) \exp\left(\beta \sum_{\boldsymbol{l}\in\Delta''} \sigma_{\boldsymbol{l}} \sum_{\boldsymbol{l}'\in\Delta^c} J_{\boldsymbol{l}\boldsymbol{l}'} \right) \right\rangle \nu_{\Delta''}(t) \right]^{-1} \\ &\quad \times \sum_{\sigma_{\Delta''}} \left[\sum_{\sigma_{\Delta'}} f(\sigma_{\Delta'}) \exp\left(-\beta H_{\Delta'} + \beta \sum_{\boldsymbol{l}_1\in\Delta', \boldsymbol{l}_2\in\Delta''} J_{\boldsymbol{l}_1\boldsymbol{l}_2}\sigma_{\boldsymbol{l}_1}\sigma_{\boldsymbol{l}_2} \right.\right. \\ &\qquad \left.\left. +\beta \sum_{\boldsymbol{l}\in\Delta'} \sigma_{\boldsymbol{l}} \sum_{\boldsymbol{l}'\in\Delta^c} J_{\boldsymbol{l}\boldsymbol{l}'} \right) \right] \exp\left(-\beta H_{\Delta''} + t \sum_{\boldsymbol{l}\in\Delta''} \sigma_{\boldsymbol{l}} \right) \\ &= \left[\left\langle Z_{\beta,\Delta'}(\sigma_{\Delta''}) \exp\left(\beta \sum_{\boldsymbol{l}\in\Delta''} \sigma_{\boldsymbol{l}} \sum_{\boldsymbol{l}'\in\Delta^c} J_{\boldsymbol{l}\boldsymbol{l}'} \right) \right\rangle \nu_{\Delta''}(t) \right]^{-1} \\ &\quad \times \left\langle Z_{\beta,\Delta'}(\sigma_{\Delta''}) F(\sigma_{\Delta''}) \exp\left(\beta \sum_{\boldsymbol{l}\in\Delta''} \sigma_{\boldsymbol{l}} \sum_{\boldsymbol{l}'\in\Delta^c} J_{\boldsymbol{l}\boldsymbol{l}'} \right) \right\rangle \nu_{\Delta''}(t). \quad (105)\end{aligned}$$

Passing here to the limit $t \to +\infty$ and employing Lemma 40 we arrive at

$$\lim_{t\to+\infty} \phi(t) = \frac{Z_{\beta,\Delta'}(\sigma^+_{\Delta''}) F(\sigma^+_{\Delta''}) \exp(\beta \sum_{\boldsymbol{l}\in\Delta''} \sum_{\boldsymbol{l}'\in\Delta^c} J_{\boldsymbol{l}\boldsymbol{l}'})}{Z_{\beta,\Delta'}(\sigma^+_{\Delta''}) \exp(\beta \sum_{\boldsymbol{l}\in\Delta''} \sum_{\boldsymbol{l}'\in\Delta^c} J_{\boldsymbol{l}\boldsymbol{l}'})} = F(\sigma^+_{\Delta''}).$$

By (102), this yields

$$\begin{aligned}&\lim_{t\to+\infty} \phi(t) \\ &= \sum_{\sigma_{\Delta'}} f(\sigma_{\Delta'}) \exp\left(-\beta H_{\Delta'} + \beta \sum_{\boldsymbol{l}_1\in\Delta'} \sigma_{\boldsymbol{l}_1} \sum_{\boldsymbol{l}_2\in\Delta''} J_{\boldsymbol{l}_1\boldsymbol{l}_2} + \beta \sum_{\boldsymbol{l}_1\in\Delta'} \sigma_{\boldsymbol{l}_1} \sum_{\boldsymbol{l}_2\in\Delta^c} J_{\boldsymbol{l}_1\boldsymbol{l}_2} \right) \\ &\quad \times \left[\sum_{\sigma_{\Delta'}} \exp\left(-\beta H_{\Delta'} + \beta \sum_{\boldsymbol{l}_1\in\Delta'} \sigma_{\boldsymbol{l}_1} \sum_{\boldsymbol{l}_2\in\Delta''} J_{\boldsymbol{l}_1\boldsymbol{l}_2} + \beta \sum_{\boldsymbol{l}_1\in\Delta'} \sigma_{\boldsymbol{l}_1} \sum_{\boldsymbol{l}_2\in\Delta^c} J_{\boldsymbol{l}_1\boldsymbol{l}_2} \right) \right]^{-1} \\ &= \sum_{\sigma_{\Delta'}} f(\sigma_{\Delta'}) \exp\left(-\beta H_{\Delta'} + \beta \sum_{\boldsymbol{l}_1\in\Delta'} \sigma_{\boldsymbol{l}_1} \sum_{\boldsymbol{l}_2\in(\Delta')^c} J_{\boldsymbol{l}_1\boldsymbol{l}_2} \right) \\ &\quad \times \left[\sum_{\sigma_{\Delta'}} \exp\left(-\beta H_{\Delta'} + \beta \sum_{\boldsymbol{l}_1\in\Delta'} \sigma_{\boldsymbol{l}_1} \sum_{\boldsymbol{l}_2\in(\Delta')^c} J_{\boldsymbol{l}_1\boldsymbol{l}_2} \right) \right]^{-1} \\ &= \langle f \rangle_{\nu_{\Delta'}(\cdot|\xi_+)}.\end{aligned}$$

Taking into account (101) we obtain (94). □

Recall that we are studying the Ising model with a non-zero homogeneous external field h. Since the interaction term in the Hamiltonian (2) and

the single-spin measure ϱ^{I} are symmetric with respect to the replacement $\sigma \to -\sigma$, it is enough to consider the case $h > 0$ only.

A function $f : \mathbb{R} \to \mathbb{R}$ is called *right-continuous* at $x_0 \in \mathbb{R}$ if $\lim_{x \to x_0 + 0} f(x) = f(x_0)$. Such a function is *left-continuous* at x_0 if $g(x) \stackrel{\mathrm{def}}{=} f(-x)$ is right-continuous at $-x_0$. If a sequence of monotone increasing continuous functions $\{f_n\}_{n \in \mathbb{N}}$, $f_n : \mathbb{R} \to \mathbb{R}$ converges pointwise on $\mathbb{R}$ to a function f, then this f is right-continuous.

The next statement follows from the one just proven.

Corollary 42: *For every $\beta > 0$ and $h \in \mathbb{R}$, the infinite-volume limits of the expectations*

$$M_{\pm}(h) = \lim_{\Lambda \to \mathbb{Z}^d} \langle \sigma_{\boldsymbol{l}} \rangle_{\nu_\Lambda(\cdot|\xi_\pm)}, \tag{106}$$

exist. They do not depend on $\boldsymbol{l}$. Moreover, $M_+(h)$ (respectively $M_-(h)$) is right-continuous (respectively left-continuous).

Proof: Let us prove the above statement for $M_+(h)$. Since the function $f(\sigma) = \sigma_{\boldsymbol{l}}$ is monotone, the above lemma yields

$$\langle \sigma_{\boldsymbol{l}} \rangle_{\nu_\Lambda(\cdot|\xi_+)} \leq \langle \sigma_{\boldsymbol{l}} \rangle_{\nu_{\Lambda'}(\cdot|\xi_+)}, \tag{107}$$

for any two boxes $\Lambda' \subset \Lambda$. On the other hand, since $\sigma_{\boldsymbol{l}} = \pm 1$,

$$-1 \leq \langle \sigma_{\boldsymbol{l}} \rangle_{\nu_\Lambda(\cdot|\xi_\pm)} \leq 1,$$

hence $\{\langle \sigma_{\boldsymbol{l}} \rangle_{\nu_\Lambda(\cdot|\xi_+)}\}_\Lambda$ converges as a bounded monotone decreasing sequence. By the FKG inequality,

$$\frac{\partial}{\partial h} \langle \sigma_{\boldsymbol{l}} \rangle_{\nu_\Lambda(\cdot|\xi_+)} = \beta \sum_{\boldsymbol{l}' \in \Lambda} K^\Lambda_{\boldsymbol{l}\boldsymbol{l}'}(h) \geq 0,$$

hence $\langle \sigma_{\boldsymbol{l}} \rangle_{\nu_\Lambda(\cdot|\xi_+)} \geq 0$ for $h \geq 0$. Since for every Λ, $\langle \sigma_{\boldsymbol{l}} \rangle_{\nu_\Lambda(\cdot|\xi_+)}$ is a continuous and monotone function of h, the limit of the above sequence is right-continuous. Finally, since the locally weak limits of $\pi_\Lambda(\cdot|\xi_\pm)$ are the extreme translation invariant states $\mu_\pm$, the above $M_+(h)$ is independent of $\boldsymbol{l}$. We remark here, that all our conclusions regarding $M_+(h)$ are valid for all $h \in \mathbb{R}$ since no assumptions restricting h were made in the above lemma. Now let us prove the statement for $M_-(h)$. By symmetry, $\langle \sigma_{\boldsymbol{l}} \rangle_{\nu_\Lambda(\cdot|\xi_-)} = -\langle \sigma_{\boldsymbol{l}} \rangle_{\tilde{\nu}_\Lambda(\cdot|\xi_+)}$, where $\tilde{\nu}_\Lambda(\cdot|\xi_+)$ is the local Gibbs measure with the external field equal to $-h$. Then the convergence of the sequence of $\langle \sigma_{\boldsymbol{l}} \rangle_{\nu_\Lambda(\cdot|\xi_-)}$ and the translation invariance of its limit follow from the above

consideration. Moreover, for these limits one has $M_-(h) = -M_+(-h)$. Finally

$$\lim_{h'\to h-0} M_-(h') = -\lim_{-h'\to -h+0} M_+(-h') = -M_+(-h) = M_-(h). \qquad \square$$

Proof of Theorem 33: By (65)

$$-\frac{\partial}{\partial h} F_{\beta,\Lambda}(\xi_\pm) = \frac{1}{|\Lambda|}\sum_{\boldsymbol{l}\in\Lambda} \langle \sigma_{\boldsymbol{l}}\rangle_{\nu_\Lambda(\cdot|\xi_\pm)}. \tag{108}$$

By Proposition 37, both $-F_{\beta,\Lambda}(\xi_\pm)$ have the same limit, which coincides with the $\beta p(h)$ studied in Lemma 39. This limit, as a convex function of $h \in \mathbb{R}$, has one-sided derivatives at any h, which are the limits of the derivatives (108). This means

$$\begin{aligned}\lim_{h'\to h\pm 0} \frac{\beta(p(h') - p(h))}{h' - h} &= -\lim_{h'\to h\pm 0} \lim_{\Lambda\to\mathbb{Z}^d} \frac{\beta F_{\beta,\Lambda}(\xi_\pm, h') - F_{\beta,\Lambda}(\xi_\pm, h)}{h' - h} \\ &= \lim_{\Lambda\to\mathbb{Z}^d} \frac{1}{|\Lambda|}\sum_{\boldsymbol{l}\in\Lambda} \langle \sigma_{\boldsymbol{l}}\rangle_{\nu_\Lambda(\cdot|\xi_\pm)} = M_\pm(h). \end{aligned} \tag{109}$$

Here we have used the results of Corollary 42. By Lemma 39, $p(h)$ is differentiable for $h \neq 0$, which means that both of its one-sided derivatives coincide at such h. Therefore, $M_+(h) = M_-(h)$ if $h \neq 0$, which implies (76). Then we may apply Lemma 35 which completes the proof. $\square$

2.7. *Self-Similarity, One-Dimensional and Hierarchical Models*

As mentioned in the Introduction, the one-dimensional Ising model with the interaction potential of finite range has no phase transition. Moreover, one may show that the set of its Gibbs states is a singleton for all $\beta > 0$ (see Ref. 4, p. 164). Is this true for the case of long-range interactions? The answer was given by F.J. Dyson in Refs. 75 and 76. Namely, the one-dimensional ferromagnetic Ising model with the zero external field and the translation invariant interaction potential $J_{\boldsymbol{l}\boldsymbol{l}'} = \phi(|\boldsymbol{l}-\boldsymbol{l}'|)$, such that $\phi(x) \sim \phi_0 x^{-1-\lambda}$ as $x \to +\infty$ with $\lambda \in (0,1)$, has a phase transition. The same model with $\lambda > 1$ has no phase transitions. The borderline case $\lambda = 1$ was studied in Ref. 77, where it was shown that the model has a phase transition, but in contrast to the case $\lambda < 1$, the order parameter has a jump at $\beta = \beta_c$.

To obtain his results Dyson introduced in Ref. 75 a spin model with a specific hierarchical structure. Later it was understood that this structure

has a very deep connection with a certain property of lattice spin models, which appears at their critical points. This property is called self-similarity. The first publication where it was discussed, though still without this name, is L.P. Kadanoff's paper[78] (see also Refs. 79 and 80, and references therein) in which he presented his known block-spin construction. Similar arguments were developed also by R.B. Griffiths in Ref. 44. Later an explosion of activity came in this direction, a consequence of which was an approach in the theory of critical phenomena known as the renormalization group method. In fact, that is not a single method but a vast variety of methods and tools with different levels of mathematical sophistication. The notion of self-similarity, first mentioned by Ya.G. Sinai in Ref. 81, was formulated as a property of a random field. Later the concept of self-similar random fields became a part of the mathematical theory of critical phenomena in models of statistical physics, lattice spin models in particular. A full and comprehensive description of this concept is given in Refs. 14 and 66. In this connection we mention also papers by K. Gawędzki.[82–84]

Renormalization group methods developed in theoretical physics have produced and still are producing a very strong impact on the theory of critical phenomena. One may say that they have created a new philosophy with its own set of concepts. In this context we mention brilliant works of K.G. Wilson[85] and I.R. Yuknovskii.[86,87]

At the same time, the mathematical tools used in modern renormalization theories, especially those applied to more realistic models, are not sufficiently elaborated. Moreover, quite often ill defined mathematical objects are employed here. As examples, one can mention nonexisting integrals, series expansions with zero convergence radii, etc. An attempt to bridge the gap between the treatments of renormalization in physics and the mathematically rigorous approach was made recently in Ref. 88.

Let us describe, briefly and schematically, the mathematical aspects of the renormalization group approach to the models we consider here. Recall that we study spin models defined on the lattice $\mathbb{Z}^d$ and described by the Hamiltonian (2) and single-spin measures ϱ, which belong to one of the types described in the preceding subsections. Recall also that Ω , $\mathcal{P}(\Omega)$ and $\mathcal{G}_\beta$ stand for the set of all spin configurations, the set of all probability measures on this set and the set of all Gibbs states of our model existing at a given β respectively. Suppose there is defined a surjection $\varkappa : \mathbb{Z}^d \to \mathbb{Z}^d$ [a map such that for every $\boldsymbol{l} \in \mathbb{Z}^d$, there exist $\boldsymbol{l}' \in \mathbb{Z}^d$, for which $\varkappa(\boldsymbol{l}') = \boldsymbol{l}$].

Suppose also that, for every $\boldsymbol{l} \in \mathbb{Z}^d$, the set

$$V_{\boldsymbol{l}} \stackrel{\text{def}}{=} \{\boldsymbol{l}' \in \mathbb{Z}^d \mid \varkappa(\boldsymbol{l}') = \boldsymbol{l}\}, \tag{110}$$

contains a fixed number of elements, the same for all such sets, i.e., $|V_{\boldsymbol{l}}| = v \in \mathbb{N}$. We will call such $V_{\boldsymbol{l}}$ *blocks*. Given a configuration $\sigma \in \Omega$, we set

$$\omega_{\boldsymbol{l}} = v^{-\zeta} \sum_{\boldsymbol{l}' \in V_{\boldsymbol{l}}} \sigma_{\boldsymbol{l}'}, \tag{111}$$

where $\zeta > 0$ is a parameter of our theory. Clearly, the vector $\omega = (\omega_{\boldsymbol{l}})_{\boldsymbol{l} \in \mathbb{Z}^d}$ is again an element of Ω, i.e., it is a configuration. This defines a transformation $O_{\varkappa,\zeta} : \Omega \to \Omega$, which maps configurations into configurations and depends on the initial map $\varkappa$ and on the parameter ζ. As a linear bounded transformation [defined in the metric $\boldsymbol{d}$ by (53)], $O_{\varkappa,\zeta}$ is continuous, hence for every open $A \subset \Omega$, its preimage $O^{-1}_{\varkappa,\zeta}(A) = \{\sigma \in \Omega \mid O_{\varkappa,\zeta}(\sigma) \in A\}$ is also an open subset. This immediately yields that $O_{\varkappa,\zeta}$ is a measurable map, i.e., for every Borel set $A \subset \Omega$, its preimage $O^{-1}_{\varkappa,\zeta}(A)$ is also a Borel set (see Subsection 2.5). For a probability measure $\mu \in \mathcal{P}(\Omega)$, we define a new measure $\tilde{\mu}$ by its values on Borel subsets of Ω as follows:

$$\tilde{\mu}(A) = \mu\left(O^{-1}_{\varkappa,\zeta}(A)\right), \tag{112}$$

which is correct in view of the properties of $O_{\varkappa,\zeta}$ discussed above. This new measure is again an element of $\mathcal{P}(\Omega)$, thus we have defined the map

$$R_{\varkappa,\zeta}(\mu) = \tilde{\mu}. \tag{113}$$

This map is called *the renormalization transformation*. The above definition of this transformation, although correct mathematically, may seem to be too formal from the "physical point of view". Let us try to explain it. First one takes an "initial" spin configuration σ and transforms it into the configuration of renormalized block-spins, i.e., into ω given by (111). Then one fixes ω and "integrates out" the measure μ under the condition that the sums (111) be fixed. The new measure $\tilde{\mu}$ obtained in such a way is called *a renormalized measure* $R_{\varkappa,\zeta}(\mu)$. This program of passing from the distribution of spins to the distribution of renormalized block-spins was a key element of all constructions mentioned above, starting from the pioneering paper of L.P. Kadanoff. A measure $\mu \in \mathcal{P}(\Omega)$ is called *self-similar* if it is a fixed point of $R_{\varkappa,\zeta}$, that is, it is a solution of

$$R_{\varkappa,\zeta}(\mu) = \mu. \tag{114}$$

The basic idea of the renormalization group theory of critical phenomena is the so-called *universality hypothesis*, which states that at the critical point

$\beta = \beta_c$, the set of all Gibbs states of the model $\mathcal{G}_\beta$ consists of one element and this element is self-similar. In other words, at the critical point the individual spins have the same probability distribution as the renormalized sums of such spins, as well as the renormalized sums of these sums, and so on. If this is the case, the critical point properties of the model may be obtained by studying $R_{\varkappa,\zeta}$. Here we are at the point of this theory where it is natural to show why it may fail to give the description of the mentioned properties. Since $R_{\varkappa,\zeta}$ is defined on the whole set $\mathcal{P}(\Omega)$, it is also defined on its subset $\mathcal{G}_\beta$, but it may not be a self-map of the latter set. This means that for a given Gibbs measure $\mu \in \mathcal{G}_\beta$, the renormalized measure $R_{\varkappa,\zeta}(\mu)$ may not be Gibbsian, i.e., it may be out of $\mathcal{G}_\beta$. Since, except for simple situations, one renormalizes local Gibbs measures, but not the elements of $\mathcal{G}_\beta$ directly, it is not clear whether or not the renormalized local Gibbs measures may give the elements of $\mathcal{G}_\beta$. A problem of this kind has appeared in practice, for example it appears in the case of the Ising model with the interaction potential of finite range. In order to be able to proceed with the renormalization, physicists apply certain approximate "decouplings" that effectively imply considering not the model itself but its caricature, for which such decouplings may be justified. This gives a hint that there might exist models for which the mentioned problems do not appear and the renormalization scheme may be realized rigorously. Proceeding along this line of arguments, the authors of Ref. 89 discovered that the approximate scheme developed in Refs. 86 and 87 for the three-dimensional Ising model becomes rigorous when applied to Dyson's hierarchical model, which was invented and used by F.J. Dyson as a tool in the study of the one-dimensional translation invariant spin model. The critical point properties of Dyson's hierarchical model were first studied by P.M. Bleher and Ya.G. Sinai in Refs. 90 and 91 (a complete description of these results is presented in Ref. 64). Among other papers on this subject we mention here Refs. 82–84 and 92.

It is not surprising that the hierarchical model (described below) has that nice property. Instead of translation invariance possessed by the models we have considered so far, this model has a symmetry which ideally fits the renormalization scheme – it is self-similar in some sense. The idea to substitute translation invariance by such a symmetry was (more or less consciously) used in the method developed by I.R. Yukhnovskii. In Ref. 89 (a slightly different version of the construction described in that paper was used in Ref. 42), it was explicitly shown how it leads from translation invariance to self-similarity possessed by hierarchical models. In this subsection we show that the translation invariant one-dimensional spin model with

the power-like decaying interaction potential also fits the renormalization scheme. A preliminary version of the theory given below has appeared in Ref. 93.

We consider the model defined on the lattice $\mathbb{Z}$ and described by the Hamiltonian (2) with the interaction potential

$$J_{\boldsymbol{l}\boldsymbol{l}'} = [|\boldsymbol{l} - \boldsymbol{l}'| + 1]^{-1-\lambda}. \tag{115}$$

Set

$$V_{\boldsymbol{l}}^{(n)} = \{\boldsymbol{l}' \in \mathbb{Z} \mid 2^n \boldsymbol{l} \leq \boldsymbol{l}' \leq 2^n \boldsymbol{l} + 2^n - 1\}, \quad n \in \mathbb{N}_0, \quad \boldsymbol{l} \in \mathbb{Z}. \tag{116}$$

The subsets $V_{\boldsymbol{l}}^{(1)}$ are the blocks mentioned above, for which $v = 2$. Then $\varkappa$ maps the two elements of such a block $V_{\boldsymbol{l}}^{(1)}$ into $\boldsymbol{l}$. Considering the blocks $V_{\boldsymbol{l}}^{(1)}$, $\boldsymbol{l} \in \mathbb{Z}$ as elements of a new lattice, which however is the same as $\mathbb{Z}$, we may apply the map $\varkappa$ to these elements, which will map $V_{\boldsymbol{l}'}^{(1)}$ into $\mathbb{Z}$ exactly as was done above. This produces a hierarchy of subsets $V_{\boldsymbol{l}}^{(n)}$ of the lattice $\mathbb{Z}$, defined by (116), organized according to the rule

$$V_{\boldsymbol{l}}^{(n)} = \bigcup_{\boldsymbol{l}' \in V_{\boldsymbol{l}}^{(n-k)}} V_{\boldsymbol{l}'}^{(k)}; \quad n \in \mathbb{N}, \quad k = 0, 1, \ldots, n-1. \tag{117}$$

Given $n \in \mathbb{N}_0$, we set $\mathcal{V}^{(n)} = \{V_{\boldsymbol{l}}^{(n)}\}_{\boldsymbol{l} \in \mathbb{Z}}$.

Definition 43: The family $\{\mathcal{V}^{(n)}\}_{n \in \mathbb{N}_0}$ is called a hierarchical structure on the lattice $\mathbb{Z}$.

For $\alpha, \alpha' = 0, 1$ and $\boldsymbol{l}, \boldsymbol{l}' \in \mathbb{Z}$, we set

$$I(2\boldsymbol{l} + \alpha, 2\boldsymbol{l}' + \alpha') = \frac{1}{[|(2\boldsymbol{l} + \alpha) - (2\boldsymbol{l}' + \alpha')| + 1]^{1+\lambda}} - \frac{2^{-(1+\lambda)}}{[|\boldsymbol{l} - \boldsymbol{l}'| + 1]^{1+\lambda}}, \tag{118}$$

which defines $I(\boldsymbol{l}, \boldsymbol{l}')$ for all $\boldsymbol{l}, \boldsymbol{l}' \in \mathbb{Z}$. In order to introduce a lattice spin model one often uses its formal Hamiltonian written on the whole lattice, which has no rigorous mathematical meaning but shows how one can define local Hamiltonians (2). Such a formal Hamiltonian in the case of the model we consider now is

$$H = -\frac{1}{2} \sum_{\boldsymbol{l}, \boldsymbol{l}' \in \mathbb{Z}} \frac{1}{(|\boldsymbol{l} - \boldsymbol{l}'| + 1)^{1+\lambda}} \sigma_{\boldsymbol{l}} \sigma_{\boldsymbol{l}'}, \tag{119}$$

which by means of (118) may be rewritten (more details on how to pass to the expression below may be found in Ref. 93)

$$H = -\frac{1}{2}\sum_{n=0}^{\infty}\sum_{\boldsymbol{l},\boldsymbol{l}'\in\mathbb{Z}} 2^{-n(1+\lambda)} I(\boldsymbol{l},\boldsymbol{l}')\sigma(V_{\boldsymbol{l}}^{(n)})\sigma(V_{\boldsymbol{l}'}^{(n)}), \tag{120}$$

where for a set $\Delta \subset \mathbb{Z}$,

$$\sigma(\Delta) = \sum_{\boldsymbol{l}\in\Delta} \sigma_{\boldsymbol{l}}. \tag{121}$$

The essence of the above representation of H is that it has a block-spin structure, which enables us to apply here the renormalization scheme described above. The local Hamiltonians may be defined on the basis of (120) by restricting the sums to finite subsets of the lattice $\mathbb{Z}$, which now are to be taken in a special way if one wants to preserve the block-spin structure of these Hamiltonians. In particular, the local Hamiltonian in

$$\Lambda_m \stackrel{\text{def}}{=} \{\boldsymbol{l} \in \mathbb{Z} \mid -2^m \leq \boldsymbol{l} \leq 2^m - 1\}, \quad m \in \mathbb{N}_0,$$

with the zero boundary conditions is

$$H_{\Lambda_m} = \frac{1}{2}\sum_{n=0}^{m}\sum_{\boldsymbol{l},\boldsymbol{l}'\in\Lambda_{m-n}} 2^{-n(1+\lambda)} I(\boldsymbol{l},\boldsymbol{l}')\sigma(V_{\boldsymbol{l}}^{(n)})\sigma(V_{\boldsymbol{l}'}^{(n)}), \quad m \in \mathbb{N}. \tag{122}$$

It should be stressed here that this Hamiltonian does not coincide with the one which can be obtained from the formal Hamiltonian in the form (119) by restricting the sums to Λ_m. But, in order to construct Gibbs states according to the scheme based on the DLR equation (see Subsection 2.4) we would need such local Hamiltonians defined on different subsets $\Delta \subset \mathbb{Z}$ and with boundary conditions outside such Δ. This means that following this scheme we could not preserve the block-spin structure of local Hamiltonians, which would make the above construction useless. This problem may be overcome as follows. Given $m \in \mathbb{N}$, we set

$$H_m = -\frac{1}{2}\sum_{n=0}^{m}\sum_{\boldsymbol{l},\boldsymbol{l}'\in\mathbb{Z}} 2^{-n(1+\lambda)} I(\boldsymbol{l},\boldsymbol{l}')\sigma(V_{\boldsymbol{l}}^{(n)})\sigma(V_{\boldsymbol{l}'}^{(n)}). \tag{123}$$

In contrast to (122) this is still a formal Hamiltonian since the sums over $\boldsymbol{l},\boldsymbol{l}'$ run through the whole lattice. In view of the way in which it was produced, such an expression can be called *a truncated Hamiltonian*. By means of (121) we may rewrite it in the form (119) but with a certain interaction potential

$J_m(\boldsymbol{l},\boldsymbol{l}')$ instead of $[|\boldsymbol{l}-\boldsymbol{l}'|+1]^{-1-\lambda}$. The effect of the above truncation is that this potential has the following asymptotics

$$J_m(\boldsymbol{l},\boldsymbol{l}') \sim J_m^{(0)}|\boldsymbol{l}-\boldsymbol{l}'|^{-2-\lambda}, \quad |\boldsymbol{l}-\boldsymbol{l}'| \to +\infty. \tag{124}$$

Due to Dyson's results mentioned above the model with such a formal Hamiltonian has no phase transitions. Moreover, for a similar model with the above asymptotics of the interaction potentials, it was proven that their sets $\mathcal{G}_\beta$ are singletons for all β (see Ref. 94 and Subsection 8.3 of Ref. 4). This opens a possibility to construct Gibbs states of the model described by (120) in the following way. First one constructs the states μ_m for (123), which are unique for every $m \in \mathbb{N}$, and then passes to the limit $m \to +\infty$. By construction, these states satisfy the recursion

$$R_{\varkappa,1+\lambda}(\mu_{m+1}) = \mu_m, \tag{125}$$

and the limit of the sequence $\{\mu_m\}$ should be a fixed point of $R_{\varkappa,1+\lambda}$. We are going to realize this program in a separate work.

Now let us turn to hierarchical models. The simplest way to get such a model from the translation invariant model we consider in this subsection, is to put in (120) $I(\boldsymbol{l},\boldsymbol{l}') = 0$ for all $\boldsymbol{l} \neq \boldsymbol{l}'$. As a consequence, the formal Hamiltonian of this new model is

$$H = -\frac{1}{2}\sum_{n=0}^{\infty}\sum_{\boldsymbol{l}\in\mathbb{Z}} 2^{-n(1+\lambda)} I(\boldsymbol{l},\boldsymbol{l})[\sigma(V_{\boldsymbol{l}}^{(n)})]^2. \tag{126}$$

Since $I(\boldsymbol{l},\boldsymbol{l}') \geq 0$, such an action decreases the interaction potential of the model (120). Thus, by Corollary 20, the order parameter of the hierarchical model $P^{\mathrm{h}}(\beta)$ [see (72)] will not exceed the corresponding parameter $P(\beta)$ of the model (120). Hence if the former is positive for big enough β, $P(\beta)$ should be positive as well. This argumentation was used by F.J. Dyson in Ref. 75, although no direct comparison of these models was made in that paper. Comparing the Hamiltonians (120) and (126) one can conclude that in the hierarchical version the interaction between different blocks of the same hierarchy level is neglected. The effect of this is that the Hamiltonian (126) is additive in $\boldsymbol{l}$, which in turn implies that instead of considering measures on infinite dimensional spaces of configurations, such as the measures μ_m, μ_{m+1} in (125), one considers measures just on the space $\mathbb{R}$, which define the probability distributions of block-spins. The corresponding recurrence will have the form of (125) but with the renormalization transformation acting on such one-dimensional measures. For further details the reader is referred to the articles describing hierarchical models mentioned above.

Finally, we remark that the hierarchical models are well studied, one can say that almost all critical point properties of such models are known. In particular, a self-similar Gibbs state of such a model was constructed in Ref. 95.

3. Quantum Models

3.1. *Local Gibbs States*

For quantum lattice systems, Gibbs states are defined by means of their Hamiltonians, which now are operators on certain complex Hilbert spaces. These spaces consist of wave functions. As usual they have countable bases, i.e., complete orthonormal systems of functions, such that every wave function may be written as a countable linear combination of the elements of such a system. For a given finite subset $\Delta \subset \mathbb{Z}^d$, let $\mathcal{H}_\Delta$ be such a Hilbert space and $\{\psi_n\}_{n\in\mathbb{N}}$ be its base. Let also $\boldsymbol{L}(\mathcal{H}_\Delta)$ be the set of all linear operators acting from $\mathcal{H}$ to $\mathcal{H}$.

An example of a quantum lattice system is the spin model described by the Hamiltonian

$$H_\Delta = -\frac{1}{2}\sum_{\boldsymbol{l},\boldsymbol{l}'\in\Delta}\sum_{\alpha=x,y,z} J^\alpha_{\boldsymbol{l}\boldsymbol{l}'}\sigma^\alpha_{\boldsymbol{l}}\sigma^\alpha_{\boldsymbol{l}'} - \sum_{\boldsymbol{l}\in\Delta}\sum_{\alpha=x,y,z} h^\alpha_{\boldsymbol{l}}\sigma^\alpha_{\boldsymbol{l}}, \tag{127}$$

where, as above, $J^\alpha_{\boldsymbol{l}\boldsymbol{l}'}$, $h^\alpha_{\boldsymbol{l}}$ are real parameters of the model, defined for all $\boldsymbol{l},\boldsymbol{l}' \in \mathbb{Z}^d$ and $\alpha = x, y, z$, and $\sigma^x_{\boldsymbol{l}}$, $\sigma^y_{\boldsymbol{l}}$, $\sigma^z_{\boldsymbol{l}}$ are the Pauli matrices. With every $\boldsymbol{l}$ we associate the space $\mathcal{H}_{\boldsymbol{l}}$ of two-dimensional complex vector-columns with the scalar product

$$\phi = \begin{pmatrix}\phi^{(1)}\\ \phi^{(2)}\end{pmatrix}, \quad \psi = \begin{pmatrix}\psi^{(1)}\\ \psi^{(2)}\end{pmatrix}, \qquad \langle\psi,\phi\rangle = \bar{\psi}^{(1)}\phi^{(1)} + \bar{\psi}^{(2)}\phi^{(2)},$$

where $\bar{\psi}^{(j)}$, $j = 1, 2$ stands for the complex conjugate. The action of the Pauli matrices on such vectors is defined by the usual multiplication of matrices. The Hilbert space $\mathcal{H}_\Delta$ is defined as a tensor product

$$\mathcal{H}_\Delta = \bigotimes_{\boldsymbol{l}\in\Delta}\mathcal{H}_{\boldsymbol{l}}. \tag{128}$$

The canonical base of the space consists of the following vectors:

$$\epsilon(s_\Delta) = \bigotimes_{\boldsymbol{l}\in\Delta}\epsilon(s_{\boldsymbol{l}}), \qquad s_{\boldsymbol{l}} = \pm 1, \quad \epsilon(1) = \begin{pmatrix}1\\0\end{pmatrix}, \quad \epsilon(-1) = \begin{pmatrix}0\\1\end{pmatrix}. \tag{129}$$

Here, in a similar fashion as was done above, s_Δ is a vector with the components $s_{\boldsymbol{l}}$, $\boldsymbol{l} \in \Delta$ taking values ± 1. Thus, the space $\mathcal{H}_\Delta$ is finite-dimensional

and $\dim \mathcal{H}_\Delta = 2^{|\Delta|}$. Every $\sigma_{\boldsymbol{l}}^\alpha$ acts on the above vectors as follows

$$\sigma_{\boldsymbol{l}}^\alpha \epsilon(s_\Delta) = \Big(\sigma_{\boldsymbol{l}}^\alpha \epsilon(s_{\boldsymbol{l}}) \bigotimes\Big) \bigotimes_{\boldsymbol{l}' \in \Delta \setminus \{\boldsymbol{l}\}} \epsilon(s_{\boldsymbol{l}'}).$$

In particular,

$$\sigma_{\boldsymbol{l}}^z \epsilon(s_\Delta) = s_{\boldsymbol{l}} \epsilon(s_\Delta).$$

Each element of the space $\mathcal{H}_\Delta$ may be associated with a $2^{|\Delta|}$-dimensional complex vector-column. Then every element of $\boldsymbol{L}(\mathcal{H}_\Delta)$ may be represented by a $2^{|\Delta|} \times 2^{|\Delta|}$-complex matrix with the standard definition of its action on the above vectors.

Various versions of the model (127) are employed as the so called *quasi-spin models*.[96] If in the Hamiltonian (127) all $J_{\boldsymbol{l}\boldsymbol{l}'}^x = J_{\boldsymbol{l}\boldsymbol{l}'}^y = 0$ and $h_{\boldsymbol{l}}^x = h_{\boldsymbol{l}}^y = 0$, it turns into the Ising model in the external field $h_{\boldsymbol{l}}^z$. The Heisenberg model, the Ising model in a transverse field may be obtained from (127) in an evident way.

Another example of quantum lattice models which is widely employed in the theory of structural phase transitions (see e.g., Ref. 32) is the model of interacting quantum anharmonic oscillators, described by the following Hamiltonian [cf. (10)]:

$$H_\Delta = \frac{1}{2m} \sum_{\boldsymbol{l} \in \Delta} p_{\boldsymbol{l}}^2 + \sum_{\boldsymbol{l} \in \Delta} P(q_{\boldsymbol{l}}) - \sum_{\boldsymbol{l} \in \Delta} h_{\boldsymbol{l}} q_{\boldsymbol{l}} - \frac{1}{2} \sum_{\boldsymbol{l}, \boldsymbol{l}' \in \Delta} J_{\boldsymbol{l}\boldsymbol{l}'} q_{\boldsymbol{l}} q_{\boldsymbol{l}'}. \tag{130}$$

Here m is the particle mass, P is the same polynomial as in (7)–(10), the external field $h_{\boldsymbol{l}}$ and the interaction potential $J_{\boldsymbol{l}\boldsymbol{l}'}$ are also the same as in the classical case. But now $p_{\boldsymbol{l}}$ and $q_{\boldsymbol{l}}$ are canonical momentum and position operators, defined in the complex Hilbert space $L^2(\mathbb{R})$ of functions, which are square integrable on $\mathbb{R}$ with respect to Lebesgue's measure. These operators obey the canonical commutation relation

$$p_{\boldsymbol{l}} q_{\boldsymbol{l}} - q_{\boldsymbol{l}} p_{\boldsymbol{l}} = -i\hbar,$$

and are unbounded (see below), which strongly complicates the theory of this model. The Hamiltonian (130) is also unbounded, and all these operators are essentially self-adjoint.

For every $\psi \in \mathcal{H}_\Delta$, we define its norm as usual $\|\psi\| = \sqrt{\langle \psi, \psi \rangle}$. An operator $T \in \boldsymbol{L}(\mathcal{H}_\Delta)$ is said to be bounded if there exists a constant $C > 0$ such that, for every ψ,

$$\|T\psi\| \leq C \|\psi\|.$$

The least such C will be denoted by $\|T\|$. We will also denote by $\boldsymbol{L}_b(\mathcal{H}_\Delta)$ the set of all bounded linear operators acting from $\mathcal{H}_\Delta$ into $\mathcal{H}_\Delta$. As usual,

every such operator is defined on the whole space $\mathcal{H}_\Delta$. For the quantum spin models described above, $\boldsymbol{L}_b(\mathcal{H}_\Delta) = \boldsymbol{L}(\mathcal{H}_\Delta)$ since the corresponding Hilbert space is finite-dimensional. For every $T \in \boldsymbol{L}_b(\mathcal{H}_\Delta)$, we define its Hermitian conjugate T^* as an operator satisfying the following relation $\langle T^*\phi, \psi\rangle = \langle \phi, T\psi\rangle$ for all $\phi, \psi \in \mathcal{H}_\Delta$. An operator $T \in \boldsymbol{L}_b(\mathcal{H}_\Delta)$ is said to be positive if

$$\langle \psi, T\psi\rangle \geq 0,$$

for all $\psi \in \mathcal{H}_\Delta$. For such an operator, one may define $\sqrt{T}$. For every $T \in \boldsymbol{L}_b(\mathcal{H}_\Delta)$, the operator T^*T is positive, hence one may set $|T| = \sqrt{T^*T}$. An operator $T \in \boldsymbol{L}_b(\mathcal{H}_\Delta)$ is said to be trace-class if, for an orthonormal base $\{\psi_n\}_{n\in\mathbb{N}}$,

$$\sum_{n=1}^{\infty} \langle \psi_n, |T|\psi_n\rangle < \infty. \tag{131}$$

Then one may set

$$\operatorname{trace}(T) = \sum_{n=1}^{\infty} \langle \psi_n, T\psi_n\rangle. \tag{132}$$

The latter series converges absolutely, its sum is independent of the particular choice of the base. The set of all trace-class operators will be denoted by $\boldsymbol{L}_t(\mathcal{H}_\Delta)$. For every $T \in \boldsymbol{L}_t(\mathcal{H}_\Delta)$ and $Q \in \boldsymbol{L}_b(\mathcal{H}_\Delta)$, the products TQ and QT are trace-class. Clearly $\boldsymbol{L}_t(\mathcal{H}_\Delta) \subset \boldsymbol{L}_b(\mathcal{H}_\Delta) \subset \boldsymbol{L}_(\mathcal{H}_\Delta)$. In finite-dimensional spaces all these sets coincide, but in the infinite-dimensional case the inclusions are proper.

For $T \in \boldsymbol{L}_b(\mathcal{H}_\Delta)$, the above introduced $\|T\|$ is a norm, and we shall call it *operator norm*. The set $\boldsymbol{L}_b(\mathcal{H}_\Delta)$ equipped with the operator norm turns into a complete normed space – a Banach space. In addition to the linear space structure we have also multiplication on the latter space. By definition, for any $T, Q \in \boldsymbol{L}_b(\mathcal{H}_\Delta)$,

$$\|TQ\| \leq \|T\|\|Q\|, \quad \|T^*\| = \|T\|. \tag{133}$$

Banach spaces with multiplication and an operation $T \mapsto T^*$, which possess the above properties, are called C^*-algebras. A detailed presentation of the theory of these algebras and their application in quantum statistical physics may be found in Ref. 2.

For an entire function $F : \mathbb{C} \to \mathbb{C}$ and $T \in \boldsymbol{L}_b(\mathcal{H}_\Delta)$, we set

$$F(T) = \sum_{n=0}^{\infty} \frac{1}{n!} F^{(n)} T^n, \quad F^{(n)} = \frac{d^n F}{dz^n}(0).$$

If this series converges in the operator norm, it defines a bounded operator $F(T)$. In both examples above the Hamiltonians [not necessarily belonging to $\boldsymbol{L}_b(\mathcal{H}_\Delta)$] are such that $\exp(-\beta H_\Delta) \in \boldsymbol{L}_t(\mathcal{H}_\Delta)$ for any finite subset Δ and every $\beta > 0$. For such models, one may set

$$Z_{\beta,\Delta} = \operatorname{trace}[\exp(-\beta H_\Delta)], \quad \rho_{\beta,\Delta} = Z_{\beta,\Delta}^{-1} \exp(-\beta H_\Delta). \tag{134}$$

The latter trace-class operator is called a density matrix. Then, for every $T \in \boldsymbol{L}_b(\mathcal{H}_\Delta)$, one may define

$$T \mapsto \langle T \rangle_{\beta,\Delta} = \operatorname{trace}\left(T \rho_{\beta,\Delta}\right), \tag{135}$$

which is a normalized positive linear functional on the C^*-algebra $\boldsymbol{L}_b(\mathcal{H}_\Delta)$. It is called a local Gibbs state of the model, and the elements of $\boldsymbol{L}_b(\mathcal{H}_\Delta)$ are called observables. Comparing with the case of classical models one can conclude that here taking trace corresponds to integration, the density matrix corresponds to the local Gibbs measure (3), and the algebra of observables $\boldsymbol{L}_b(\mathcal{H}_\Delta)$ corresponds to the set of functions $\mathcal{F}_\Delta$.

To simplify the notation we set

$$\mathfrak{A}_\Delta = \boldsymbol{L}_b(\mathcal{H}_\Delta).$$

As above, for $\Delta \subset \Delta'$, we may include $\mathfrak{A}_\Delta$ into $\mathfrak{A}_{\Delta'}$ and define

$$\mathfrak{A} = \bigcup_{\Delta \in \mathcal{D}} \mathfrak{A}_\Delta, \tag{136}$$

where $\mathcal{D}$ is an increasing sequence of subsets, which exhausts the lattice $\mathbb{Z}^d$.

3.2. *Green and Matsubara Functions*

The time evolution of a quantum system is described by the corresponding Schrödinger equation, the solutions of which define the evolution of the states (135). In the Heisenberg approach wave functions, and hence the states, do not evolve. Instead the evolution of the system is described by the evolution of the observables, which constitute the algebras $\mathfrak{A}_\Delta$. This is described by the following map. Given $t \in \mathbb{R}$, considered as time, we set

$$\mathfrak{a}_\Delta^t(T) = \exp(i(t/\hbar) H_\Delta) T \exp(-i(t/\hbar) H_\Delta), \quad T \in \mathfrak{A}_\Delta. \tag{137}$$

In what follows, an observable T at time $t = 0$ evolves into the observables $\mathfrak{a}_\Delta^t(T)$. The evolution maps $\mathfrak{a}_\Delta^t$ have the following properties.

Since $U_t = \exp(i(t/\hbar)H_\Delta)$ and $t \in \mathbb{R}$ is a unitary operator, one has

$$\|\mathfrak{a}_\Delta^t(T)\| = \|T\|, \tag{138}$$

i.e., $\mathfrak{a}_\Delta^t$ are norm-preserving hence continuous as maps acting between normed spaces. Furthermore, they are linear, that is

$$\mathfrak{a}_\Delta^t(\kappa T + \lambda Q) = \kappa \mathfrak{a}_\Delta^t(T) + \lambda \mathfrak{a}_\Delta^t(Q),$$

for all $\kappa, \lambda \in \mathbb{C}$ and $T, Q \in \mathfrak{A}_\Delta$. For any $t, s \in \mathbb{R}$ and $T \in \mathfrak{A}_\Delta$, one has

$$\mathfrak{a}_\Delta^s\left(\mathfrak{a}_\Delta^t(T)\right) = \mathfrak{a}_\Delta^{t+s}(T), \tag{139}$$

which means that they constitute a group of algebraic isomorphisms. Finally, they are called time automorphisms since they map the algebra of observables $\mathfrak{A}_\Delta$ into itself. For $T_1, \ldots, T_n \in \mathfrak{A}_\Delta$ and $t_1, \ldots, t_n \in \mathbb{R}$, we set

$$G^{\beta,\Delta}_{T_1,\ldots,T_n}(t_1, \ldots, t_n) = \operatorname{trace}\left(\mathfrak{a}_\Delta^{t_1}(T_1) \cdots \mathfrak{a}_\Delta^{t_n}(T_n)\rho_{\beta,\Delta}\right), \tag{140}$$

where the density matrix $\rho_{\beta,\Delta}$ was defined in (134). For fixed $T_1, \ldots, T_n \in \mathfrak{A}_\Delta$, this is a function of $t_1, \ldots, t_n$ defined on the whole $\mathbb{R}^n$. It is called a Green function for those observables. Clearly, the whole information about the evolution is contained in these functions defined for all observables $T \in \mathfrak{A}_\Delta$. Here it would be quite natural to try to find a smaller set of observables such that the Green functions defined for the elements of this set completely describe the evolution of the whole algebra. For the models considered in this section, such a smaller set was found by R. Høegh-Krohn in Ref. 97.

In order to formulate these results we have to introduce new notions. A subset $\mathfrak{M} \subset \mathfrak{A}_\Delta$ is called subalgebra if it is an algebra with respect to the linear operations and multiplication, which means that it is closed with respect to these operations. A subalgebra is called abelian if all its elements commute with each other. For the model of interacting quantum anharmonic oscillators described by the Hamiltonian (130), such a subalgebra consists of multiplication operators on bounded continuous functions. An operator $T : L^2(\mathbb{R}^{|\Delta|}) \to L^2(\mathbb{R}^{|\Delta|})$ is called a multiplication operator on the bounded continuous function $F : \mathbb{R}^{|\Delta|} \to \mathbb{C}$ if for every $\psi \in L^2(\mathbb{R}^{|\Delta|})$,

$$(T\psi)(x_\Delta) = F(x_\Delta)\psi(x_\Delta). \tag{141}$$

In the sequel, we will denote such operators also by F. Of course, linear combinations and products of multiplication operators are again multiplication operators, they commute with each other. The algebra of such operators will be denoted by $\mathfrak{F}_\Delta$. Now we are in a position to present the result of R. Høegh-Krohn.

Proposition 44: *Let $\mathfrak{A}_\Delta^{(0)} \subset \mathfrak{A}_\Delta$ be the set of all observables which are linear combinations of the operators*

$$\mathfrak{a}_\Delta^{t_1}(F_1) \cdots \mathfrak{a}_\Delta^{t_1}(F_n)$$

for all possible choices $n \in \mathbb{N}$, $t_1, \ldots, t_n \in \mathbb{R}$ and $F_1, \ldots, F_n \in \mathfrak{F}_\Delta$. Then the σ-weak closure of this set coincides with the whole algebra $\mathfrak{A}_\Delta$.

The meaning of this statement is that the Green functions defined on the multiplication operators only fully determine the local Gibbs state $\langle\cdot\rangle_{\beta,\Delta}$ defined in (134). A similar statement may be proven also for certain quantum spin models described by the Hamiltonian (127). In this case the role of $\mathfrak{F}_\Delta$ will be played by the algebra generated by the Pauli matrices $\sigma_{\boldsymbol{l}}^z$ with $\boldsymbol{l} \in \Delta$. The next step in developing the tools for studying local Gibbs states of quantum models is to extend analytically the Green functions to imaginary values of $t_1, \ldots, t_n$ and to obtain Matsubara functions. In a general situation the corresponding theorem was proven in Ref. 98. The proof is quite complicated. For the model of interacting quantum anharmonic oscillators, the proof was given in Ref. 33, its extended and simplified version may be found in the Ref. 34. Given $n \in \mathbb{N}$ and a domain $\mathcal{O} \subset \mathbb{C}^n$, let $\mathrm{Hol}(\mathcal{O})$ be the set of all functions holomorphic on $\mathcal{O}$. Given $\beta > 0$ and $n \in \mathbb{N}$, we set

$$\mathcal{D}_n^\beta = \{(t_1, \ldots, t_n) \in \mathbb{C}^n \mid 0 < \Im(t_1) < \Im(t_2) < \cdots < \Im(t_n) < \beta\}, \quad (142)$$

where $\Im(t_j)$ stands for the imaginary part of t_j, $j = 1, \ldots, n$. By $\overline{\mathcal{D}_n^\beta}$ we denote the closure of $\mathcal{D}_n^\beta$. Given $\xi_1, \ldots, \xi_n \in \mathbb{R}$, we also set

$$\mathcal{D}_n^\beta(\xi_1, \ldots, \xi_n) = \{(t_1, \ldots, t_n) \in \mathcal{D}_n^\beta \mid \Re(t_j) = \xi_j, \quad \text{for} \quad j = 1, \ldots, n\}. \quad (143)$$

Proposition 45: *For every $T_1, \ldots, T_n \in \mathfrak{A}_\Delta$,*

(a) the function $G_{T_1,\ldots,T_n}^{\beta,\Delta}$ may be extended to a holomorphic function on $\mathcal{D}_n^\beta$;

(b) this extension (which will also be written as $G_{T_1,\ldots,T_n}^{\beta,\Delta}$) is continuous on $\overline{\mathcal{D}_n^\beta}$ and for all $(t_1, \ldots, t_n) \in \overline{\mathcal{D}_n^\beta}$,

$$|G_{T_1,\ldots,T_n}^{\beta,\Delta}(t_1, \ldots, t_n)| \leq \|T_1\| \cdots \|T_n\|, \quad (144)$$

where $\|\cdot\|$ stands for the operator norm;

(c) for every $\xi_1, \ldots, \xi_n \in \mathbb{R}$, the set $\mathcal{D}_n^\beta(\xi_1, \ldots, \xi_n)$ is such that for any $f, g \in \mathrm{Hol}(\mathcal{D}_n^\beta)$, the equality $f = g$ on $\mathcal{D}_n^\beta(\xi_1, \ldots, \xi_n)$ implies that these functions are equal on the whole $\mathcal{D}_n^\beta$.

The meaning of this result may be explained as follows. If one has the Green functions for all possible choices of $F_j \in \mathfrak{F}_\Delta$, defined on one of such $\mathcal{D}_n^\beta(\xi_1, \ldots, \xi_n)$ only, then one has the complete information about the state. Indeed, by claims (a) and (c) of the above proposition, the values of the Green functions for real $t_1, \ldots, t_n$ may be uniquely determined by their values on such $\mathcal{D}_n^\beta(\xi_1, \ldots, \xi_n)$. Then, by Proposition 44, the values of the Green functions constructed for $F_j \in \mathfrak{F}_\Delta$ only, uniquely determine the values of such functions constructed for all operators, which in turn determines the state $\langle\cdot\rangle_{\beta,\Delta}$. By claim (a) of Proposition 45, the Green functions are differentiable for all real $t_1, \ldots, t_n$, which can be used to study them by means of differential equations.

The restrictions of the Green functions $G^{\beta,\Delta}_{T_1,\ldots,T_n}$ to $\mathcal{D}_n^\beta(0, \ldots, 0)$, i.e.,

$$\Gamma^{\beta,\Delta}_{T_1,\ldots,T_n}(\tau_1, \ldots, \tau_n) = G^{\beta,\Delta}_{T_1,\ldots,T_n}(it_1, \ldots, it_n), \tag{145}$$

are called Matsubara functions for the observables $T_1, \ldots, T_n$. In the light of the above discussion, these functions constructed for all possible choices of $F_1, \ldots, F_n \in \mathfrak{F}_\Delta$ completely determine the state $\langle\cdot\rangle_{\beta,\Delta}$.

3.3. *Euclidean Approach*

Integration in spaces of functions is one of the most popular and powerful methods of modern quantum theory. It appeared as a result of the mathematical development of R. Feynman's ideas[1] to formulate quantum theory in terms of path integrals. This development has revealed deep connections between quantum theory and stochastic analysis. A profound description of these connections, as well as of the method and its various applications, is given in B. Simon's book.[12]

An approach to the construction of Gibbs states of quantum lattice models of the type of (130) based on integration in function spaces was initiated in 1975 in Refs. 33 and 97. In the case of the Ising model with transverse field, similar methods were used in Ref. 65. The essence of the approach of Ref. 33 may be expressed in the following formula derived in that paper

$$\Gamma^{\beta,\Delta}_{F_1,\ldots,F_n}(\tau_1, \ldots, \tau_n) = \int_{\Omega_{\beta,\Delta}} F_1(\sigma_\Delta(\tau_1)) \cdots F_n(\sigma_\Delta(\tau_n))\, d\nu_{\beta,\Delta}(\sigma_\Delta), \tag{146}$$

which is strongly reminiscent of expressions from the preceding section like (17). The main dissimilarity of (146) and (17) is that the above integral is taken in an infinite dimensional space. Let us describe all components of

the right-hand side of (146). First we introduce $\Omega_{\beta,\Delta}$. By $C[0,\beta]$ we denote the real linear space of continuous functions $\phi : [0,\beta] \to \mathbb{R}$. This space endowed with the norm $\|\phi\| = \sup\{|\phi(\tau)| \mid \tau \in [0,\beta]\}$ becomes a Banach space. Set

$$\mathcal{C}_\beta = \{\phi \in C[0,\beta] \mid \phi(0) = \phi(\beta)\}. \tag{147}$$

This space consists of continuous periodic functions on the interval $[0,\beta]$. This is a closed subspace of $C[0,\beta]$, which means that it is a Banach space with the same norm. Furthermore, we set

$$\Omega_{\beta,\Delta} = \{\sigma_\Delta = (\sigma_{\boldsymbol{\imath}})_{\boldsymbol{\imath}\in\Delta} \mid \sigma_{\boldsymbol{\imath}} \in \mathcal{C}_\beta\}. \tag{148}$$

Each element of $\Omega_{\beta,\Delta}$ is a vector $\sigma_\Delta = (\sigma_{\boldsymbol{\imath}})_{\boldsymbol{\imath}\in\Delta}$ with the components $\sigma_{\boldsymbol{\imath}}$, which may also be called *spins*, but this time the spins are periodic continuous functions defined on $[0,\beta]$, i.e., they are infinite dimensional.

Now we describe the measure $\mathrm{d}\nu_{\beta,\Delta}$, which plays here a similar role as the local Gibbs measure $\mathrm{d}\nu_\Delta$ (3) does in the classical case. First we define a reference measure γ_β. It is a symmetric Gaussian measure on the Banach space $\mathcal{C}_\beta$ (the theory of such measures may be found in Refs. 12, 19 and 20), which is completely determined by its covariation operator. The latter is an integral operator with the integral kernel

$$S(\tau,\tau') = \frac{1}{2\sqrt{m}} \frac{\exp\left(-|\tau-\tau'|/\sqrt{m}\right) + \exp\left(-(\beta-|\tau-\tau'|)/\sqrt{m}\right)}{1-\exp\left(-\beta/\sqrt{m}\right)}, \tag{149}$$

where m is the same as in the Hamiltonian (130), i.e., it is the particle mass. It appears that this is nothing else but the Matsubara function of the quantum harmonic oscillator of mass m described by the Hamiltonian

$$H^{\mathrm{har}} = \frac{1}{2m}p^2 + \frac{1}{2}q^2.$$

On the other hand, $S(\tau,\tau')$ is the correlation function of the so called *periodic Ornstein–Uhlenbeck process with period* β. First this process has appeared in the pioneering paper of Ref. 97, the study of such processes and their applications in quantum statistical physics is given in Refs. 98 and 99.

In what follows, the Gaussian measure γ_β describes the states of a single quantum harmonic oscillator. The states of interacting quantum anharmonic oscillators located at sites of the subset Δ are described by the measure which is constructed from γ_β and the energy functions $E_{\beta,\Delta}$ on

the base of the famous Feynman–Kac formula (see e.g., Ref. 12)

$$\mathrm{d}\nu_{\beta,\Delta}(\sigma_\Delta) = \frac{1}{Z_{\beta,\Delta}} \exp\left(-E_{\beta,\Delta}(\sigma_\Delta)\right) \prod_{\boldsymbol{l}\in\Delta} d\gamma_\beta(\sigma_{\boldsymbol{l}}), \tag{150}$$

where

$$Z_{\beta,\Delta} = \int_{\Omega_{\beta,\Delta}} \exp(-E_{\beta,\Delta}(\sigma_\Delta)) \prod_{\boldsymbol{l}\in\Delta} d\gamma_\beta(\sigma_{\boldsymbol{l}}), \tag{151}$$

$$E_{\beta,\Delta}(\sigma_\Delta) = -\frac{1}{2} \sum_{\boldsymbol{l},\boldsymbol{l}'\in\Delta} J_{\boldsymbol{l}\boldsymbol{l}'} \int_0^\beta \sigma_{\boldsymbol{l}}(\tau)\sigma_{\boldsymbol{l}'}(\tau)\, d\tau - \sum_{\boldsymbol{l}\in\Delta} h_{\boldsymbol{l}} \int_0^\beta \sigma_{\boldsymbol{l}}(\tau)\, d\tau + \sum_{\boldsymbol{l}\in\Delta} \int_0^\beta \tilde{P}(\sigma_{\boldsymbol{l}}(\tau))\, d\tau, \tag{152}$$

and where $\tilde{P}(t) = P(t) - (t^2/2)$; we have extracted $t^2/2$ into the Gaussian measure γ_β. The measure (150) is called *the local Euclidean Gibbs measure*. Since this measure completely determines the Matsubara functions (145) for all $F_1, \ldots, F_n \in \mathfrak{F}_\Delta$, it determines the local Gibbs state $\langle\cdot\rangle_{\beta,\Delta}$, it is also called *the local Euclidean Gibbs state*. In what follows, the Euclidean approach allows one to study local Gibbs states of the model (130) by means of probability measures as if it is a system of classical spins with the only difference that these spins are infinite dimensional. This approach was developed in Refs. 34, 54, 61, 73, 74 and 100–111. Its full description and an extended related bibliography are given in Ref. 34. Here we mention certain results obtained in this approach. First of all it would make sense to study these states in the quasi-classical limit $m \to +\infty$. In Ref. 101 (see also Section 3 in Ref. 34) a statement describing such a limit was proven. Its corollary may be formulated as follows. We recall that in Section 2 we introduced the set $\mathcal{F}_\Delta$ of all continuous polynomially bounded functions $f : \Omega_\Delta = \mathbb{R}^{|\Delta|} \to \mathbb{R}$. Let $\mathcal{F}_\Delta^{(0)} \subset \mathcal{F}_\Delta$ be the set of such functions which are bounded. We shall use the set $\boldsymbol{F}_{\beta,\Delta}$ consisting of all bounded continuous functions $F : \Omega_{\beta,\Delta} \to \mathbb{R}$, where $\Omega_{\beta,\Delta}$ is defined by (148). By $\Omega^{\mathrm{c}}_{\beta,\Delta}$ we denote the subset of $\Omega_{\beta,\Delta}$ consisting of all constant vectors, i.e.,

$$\Omega^{\mathrm{c}}_{\beta,\Delta} = \{\sigma_\Delta = (\sigma_{\boldsymbol{l}})_{\boldsymbol{l}\in\Delta} \in \Omega_{\beta,\Delta} \mid \exists \xi_\Delta = (\xi_{\boldsymbol{l}})_{\boldsymbol{l}\in\Delta} \in \Omega_\Delta, \quad \forall \tau \in [0,\beta] \;\; \forall \boldsymbol{l} \in \Delta : \;\; \sigma_{\boldsymbol{l}}(\tau) \equiv \xi_{\boldsymbol{l}}\}.$$

For the elements of this set we write $\sigma_\Delta(\tau) \equiv \xi_\Delta$ meaning that all the components of σ_Δ, which are constant functions of τ, coincide with the corresponding components of the vector $\xi_\Delta \in \Omega_\Delta$. Given a function $f \in$

$\mathcal{F}_\Delta^{(0)}$, we set

$$\Psi_f = \{F \in \boldsymbol{F}_{\beta,\Lambda} \mid \forall \sigma_\Delta \in \Omega^{\mathrm{c}}_{\beta,\Delta} : \quad F(\sigma_\Delta) = f(\xi_\Delta)\}. \tag{153}$$

In other words, the above set consists of the functions which have constant σ_Δ values coinciding with the corresponding values of this chosen function f.

Proposition 46: *For any finite Δ, for every $\beta > 0$, for any $f \in \mathcal{F}_\Delta^{(0)}$ and all $F \in \Psi_f$,*

$$\lim_{m\to+\infty} \int_{\Omega_{\beta,\Delta}} F(\sigma_\Delta)\, d\nu_{\beta,\Delta}(\sigma_\Delta) = \int_{\Omega_\Delta} f(\xi_\Delta)\, d\nu_\Delta(\xi_\Delta), \tag{154}$$

where the measure ν_Δ is defined by (11) with the same P, $h_{\boldsymbol{l}}$ and $J_{\boldsymbol{l}\boldsymbol{l}'}$ as in (150)–(152).

We recall that the Gibbs states of classical systems were introduced as solutions of the DLR equation (see Definition 21). In the quantum case the equilibrium states are defined by means of the *Kubo–Martin–Schwinger (KMS) conditions* (see the second volume of Ref. 2). We are not going to pay here more attention to this condition and just remark that for the models with unbounded operators, like the one described by (130), this construction is impossible (see the discussion in Ref. 34). The only possibility for such models, at least so far, is to construct Euclidean Gibbs states following the scheme:

$$\text{local Gibbs measures} \;\Rightarrow\; \text{DLR equation} \;\Rightarrow\; \text{Gibbs measure, its solution}$$

described in the preceding section. We refer to Ref. 34 where this scheme has been realized.

3.4. *Phase Transitions and Critical Points*

Since the main place in our consideration of quantum models belongs to the model (130), we restrict ourselves to presenting here results on phase transitions and critical phenomena based on this model only. The corresponding results for a number of quantum spin models described by the Hamiltonian (127) may be found in Refs. 65 and 112.

Thus, we consider the model described by the Hamiltonian (130) with the zero external field and an even polynomial P. All the methods employed to prove the existence of the long range order for the model (130) are based on the so called infrared bounds[113] (see also Ref. 112 for more details and

appropriate modifications to the quantum case). As in the classical case the order parameter is defined by the expression

$$P(\beta) = \lim_{n\to+\infty} \frac{1}{|\Lambda_n|^2} \sum_{\boldsymbol{l},\boldsymbol{l}'\in\Lambda_n} \langle q_{\boldsymbol{l}} q_{\boldsymbol{l}'} \rangle^{(p)}_{\beta,\Lambda}, \tag{155}$$

where, as in (71), $\{\Lambda_n\}_{n\in\mathbb{N}}$ is a sequence of boxes and the state $\langle\cdot\rangle^{(p)}_{\beta,\Lambda}$ is defined by (134), (135) with the Hamiltonian (130) in which the interaction potential has been modified to take into account the periodic boundary conditions, exactly as was done in the classical case. Here one has to mention that the states $\langle\cdot\rangle_{\beta,\Lambda}$, and hence the periodic state $\langle\cdot\rangle^{(p)}_{\beta,\Lambda}$, were defined for bounded operators only, whereas the displacement operators $q_{\boldsymbol{l}}$ are unbounded. In general, this is a problem, which takes some effort to be overcome, see Refs. 114 and 115. But in the case considered we may use the representation (146) (fortunately $q_{\boldsymbol{l}}$ is a multiplication operator), which yields

$$\langle q_{\boldsymbol{l}} q_{\boldsymbol{l}'} \rangle^{(p)}_{\beta,\Lambda} = \int_{\Omega_{\beta,\Lambda}} \sigma_{\boldsymbol{l}}(0)\sigma_{\boldsymbol{l}'}(0)\, d\nu^{(p)}_{\beta,\Lambda}(\sigma_\Lambda), \tag{156}$$

where the Euclidean Gibbs measure $\nu^{(p)}_{\beta,\Lambda}$ is defined by (150)–(152) with $h_{\boldsymbol{l}} = 0$ and $J^{\Lambda}_{\boldsymbol{l}\boldsymbol{l}'}$ instead of $J_{\boldsymbol{l}\boldsymbol{l}'}$; see (66). We also suppose that $J^{\Lambda}_{\boldsymbol{l}\boldsymbol{l}'} \geq 0$ and the condition (15) is satisfied. The following statement was proven in Ref. 105, see also Refs. 61 and 107.

Proposition 47: *Let the polynomial $P(8)$ in (152) be even, with $r \geq 2$, and possess two nondegenerate minima at some points $\pm t_0$ with $t_0 > 0$. Then for $d \geq 3$, there exists $m_* > 0$ such that for the particle mass $m > m_*$, there exists $\beta_C > 0$ such that: (a) for $\beta < \beta_C$, the order parameter (155) is zero; (b) for $\beta > \beta_C$, $P(\beta) > 0$.*

A particular case of this statement, where the polynomial P was as above but with $r = 2$ was proven in Refs. 65 and 116.

The only theorem describing a critical point of a model of this type was proven in Ref. 103, where a hierarchical version of the model (130) was considered. Its formal Hamiltonian may be written in the form

$$H = \frac{1}{2m} \sum_{\boldsymbol{l}\in\mathbb{Z}} p^2_{\boldsymbol{l}} + \sum_{\boldsymbol{l}\in\mathbb{Z}} \left(a q^2_{\boldsymbol{l}} + b q^4_{\boldsymbol{l}}\right) - \frac{1}{2} \sum_{n=0}^{\infty} \sum_{\boldsymbol{l}\in\mathbb{Z}} 2^{-n(1+\lambda)} I(\boldsymbol{l},\boldsymbol{l}) [q(V^{(n)}_{\boldsymbol{l}})]^2, \tag{157}$$

where $I(\boldsymbol{l},\boldsymbol{l})$ and $V_{\boldsymbol{l}}^{(n)}$ are the same as in (126), $a \in \mathbb{R}$, $b > 0$ and

$$q(V_{\boldsymbol{l}}^{(n)}) = \sum_{\boldsymbol{l} \in V_{\boldsymbol{l}}^{(n)}} q_{\boldsymbol{l}}.$$

The statement below is a corollary of the main theorem of Ref. 103.

Proposition 48: *For the model described by (157) with $\lambda \in (0, 1/2)$, there exist such values of the parameters m, a and b that the following holds. There exists $\beta_* > 0$ such that:*
(a) for $\beta = \beta_*$ [cf., (74)],

$$0 < \lim_{n \to +\infty} 2^{-n(1+\lambda)} \sum_{\boldsymbol{l},\boldsymbol{l}' \in V_{\boldsymbol{0}}^{(n)}} \langle q_{\boldsymbol{l}} q_{\boldsymbol{l}'} \rangle_{\beta, V_{\boldsymbol{0}}^{(n)}} < \infty; \tag{158}$$

(b) for $\beta < \beta_*$,

$$2^{-n} \sum_{\boldsymbol{l},\boldsymbol{l}' \in V_{\boldsymbol{0}}^{(n)}} \langle q_{\boldsymbol{l}} q_{\boldsymbol{l}'} \rangle_{\beta, V_{\boldsymbol{0}}^{(n)}} \leq C < \infty; \tag{159}$$

for all $n \in \mathbb{N}$.

We remark here that (159) means that the static susceptibility $\chi_{V_{\boldsymbol{0}}^{(n)}}$ [cf. (73) and the final part of Subsection 2.5] remains bounded as $n \to +\infty$. Here for a finite subset Δ, we set

$$\chi_\Delta = \frac{1}{|\Delta|} \sum_{\boldsymbol{l},\boldsymbol{l}' \in \Delta} \langle q_{\boldsymbol{l}} q_{\boldsymbol{l}'} \rangle_{\beta,\Delta}. \tag{160}$$

As follows from Proposition 47, the long-range order appears when the particle mass is big enough, which corresponds to the quasi-classical limit (see Proposition 46). What can be said about the opposite limit $m \to 0$? In other words, which quantum effects may one expect in such models? This question was first studied in Ref. 117, where it was shown that the long-range order does not appear in the small-mass limit. A mathematically rigorous proof of this effect was given in Ref. 118. Here we present a result, proven in Ref. 100, which shows that not only the long-range order, but any critical point anomaly, is suppressed if a certain condition involving the particle mass is satisfied.

The Hamiltonian (130) may be written in the form

$$H_\Delta = \sum_{\boldsymbol{l} \in \Delta} H_{\boldsymbol{l}} - \frac{1}{2} \sum_{\boldsymbol{l},\boldsymbol{l}' \in \Delta} J_{\boldsymbol{l}\boldsymbol{l}'} q_{\boldsymbol{l}} q_{\boldsymbol{l}'}, \tag{161}$$

where the one-particle Hamiltonian is

$$H_{\boldsymbol{l}} = \frac{1}{2m} p_{\boldsymbol{l}}^2 + P(q_{\boldsymbol{l}}). \tag{162}$$

It is well known that its spectrum consists of non-degenerate eigenvalues λ_n, $n \in \mathbb{N}_0$. Set

$$\delta = \min_{n \in \mathbb{N}} (\lambda_n - \lambda_{n-1}), \tag{163}$$

which is the minimal distance between the one-particle energy levels. For the quantum harmonic oscillator described by (162) with $P(q_{\boldsymbol{l}}) = (b/2) q_{\boldsymbol{l}}^2$, where $b > 0$ is its *rigidity*, one has

$$\delta_{\mathrm{h}} = \hbar \sqrt{b/m}. \tag{164}$$

The following statement is a corollary of the main theorem proven in Ref. 100.

Proposition 49: *For the model described by the Hamiltonian (130), (161) let the following condition be satisfied:*

$$(m\delta^2/\hbar^2) > \|J\| \stackrel{\text{def}}{=} \sup_{\boldsymbol{l} \in \mathbb{Z}^d} \sum_{\boldsymbol{l}' \in \mathbb{Z}^d} J_{\boldsymbol{l}\boldsymbol{l}'}. \tag{165}$$

Then for every $\beta > 0$ and for any increasing sequence $\mathcal{D}$ of subsets which exhausts the lattice $\mathbb{Z}^d$, the sequence of static susceptibilities $\{\chi_\Delta\}_{\Delta \in \mathcal{D}}$ defined by (160) remains bounded, i.e., no critical point anomalies are possible at all temperatures.

As shown in Ref. 100, if in (161) P is an even polynomial of degree $2r \geq 4$, then $m\delta^2$ is a continuous function of m such that

$$m\delta^2 \sim C m^{-(r-1)/(r+1)} \quad \text{as } m \to 0$$

which means that there should exist a constant m_*, depending on $\|J\|$ and on the coefficients of the polynomial P, such that the condition (165) is satisfied for $m < m_*$. This yields the following corollary of the above statement.

Corollary 50: *For the model described by the Hamiltonian (130), (161), there exists a constant $m_* > 0$, which depends solely on the coefficients of the polynomial P and on the interaction parameter $\|J\|$ and is independent of β, such that for $m < m_*$, no critical point anomalies, and all the more, no long-range order, are possible at all temperatures.*

The extension of the above results to the case of vector quantum oscillators was given in Refs. 108 and 109.

Let us analyze these statements. By (164), for the harmonic oscillators, one has $m\delta_{\rm h}^2 = \hbar^2 b$. Then the condition (165) gets the form

$$b > \|J\|,$$

which is nothing else but the stability condition (16). Then for the anharmonic oscillators, the parameter $m\delta^2$ may be considered as a measure of its quantum rigidity and the effect described by the above statements may be called *a quantum stabilization* of the system of quantum anharmonic oscillators described by (130), (161). Stronger statements of this kind establishing uniqueness of Euclidean Gibbs states for this system, were proven in Refs. 73, 74 and 102.

Acknowledgments

The author is grateful to his teachers Igor Stasyuk and Igor Yukhnovskii who introduced him into the subject of this article. He thanks Sergio Albeverio, Yuri Kondratiev, Agnieszka Kozak, Mykhailo Kozlovskii, Taras Krokhmalskii, Mykola Melnyk, Michael Röckner and Lech Wołowski for collaboration – certain parts of the results described in this article were obtained and/or discussed jointly. He also thanks Yuri Holovatch and Igor Stasyuk for organizing in March 2002 (in ICMP, Lviv) the Ising Lectures in which the main part of the above material was presented. Helpful comments and suggestions by Yuri Holovatch substantially improved the presentation of the article. The author is also grateful for the hospitality of the Research Centre BiBoS, Bielefeld University where this article was brought into its final form. His research was supported in part by the Deutsche Forschungsgemeinschaft through the German–Polish project 436 POL 113/98/0-1 "Probability Measures"; that support is gratefully acknowledged.

References

1. S. Albeverio and R. Høegh-Krohn, *Mathematical Theory of Feynman Path Integrals* (Lect. Notes in Math. 523, Springer-Verlag, Berlin, 1976).
2. O. Bratteli and D.W. Robinson, *Operators Algebras and Quantum Statistical Mechanics, I* (Springer-Verlag, New York Heidelberg, 1979); *Operators Algebras and Quantum Statistical Mechanics, II* (Springer-Verlag, New York Berlin, 1981).
3. R. Fernández, J. Fröhlich and A.D. Sokal, *Random Walks, Critical Phenomena and Triviality in Quantum Field Theory* (Springer-Verlag, Berlin, 1992).

4. H.-O. Georgii, *Gibbs Measures and Phase Transitions* (Walter de Gruyter, Berlin New York, 1988).
5. R.B. Israel, *Convexity in the Theory of Lattice Gases* (Princeton Series in Physics, Princeton University Press, Princeton, N.J., 1979).
6. V.A. Malyshev and R.A. Minlos, *Gibbsovskie sluchaĭnye polya. Metod klasternykh razlozheniĭ.* ("Nauka", Moscow, 1985); translation: *Gibbs random fields. Cluster expansions* (Mathematics and its Applications (Soviet Series), 44. Kluwer Academic Publishers Group, Dordrecht, 1991).
7. V.A. Malyshev and R.A. Minlos, *Linear infinite-particle operators* (Translations of Mathematical Monographs, 143. American Mathematical Society, Providence, RI, 1995).
8. R.A. Minlos, *Introduction to Mathematical Statistical Physics* (University Lecture Series, 19, Amer. Math. Soc. Providence, RI, 2000).
9. G. Roepstorff, *Path Integral Approach to Quantum Physics. An Introduction* (Springer-Verlag, Berlin Heidelberg, 1994).
10. D. Ruelle, *Statistical Mechanics: Rigorous Results* (W. A. Benjamin, Inc., New York-Amsterdam, 1969).
11. B. Simon, *The $P(\varphi)_2$ Euclidean (Quantum) Field Theory* (Princeton University Press, Princeton, N.J., 1974).
12. B. Simon, *Functional Integration and Quantum Physics* (Academic Press, New York London, 1979).
13. B. Simon, *The Statistical Mechanics of Lattice Gases. I* (Princeton University Press, Princeton, N.J., 1993).
14. Ya. G. Sinai, *Theory of Phase Transitions: Rigorous Results* (Pergamon Press, Oxford-Elmsford, N.Y., 1982).
15. M. Reed and B. Simon, *Methods of Modern Mathematical Physics. I. Functional Analysis* (Academic Press, New York London, 1972).
16. L. Iliev, *Laguerre Entire Functions* (Second edition, Publishing House of the Bulgarian Academy of Sciences, Sofia, 1987).
17. B. Ya. Levin, *Lectures on Entire Function* (American Mathematical Society, Providence, RI, 1996).
18. P. Billingsley,*Probability and Measure* (Third edition. Wiley Series in Probability and Mathematical Statistics. A Wiley-Interscience Publication. John Wiley & Sons, Inc., New York, 1995).
19. K.R. Parthasarathy, *Probability Measures on Metric Spaces* (Academic Press, New York, 1967).
20. A.V. Skorohod, *Intergration in Hilbert Space* (Springer-Verlag, Berlin, 1974).
21. Vivek S. Borkar, *Probability Theory. An Advanced Course* (Springer-Verlag, New York, 1995).
22. E. Ising, *Z. Phys.* **31**, 253 (1925).
23. S.G. Brush, *Rev. Mod. Phys.* **39**, 883 (1967).
24. S. Kobe, *J. Stat. Phys.* **88**, 991 (1997).
25. L. Onsager, *Phys. Rev.* **65**, 117 (1944).
26. D. Gandolfo, Private communication, 2002.

27. A.K. Hartmann and H. Rieger, *Optimization Algorythms in Physics* (Wiley-VCH Verlag Berlin GmbH, Berlin, 2002).
28. http://www.physik.uni-bielefeld.de/complexity/
29. B. Simon and R. Griffiths, *Comm. Math. Phys.* **33**, 145 (1973).
30. P.M. Bleher and N.N. Ganikhodzhaev, *Teor. Veroyatnost. i Primenen.* **35**, 220 (1990); translation in *Theory Probab. Appl.* **35**, 216 (1990).
31. N.N. Ganikhodzhaev, *Teoret. Mat. Fiz.* **130**, 493 (2002); translation in *Theoret. and Math. Phys.* **130**, 419 (2002).
32. S. Stamenković, *Condens. Matter Phys.* **1**(14), 257 (1998).
33. S. Albeverio and R. Høegh-Krohn, *J. Func. Anal.* **19**, 242 (1975).
34. S. Albeverio, Yu. Kondratiev, Yu. Kozitsky, and M. Röckner, *Rev. Math. Phys.* **14**, 1335 (2002).
35. J. Abdullaev and R.A. Minlos, in *Probability Contributions to Statistical Mechanics* (Adv. Soviet Math., 20, Amer. Math. Soc., Providence, RI, 1994), p. 1.
36. T.D. Lee and C.N. Yang, *Phys. Rev.* **87**, 410 (1952).
37. E.H. Lieb and A.D. Sokal, *Comm. Math. Phys.* **80**, 153 (1981).
38. C.M. Newman, *Comm. Pure Appl. Math.* **27**, 143 (1974).
39. C.M. Newman, *J. Stat. Phys.* **15**, 399 (1976).
40. Yu. Kozitsky and N.O. Melnik, *Teoret. Mat. Fiz.* **78**, 177 (1989); translation in *Theoret. and Math. Phys.* **78**, 127 (1989).
41. Yu. Kozitsky, *Teoret. Mat. Fiz.* **58**, 96 (1984).
42. Yu. Kozitsky, *Rep. Math. Phys.* **26**, 429 (1988).
43. C. Fortuin, P. Kastelyn and J. Ginibre, *Comm. Math. Phys.* **22**, 89 (1971).
44. R.B. Griffiths, *J. Math. Phys.* **10**, 1559 (1969).
45. G. Sylvester, *J. Stat. Phys.* **15**, 327 (1976).
46. R.S. Ellis and J.S Rosen, *Ann. Probab.* **10**, 47 (1982).
47. M. Aizenman, *Comm. Math. Phys.* **86**, 1 (1982).
48. S.B. Shlosman, *Comm. Math. Phys.* **102**, 679 (1986).
49. C.M. Newman, *Comm. Math. Phys.* **74**, 119 (1980).
50. N.N. Bogolyubov, in *Problems in the Theory and History of Differential Equations* (Naukova Dumka, Kiev, 1968), p. 13.
51. R.L. Dobrushin, *Teor. Veroyatnost. i Primenen.* **13**, 201 (1968); translation in *Theor. Probab. Appl.* **13**, 179 (1968).
52. R.L. Dobrushin, *Funcional. Anal. i Priložen.* **3**, 27 (1969).
53. O.E. Lanford and D. Ruelle, *Comm. Math. Phys.* **13**, 194 (1969).
54. S. Albeverio, Yu. Kondratiev, T. Pasurek and M. Röckner, *A Priori Estimates and Existence for Euclidean Gibbs Measures* (Preprint BiBoS Nr 02-06-089, Bielefeld, 2002).
55. R.L. Dobrushin, *Teor. Veroyatnost. i Primenen.* **18**, 261 (1973); translation in *Theor. Probab. Appl.* **18**, 253 (1973).
56. R.L. Dobrushin, *Teor. Veroyatnost. i Primenen.* **17**, 619 (1972); translation in *Theor. Probab. Appl.* **17**, 619 (1972).
57. M. Aizenman, *Comm. Math. Phys.* **73**, 83 (1980).
58. M. Aizenman, D.J. Barsky and R. Fernández, *J. Stat. Phys.* **47**, 343 (1987).
59. D. Ruelle, *Comm. Math. Phys.* **50**, 189 (1976).

60. J.L. Lebowitz and E. Presutti, *Comm. Math. Phys.* **50**, 195 (1976). Erratum: *Comm. Math. Phys.* **78**, 151 (1980).
61. V.S. Barbulyak and Yu. G. Kondratiev, *Dokl. Akad. Nauk Ukrain. SSR* **8**, 31 (1991).
62. M. Aizenman, in *Statistical Physics and Dynamical Systems (Köszeg, 1984)* (Progr. Phys., 10, Birkhäuser Boston, Boston, MA, 1985), p 453.
63. M. Aizenman and R. Fernández, *J. Stat. Phys.* **44**, 393 (1986).
64. P.M. Bleher and P. Major, *Ann. Probab.* **15**, 153 (1987).
65. W. Driessler, L. Landau and J.F. Perez, J. Stat. Phys. **20**, 123 (1979).
66. Ya.G. Sinai, in *Mathematical problems in theoretical physics (Proc. Internat. Conf., Univ. Rome. Rome, 1977)* (Lecture Notes in Phys., 80, Springer, Berlin New York, 1978), p 303.
67. R. Peierls, *Proc. Cambridge Phil. Soc.* **32**, 477 (1936).
68. S.A. Pirogov and Ja.G. Sinai, *Teoret. Mat. Fiz.* **25**, 358 (1975); *ibid.* **26**, 61 (1976).
69. M. Zahradník, *Rend. Math. Appl. (7)* **18**, 411 (1998).
70. R.L. Dobrushin and S.B. Shlosman, *Selecta Math. Sov.* **1**, 317 (1981).
71. D. Iagolnitzer and B. Souillard, *Phys. Rev.* **B19**, 1515 (1979).
72. J.L. Lebowitz and A. Martin-Löf, *Comm. Math. Phys.* **25**, 276 (1972).
73. S. Albeverio, Yu. Kondratiev, Yu. Kozitsky and M. Röckner, *C.R. Acad. Sci. Paris, Ser I* **335**, 693 (2002).
74. S. Albeverio, Yu. Kondratiev, Yu. Kozitsky and M. Röckner, *Small Mass Implies Uniqueness of Gibbs States of a Quantum Crystal* (Preprint BiBoS Nr 02-12-104, Bielefeld, 2002, subm. in *Comm. Math. Phys.*).
75. F.J. Dyson, *Comm. Math. Phys.* **12**, 91 (1969).
76. F.J. Dyson, in *Mathematical aspects of statistical mechanics (Proc. Sympos. Appl. Math., New York, 1971)* (SIAM-AMS Proceedings, Vol. V, Amer. Math. Soc., Providence, R. I., 1972), p. 1.
77. M. Aizenman, J.T. Chayes, L. Chayes and C.M. Newman, *J. Stat. Phys.* **50**, 1 (1988).
78. L.P. Kadanoff, *Physics* **2**, 263 (1966).
79. L.P. Kadanoff, in *Phase transitions and critical phenomena, Vol. 5a* (Academic Press, London, 1976), p. 1.
80. L.P. Kadanoff, *Statistical Physics. Statics, Dynamics and Renormalization* (World Scientific Publishing Co., Inc., River Edge, NJ, 2000).
81. Ya.G. Sinai, *Teor. Verojatnost. i Primenen.* **21**, 63 (1976).
82. K. Gawędzki, in *Mathematics + physics. Vol. 1* (World Sci. Publishing, Singapore, 1985), p 99.
83. K. Gawędzki and A. Kupiainen, *Comm. Math. Phys.* **89**, 191 (1983).
84. K. Gawędzki and A. Kupiainen, *Comm. Math. Phys.* **99**, 197 (1985).
85. K.G. Wilson, *Rev. Modern Phys.* **55**, 583 (1983).
86. I.R. Yukhnovskii, *Phase Transitions of the Second Order* (World Scientific Publishing Co., Singapure, 1987).
87. I.R. Yukhnovskii, *Riv. Nuovo Cimento (3)* **12**, 1 (1989).
88. M. Salmhofer, *Renormalization. An Introduction* (Springer-Verlag, Berlin Heidelberg, 1999).

89. Yu. Kozitsky and I.R. Yukhnovskii, *Teoret. Mat. Fiz.* **51**, 268 (1982).
90. P.M. Bleher and Ya.G. Sinai, *Comm. Math. Phys.* **33**, 23 (1973).
91. P.M. Bleher and Ya.G. Sinai, *Comm. Math. Phys.* **45**, 247 (1975).
92. Yu. Kozitsky, M. Kozlovskii and T. Krokhmalskii, *Condens. Matter Phys.* **2**, 15 (1999).
93. Yu. Kozitsky, *Condens. Matter Phys.* **5**, 74 (1995).
94. E. Olivieri, P. Picco and Yu.M. Suhov, *J. Stat. Phys.* **70**, 985 (1993).
95. P.M. Bleher, *Comm. Math. Phys.* **84**, 557 (1982).
96. I.V. Stasyuk, *Condens. Matter Phys.* **2**(19), 435 (1999).
97. R. Høegh-Krohn, *Comm. Math. Phys.* **38**, 195 (1974).
98. A. Klein and L.D. Landau, *J. Func. Anal.* **42**, 368 (1981).
99. A. Klein and L.D. Landau, *Pacif. Journ. Math.* **94**, 341 (1981).
100. S. Albeverio, Yu. Kondratiev and Yu. Kozitsky, *Comm. Math. Phys.* **194**, 493 (1998).
101. S. Albeverio, Yu. Kondratiev and Yu. Kozitsky, *Lett. Math. Phys.* **48**, 221 (1999).
102. S. Albeverio, Yu. Kondratiev, Yu. Kozitsky and M. Röckner, *Ann. Inst. H. Poincaré, Probab. Statist.* **37**, 43 (2001).
103. S. Albeverio, Yu. Kondratiev, A. Kozak and Yu. Kozitsky, *A System of Quantum Anharmonic Oscillators with Hierarchical Structure: Critical Point Convergence* (Preprint BiBoS Universitaet Bielefeld, Nr 02-07-092, 2002, submitted in *Comm. Math. Phys.*).
104. V.S. Barbulyak and Yu.G. Kondratiev, *Dokl. Akad. Nauk Ukrain. SSR* **9**, 38 (1991).
105. V.S. Barbulyak and Yu.G. Kondratiev, *Funktsional. Anal. i Prilozhen.* **26**, 61 (1992); translation in *Funct. Anal. Appl.* **26**, 124 (1992).
106. S.A. Globa and Yu.G. Kondratiev, *Selecta Math. Sov.* **9**, 297 (1990).
107. Ju.G. Kondratiev, in *Stochastic Processes, Physics and Geometry II* (World Scientific, Singapure, 1994), p 465.
108. Yu. Kozitsky, *Lett. Math. Phys.* **51**, 71 (2000).
109. Yu. Kozitsky, *Lett. Math. Phys.* **53**, 289 (2000).
110. Yu. Kozitsky, in *Stochastic Processes, Physics and Geometry: New Interplays, II (Leipzig, 1999)* (Canad. Math. Soc. Conf. Proc., 29, Amer. Math. Soc., Providence, RI, 2000), p. 403.
111. Yu. Kozitsky, in *Noncommutative Structures in Mathematics and Physics (Kiev, 2000, S. Duplij and J. Wess eds.)* (NATO Sci Ser. II Math. Phys. Chem. 22. Kluwer Acad. Publ. Dordrecht, 2001), p. 415.
112. F.J. Dyson, E.H. Lieb and B. Simon, *J. Stat. Phys.* **18**, 335 (1978).
113. J. Fröhlich, B. Simon and T. Spencer, *Comm. Math. Phys.* **50**, 79 (1976).
114. G.L. Sewell, *J. Math. Phys.* **11**, 1868 (1970).
115. G.L. Sewell, *Quantum Theory of Collective Phenomena* (Clarendon Press, Oxford, 1986).
116. L.A. Pastur, B.A. Khoruzhenko, *Teoret. Mat. Fiz.* **73**, 111 (1987).
117. T. Schneider, H. Beck and E. Stoll, *Phys. Rev.* **B13**, 1123 (1976).
118. A. Verbeure and V.A. Zagrebnov, *J. Phys. A.: Math. Gen.* **28**, 5415 (1995).

CHAPTER 2

RELAXATION IN QUANTUM SPIN CHAINS: FREE FERMIONIC MODELS

Dragi Karevski

Laboratoire de Physique des Matériaux, UMR CNRS 7556,
Université Henri Poincaré
BP 239, 54506 Vandoeuvre lès Nancy Cedex, France
E-mail: karevski@lpm.u-nancy.fr

The aim of this chapter is to give a pedagogical introduction to the exact equilibrium and non-equilibrium properties of free fermionic quantum spin chains, whether disordered or otherwise. In the first part we present in full detail the canonical diagonalization procedure. The phase diagram is analysed and phase transitions are discussed on simple grounds. Equilibrium dynamical properties are reviewed. The remaining part is devoted to the non-equilibrium dynamical behaviour of such quantum chains relaxing from a non-equilibrium pure initial state to a final stationary state. In particular, special attention is paid to the relaxation of transverse magnetization. Two-time functions are also considered, giving insights on the nature of the final non-equilibrium stationary state and the possibility of aging in such systems.

1. Introduction

Quantum spin chains are probably the simplest quantum mechanical systems showing a wide variety of interesting properties,[1–5] a main one being the existence of quantum phase transitions, that is transitions at zero temperature driven by large quantum fluctuations.[6] Singularities occuring strictly[7] at the zero-temperature transition point can, however, produce a typical signature at a (very) low temperature. On the experimental side, physicists are nowadays able to produce artificial samples with behaviour that fits very well with the theoretical descriptions.[8–10]

The low dimensionality of these systems allows the use of efficient analytical and numerical tools such as the Bethe ansatz,[11,12] bosonization[13,14]

or fermionization,[1,15] exact diagonalization of finite chains or the numerical density matrix (DMRG) approach.[16–18] We focus our attention in this review on free-fermionic quantum spin chains, which are spin models that can be mapped on systems of non-interacting fermions.[1] The free nature of the elementary excitations allows for an exact diagonalization of the Hamiltonian. It is not here necessary to argue on the usefulness of exact solutions for the implementation of the general comprehension we have of such many-body systems. In particular, they can be used as a *garde fou* when dealing with more complex systems, unsolved or unsolvable. Moreover, some of the properties they show can still be present in truly interacting systems, that is, models that cannot be or have not yet been mapped on free particles or solvable problems.

Most of the studies during the last decades, have been devoted to understand the influence of inhomogeneities,[19] such as regular alternation (see Derzhko in this volume), aperiodic[20] modulation of the couplings between spins or the presence of quenched disorder,[21] on the nature of the phase transition (one can refer to Berche and Chatelain in this volume for a general review of the influence of quenched disorder on classical, that is thermally activated, phase transitions). This has culminated in the work of D. Fisher[22] on the random transverse field Ising quantum chain. The extremely broad distribution of energy scales near the critical point, for such random chains, allows the use of a decimation-like renormalization group transformation.[23] However, all these works deal with equilibrium properties, but here we will pay attention to another less worked out aspect, which is the non-equilibrium behaviour of such fermionic spin chains. The focus will be on homogeneous systems, since they allow analytical calculations, although expressions are given which are valid for general coupling distributions.

The paper is organised as follows: in the next section, we present the general features of the free fermionic spin models and the canonical diagonalization procedure first introduced by Lieb *et al.*[1] A detailed discussion is given on the excitation spectrum and the associated eigenvectors. In Section 3 we turn on the discussion of equilibrium properties, static as well as dynamic. In particular we point out that one can extract the full phase diagram of such spin chains from the knowledge of the surface magnetization. Results on dynamical correlation functions are reviewed. The following section deals with the non-equilibrium behaviour. After solving the Heisenberg equations of motion for the basic dynamical variables, we present some aspects of the relaxation of the transverse magnetization.

We show that systems with either conserved or non-conserved dynamics present, however, some similarities in their relaxation behaviour. This is illustrated with the XX-chain for conserved dynamics, and with the Ising chain for non-conserved dynamics. Two-time functions are also considered and aging, that is, the dependence of the relaxation process on the age of the system, is also discussed. Results reviewed here are summarised in the last section.

2. Quantum Spin Chains

2.1. *Free Fermionic Models*

The generic XY Hamiltonian that we will consider is[24–26]

$$H = -\frac{1}{2}\sum_{n=1}^{L-1}\left(\frac{1+\kappa}{2}\sigma_n^x\sigma_{n+1}^x + \frac{1-\kappa}{2}\sigma_n^y\sigma_{n+1}^y\right) - \frac{1}{2}\sum_{n=1}^{L} h\sigma_n^z, \qquad (1)$$

where the

$$\sigma_n = 1 \otimes 1 \cdots \otimes \sigma \otimes 1 \cdots \otimes 1$$

are Pauli matrices at site n and κ is an anisotropy parameter with limiting values: $\kappa = 1$ corresponding to the Ising case with a Z_2 symmetry; and $\kappa = 0$ describing the XX-model which has $U(1)$ symmetry. We will consider here only free boundary conditions. The phase diagram and the critical behaviour of this model are known exactly since the work of Barouch and McCoy in 1971 who generalized[27,28] results obtained previously in the case of a vanishing transverse field,[1] or at $\kappa = 1$.[26] It was first considered in the framework of conformal invariance[29] in Ref. 30. In this section, to give a self-consistent presentation, we present in full detail the diagonalization procedure, following, more or less closely, the initial work of Lieb *et al.*[1]

The Hamiltonian can be mapped exactly on a free fermion model, consisting of an assembly of non-interacting Fermi–Dirac oscillators. To proceed, let us first introduce the ladder operators

$$\sigma^{\pm} = \frac{1}{2}(\sigma^x \pm i\sigma^y).$$

In the diagonal base of the σ^z component, they simply act as $\sigma^+|\downarrow\rangle = |\uparrow\rangle$ and $\sigma^-|\uparrow\rangle = |\downarrow\rangle$. They satisfy the anticommutation rules at the same site

$$\{\sigma^+, \sigma^-\} = 1,$$

and by construction they commute at different sites. They look like Fermi operators except that they commute on different sites. True fermionic operators are obtained through a Jordan–Wigner transformation.[15]

Consider a basis vector with all spins down (in the z-direction) and use the notation $|1\rangle \equiv |\uparrow\rangle$ and of course $|0\rangle \equiv |\downarrow\rangle$; then this state will be the vacuum state destroyed by all the lowering operators σ^-,

$$\sigma_n^-|00\cdots0\rangle = 0, \quad \forall n.$$

From this vacuum state, all the other states can be built up by applying raising operators σ^+. The situation looks very much the same as with fermions. But to have really fermions we need antisymmetry, i.e. anticommutation rules also at different sites. We introduce new operators,

$$c_n = A(n)\sigma_n^-, \qquad c_n^+ = \sigma_n^+ A^+(n),$$

where $A(n)$ is a unitary operator commuting with $\sigma_n^\pm$,

$$[A(n), \sigma_n^\pm] = 0.$$

Then automatically we have

$$\{c_n^+, c_n\} = \{\sigma_n^+, \sigma_n^-\} = 1$$

and in particular

$$\sigma_n^z = 2\sigma_n^+\sigma_n^- - 1 = 2c_n^+c_n - 1. \tag{2}$$

In order to fulfil the antisymmetry principle (sign change under particle exchange), the creation and annihilation operators must satisfy[31]

$$c_l^+|n_1, n_2, \ldots, n_l, \ldots\rangle = (-1)^{\Sigma_l}(1-n_l)|n_1, n_2, \ldots, n_l+1, \ldots\rangle,$$
$$c_l|n_1, n_2, \ldots, n_l, \ldots\rangle = (-1)^{\Sigma_l} n_l|n_1, n_2, \ldots, n_l-1, \ldots\rangle,$$

where $\Sigma_l = \sum_{i=1}^{l-1} n_i$ is the number of particles on the left of the l site. We should find now an operator representation of the sign factor $(-1)^{\Sigma_l}$. It is obvious that the choice

$$A(l) = \prod_{i=1}^{l-1}(-\sigma_i^z)$$

will perfectly do the job.[31] This leads finally to the so-called Jordan–Wigner transformations[15]

$$c_n = \prod_{i=1}^{n-1}(-\sigma_i^z)\sigma_n^- = \prod_{i=1}^{n-1} \exp\left(i\pi\sigma_i^+\sigma_i^-\right)\sigma_n^- \tag{3}$$

and the adjoint relation. Inverting these relations, we obtain expressions of the ladder operators and the original Pauli matrices in terms of the

fermionic creation and annihilation operators c^+ and c. Replacing this into our Hamiltonian we obtain the quadratic form

$$H = \sum_{n,m=1}^{L} c_n^+ A_{nm} c_m + \frac{1}{2}(c_n^+ B_{nm} c_m^+ - c_n B_{nm} c_m), \tag{4}$$

where the real matrices A and B are, respectively, symmetric, and antisymmetric since the Hamiltonian is hermitian. The quadratic nature of the Hamiltonian in terms of the Fermi operators insures the integrability of the model. As in the bosonic case, this form can be diagonalized by a Bogoliubov transformation.[1,32]

Let us mention here briefly that more general quantum spin-$\frac{1}{2}$ chains are not tractable using this approach. For example, in the Heisenberg model[11]

$$H = J \sum_n \vec{\sigma}_n \vec{\sigma}_{n+1},$$

there are terms of the form

$$\sigma_n^z \sigma_{n+1}^z \propto c_n^+ c_n c_{n+1}^+ c_{n+1},$$

leading to interacting fermions. With longer range interactions, such as $\sigma_n^x \sigma_{n+p}^x$, or magnetic fields in the x or y directions, another problem arises due to the non-locality of the Jordan–Wigner transformations. For example a next nearest neighbour interaction $\sigma_n^x \sigma_{n+2}^x$ generates quartic terms like

$$c_n^\mu c_{n+1}^+ c_{n+1} c_{n+2}^\nu,$$

where the μ and ν superscripts refer to either creation or annihilation operators. In the case of a magnetic field, let us say in the x direction, we have additional terms proportional to the spin operators

$$\sigma_n^x = \left(\prod_{i=1}^{n-1} (c_i^+ + c_i)(c_i^+ - c_i) \right) (c_n^+ + c_n),$$

which are clearly even worse. Non-local effects also appear when dealing with closed boundary conditions.[1,25]

Nevertheless, the Hamiltonian (1) is not the most general free-fermionic expression. We can still add for example terms of the form $\sigma_n^x \sigma_{n+1}^y - \sigma_n^y \sigma_{n+1}^x$, the so-called Dzyaloshinskii–Moriya interaction[33,34] or play with the boundary conditions.[35]

2.2. *Canonical Diagonalization*

We now come to the diagonalization of the Hamiltonian (1). For that purpose, we express the Jordan–Wigner transformation in terms of Clifford operators[36] Γ_n^1, Γ_n^2,

$$\Gamma_n^1 = \left(\prod_{i=1}^{n-1} -\sigma_i^z\right)\sigma_n^x, \qquad \Gamma_n^2 = -\left(\prod_{i=1}^{n-1} -\sigma_i^z\right)\sigma_n^y. \tag{5}$$

These operators are the $2L$-generators of a Clifford algebra since

$$\{\Gamma_n^i, \Gamma_k^j\} = 2\delta_{ij}\delta_{nk}, \quad \forall i,j = 1,2; \ \forall n,k = 1,\ldots,L, \tag{6}$$

and are real operators, that is ${\Gamma_n^i}^+ = \Gamma_n^i$. They can be viewed as non-properly normalised Majorana fermions. The different terms in the original Hamiltonian are expressed as

$$\sigma_n^z = i\Gamma_n^1\Gamma_n^2, \qquad \sigma_n^x\sigma_{n+1}^x = -i\Gamma_n^2\Gamma_{n+1}^1, \qquad \sigma_n^y\sigma_{n+1}^y = i\Gamma_n^1\Gamma_{n+1}^2\,. \tag{7}$$

Introducing the two-component spinor

$$\Gamma_n = \begin{pmatrix}\Gamma_n^1\\ \Gamma_n^2\end{pmatrix},$$

one can write the Hamiltonian in the form

$$H = \frac{1}{4}\sum_{n=1}^{L-1}\Gamma_n^\dagger\left[\sigma^{\mathbf{y}} + i\kappa\sigma^{\mathbf{x}}\right]\Gamma_{n+1} + \frac{1}{4}\sum_{n=1}^{L}\Gamma_n^\dagger h\sigma^{\mathbf{y}}\Gamma_n, \tag{8}$$

where $\Gamma_n^\dagger = (\Gamma_n^1, \Gamma_n^2)$ and

$$\sigma^{\mathbf{y}} = \begin{pmatrix}0 & -i\\ i & 0\end{pmatrix}, \qquad \sigma^{\mathbf{x}} = \begin{pmatrix}0 & 1\\ 1 & 0\end{pmatrix},$$

are the Pauli matrices, not to be confused with the initial spin operators. Introducing the $2L$-component operator $\mathbf{\Gamma}^\dagger = (\Gamma_1^\dagger, \Gamma_2^\dagger, \ldots, \Gamma_L^\dagger)$, the Hamiltonian is given by

$$H = \frac{1}{4}\mathbf{\Gamma}^\dagger\mathbf{T}\mathbf{\Gamma}, \tag{9}$$

where $\mathbf{T}$ is a $2L \times 2L$ hermitian matrix[37,38] given by

$$\mathbf{T} = \begin{pmatrix} \mathbf{D} & \mathbf{F} & 0 & \dots & & 0 \\ \mathbf{F}^\dagger & \mathbf{D} & \mathbf{F} & 0 & \dots & 0 \\ 0 & \ddots & \ddots & \ddots & 0 & \\ & & & & & \\ & & & & & \\ 0 & \dots & 0 & \mathbf{F}^\dagger & \mathbf{D} & \mathbf{F} \\ 0 & \dots & & 0 & \mathbf{F}^\dagger & \mathbf{D} \end{pmatrix}, \tag{10}$$

$$\mathbf{D} = h\sigma^{\mathbf{y}}, \qquad \mathbf{F} = \frac{1}{2}\left(\sigma^{\mathbf{y}} + i\kappa\sigma^{\mathbf{x}}\right). \tag{11}$$

To diagonalize H, we introduce the unitary transformation matrix $\mathbf{U}$ built up on the eigenvectors of the $\mathbf{T}$ matrix,

$$\mathbf{T}V_q = \epsilon_q V_q, \quad q = 1, \dots, 2L,$$

with the orthogonality and completeness relations

$$\sum_{i=1}^{2L} V_q(i)V_{q'}(i) = \delta_{qq'}, \qquad \sum_{q=1}^{2L} V_q(i)V_q(i') = \delta_{ii'}.$$

Inserting into (9) the expression $\mathbf{T} = \mathbf{U}\mathbf{\Lambda}\mathbf{U}^\dagger$ where $\mathbf{\Lambda}_{pq} = \epsilon_q\delta_{pq}$ is the diagonal matrix, one arrives at

$$H = \frac{1}{4}\mathbf{\Gamma}^\dagger\mathbf{U}\mathbf{\Lambda}\mathbf{U}^\dagger\mathbf{\Gamma} = \frac{1}{4}\mathbf{X}^\dagger\mathbf{\Lambda}\mathbf{X} = \frac{1}{4}\sum_{q=1}^{2L}\epsilon_q x_q^+ x_q,$$

with the diagonal $2L$-component operator

$$\mathbf{X} = \mathbf{U}^\dagger\mathbf{\Gamma}.$$

We introduce now the following parametrisation, which will become clear later, of the eigenvectors V_q:

$$V_q = \frac{1}{\sqrt{2}}\begin{pmatrix} \phi_q(1) \\ -i\psi_q(1) \\ \phi_q(2) \\ -i\psi_q(2) \\ \vdots \\ \phi_q(L) \\ -i\psi_q(L) \end{pmatrix}. \tag{12}$$

Using this parametrisation, the operators x_q and their adjoints are given by

$$x_q = \frac{1}{\sqrt{2}} \sum_{i=1}^{L} \left[\phi_q^*(i)\Gamma_i^1 + i\psi_q^*(i)\Gamma_i^2 \right],$$
$$x_q^+ = \frac{1}{\sqrt{2}} \sum_{i=1}^{L} \left[\phi_q(i)\Gamma_i^1 - i\psi_q(i)\Gamma_i^2 \right].$$

Now, if we consider the normalised operators

$$d_q = \frac{1}{\sqrt{2}} x_q,$$

we can easily check that together with the adjoints d_q^+, they define Dirac fermions, that is they satisfy the anticommutation rules

$$\{d_q^+, d_{q'}\} = \delta_{q,q'}, \qquad \{d_q^+, d_{q'}^+\} = 0, \qquad \{d_q, d_{q'}\} = 0. \tag{13}$$

For example, the first bracket is evaluated as

$$\begin{aligned}\{d_q^+, d_{q'}\} = \; & \frac{1}{4} \sum_{i,j} \phi_q(i)\phi_{q'}^*(j)\{\Gamma_i^1, \Gamma_j^1\} + \psi_q(i)\psi_{q'}^*(j)\{\Gamma_i^2, \Gamma_j^2\} \\ & -i\psi_q(i)\phi_{q'}^*(j)\{\Gamma_i^2, \Gamma_j^1\} + i\phi_q(i)\psi_{q'}^*(j)\{\Gamma_i^1, \Gamma_j^2\},\end{aligned}$$

and using the anticommutation rules for the Clifford operators and the normalisation of the eigenvectors one is led to the above mentioned result.

Finally we have the free fermion Hamiltonian

$$H = \frac{1}{2} \sum_{q=1}^{2L} \epsilon_q d_q^+ d_q. \tag{14}$$

We now take into account the particular structure of the $\mathbf{T}$ matrix. Due to the absence of the diagonal Pauli matrix $\sigma^{\mathbf{z}}$ in the expression of $\mathbf{T}$, the non-vanishing elements $\mathbf{T}_{ij}$ are those with $i+j$ odd, all even terms are vanishing. This means that by squaring the $\mathbf{T}$ matrix we can decouple the original $2L$-eigenproblem into two L-eigenproblems. The easiest way to see this is to rearrange the matrix $\mathbf{T}$ in the form

$$\mathbf{T} = \begin{pmatrix} 0 & \mathbf{C} \\ \mathbf{C}^\dagger & 0 \end{pmatrix}, \tag{15}$$

where the $L \times L$ matrix $\mathbf{C}$ is given by

$$\mathbf{C} = -i \begin{pmatrix} h & J_y & & & \\ J_x & h & J_y & \mathcal{O} & \\ & J_x & \ddots & \ddots & \\ & \mathcal{O} & \ddots & \ddots & J_y \\ & & & J_x & h \end{pmatrix}, \tag{16}$$

with $J_x = (1+\kappa)/2$ and $J_y = (1-\kappa)/2$. Squaring the $\mathbf{T}$ matrix gives[g]

$$\mathbf{T}^2 = \begin{pmatrix} \mathbf{C}\mathbf{C}^\dagger & 0 \\ 0 & \mathbf{C}^\dagger\mathbf{C} \end{pmatrix}. \tag{17}$$

In this new basis the eigenvectors V_q are simply given by

$$V_q = \frac{1}{\sqrt{2}} \begin{pmatrix} \phi_q(1) \\ \phi_q(2) \\ \vdots \\ \phi_q(L) \\ -i\psi_q(1) \\ \vdots \\ -i\psi_q(L) \end{pmatrix},$$

and together with $\mathbf{T}^2$ we finally obtain the decoupled eigenvalue equations

$$\mathbf{C}\mathbf{C}^\dagger \phi_q = \epsilon_q^2 \phi_q, \tag{18}$$

$$\mathbf{C}^\dagger\mathbf{C} \psi_q = \epsilon_q^2 \psi_q. \tag{19}$$

Since the $\mathbf{C}\mathbf{C}^\dagger$ and $\mathbf{C}^\dagger\mathbf{C}$ are real symmetric matrices, their eigenvectors can be chosen real and they satisfy completeness and orthogonality relations. This justifies the initial parametrisation of the vectors V_q and one recovers the original formulation of Lieb, Schultz and Mattis.[1]

Finally, one can notice another interesting property of the $\mathbf{T}$ matrix which is related to the particle–hole symmetry.[37] Due to the off-diagonal structure of $\mathbf{T}$, we have

$$-i\mathbf{C}\psi_q = \epsilon_q \phi_q, \qquad \mathbf{C}^\dagger \phi_q = -i\epsilon_q \psi_q \tag{20}$$

and we see that these equations are invariant under the simultaneous change $\epsilon_q \to -\epsilon_q$ and $\psi_q \to -\psi_q$. So, to each eigenvalue $\epsilon_q \geq 0$ associated to the

[g]The supersymmetric structure appearing in the $\mathbf{T}^2$ matrix has been used in Ref. 39.

vector V_q corresponds an eigenvalue $\epsilon_{q'} = -\epsilon_q$ associated to the vector

$$V_{q'} = \frac{1}{\sqrt{2}} \begin{pmatrix} \phi_q(1) \\ \phi_q(2) \\ \vdots \\ \phi_q(L) \\ i\psi_q(1) \\ \vdots \\ i\psi_q(L) \end{pmatrix} .$$

Let us classify the eigenvalues such as

$$\epsilon_{q+L} = -\epsilon_q, \quad \forall q = 1, \ldots, L,$$

with $\epsilon_q \geq 0$ $\forall q = 1, \ldots, L$. Then the Hamiltonian can be written as

$$H = \frac{1}{2} \sum_{q=1}^{L} (\epsilon_q d_q^+ d_q - \epsilon_q d_{q+L}^+ d_{q+L}),$$

where the operators with $q = 1, \ldots, L$ are associated with particles and the operators with $q = L+1, \ldots, 2L$ are associated with holes, that is, negative energy particles. Thus, by the usual substitution

$$\eta_q^+ = d_q^+, \quad \forall q = 1, \ldots, L; \qquad \eta_q^+ = d_{q+L}, \quad \forall q = 1, \ldots, L, \tag{21}$$

we rewrite now the Hamiltonian in the form

$$H = \frac{1}{2} \sum_{q=1}^{L} \left(\epsilon_q \eta_q^+ \eta_q - \epsilon_q \eta_q \eta_q^+ \right) = \sum_{q=1}^{L} \epsilon_q \left(\eta_q^+ \eta_q - \frac{1}{2} \right). \tag{22}$$

2.3. *Excitation Spectrum and Eigenvectors*

The problem now essentially resides in solving the two linear coupled equations $-i\mathbf{C}\psi_q = \epsilon_q \phi_q$ and $i\mathbf{C}^\dagger \phi_q = \epsilon_q \psi_q$. We will present here the solutions of two particular cases, namely the XY-chain without field[1,25] and the Ising quantum chain in a transverse field.[26] In the following we assume, without loss of generality, that the system size L is even number and $\kappa \geq 0$.

2.3.1. *XY-Chain*

From $i\mathbf{C}^\dagger\phi_q = \epsilon_q\psi_q$, we have the bulk equations

$$\begin{aligned}\frac{1-\kappa}{2}\phi_q(2k-1) + \frac{1+\kappa}{2}\phi_q(2k+1) &= -\epsilon_q\psi_q(2k),\\ \frac{1-\kappa}{2}\phi_q(2k) + \frac{1+\kappa}{2}\phi_q(2k+2) &= -\epsilon_q\psi_q(2k+1).\end{aligned} \tag{23}$$

Due to the parity coupling of these equations, we have two types of solutions:

$$\phi_q^I(2k) = \psi_q^I(2k-1) = 0, \quad \forall k, \tag{24}$$

and

$$\phi_q^{II}(2k-1) = \psi_q^{II}(2k) = 0, \quad \forall k. \tag{25}$$

In the first case, the bulk equations that remain to be solved are

$$\frac{1-\kappa}{2}\phi_q^I(2k-1) + \frac{1+\kappa}{2}\phi_q^I(2k+1) = -\epsilon_q\psi_q^I(2k),$$

with the boundary conditions

$$\phi_q^I(L+1) = \psi_q^I(0) = 0\ . \tag{26}$$

Here we absorb the minus sign in Eq. (23) into the redefinition

$$\widetilde{\psi}_q = -\psi_q\ .$$

Using the ansatz $\phi_q^I(2k-1) = e^{iq(2k-1)}$ and $\widetilde{\psi}_q^I(2k) = e^{iq2k}e^{i\theta_q}$ to solve the bulk equations (23), we obtain

$$\cos q + i\kappa\sin q = \epsilon_q e^{i\theta_q}, \tag{27}$$

that is

$$\epsilon_q = \sqrt{\cos^2 q + \kappa^2\sin^2 q} \geq 0 \tag{28}$$

and the phase shift

$$\theta_q = \arctan(\kappa\tan q)\ , \tag{29}$$

with $0 < \theta_q \leq 2\pi$ to avoid ambiguity. The eigenvectors associated to the positive excitations satisfying the boundary equations are then

$$\begin{aligned}\phi_q^I(2k+1) &= A_q\sin\left(q(2k+1) - \theta_q\right),\\ \widetilde{\psi}_q^I(2k) &= A_q\sin(q2k),\end{aligned} \tag{30}$$

with

$$q(L+1) = n\pi + \theta_q, \tag{31}$$

or more explicitly

$$q = \frac{\pi}{L+1}\left(n + \frac{1}{\pi}\arctan\left(\kappa \tan q\right)\right) . \tag{32}$$

The normalisation constant A_q is easy to evaluate and is actually dependent on q. Using $\theta_q = q(L+1) + n\pi$, one can write ϕ_q^I in the form

$$\phi_q^I(2k+1) = -A_q \delta_q \sin q(L-2k) ,$$

where $\delta_q = (-1)^n$ is given by the sign of $\cos q(L+1)$. Equation (32) has $L/2-1$ real solutions, that in the lowest order in $1/L$ are given by

$$q_n \simeq \frac{\pi}{L}\left(n - \nu_n\right), \tag{33}$$

$$\nu_n = \frac{n}{L} - \frac{1}{\pi}\arctan\left(\kappa \tan\left(\frac{n\pi}{L}\right)\right), \quad n = 1, 2, \ldots, \frac{1}{2}L - 1. \tag{34}$$

There is also a complex root of (32)

$$q_0 = \frac{1}{2}\pi + iv, \tag{35}$$

where v is the solution of

$$\tanh v = \kappa \tanh[v(L+1)] . \tag{36}$$

With the parametrisation $x = e^{-2v}$ and $\rho^2 = (1-\kappa)/(1+\kappa)$, one is led to the equation

$$x = \frac{\rho^2}{1 - x^L(1-\rho^2 x)}$$

and the first nontrivial approximation leads to

$$x^{-1} \simeq \rho^{-2} - (1-\rho^4)\rho^{-2(L-1)}. \tag{37}$$

The excitation associated with this localised mode (see the form of ϕ_{q_0} and ψ_{q_0} with $q_0 = \pi/2 + iv$) is exponentially close to the ground state, that is

$$\epsilon_{q_0} \simeq (1+\rho^2)\rho^L. \tag{38}$$

From this observation, together with some weak assumptions, the complete phase diagram of the system can be obtained. We will discuss this point later.

The solutions of the second type satisfy the same bulk equations but the difference lies in the boundary conditions $\phi_q^{II}(0) = \psi_q^{II}(L+1) = 0$. The eigenvectors are given by

$$\begin{aligned} \phi_q^{II}(2k) &= A_q \sin(q2k), \\ \widetilde{\psi}_q^{II}(2k+1) &= A_q \sin(q(2k+1)+\theta_q) = -A_q \delta_q \sin q(L-2k), \end{aligned} \tag{39}$$

with

$$q = \frac{\pi}{L+1}\left(n - \frac{1}{\pi}\arctan\left(\kappa \tan q\right)\right), \tag{40}$$

which has $L/2$ real roots. To the leading order, one gets

$$q_n = \frac{\pi}{L}\left(n - \nu_n\right), \tag{41}$$

$$\nu_n = \frac{n}{L} + \frac{1}{\pi}\arctan\left(\kappa \tan\left(\frac{n\pi}{L}\right)\right), \quad n = 1, 2, \ldots, \frac{1}{2}L \tag{42}$$

which completes the solution of the XY-chain.

2.3.2. *Ising Chain*

The solution of the Ising chain ($\kappa = 1$) proceeds along the same lines.[26] The bulk equations are

$$h\phi_q(k) + \phi_q(k+1) = \epsilon_q \widetilde{\psi}_q(k), \tag{43}$$

with the boundary conditions

$$\phi_q(L+1) = \psi_q(0) = 0. \tag{44}$$

With the same ansatz as before, one arrives at

$$h + e^{iq} = \epsilon_q e^{i\theta_q}, \tag{45}$$

that is,

$$\epsilon_q = \sqrt{(h+\cos q)^2 + \sin^2 q}, \tag{46}$$

$$\theta_q = \arctan\left(\frac{\sin q}{h+\cos q}\right). \tag{47}$$

Taking into account the boundary conditions, the solutions are readily expressed as

$$\phi_q(k) = A \sin(qk - \theta_q), \qquad \psi_q(k) = -A \sin(qk), \tag{48}$$

where q is a solution of the equation

$$q = \frac{\pi}{L+1}\left(n + \frac{1}{\pi}\arctan\left(\frac{\sin q}{h+\cos q}\right)\right) . \tag{49}$$

The eigenvectors can then also be written in the form

$$\phi_q(k) = -A(-1)^n \sin(q(L+1-k)), \qquad \psi_q(k) = -A\sin(qk). \tag{50}$$

In the thermodynamic limit, $L \to \infty$, for $h \geq 1$, Eq. (49) gives rise to L real roots. On the other hand, for $h < 1$, there is also one complex root $q_0 = \pi + iv$ associated to a localised mode such that v is solution of

$$\tanh(v(L+1)) = -\frac{\sinh v}{h - \cosh v} . \tag{51}$$

To the leading order, we have $v \simeq \ln h$. The eigenvectors associated to this localised mode are

$$\begin{aligned} \phi_{q_0}(k) &= A(-1)^k \sinh(v(L+1-k)), \\ \psi_{q_0}(k) &= -A(-1)^k \sinh(vk). \end{aligned} \tag{52}$$

Exactly at the critical value $h = 1$, we have $\theta_q = q/2$, which gives a simple quantisation condition:

$$q = \frac{2n\pi}{2L+1}, \quad n = 1, 2, \ldots, L. \tag{53}$$

Changing q into $\pi - q$, we have[40]

$$\begin{aligned} \phi_q(k) &= \frac{2}{\sqrt{2L+1}}(-1)^{k+1}\cos(q(k-1/2)), \\ \psi_q(k) &= \frac{2}{\sqrt{2L+1}}(-1)^k \sin(qk), \end{aligned} \tag{54}$$

$$\epsilon_q = 2\left|\sin\frac{1}{2}q\right|, \tag{55}$$

with $q = (2n+1)\pi/(2L+1)$ and $n = 0, 1, \ldots, L-1$.

3. Equilibrium Behaviour

3.1. *Critical Behaviour*

From the knowledge of the eigenvectors ϕ and ψ, and the corresponding one-particle excitations, we can in principle calculate all the physical quantities, such as magnetization, energy density or correlation functions. However, they are, in general, complicated many-particles expectation values due to the non-local expression of the spin operators in terms of fermions. We will

come later to this aspect when considering the dynamics. Nevertheless, quantities that can be expressed locally in terms of fermions are simple, such as correlations involving only σ^z operators or σ_1^x.

3.1.1. *Surface Magnetization*

A very simple expression is obtained for the surface magnetization, that is the magnetization on the x (or y) direction of the first site. The behaviour of the first spin[41,42] gives general information on the phase diagram of the chain.[27–29] Since the expectation value of the magnetization operator in the ground state vanishes, we have to find a bias. The usual way will be to apply a magnetic field in the desired direction, in order to break the ground state symmetry. Of course this procedure has the disadvantage of breaking the quadratic structure of the Hamiltonian. Another route is to extract the magnetization behaviour from that of the correlation function. In this respect, the $x(y)$ component of the surface magnetization is obtained from the autocorrelation function $G(\tau) = \langle \sigma_1^x(0)\sigma_1^x(\tau)\rangle$ in imaginary time τ where $\sigma_1^x(\tau) = e^{\tau H}\sigma_1^x e^{-\tau H}$. Introducing the diagonal basis of H, we have

$$G(\tau) = |\langle\sigma|\sigma_1^x|0\rangle|^2 e^{-\tau(E_\sigma - E_0)} + \sum_{i>1} |\langle i|\sigma_1^x|0\rangle|^2 e^{-\tau(E_i - E_0)}, \qquad (56)$$

where $|0\rangle$ is the ground state with energy E_0 and $|\sigma\rangle = \eta_1^+|0\rangle$ is the first excited state with one diagonal fermion of which the energy is $E_\sigma = E_0 + \epsilon_1$. From the previous section we see that we have a vanishing excitation for $h < 1$ in the thermodynamic limit $L \to \infty$ leading to a degenerate ground state. This implies that in the limit of large τ, only the first term in the previous expression of the autocorrelation function contributes,

$$\lim_{\tau\to\infty} G(\tau) = [m_s^x]^2, \qquad (57)$$

where $m_s^x = \langle\sigma|\sigma_1^x|0\rangle$. Noticing that $\sigma_1^x = \Gamma_1^1 = c_1^+ + c_1$ and making use of the inverse expression, $\Gamma_n^1 = \sum_q \phi_q(n)(\eta_q^+ + \eta_q)$, one obtains

$$m_s^x = \langle\sigma|\sigma_1^x|0\rangle = \phi_1(1). \qquad (58)$$

Similarly, one can obtain $m_s^y = \langle\sigma|\sigma_1^y|0\rangle = \psi_1(1)$.

Following Peschel,[41] it is now possible to obtain a closed formula for the surface magnetization.[42] In the semi-infinite limit $L \to \infty$, for $h < 1$, the first gap $E_\sigma - E_0 = \epsilon_1$ vanishes due to spontaneous symmetry breaking. In this case, Eqs. (20) simplify into

$$\mathbf{C}^\dagger\phi_1 = 0, \qquad \mathbf{C}\psi_1 = 0. \qquad (59)$$

Noticing that by changing κ into $-\kappa$, m^x and m^y are interchanged, in the following we will consider only the x-component.

To find the eigenvector ϕ_1, we rewrite $\mathbf{C}^\dagger\phi_1 = 0$ in the iterative form

$$\begin{pmatrix} \phi_1(n+1) \\ \phi_1(n) \end{pmatrix} = \mathbf{K}_n \begin{pmatrix} \phi_1(n) \\ \phi_1(n-1) \end{pmatrix}, \tag{60}$$

where $\mathbf{K}_n$ is a 2×2 matrix associated to the site n, for homogeneous coupling constants it can be written explicitly as

$$\mathbf{K}_n = \mathbf{K} = -\begin{pmatrix} 2h/(1+\kappa) & (1-\kappa)/(1+\kappa) \\ -1 & 0 \end{pmatrix}. \tag{61}$$

By iterations, we obtain for the $(n+1)$th component of the eigenvector ϕ_1 the expression

$$\phi_1(n+1) = (-1)^n \phi_1(1) \left(\mathbf{K}^n\right)_{11}, \tag{62}$$

where the indices 11 stand for the 1,1 component of the matrix $\mathbf{K}^n$. The normalisation of the eigenvector, $\sum_i \phi_1^2(i) = 1$, leads to the final expression[42]

$$m_s^x = \left(1 + \sum_{n=1}^{\infty} \left|\left(\mathbf{K}^n\right)_{11}\right|^2\right)^{-1/2}. \tag{63}$$

First we note that the transition from a paramagnetic to an ordered phase is characterised by the divergence of the sum entering (63). On the other hand, since for a one-dimensional quantum system with short-range interactions, the surface cannot order by itself, the surface transition is the signal of a transition in the bulk. It means that one can obtain some knowledge of the bulk by studying surface quantities. To do so, we first diagonalize the $\mathbf{K}$ matrix. The eigenvalues are

$$\lambda_\pm = \frac{1}{1+\kappa}(h \pm \sqrt{h^2 + \kappa^2 - 1}) \tag{64}$$

for $h^2 + \kappa^2 > 1$ and complex conjugates, otherwise

$$\lambda_\pm = \frac{1}{1+\kappa}(h \pm i\sqrt{1 - h^2 - \kappa^2}) = \rho \exp(\pm i\vartheta), \tag{65}$$

with $\rho = \sqrt{(1-\kappa)/(1+\kappa)}$ and $\vartheta = \arctan(\sqrt{1-h^2-\kappa^2}/h)$ and they become degenerate on the line $h^2 + \kappa^2 = 1$. The leading eigenvalue gives the behaviour of $\phi_1^2(n) \sim |\lambda_+|^{2n}$ which, for an ordered phase, implies that $|\lambda_+| < 1$. The first mode is then localised near the surface. From this condition on λ_+, we see that it corresponds to $h < h_c = 1$. For $h > 1$, the

surface magnetization exactly vanishes and we infer that the bulk is also unordered. So that for any anisotropy κ, the critical line is at $h = 1$ and in fact it belongs to the $2d$-Ising[43] universality class.[h] As shown hereafter, the special line $h^2 + \kappa^2 = 1$, where the two eigenvalues collapse, separates an ordinary ferromagnetic phase ($h^2 + \kappa^2 > 1$) from an oscillatory one ($h^2 + \kappa^2 < 1$).[27] This line is known as the disorder line of the model. The line at vanishing anisotropy, $\kappa = 0$, is a continuous transition line (with diverging correlation length) called the anisotropic transition where the magnetization changes from the x to the y direction.

In the ordered phase, the decay of the eigenvector ϕ_1 gives the correlation length of the system, which is related to the leading eigenvalue by

$$\phi_1^2(n) \sim |\lambda_+|^2 \sim \exp(-n/\xi), \tag{66}$$

so that

$$\xi = \frac{1}{2|\ln|\lambda_+||}\,. \tag{67}$$

By analysing λ_+, it is straightforward to see that the correlation length exponent defined as $\xi \sim \delta^{-\nu}$, with $\delta \propto 1 - h$ for the Ising transition and $\delta \propto \kappa$ for the anisotropic one, is $\nu = 1$. Of course, a specific analysis of formula (63) leads to the behaviour of the surface magnetization. At fixed anisotropy κ, close enough to the Ising transition line we have

$$m_s^x \sim (1 - h)^{1/2}, \tag{68}$$

giving the surface critical exponent $\beta_s^I = 1/2$. In the oscillatory phase, a new length scale appears given by ϑ^{-1}. A straightforward calculation gives for the eigenvector ϕ_1 the expression

$$\phi_1(n) = (-1)^n \rho^n \frac{1+\kappa}{h \tan\vartheta} \sin(n\vartheta)\phi_1(1), \tag{69}$$

which leads to

$$m_s^x \sim \kappa^{1/2}, \tag{70}$$

close to the anisotropy line, so $\beta_s^a = 1/2$ too.

We have seen here how from the study of surface properties[42] one can determine very simply (by the diagonalization of a 2×2 matrix) the bulk

[h] To get an account on the connection between d-dimensional quantum systems and $d+1$-dimensional classical systems, one can refer to Kogut's celebrated review.[44] The idea lies in the fact that, in imaginary (Euclidean) time τ, the evolution operator $e^{-\tau H}$, where H is the Hamiltonian of the d-dimensional quantum system, can be interpreted as the transfer matrix of a $d + 1$ classical system.

phase diagram and also the exact correlation length.[27] One may also notice that expression (63) is suitable for finite size analysis,[45] cut off at some size L. In fact for the Ising chain, to be precise, one can work with symmetry breaking boundary conditions.[48] That is, working on a finite chain, we fix the spin at one end (which is equivalent to setting $h_L = 0$) and evaluate the magnetization at the other end. In this case, the surface magnetization is exactly given by (63) where the sum is truncated at $L-1$. The fixed spin at the end of the chain, let us say $\sigma_L^x = +$, leads to an extra Zeeman term since we have now in the Hamiltonian the term $-(J_{L-1}/2)\sigma_{L-1}^x$, where the last coupling J_{L-1} plays the role of a magnetic field. The vanishing of h_L induces a two-fold degeneracy of the Hamiltonian which is due to the exact vanishing of one excitation, say ϵ_1. This degeneracy simply reflects the fact that $[\sigma_L^x, H] = 0$. On a mathematical ground, we can see this from the form of the $\mathbf{T}$ matrix which has a block-diagonal structure with a vanishing 2×2 last block. From the vacuum state associated to the diagonal fermions, $|0\rangle$, and its degenerate state $\eta_1^+|0\rangle$, we can form the two ground states

$$|\pm\rangle = \frac{1}{\sqrt{2}}\left(|0\rangle \pm \eta_1^+|0\rangle\right), \tag{71}$$

associated respectively to $\sigma_L^x = +$ and $\sigma_L^x = -$. Since we have a boundary symmetry breaking field, we can directly calculate the surface magnetization from the expectation value of σ_1^x in the associated ground state. It gives $\langle +|\sigma_1^x|+\rangle = \phi_1(1)$, where $\phi_1(1)$ is exactly obtained for any finite size from $\mathbf{C}^\dagger\phi_1 = 0$. This finite-size expression has been used extensively to study the surface properties of several inhomogeneous Ising chains with quenched disorder,[51–54] where a suitable mapping to a surviving random walk[48] problem permits one to obtain exact results.

3.1.2. *Bulk Magnetization*

As stated at the beginning of this section, quantities involving σ^x or σ^y operators are much more involved. Nevertheless, thanks to Wick's theorem, they are computable in terms of Pfaffians[27,46] or determinants whose size is linearly increasing with the site index. For example, if one wants to compute $\langle\sigma|\sigma_l^x|0\rangle$, the magnetization at site l, one has to evaluate the expectation value[47]

$$m_l = \langle\sigma|\sigma_l^x|0\rangle = \langle 0|\eta_1 A_1 B_1 A_2 B_2 \cdots A_{l-1} B_{l-1} A_l|0\rangle, \tag{72}$$

where we have defined $A_i = \Gamma_i^1$ and $B_i = -i\Gamma_i^2$ in order to absorb unnecessary i factors. These notations were initially introduced by Lieb *et al.*[1] Note

that $B^2 = -1$. Since A_l and B_l are linear combinations of Fermi operators,

$$A_l = \sum_q \phi_q(l) \left(\eta_q^+ + \eta_q\right), \qquad B_l = \sum_q \psi_q(l) \left(\eta_q^+ - \eta_q\right), \tag{73}$$

we can apply Wick's theorem for fermions.[1] The theorem states that we may expand the canonical (equilibrium) expectation value, with respect to a bilinear fermionic Hamiltonian, of a product of operators obeying anti-commutation rules, in terms of contraction pairs. For example, if we have to evaluate the product $\langle C_1 C_2 C_3 C_4 \rangle$, we can expand it as

$$\langle C_1 C_2 C_3 C_4 \rangle = \langle C_1 C_2 \rangle \langle C_3 C_4 \rangle - \langle C_1 C_3 \rangle \langle C_2 C_4 \rangle + \langle C_1 C_4 \rangle \langle C_2 C_3 \rangle \, .$$

Due to the fermionic nature of the operators involved, a minus sign appears at each permutation. In our case, it is easy to see that the basic contractions $\langle 0|A_i A_j|0\rangle$ and $\langle 0|B_i B_j|0\rangle$ are vanishing for $i \neq j$. The only contributing terms are those products involving only pairs of the type $\langle 0|\eta_1 A|0\rangle$, $\langle 0|\eta_1 B|0\rangle$ or $\langle 0|BA|0\rangle$. One may also remark that it is unnecessary to evaluate terms of the form $\langle 0|\eta_1 B|0\rangle$ since in this case there is automatically in the product a vanishing term $\langle 0|A_i A_j|0\rangle$ with $i \neq j$. The simplest non-vanishing product appearing in the Wick expansion is

$$\langle 0|\eta_1 A_1|0\rangle \langle 0|B_1 A_2|0\rangle \cdots \langle 0|B_{l-1} A_l|0\rangle \, .$$

The local magnetization m_l is then given by the $l \times l$ determinant[47,48]

$$m_l = \begin{vmatrix} H_1 & G_{11} & G_{12} & \dots & G_{1l-1} \\ H_2 & G_{21} & G_{22} & \dots & G_{2l-1} \\ \vdots & \vdots & \vdots & & \vdots \\ H_l & G_{l1} & G_{l2} & \dots & G_{ll-1} \end{vmatrix}, \tag{74}$$

with

$$H_j = \langle 0|\eta_1 A_j|0\rangle = \phi_1(j), \tag{75}$$

$$G_{jk} = \langle 0|B_k A_j|0\rangle = -\sum_q \phi_q(j)\psi_q(k) \, . \tag{76}$$

This expression for the local magnetization enables one to compute, at least numerically, magnetization profiles[49,50] and to extract scaling behaviour. For example far in the bulk of the Ising chain we have near the transition the power law behaviour $m_b \sim (1-h)^{1/8}$ for $h < 1$ and zero otherwise.[26] To conclude this section, one can also consider more complicated quantities such as two-point correlation functions[1,26] in the same spirit.

3.2. *Time-Dependent Correlation Functions*

Time-dependent correlations functions are of primary importance since experimentally accessible dynamical quantities are, more or less simply, related to them. For general spin chains, the exact analysis of the long time behaviour of spin–spin correlations is a particularly difficult task. The generic time-dependent spin–spin correlation function is

$$\langle \sigma_i^\mu(t)\sigma_j^\nu\rangle,$$

where i, j are space indices, $\mu, \nu = x, y, z$ and where $\langle \ . \ \rangle \equiv \mathrm{Tr}\{ \ . \ e^{-\beta H}\}/\mathrm{Tr}\{e^{-\beta H}\}$ is the canonical quantum expectation at temperature $T = 1/\beta$. The time-dependent operator $\sigma_i^\mu(t) = e^{iHt}\sigma_i^\mu e^{-iHt}$ is given by the usual Heisenberg representation. Most of the approximation schemes developed so far[55,56] are not really relevant for such many-body systems, at least at finite temperature. One is ultimately forced to go on numerical analyses, basically by exact diagonalization of very short chains, although recently there has been significant numerical progress using a time-dependent DMRG (Density Matrix Renormalization Group) procedure.[57]

Nontrivial exact solutions for time-dependent correlations do exist for free fermionic spin chains,[28,58,60–63] due to the non-interacting nature of the excitations. For such chains, not only bulk regimes were investigated but also boundary effects.[64,68–71] On one hand, the z–z correlations are easily calculable due to their local expression in terms of the Fermi operators. They are basically fermion density correlation functions. On the other hand, the x–x correlations are much more involved since in the Fermi representation one has to evaluate string operators. Nevertheless, as for the static correlators, one may use Wick's theorem to reduce them to the evaluation of a Pfaffian, or determinant, whose size is linearly increasing with $i + j$.

For the N-sites free boundary isotropic XY-chain in a transverse field,

$$H = \frac{J}{4}\sum_{j=1}^{N-1}(\sigma_j^x\sigma_{j+1}^x + \sigma_j^x\sigma_{j+1}^x) - \frac{h}{2}\sum_{j=1}^{N}\sigma_j^z,$$

the basic contractions at inverse temperature β are given by:[64]

$$\begin{aligned}\langle A_j(t)A_l\rangle &= \frac{2}{N+1}\sum_q \sin qj \sin ql\left(\cos\varepsilon_q t - i\sin\varepsilon_q t\tanh\frac{\beta\varepsilon_q}{2}\right),\\ \langle A_j(t)B_l\rangle &= \frac{2}{N+1}\sum_q \sin qj \sin ql\left(i\sin\varepsilon_q t - \cos\varepsilon_q t\tanh\frac{\beta\varepsilon_q}{2}\right),\end{aligned} \quad (77)$$

and the symmetry relations

$$\langle B_j(t)B_l\rangle = -\langle A_j(t)A_l\rangle, \qquad \langle B_l(t)A_j\rangle = -\langle A_j(t)B_l\rangle, \tag{78}$$

where the excitation energies are $\varepsilon_q = J\cos q - h$ with $q = n\pi/(N+1)$, $n = 1, \ldots, N$. With the help of these expressions, one is able to evaluate the desired time-dependent correlations, at least numerically.

The z–z correlator, namely $\langle \sigma_j^z(t)\sigma_l^z\rangle$, is given in the thermodynamic limit at infinite temperature $T = \infty$ by[64,65]

$$\langle \sigma_j^z(t)\sigma_l^z\rangle = \left[J_{j-l}(Jt) - (-1)^l J_{j+l}(Jt)\right]^2, \tag{79}$$

where J_n is the Bessel function of the first kind. One has to notice that this result is field independent. The bulk behaviour is obtained by putting j, $l \to \infty$ and keeping $l - j$ finite. One has

$$\langle \sigma_j^z(t)\sigma_l^z\rangle = J_{j-l}^2(Jt) \overset{Jt\gg 1}{\sim} t^{-1}, \tag{80}$$

leading to a power law decay in time. For large time, the boundary effects lead to

$$\langle \sigma_j^z(t)\sigma_l^z\rangle \simeq \frac{8}{\pi J^3 t^3}\left[\sin^2\left(Jt - \frac{\pi r}{2}\right)\right] l^2(l+r)^2, \tag{81}$$

with $r = j - l$ the distance between the two sites. Therefore, the decay in time changes from t^{-1} to t^{-3} near the boundaries.[64]

In the low-temperature limit ($T = 0$), we have a closed expression for $h \geq J$ which is time- and site-independent[64]

$$\langle \sigma_j^z(t)\sigma_l^z\rangle = 1, \tag{82}$$

revealing an ordered ground state. This can be related to the fact that the ground state corresponds to a completely filled energy band, since all the energy excitations are negative. As already stated before, the calculation of the z–z correlation function is an easy task and we will not go on other models.

In order to calculate the x–x time-dependent correlation functions for such free-fermionic chains, one has to evaluate

$$\langle \sigma_j^x(t)\sigma_l^x\rangle = \langle A_1(t)B_1(t)\cdots A_{j-1}(t)B_{j-1}(t)A_j(t)A_1B_1\cdots A_{l-1}B_{l-1}A_l\rangle. \tag{83}$$

In the high temperature limit ($T = \infty$), the bulk correlation function of the isotropic XY-chain in a transverse field h is given by the Gaussian

behaviour[58,60,72]

$$\langle \sigma_j^x(t)\sigma_l^x\rangle = \delta_{jl}\cos ht \exp(-J^2t^2/4), \tag{84}$$

where δ_{jl} is the Kronecker symbol. The boundary effects are hard to take into account due to the fact that the Pfaffian to be evaluated is a Toeplitz determinant[58,59,73] that can be treated only for large order.[58] Nevertheless for a vanishing transverse field, a conjecture was inferred from exact calculations for the boundary nearest sites $i = 1, 2, \ldots, 5$, claiming an asymptotic power-like decay,[68]

$$\langle \sigma_j^x(t)\sigma_l^x\rangle \sim \delta_{jl}t^{-3/2-(j-1)(j+1)} \ . \tag{85}$$

At vanishing temperature and for $h \geq J$, the basic contractions can be evaluated in a closed form too. These lead to[62,64,66,67]

$$\langle \sigma_j^x(t)\sigma_l^x\rangle = \exp(-iht)\exp[i(j-l)\pi/2]\, J_{j-l}(Jt) \tag{86}$$

for the bulk correlation function. The Bessel function gives rise to a $t^{-1/2}$ asymptotic behaviour. So moving from $T = \infty$ to $T = 0$ there is a dramatic change in the time decay behaviour.[64] Finally, one is also able to take into account the free boundary effects. In this case, for large enough time, the behaviour changes from $t^{-1/2}$ to $t^{-3/2}$.[64]

At finite temperature the asymptotic decay of the time-dependent correlators is exponential,[74]

$$\langle \sigma_i^x(t)\sigma_{i+n}^x\rangle \propto t^{2(\nu_+^2+\nu_-^2)} \exp f(n,t), \tag{87}$$

where $f(n,t)$ is a negative monotonically decreasing function with increasing T. The pre-exponents $\nu_\pm$ are known functions[74] of the field h, the temperature and the ratio n/t. When $T \to \infty$, the function $f(n,t)$ diverges logarithmically indicating the change of the decay shape from exponential to Gaussian.[69]

To end this section, one may mention that the decay laws for the x–x time-dependent correlation functions of the anisotropic XY-chain are basically the same as for the isotropic case, namely power law at zero temperature and Gaussian at infinite temperature.[59]

4. Non-Equilibrium Behaviour

4.1. *Heisenberg Equations of Motion*

Non-equilibrium properties of quantum systems have attracted a lot of interest throughout the decades.[75] Precursor studies on free-fermionic spin

chains were performed by Niemeijer[25] and Tjion[76] at the end of the sixties. Soon after, Barouch, McCoy and Dresden[77,78] solved exactly the Liouville equation for the XY-chain and computed the time-dependent transverse magnetization for several non-equilibrium situations. They have shown the occurrence of an algebraic relaxation instead of exponential as predicted by Terwiel and Mazur[79] using a weak coupling limit. More recently, a special focus was pointed on non-equilibrium quantum steady states, which are driven by some currents.[80–82] These studies are motivated by the fact that quantum systems have a natural dynamics, given by the quantum Liouville equation[83]

$$\frac{\partial \rho(t)}{\partial t} = -i[H_T, \rho(t)] \equiv \mathcal{L}(\rho(t)),$$

where ρ is the density operator, H_T the Hamiltonian and where $\mathcal{L}$ is the quantum Liouville super-operator acting on the vector space of linear operators. The expectation value of an operator Q at time t is given by

$$\langle Q \rangle(t) = \mathrm{Tr}\{\rho(t)Q\},$$

where we have assumed that the density operator is normalised to one. The traditional way to study the non-equilibrium properties of a quantum system is to couple it with a bath that can itself be described quantum mechanically, for example an assembly of harmonic oscillators.[84] The total Hamiltonian is then split into three different pieces,

$$H_T = H_s + H_I + H_b$$

where H_s is the system Hamiltonian, H_b the Hamiltonian of the bath and H_I stands for the interaction between the bath and system dynamical variables. Now, the average quantities of the system are obtained with the help of the reduced density operator, that is, the density operator traced over the bath dynamical degrees of freedom,

$$\rho_s(t) = \mathrm{Tr}_b\{\rho(t)\} \ .$$

The expectation value of a dynamical variable Q of the system is given by

$$\langle Q \rangle(t) = \mathrm{Tr}_s\{Q\rho_s(t)\} \ .$$

For a complete review of this approach one can refer to Ref. 85.

Another, simpler, route to out-of-equilibrium problems, is to investigate the relaxation of a non-equilibrium initial state, in which a closed system

has been prepared at time $t = 0$. For a pure initial state, $|\Psi\rangle$, the initial density operator is just the projector

$$\rho = |\Psi\rangle\langle\Psi| \ .$$

The time evolution of the state $|\Psi\rangle$ is thus simply given by the Schrödinger equation and is formally given by

$$|\Psi(t)\rangle = \exp(-iHt)|\Psi\rangle,$$

where H is the Hamiltonian of the closed system.

In the framework of free fermionic models, the easiest way to handle the problem is to solve the Heisenberg equations of motion,[58,59]

$$\frac{d}{dt}X = i[H, X]. \tag{88}$$

Since all the spin variables of the quantum chains can be expressed in terms of the Clifford generators $\{\Gamma\}$, the first step is to solve the equation of motion for these operators. In order to avoid unnecessary minus signs, let us redefine the generators in the form of Ref. 58:

$$\begin{aligned} P_{2n} = X_n &= \left(\prod_{i=-\infty}^{n-1} \sigma_i^z\right)\sigma_n^x \quad (= (-1)^{n-1}\Gamma_n^1), \\ P_{2n+1} = Y_n &= \left(\prod_{i=-\infty}^{n-1} \sigma_i^z\right)\sigma_n^y \quad (= (-1)^{n}\Gamma_n^2), \end{aligned} \tag{89}$$

where the chain sites run from $i = -N$ to $i = N$ with the thermodynamic limit $N \to \infty$ implicitly taken. With the anisotropic Hamiltonian

$$H = -\frac{1}{2}\sum_i \left(J^x\sigma_i^x\sigma_{i+1}^x + J^y\sigma_i^y\sigma_{i+1}^y + h\sigma_i^z\right),$$

the equations of motion are

$$\begin{aligned} \frac{d}{dt}X_n &= J^xY_{n-1} + J^yY_{n+1} - hY_n, \\ \frac{d}{dt}Y_n &= -J^xX_{n+1} - J^yX_{n-1} + hX_n. \end{aligned} \tag{90}$$

The solutions are linear combinations of the initial time operators $\{P_n\}$:

$$\begin{aligned} X_n &= \sum_m X_{n-m}f_m(t) + Y_{n-m}h_m(t), \\ Y_n &= \sum_m -X_{n-m}h_{-m}(t) + Y_{n-m}f_m(t), \end{aligned} \tag{91}$$

with

$$f_m(t) = \frac{1}{2\pi}\int_{-\pi}^{\pi} dq \exp(-imq)\cos(\epsilon_q t), \tag{92}$$

$$h_m(t) = \frac{1}{2\pi}\int_{-\pi}^{\pi} dq\ \exp(-imq)\frac{\sin(\epsilon_q t)}{\epsilon_q}\left(J^x e^{iq} - h + J^y e^{-iq}\right), \tag{93}$$

where the excitation energies are

$$\epsilon_q = [((J^x + J^y)\cos q - h)^2 + (J^x - J^y)^2 \sin^2 q]^{1/2}. \tag{94}$$

In the special cases of the critical Ising chain, corresponding to $J^x = h = 1$ and $J^y = 0$, and the isotropic XX-chain with $J_x = J_y = 1/2$, one obtains closed analytical expressions for the basic time-dependent operators.[59] These closed forms permit one to analyse exactly the long time behaviour of transverse magnetization profiles, end-to-end correlations,[86,88] two-time transverse correlation functions and so on. In order to illustrate the procedure we concentrate on the critical Ising chain following Ref. 58. The isotropic chain can be treated on the same footings. At $J^x = h = 1$ and $J^y = 0$, the equations of motion simplify into

$$\frac{d}{dt}P_n = P_{n-1} - P_{n+1}, \tag{95}$$

where we have used the operator notation P in order to have more compact expressions. By iteration, one obtains for the lth order term

$$\left(\frac{d}{dt}\right)^l P_n = \sum_{k=0}^{l}(-1)^l \binom{k}{l} P_{n-l+2k}, \tag{96}$$

where the $\binom{k}{l}$ are the binomial coefficients. One can now sum up the Taylor series

$$\sum_{l=0}^{\infty}\frac{z^l}{l!}\left(\frac{d}{dt}\right)^l P_n = \sum_{k=-\infty}^{\infty} P_{n-k}J_k(2z)\ , \tag{97}$$

where J_n is the Bessel function of integer order n. Finally one has

$$P_n(t) = \sum_{k=-\infty}^{\infty} P_k J_{n-k}(2t)\ , \tag{98}$$

which gives the time dependence of the basic operators. Putting $F_t(j) = J_j(2t)$, the time evolution of the operators P_n is expressed as a discrete

convolution product,

$$P_n(t) = \sum_k F_t(n-k)P_k = (F_t \star P)(n) \ , \tag{99}$$

where the kernel for the critical Ising chain is simply the integer Bessel function $J_k(2t)$. This formula is exact for an infinite chain. In the case of a finite size system, one has to take care for site indices close to the boundaries. We will come back later on this point. Alternatively, one can express in closed form the functions f and h introduced previously. One has for the critical Ising chain

$$\begin{aligned} f_m(t) &= \frac{1}{2\pi}\int_{-\pi}^{\pi} dq\, e^{-imq} \cos\left(2t \sin\frac{q}{2}\right) = J_{2m}(2t), \\ h_m(t) &= \frac{1}{2\pi}\int_{-\pi}^{\pi} dq\, e^{-i(m-1/2)q} \sin\left(2t \sin\frac{q}{2}\right) = J_{2m-1}(2t), \end{aligned} \tag{100}$$

leading together with (91) to the time behaviour (98).

Having solved explicitly the equations of motion for the Clifford operators, we can now express the time dependence of physical quantities in terms of the initial-time P_n operators. For example, the transverse magnetization at site n is given by

$$\sigma_n^z(t) = iP_{2n+1}(t)P_{2n}(t) = i\sum_{kk'} F_t(2n+1-k)F_t(2n-k')P_kP_{k'}, \tag{101}$$

which can be rewritten

$$\begin{aligned} \sigma_n^z(t) = & \sum_p \left[F_t^2(2(n-p)) - F_t(2(n-p)+1)F_t(2(n-p)-1)\right]\sigma_p^z \\ & + i{\sum_{kk'}}^{*} F_t(2n+1-k)F_t(2n-k')P_kP_{k'}, \end{aligned} \tag{102}$$

where $\sum^*$ restricts the summation over all k and k' except $k' = k \pm 1$. The case $k = k'$, with $P_k^2 = 1$, gives zero since

$$\sum_k F_t(2n+1-k)F_t(2n-k) = \sum_k J_k(2t)J_{k+1}(2t) = J_1(0) = 0 \ .$$

Equation (102) will be our starting point for the study of the transverse profile time evolution with a specific initial state.

In the same way, the operator σ_n^x at time t is given by

$$\sigma_n^x(t) = (-i)^n \prod_{j=0}^{2n} \sum_{k_j} P_{k_j} J_{j-k_j}(2t), \tag{103}$$

where we have labelled the first site of the chain by $l = 0$ and taken a bulk site n, that is infinitely far away from the boundaries. In the string $\prod_{k_j} P_{k_j}$,

only those terms with all k_j different will give a non-vanishing contribution, since if at least two identical labels appear, we have a factor

$$\sum_k J_{j-k}(2t)J_{i-k}(2t) = \delta_{ij}$$

vanishing for $i \neq j$. Finally one arrives at

$$\sigma_n^x(t) = (-i)^n \sum_{k_0<k_1<\cdots<k_{2n}} P_{k_0}P_{k_1}\cdots P_{k_{2n}} \det(a_{ij}), \tag{104}$$

$$a_{ij} = J_{i-k_j}(2t) \quad 0 \leq i,j \leq 2n. \tag{105}$$

The developments given so far are of course valid for infinite homogeneous chains. In the case of inhomogeneous chains, as for example in the presence of disorder,[88] the time-dependent coefficients of the linear development of the operators $P_n(t)$ are no longer given in terms of Bessel functions. Moreover, for finite homogeneous chains, there are also terms proportional not only to $J_{n-k}(2t)$ but also to $J_{n+k}(2t)$, where the last terms play a significant role for the near-boundary behaviour. In order to take into account these facts, we present now quickly the general expressions[87] valid for finite chains of the type (1). By introducing the Clifford Γ_n^i operators we arrived at $H = (1/4)\Gamma^\dagger \mathbf{T}\Gamma$ with the $2L$-component Clifford operator given by $\Gamma^\dagger = (\Gamma_1^\dagger, \Gamma_2^\dagger, \ldots, \Gamma_L^\dagger)$ and $\Gamma_n^\dagger = (\Gamma_n^1, \Gamma_n^2)$. The diagonalization of the Hamiltonian can then be performed by the introduction of the diagonal Clifford generators $\gamma_q^\dagger = (\gamma_q^1, \gamma_q^2)$ related to the lattice one by $\Gamma_n^1 = \sum_q \phi_q(n)\gamma_q^1$ and $\Gamma_n^2 = \sum_q \psi_q(n)\gamma_q^2$ with ϕ and ψ defined previously as the eigenvector components of the matrix $\mathbf{T}$ given in (10). It leads to

$$H = i\sum_q \frac{\epsilon_q}{2}\gamma_q^1\gamma_q^2 \,. \tag{106}$$

The time dependence of the diagonal operators is then simply given by $\gamma_q(t) = U_q^\dagger(t)\gamma_q U_q(t)$ with

$$U_q(t) = \exp\left(\frac{\epsilon_q t}{2}\gamma_q^1\gamma_q^2\right) = \cos\frac{\epsilon_q t}{2} + \gamma_q^1\gamma_q^2 \sin\frac{\epsilon_q t}{2} \,. \tag{107}$$

Utilising the fact that $\{\gamma_q^i, \gamma_{q'}^j\} = 2\delta_{ij}\delta_{qq'}$, we obtain

$$\gamma_q^i(t) = \sum_{j=1}^{2} \langle \gamma_q^j | \gamma_q^i(t) \rangle \gamma_q^j, \tag{108}$$

where we have defined the pseudo-scalar product as

$$\langle C|D\rangle = \frac{1}{2}\{C^\dagger, D\}, \tag{109}$$

with $\{\cdot\,,\cdot\}$ the anticommutator. The time-dependent lattice Clifford generators, $\Gamma_n^i(t)$, can then be re-expressed in terms of the initial time operators Γ with the help of the inverse transforms $\gamma_q^1 = \sum_k \phi_q(k)\Gamma_k^1$ and $\gamma_q^2 = \sum_k \psi_q(k)\Gamma_k^2$. Finally, one obtains

$$\Gamma_n^j(t) = \sum_{k,i} \langle \Gamma_k^i | \Gamma_n^j(t) \rangle \Gamma_k^i, \tag{110}$$

with components

$$\begin{aligned}
\langle \Gamma_k^1 | \Gamma_n^1(t) \rangle &= \sum_q \phi_q(k)\phi_q(n)\cos\epsilon_q t, \\
\langle \Gamma_k^1 | \Gamma_n^2(t) \rangle &= \langle \Gamma_n^2 | \Gamma_k^1(-t) \rangle = -\sum_q \phi_q(k)\psi_q(n)\sin\epsilon_q t, \\
\langle \Gamma_k^2 | \Gamma_n^2(t) \rangle &= \sum_q \psi_q(k)\psi_q(n)\cos\epsilon_q t.
\end{aligned} \tag{111}$$

These general expressions are exact for all finite size free boundaries free fermionic quantum chains.

Formally, since $\langle \Gamma_k^i | \Gamma_l^j \rangle = \delta_{ij}\delta_{kl}$, the set $\{\Gamma_k^i\}$ forms an orthonormal basis of a $2L$-dimensional linear vector space $\mathcal{E}$ with inner product defined by $\langle \cdot | \cdot \rangle \equiv \frac{1}{2}\{\cdot^\dagger, \cdot\}$. Hence, every vector $X \in \mathcal{E}$ has a unique expansion $X = \sum_{i,k} \langle \Gamma_k^i | X \rangle \Gamma_k^i$. The string expression $X_1 X_2 \cdots X_n$, with $X_j \in \mathcal{E}$, is a direct product vector of the space $\mathcal{E}_1 \otimes \mathcal{E}_2 \otimes \cdots \otimes \mathcal{E}_n$ which decomposition is

$$X_1 X_2 \cdots X_n = \sum_{i_1,k_1,\ldots,i_n,k_n} \langle \Gamma_{k_1}^{i_1} | X_1 \rangle \cdots \langle \Gamma_{k_n}^{i_n} | X_n \rangle \Gamma_{k_1}^{i_1} \cdots \Gamma_{k_n}^{i_n}. \tag{112}$$

With the help of this time-development and the specific solutions ϕ and ψ, we are able to analyse any non-homogeneous finite chain. One has to solve first the eigenvalue equation $\mathbf{T}V_q = \epsilon_q V_q$ and re-inject the ϕ and ψ into the basic components given in (111) and then use the general expression (112).

4.2. *Time-Dependent Behaviour*

4.2.1. *Transverse Magnetization*

In this section we consider initial pure states of the form

$$|\Psi\rangle = |\cdots \sigma(k)\sigma(k+1)\cdots\rangle,$$

where $\sigma(k)$ is the value of the z-component spin at site k. Such initial states are physically relevant since they are quite easily accessible by the application of a strong modulated magnetic field in the desired direction. On the theoretical side, these states permit one to obtain exact

solutions.[89,90] The question we ask is how the magnetization will relax as time evolves[86,90–92,94] and how topological defects, such as droplets or kinks will spread out?[80,81,87,94] In order to give an answer, we compute the transverse magnetization profile

$$\langle\Psi|\sigma_l^z(t)|\Psi\rangle = \sum_{k_1,i_1,k_2,i_2} \langle\Gamma_{k_1}^{i_1}|\Gamma_l^2(t)\rangle\langle\Gamma_{k_2}^{i_2}|\Gamma_l^1(t)\rangle\langle\Psi| - i\Gamma_{k_1}^{i_1}\Gamma_{k_2}^{i_2}|\Psi\rangle \ . \quad (113)$$

Since in the z-state $|\Psi\rangle = \cdots \otimes |\sigma(k)\rangle \otimes |\sigma(k+1)\rangle \otimes \cdots$, the only non-vanishing contributions come from terms $-i\Gamma_k^2\Gamma_k^1 = \sigma_k^z$; the expectation value of the transverse magnetization at time t in such a state is given by

$$\langle\Psi|\sigma_l^z(t)|\Psi\rangle = \sum_k \left[\langle\Gamma_k^2|\Gamma_l^2(t)\rangle\langle\Gamma_k^1|\Gamma_l^1(t)\rangle - \langle\Gamma_k^1|\Gamma_l^2(t)\rangle\langle\Gamma_k^2|\Gamma_l^1(t)\rangle\right]\sigma(k) \ . \quad (114)$$

Clearly, for a translation invariant Hamiltonian this equation can be rewritten as a discrete convolution product,[87]

$$m(l,t) = \sum_k G_t(l-k)\sigma(k) = \big(G_t \star \sigma\big)(l) \ , \quad (115)$$

with $m(l,t) = \langle\Psi|\sigma_l^z(t)|\Psi\rangle$. As seen from (102) for the critical infinite Ising chain the kernel G_t is given in terms of Bessel functions,

$$G_t(l) = F_t^2(2l) - F_t(2l+1)F_t(2l-1), \quad (116)$$

with $F_t(n) = J_n(2t)$ as already defined. Due to the different asymptotic properties of the Bessel functions one has to distinguish between the cases $n/t = v > 1$ and $v < 1$. For $v > 1$, corresponding in (115) to a distance $n = l - k$ between sites l and k larger than t, we are in the acausal region since the elementary excitations, travelling with velocity equal to one by appropriate normalisation of the Hamiltonian (1), have no time to propagate from the initial position l up to site k. This is exactly what is seen from the asymptotic behaviour of the Bessel function $J_n(t)$ which is vanishing exponentially as $\exp(-\lambda(v)n)$ with $\lambda(v) > 0$ for $n > t$. So the behaviour of the local magnetization will be completely governed by the local environnement, since we have a compact support kernel, insuring the existence of the convolution product. Inside the causal region, $v < 1$, with the help of

the asymptotic[95] for $\nu \gg 1$

$$J_\nu\left(\frac{\nu}{\cos\beta}\right) = \sqrt{\frac{2}{\pi\nu\tan\beta}}\cos\delta, \tag{117}$$

where $\delta \equiv \nu(\tan\beta - \beta) - \pi/4$, one obtains in the continuum limit

$$G_t(vt) = \frac{1}{t}g(v), \tag{118}$$

$$g(v) = \begin{cases} (1/\pi)\left(1-v^2\right)^{1/2} & |v|<1 \\ 0 & |v|>1 \end{cases}. \tag{119}$$

In the continuum limit, the local magnetization $m(n,t) = m_t(v)$ is then given by the convolution product

$$m_t(v) = \big(g \star \sigma_t\big)(v), \tag{120}$$

with the initial state function $\sigma_t(v) = \sigma(tv)$.

The same analysis for the XX-chain[87] leads for the Green function $g(v)$ to

$$g(v) = \begin{cases} (1/\pi)(1-v^2)^{-1/2} & |v|<1 \\ 0 & |v|>1 \end{cases}, \tag{121}$$

that is an inverse square-root behaviour. From these expressions one is able to evaluate the long time behaviour of the relaxation process from any initial z-state. With a homogeneous initial state, $m(0) = 1$, one obtains for the XX-chain $m(t) = m(0) = 1$ as it should be, since the dynamics is conservative. On the contrary, in the Ising case, one has from (115) together with (119) $m(t) = \frac{1}{2}$, that is, in the long time regime half of the initial magnetization remains in the z-direction. A more careful analysis[i] leads to[86,94]

$$m(t) = \frac{1}{2} + \frac{1}{4t}J_1(4t), \tag{122}$$

so that the final constant is in fact reached with a power law behaviour $t^{-3/2}$. One remarkable property of the relaxation of the magnetization of the Ising chain is that the remaining half magnetization has a conservative dynamics. For example, if we start with a droplet of L down spins inside an

[i]The continuum analysis performed here is valid up to order t^{-1}.

environment of up spins, in the long time limit $t \gg L$, the magnetization profile is given by

$$m_t(v) = g(v) \star \left(1 - \frac{2L}{t}\delta(v)\right) = \frac{1}{2} - \frac{2L}{\pi t}\sqrt{1-v^2}\,. \tag{123}$$

The excess magnetization $m^c = m - 1/2$ is a scaling function and spreads out into the bulk of the up-spins without loosing any weight. In fact, one can write down a continuity equation $\partial_t m^c(n,t) + j(n,t) - j(n-1,t) = 0$ where the current density is given in the continuum limit by[87]

$$j(x,t) = \frac{x}{t} m^c(x,t)\,. \tag{124}$$

For a general initial z-state the Fourier transform of Eq. (115) is

$$\tilde{m}_t(q) = \tilde{\sigma}_t(q)\tilde{g}(q), \tag{125}$$

where the kernel in Fourier space is

$$\tilde{g}(q) = J_0(2\pi q) \tag{126}$$

for the XX-chain, and

$$\tilde{g}(q) = \frac{J_1(2\pi q)}{2\pi q} \tag{127}$$

for the Ising one. By inverse Fourier transformation one obtains the desired magnetization profile.

One may notice that the relaxation of spatially inhomogeneous initial states has been treated for several variants of the XY quantum chains, modulated, dimerised and so on.[93] A slowing down of the relaxation may occur for fermionic models that have a gaped excitation spectrum at some special points of the modulation wave vector.[91–93] Disordered quantum chains have been investigated numerically in Ref. 88. For the transverse magnetization, they show similar behaviour to the homogeneous chain, that is an algebraic decay in time. During the time evolution, the spatial correlations are building up and at long time they reach a size-dependent constant depending on the distance from criticality.[88] This behaviour is related to the distribution of rare samples that are strongly correlated due to large domains of strong couplings.

4.2.2. *Boundary Effects*

For an open chain, one has to take care of boundary effects that could for a near-boundary spin modify the relaxation behaviour compared to

the bulk one. We will illustrate this with the behaviour of the transverse magnetization in the case of the XX-chain. Consider as an initial state a droplet of L down spins (in the z direction) at the boundary of a semi-infinite chain, the rest pointing in the opposite direction. The transverse magnetization at site l and at time t can be written

$$m(l,t) = 1 - 2\sum_{k=1}^{L} F_t(l,k), \tag{128}$$

with the Green function $F_t(l,k)$, using the symmetry properties of the basic contractions, given by

$$\begin{aligned} F_t(l,k) &= |\langle \Gamma_k^1 | \Gamma_l^1(t)\rangle|^2 + |\langle \Gamma_k^1 | \Gamma_l^2(t)\rangle|^2 \\ &= [J_{l-k}(t) - (-1)^k J_{l+k}(t)]^2, \end{aligned} \tag{129}$$

which is exactly the form given in (79) for the z–z correlator $\langle \sigma_l^z(t)\sigma_k^z\rangle$ at infinite temperature. The reason for this coincidence lies in the fact that the expectations of the string operators $\prod_i P_{2i}$ for the correlator at infinite temperature appear in the very same form in the z-state expectations of the transverse magnetization. Thus, this is also true for the Ising chain. From this coincidence, we see the long time behaviour of the Green function is $F_t \sim t^{-3}$ near the boundary. In fact, from the asymptotic analysis of (79) we can calculate explicitly the long time behaviour of the magnetization. The droplet magnetization, $M^z(t) = (1/2)\sum_{k=1}^{L} \sigma_k^z(t)$ spreads in the bulk, for $t \gg L$, as

$$M^z(t) = \frac{L}{2} - \frac{1}{9\pi}\left(\frac{L^2}{t}\right)^3, \tag{130}$$

which may be compared to[94]

$$M^z(t) = \frac{L}{2} - \frac{1}{\pi}\frac{L^2}{t}, \tag{131}$$

for a bulk droplet.

4.2.3. *Two-Time Functions*

Two-time functions $\langle \mathcal{Q}(t_1)\mathcal{Q}(t_2)\rangle$ are of primary importance in characterising non-equilibrium dynamics. In particular, they show the phenomenon of aging, that is, the dependence of the correlation functions on both times t_1 and $t_2 > t_1$, where t_1 is usually called the waiting time and specifies the age of the system. This is in contrast to the equilibrium situation where the

dependence is only on the time difference $t_2 - t_1$. Usually, at large waiting times, two distinct regimes develop: *(i)* at short time differences the correlations are time translation invariant whereas *(ii)* at long time differences, the relaxation is very slow and depends on the waiting time too. Aging was first considered in ultra-slow glassy dynamics[96] but it has been also investigated in simpler systems, classical[97] as well as quantum.[86,94,98,99] The first attempt in this direction on a homogeneous short range quantum spin chain was made in Ref. 94.

The two-time non-equilibrium correlation function we consider is defined by

$$C_{ij}(t_1, t_2) = \langle \Psi | \sigma_i^z(t_1) \sigma_j^z(t_2) | \Psi \rangle \ , \tag{132}$$

with a z-initial state $|\Psi\rangle$ as already defined and $t_2 > t_1$. In terms of the time-independent basic operators, the two-spins product $\sigma_i^z(t_1)\sigma_j^z(t_2)$ takes the form

$$\sigma_i^z(t_1)\sigma_j^z(t_2) = - \sum_{i_1 k_1 \cdots i_4 k_4} C^{i_1,i_2,i_3,i_4}_{k_1,k_2,k_3,k_4}(t_1,t_2) \Gamma^{i_1}_{k_1} \Gamma^{i_2}_{k_2} \Gamma^{i_3}_{k_3} \Gamma^{i_4}_{k_4}, \tag{133}$$

where the coefficients of that development are given by applying formula (112) with $\sigma_i^z(t_1)\sigma_j^z(t_2) = -\Gamma_i^2(t_1)\Gamma_i^1(t_1)\Gamma_j^2(t_2)\Gamma_j^1(t_2)$. Using Wick's theorem, the expectation in the $|\Psi\rangle$ state is given by

$$C_{ij}(t_1, t_2) = \sum_{k=0}^{6} T_k^{ij}(t_1, t_2) + \langle \Psi | \sigma_i^z(t_1) | \Psi \rangle \langle \Psi | \sigma_j^z(t_2) | \Psi \rangle \ , \tag{134}$$

with a time-translation invariant element

$$T_0^{ij}(t_1, t_2) = \langle A_i A_j \rangle^{t_2 - t_1} \langle B_i B_j \rangle^{t_2 - t_1} - \langle B_i A_j \rangle^{t_2 - t_1} \langle A_i B_j \rangle^{t_2 - t_1} \tag{135}$$

and non-invariant terms

$$T_1^{ij}(t_1, t_2) = - \langle A_i A_j \rangle^{t_2 - t_1} [BB]_{i,j}^{t_1,t_2}, \tag{136}$$

$$T_2^{ij}(t_1, t_2) = \langle A_i B_j \rangle^{t_2 - t_1} [BA]_{i,j}^{t_1,t_2}, \tag{137}$$

$$T_3^{ij}(t_1, t_2) = \langle B_i B_j \rangle^{t_2 - t_1} [AA]_{i,j}^{t_1,t_2}, \tag{138}$$

$$T_4^{ij}(t_1, t_2) = - \langle B_i A_j \rangle^{t_2 - t_1} [AB]_{i,j}^{t_1,t_2}, \tag{139}$$

$$T_5^{ij}(t_1, t_2) = -[AA]_{i,j}^{t_1,t_2} [BB]_{i,j}^{t_1,t_2}, \tag{140}$$

$$T_6^{ij}(t_1, t_2) = [AB]_{i,j}^{t_1,t_2} [BA]_{i,j}^{t_1,t_2}, \tag{141}$$

with

$$[CD]_{i,j}^{t_1,t_2} = \sum_k \sigma_k (\langle B_k C_i \rangle^{t_1} \langle A_k D_j \rangle^{t_2} - \langle A_k C_i \rangle^{t_1} \langle B_k D_j \rangle^{t_2}). \tag{142}$$

Here we have used the short notation of Ref. 86 that is to recall, $A_i = \Gamma_i^1$, $B_i = -i\Gamma_i^2$ and for the basic time contractions

$$\langle XY \rangle^t \equiv \langle X|Y(t)\rangle = \frac{1}{2}\{X^\dagger, Y(t)\}$$

that can be read from Eq. (111). The elements $T_k^{ij}(t_1,t_2)$ satisfy the set of symmetry relations

$$\begin{array}{ll} T_0^{ij}(t_1,t_2) = T_0^{ji}(t_2,t_1), & T_1^{ij}(t_1,t_2) = -T_1^{ji}(t_2,t_1), \\ T_2^{ij}(t_1,t_2) = -T_4^{ji}(t_2,t_1), & T_3^{ij}(t_1,t_2) = -T_3^{ji}(t_2,t_1), \\ T_5^{ij}(t_1,t_2) = T_5^{ji}(t_2,t_1), & T_6^{ij}(t_1,t_2) = T_6^{ji}(t_2,t_1). \end{array} \tag{143}$$

From the previous equations, together with the symmetry relations, one obtains for the connected symmetrised spin–spin correlation,

$$\tilde{C}_{ij}(t_1,t_2) = \frac{1}{2}\langle\Psi|\{\sigma_i^z(t_1),\sigma_j^z(t_2)\}|\Psi\rangle - \langle\Psi|\sigma_i^z(t_1)|\Psi\rangle\langle\Psi|\sigma_j^z(t_2)|\Psi\rangle, \tag{144}$$

the simpler expression

$$\tilde{C}_{ij}(t_1,t_2) = T_0^{ij}(t_1,t_2) - [AA]_{i,j}^{t_1,t_2}[BB]_{i,j}^{t_1,t_2} + [AB]_{i,j}^{t_1,t_2}[BA]_{i,j}^{t_1,t_2}, \tag{145}$$

which is valid for all free fermionic spin chains, prepared in an initial z-state. One may notice that for an initial x-state,[86] the formula for the correlation function is the same, except that one has to replace the initial definition of the $[CD]$.[86]

4.2.4. *Critical Ising Chain*

We concentrate now on the critical Ising chain, since at this point the contractions are simpler and one is able to give exact closed analytical expressions.[86]

In particular, the two-time autocorrelation function, that is, $i = j$, takes a very simple form for a completely ordered z-initial state. Together with $\langle A_i A_j\rangle^t = (-1)^{i+j} J_{2(i-j)}(2t)$ and $\langle A_i B_j\rangle^t = i(-1)^{i+j+1} J_{2(i-j)+1}(2t)$ for the infinite chain, one obtains

$$\tilde{C}(t_1,t_2) = J_0^2(2(t_2-t_1)) - \frac{1}{4}[f(t_2+t_1) - g(t_2-t_1)]^2, \tag{146}$$

with $f(x) = J_2(2x) + J_0(2x)$ and $g(x) = J_2(2x) - J_0(2x)$. The two-time autocorrelation can be rewritten as

$$\tilde{C}(t_1,t_2) = J_0^2(2(t_2-t_1)) - \left(\frac{J_1(2(t_2+t_1))}{2(t_2+t_1)} + J_1'(2(t_2-t_1))\right)^2. \tag{147}$$

The dependence of the correlation function on both t_1 and t_2 reflects the non-equilibrium behaviour of the system. However, in the long-time regime

$t_1 \gg 1$ with small difference times $\tau = t_2 - t_1 \ll t_1$ one recovers time translation invariance, that is, the two-time function depends only on the difference τ and decays algebraically as τ^{-2}. This power law decay subsists with the same exponent for any value of the transverse field h.[86]

By Kubo's formula,[75] the linear response function $R_{ij}^{zz}(t_1, t_2)$ at site j to an infinitesimal transverse field at site i is given by the commutator $i\langle\Psi|[\sigma_i^z(t_1), \sigma_j^z(t_2)]|\Psi\rangle$ and, along the same lines as before, it is expressed at the critical field as

$$R_{ij}^{zz}(t_1, t_2) = Q_{ij}^1(t_1, t_2) + Q_{ij}^2(t_1, t_2), \tag{148}$$

with

$$\begin{aligned} Q_{ij}^1(t_1, t_2) = {} & J_{2r-1}(2\tau) J_{2r+1}(2(t_1 + t_2)) \frac{2r+1}{t_1 + t_2} \\ & - J_{2r+1}(2\tau) J_{2r-1}(2(t_1 + t_2)) \frac{2r-1}{t_1 + t_2} \end{aligned} \tag{149}$$

and a time-translation invariant element

$$Q_{ij}^2(t_1, t_2) = Q_{ij}^2(\tau) = -\frac{2}{\tau} J_{2r-1}(2\tau) J_{2r+1}(2\tau), \tag{150}$$

with $r = j - i$ the distance between the two sites i and j. Translation invariance in time is restored at small difference times, $1 \ll \tau = t_2 - t_1 \ll t_1$, since the dominant term is then $Q_{ij}^2(\tau)$ and it leads to a τ^{-2} behaviour.

4.2.5. *XX-Chain*

For the XX-chain, the dynamics is conservative, that is the total magnetization in the z direction is conserved during time evolution. Therefore, in order to consider a relaxation process one cannot use the same procedure as in the Ising case. Instead of an infinite chain fully magnetized in the up-direction, we take as the initial state of the infinite chain a droplet of L-spins pointing upward in the z-direction, from site labels $i = 0$ to $i = L - 1$, the rest of the spins pointing in the opposite direction.[94] This can be assimilated to a system of size L interacting through its boundaries with a bath, where it can dissipate magnetization. The final stationary state reached by the system is the completely magnetized state, with all the system spins down, which is not the equilibrium state.

The two-time connected autocorrelation function of the droplet is defined by

$$\tilde{C}(t_1, t_2) = \langle\Psi|M^z(t_1) M^z(t_2)|\Psi\rangle - \langle\Psi|M^z(t_1)|\Psi\rangle\langle\Psi|M^z(t_2)|\Psi\rangle, \tag{151}$$

with $M^z(t) = \frac{1}{2}\sum_{i=0}^{L-1} \sigma_i^z(t)$ the total transverse magnetization of the droplet subsystem. The $\frac{1}{2}$ factor has been introduced in order to follow

Ref. 94. The Heisenberg equations are easily solved in this case and one obtains for the lattice fermions

$$c_k(t) = e^{-iht} \sum_r i^{k-r} J_{k-r}(t) c_r. \tag{152}$$

Introducing these solutions inside (151), using Wick's theorem and the initial droplet state, one obtains

$$\tilde{C}(t_1, t_2) = \sum_{k,l=0}^{L-1} J_{k-l}(t_2 - t_1) \sum_{r=0}^{L-1} J_{k-r}(t_2) J_{l-r}(t_1) - \sum_{k,l,r,s=0}^{L-1} J_{k-r}(t_2) J_{k-s}(t_2) J_{l-r}(t_1) J_{l-s}(t_1) \; . \tag{153}$$

The long-time behaviour of that expression is obtained with the help of the asymptotic expansion of the Bessel function $J_n(t) \sim \sqrt{2/\pi t} \cos(t - n\pi/2 - \pi/4)$. For $t_1, t_2 \gg L$, one obtains the asymptotic form

$$\tilde{C}(t_1, t_2) = \frac{L^3}{2\sqrt{\pi^3 t_1 t_2 (t_2 - t_1)}} - \frac{L^4}{2\pi^2 t_1 t_2} \; . \tag{154}$$

In the finite magnetization density regime,[94] that is for times smaller than L^2, the second term dominates and one has finally

$$\tilde{C}(t_1, t_2) = -\frac{L^4}{2\pi^2 t_1 t_2} = t_1^{-2} f\left(\frac{t_2}{t_1}\right), \quad L \ll t_1, t_2 \ll L^2, \tag{155}$$

with $f(x) \sim x^{-1}$. One may notice that this scaling form is specific of aging at a critical point where critical coarsening takes place.[100–102] This means that aging occurs in the ordered isotropic XX-chain with deterministic quantum dynamics.[94] In fact, to conclude positively about the occurrence of aging in such system, Schütz and Trimper[94] have restricted their definition of aging to the phenomenon of increasing relaxation times, i.e. the longer one waits, the slower the relaxation becomes. For that purpose they considered the ratio

$$R(t_1, t_2) = \tilde{C}(t_1, t_2) / \tilde{C}(t_1, t_1) = t_1/t_2 \; , \tag{156}$$

that is a kind of normalized autocorrelation function with respect to the waiting time t_1, which clearly shows that aging occurs in this homogeneous deterministic quantum system.

5. Discussion and Summary

We have presented in this review the general "almost" canonical approach to free fermionic quantum spin chains. Almost canonical in the sense that, several variants of notations and approaches appear all along the enormous literature devoted to this topic, and one is sometimes confused. However, we tried to give a systematic analysis and emphasise the basic technical tools, such as the Wick expansion, pair contractions and operator time development.

We have presented very few results on the well known static properties of these spin chains but merely insisted on the way to calculate them, in this sense it is a pedagogical attempt. Moreover, we have shown explicitly how one can reconstruct the zero temperature quantum phase diagram from the study of the boundary magnetization. Since it is very easy to compute the first site magnetization,[41,42] one has paid a very low price for the knowledge of the bulk behaviour, compared to standard approaches.[27] Of course, the present analysis was *a posteriori* and, as everyone knows, it is an easy task and sometimes pathetic to recover old results by new approaches. However, one can imagine that the present approach can be used to tackle really new systems, so to say to infer bulk behaviour from surface properties.

Results on equilibrium time-dependent correlation functions are quickly reviewed and I apologise for important works that have not been cited here for various reasons, the main being fortuitous omission or lack of knowledge. One should not worry too much about it, since the science is, or should be, a public good. Phrased differently, intellectual property is still a property. To summarise on the spin–spin time dependent correlations, the calculation of the transverse functions is an easy task, since they have a local expression in terms of the non-interacting fermions. They are basically fermion density correlation functions and show up power law decay in time. The x spin component correlations are much more difficult to evaluate, since in this case the Jordan–Wigner transformation leads to string Fermi operators. Nevertheless, using Wick's theorem their asymptotic behaviour can be extracted. At vanishing temperature, they decay with a power law whereas at infinite temperature they have a Gaussian shape. In the intermediate temperature regime, the decay is exponential with a power law prefactor.

Finally, in the main part of this paper we dealt with some of the non-equilibrium properties of these systems. We focused our attention, after solving the Heisenberg equations of motions for the Fermi operators, on the relaxation of the transverse magnetization in the critical Ising chain

and the isotropic XY-chain. For some particular initial states, magnetized in a given direction, we derived analytically a general expression that can be used to calculate at late times the transverse magnetization profile. In fact, the long time relaxation of the magnetization is expressed as a convolution product of the initial state with a response kernel obtained analytically for both the XX- and Ising chains. It is seen in particular that the Ising chain exhibits some similarities with the conserved dynamics XX-chain. That is, after a transient regime, the relaxation process in the Ising case is conservative too. Two-time functions are also discussed in the light of aging phenomena. It is shown how, starting with some non-equilibrium initial state, the correlations depend explicitly on both the waiting time, characterising the age of the system, and the later measurement time. Although aging was first considered in complex systems such as structural glasses or spin glasses, it is in fact also present in simple homogeneous systems with a completely deterministic dynamics. This final result is in fact very recent and it has been demonstrated in classical[97] and quantum systems.[94]

Acknowledgements

It is here a pleasure to acknowledge Yurij Holovatch for his very kind invitation in Lviv's Ising Lectures where part of the work discussed here was presented. It was also my pleasure to spend this time in Lviv with my very smart fellow traveller Bertrand Berche.

References

1. E. H. Lieb, T. D. Schultz and D. C. Mattis, *Ann. Phys., NY* **16**, 406 (1961).
2. H. J. Schulz and T. Ziman, *Phys. Rev.* **B33**, 6545 (1986).
3. F. D. M. Haldane, *Phys. Lett.* **A93**, 454 (1983).
4. F. D. M. Haldane, *Phys. Rev. Lett.* **50**, 1153 (1983).
5. N. Nagaosa, *Quantum field theory in strongly correlated electronic systems* (Springer-Verlag, Berlin, 1999).
6. S. Sachdev, *Quantum Phase Transitions* (Cambridge Univ. Press, 1999).
7. J. L. Cardy, *Scaling and renormalization in statistical physics* (Cambridge Univ. Press, 1996).
8. M. Steiner, J. Villain and C. G. Windsor, *Adv. Phys.* **25**, 87 (1976).
9. P. Lemmens, G. Güntheroldt and C. Gros, *Physics Reports* **376**, 1 (2003).
10. D. Bitko, T. F. Rosenbaum and G. Aeppli, *Phys. Rev. Lett.* **77**, 940 (1996).
11. H. Bethe, *Z. Physik* **71**, 205 (1931).
12. J. Gaudin, *La fonction d'onde de Bethe* (CEA ed., 1970).
13. A. O. Gogolin, A. A. Nersesyan and A. M. Tsvelik, *Bosonization and strongly correlated systems* (Cambridge University Press, 1998).

14. J. von Delft and H. Schoeller, *Annalen Phys.* **7**, 225 (1998).
15. P. Jordan and E. Z. Wigner, *Z. Phys.* **47**, 631 (1928).
16. S. R. White, *Phys. Rev. Lett.* **69**, 2863 (1992).
17. S. R. White, *Phys. Rev.* **B48**, 10345 (1993).
18. I. Peschel, X. Wang and M. Kaulke, Eds., *Density-matrix renormalization: A new numerical method in physics* (Springer-Verlag, Berlin, 1999).
19. F. Iglói, I. Peschel and L. Turban, *Advances in Physics* **42**, 683 (1993).
20. J. M. Luck, *J. Stat. Phys.* **72**, 417 (1993).
21. H. Rieger and A. P. Young, in *Lecture notes in Physics 492 "Complex behaviour of glassy systems"*, Ed. J. M. Rubi and C. Perez-Vicente (Springer-Verlag, Berlin Heidelberg, 1997), p. 254.
22. D. S. Fisher, *Phys. Rev. Lett.* **69**, 534 (1992); *Phys. Rev.* **B51**, 6411 (1995).
23. S. K. Ma, C. Dasgupta and C. K. Hu, *Phys. Rev. Lett.* **43**, 1434 (1979).
24. S. Katsura, *Phys. Rev.* **127**, 1508 (1962).
25. Th. Niemeijer, *Physica* **36**, 377 (1967).
26. P. Pfeuty, *Ann. Phys., NY* **57**, 79 (1970).
27. E. Barouch and B. M. McCoy, *Phys. Rev.* **A3**, 786 (1971).
28. B. M. McCoy, E. Barouch and D. B. Abraham, *Phys. Rev.* **A4**, 2331 (1971).
29. M. Henkel, *Conformal invariance and critical phenomena* (Springer-Verlag, Berlin Heidelberg, 1999).
30. G.v. Gehlen, V. Rittenberg and H. Ruegg, *J. Phys.* **A18**, 107 (1985).
31. R. D. Mattuck, *A guide to Feynman diagrams in the many body problem* (McGraw-Hill, 1967), p. 110.
32. J. Avery, *Creation and annihilation operators* (McGraw-Hill, 1976), p. 139.
33. I. Tsukada, J. Takeya, T. Masuda and K. Uchinokura, *Phys. Rev. Lett.* **87**, 127203 (2001).
34. O. Derzhko and T. Krokhmalskii, *Phys. Rev.* **B56**, 11659 (1997).
35. U. Bilstein and B. Wehefritz, *J. Phys.* **A32**, 191 (1999).
36. H. Hinrichsen, *J. Phys.* **A27**, 5393 (1994).
37. F. Iglói and L. Turban, *Phys. Rev. Lett.* **77**, 1206 (1996).
38. F. Iglói, L. Turban, D. Karevski and F. Szalma, *Phys. Rev.* **B56**, 11031 (1997).
39. B. Berche and I. Iglói, *J. Phys.* **A28**, 3579 (1995).
40. L. Turban and B. Berche, *J. Phys.* **A26**, 3131 (1993).
41. I. Peschel, *Phys. Rev.* **B30**, 6783 (1984).
42. D. Karevski, *J. Phys.* **A33**, L313 (2000).
43. L. Onsager, *Phys. Rev.* **65**, 117 (1944).
44. J. B. Kogut, *Rev. Mod. Phys.* **51**, 659 (1979).
45. M. N. Barber, in *Phase transitions and critical phenomena*, Vol. **8**, Ed. C. Domb and J. L. Lebowitz (London: Academic Press, 1983), p. 145.
46. E. R. Caianello and S. Fubini, *Nuovo Cimento* **9**, 1218 (1952).
47. P. E. Berche, B. Berche and L. Turban, *J. Physique* **I6**, 621 (1996).
48. F. Iglói and H. Rieger, *Phys. Rev.* **B57**, 11404 (1998).
49. L. Turban and F. Iglói, *J. Phys.* **A30**, L105 (1997).
50. D. Karevski, L. Turban and F. Iglói, *J. Phys.* **A33**, 2663 (2000).
51. F. Iglói, D. Karevski and H. Rieger, *Eur. Phys. J.* **B1**, 513 (1998).

52. L. Turban, D. Karevski and F. Iglói, *J. Phys.* **A32**, 3907 (1999).
53. D. Karevski, R. Juhász, L. Turban and F. Iglói, *Phys. Rev.* **B60**, 4195 (1999).
54. D. Karevski, Y.-C. Lin, H. Rieger, N. Kawashima and F. Iglói, *Eur. Phys. J.* **B20**, 267 (2001).
55. E. R. Gagliano and C. A. Balseiro, *Phys. Rev. Lett.* **59**, 2999 (1987).
56. E. R. Gagliano and C. A. Balseiro, *Phys. Rev.* **B38**, 11766 (1988).
57. T. D. Kühner and S. R. White, *Phys. Rev.* **B60**, 335 (1999).
58. U. Brandt and K. Jacoby, *Z. Physik* **B25**, 181 (1976).
59. U. Brandt and K. Jacoby, *Z. Physik* **B26**, 245 (1977).
60. H. W. Capel and J. H. H. Perk, *Physica* **87A**, 211 (1977).
61. S. Katsura, T. Horiguchi and M. Suzuki, *Physica* **46**, 67 (1970).
62. D. B. Abraham, *Stud. Appl. Math.* **51**, 179 (1972).
63. H. G. Vaidya and C. A. Tracy, *Physica* **92A**, 1 (1977).
64. H. B. Cruz and L. L. Gonçalves, *J. Phys.* **C14**, 2785 (1981).
65. L. L. Gonçales and H. B. Cruz, *J. Magn. Magn. Mater.* **15–18**, 1067 (1980).
66. B. M. McCoy, J. H. H. Perk and R. E. Shrock, *Nucl. Phys.* **B220**, [FS8], 35 (1983).
67. G. Müller and R. E. Shrock, *Phys. Rev.* **B29**, 288 (1984).
68. J. Stolze, V. S. Viswanath and G. Müller, Z. Physik **B89**, 45 (1992).
69. J. Stolze, A. Nöppert and G. Müller, *Phys. Rev.* **B52**, 4319 (1995).
70. W. Pesch and H. J. Mikeska, *Z. Physik* **B26**, 351 (1977).
71. W. Pesch and H. J. Mikeska, *Z. Physik* **B30**, 177 (1978).
72. A. Sur, D. Jasnow and I. J. Lowe, *Phys. Rev.* **B12**, 3845 (1975).
73. T. T. Wu, *Phys. Rev.* **149**, 380 (1966).
74. A. R. Its, A. G. Izergin, V. E. Korepin and N. A. Slavnov, *Phys. Rev. Lett.* **70**, 1704 (1993).
75. R. Kubo, M. Toda and N. Hashitsume, *Statistical Physics II* (Springer-Verlag, Berlin, 1985).
76. J. A. Tjion, *Phys. Rev.* **B2**, 2411 (1970).
77. E. Barouch, B. M. McCoy and M. Dresden, *Phys. Rev.* **A2**, 1075 (1970).
78. E. Barouch and B. M. McCoy, *Phys. Rev.* **A3**, 2137 (1971).
79. R. H. Terwiel and P. Mazur, *Physica* **32**, 1813 (1966).
80. T. Antal, Z. Rácz and L. Sasvári, *Phys. Rev. Lett.* **78**, 167 (1997).
81. T. Antal, Z. Rácz, A. Rákos and G. M. Schütz, *Phys. Rev.* **E59**, 4912 (1999).
82. V. Eisler, Z. Rácz and F. van Wijland, cond-mat/0301473 (v1).
83. K. Blum, *Density matrix theory and applications* (Plenum Press, New York, 1981).
84. A. O. Caldeira and A. J. Leggett, *Ann. Phys. N.Y.* **149**, 374 (1983).
85. U. Weiss, *Quantum dissipative systems*, 2nd edn., Series in Modern Condensed Matter Physics, Vol 10 (World Scientific, Singapore, 1999).
86. F. Iglói and H. Rieger, *Phys. Rev. Lett.* **85**, 3233 (2000).
87. D. Karevski, *Eur. Phys. J.* **B27**, 147 (2002).
88. S. Abriet and D. Karevski, *Eur. Phys. J.* **B30**, 77 (2002).
89. G. O. Berim and A. R. Kessel, *Teor. Mat. Fiz.* **58**, 388 (1984).
90. G. O. Berim, *Sov. J. Low Temp. Phys.* **17**, 329 (1991).

91. G. O. Berim and G. G. Cabrera, *Physica* **A238**, 211 (1997).
92. G. O. Berim, *Sov. Phys. JETP* **75**, 86 (1992).
93. G. O. Berim, S. Berim and G. G. Cabrera, *Phys. Rev.* **B66**, 094401 (2002).
94. G. M. Schütz and S. Trimper, *Europhys. Lett.* **47**, 164 (1999).
95. I. S. Gradshteyn and I. M. Ryszhik, *Table of integrals series and products* (Academic, London, 1980).
96. J. P. Bouchaud, L. F. Cugliandolo, J. Kurchan and M. Mézard, in *Spin glasses and random fields*, Ed. A. P. Young (World Scientific, Singapore, 1997).
97. L. F. Cugliandolo, J. Kurchan and G. Parisi, *J. Phys.* **4**, 1641 (1994).
98. L. F. Cugliandolo and G. Lozano, *Phys. Rev. Lett.* **80**, 4979 (1998).
99. N. Pottier and A. Mauger, *Physica* **A282**, 77 (2000).
100. A. J. Bray, *Adv. Phys.* **43**, 357 (1994).
101. C. Godrèche and J. M. Luck, *J. Phys. Cond. Matter* **14**, 1589 (2002).
102. A. Picone and M. Henkel, *J. Phys.* **A35**, 5575 (2002).

This page intentionally left blank

CHAPTER 3

QUANTUM PHASE TRANSITIONS IN ALTERNATING TRANSVERSE ISING CHAINS

Oleg Derzhko

Institute for Condensed Matter Physics
of the National Academy of Sciences of Ukraine
1 Svientsitskii Str., Lviv-11, 79011, Ukraine
E-mail: derzhko@icmp.lviv.ua

This chapter is devoted to a discussion of quantum phase transitions in a regularly alternating spin-$\frac{1}{2}$ Ising chain in a transverse field. After recalling some generally known topics of the classical (temperature-driven) phase transition theory and some basic concepts of the quantum phase transition theory I pass to the statistical mechanics calculations for a one-dimensional spin-$\frac{1}{2}$ Ising model in a transverse field, which is the simplest possible system exhibiting the continuous quantum phase transition. The essential tool for these calculations is the Jordan–Wigner fermionization. The latter technique being completed by the continued fraction approach enables one to obtain analytically the thermodynamic quantities for a "slightly complicated" model in which the intersite exchange interactions and on-site fields vary regularly along a chain. Rigorous analytical results for the ground-state and thermodynamic quantities, as well as exact numerical data for the spin correlations computed for long chains demonstrate how the regularly alternating bonds/fields affect the quantum phase transition. I discuss in detail the case of period 2, swiftly sketch the case of period 3 and finally summarize emphasizing the effects of periodically modulated Hamiltonian parameters on quantum phase transitions in the transverse Ising chain and in some related models.

1. Classical and quantum phase transitions

In this chapter I consider the effects of regular alternation of the Hamiltonian parameters on the quantum phase transition inherent in a one-dimensional spin-$\frac{1}{2}$ Ising model in a transverse field. Before starting

to discuss this issue let me recall some common wisdoms from statistical physics. One of the aims of statistical physics is to describe different phases which may occur in many-particle systems and the transitions between different phases, i.e. the phase transitions. We often face phase transitions in everyday life. Melting of ice, boiling of water or vanishing of the magnetic properties of iron after heating are well known phenomena for everyone. Normally we associate the changes in properties of a substance as the temperature varies. However, such changes may occur at a fixed finite temperature while some other parameter (such as pressure) varies.

P. Ehrenfest proposed a classification of phase transitions. In the Ehrenfest classification of phase transitions we say that the phase transition is of the order one if the free energy is continuous across the phase transition whereas its first derivative with respect to temperature and other variables (for example, pressure) are discontinuous. Similarly, we say that the phase transition is of the order two (three) if the free energy and its first derivative (first two derivatives) are continuous across the phase transition whereas the second (third) derivatives are discontinuous.

A few years later L. Landau proposed to consider discontinuous or continuous phase transitions. In the Landau sense the discontinuous (continuous) phase transition is characterized by a discontinuous (continuous) change in the order parameter and, therefore, it is usually viewed as of the first- (second- or higher-) order. In the first-order phase transitions the two phases coexist at the phase transition temperature. Thus, if ice is melting one observes two phases, i.e., liquid and solid, which coexist at the temperature of phase transition. This is an example of discontinuous phase transition. In the second-order (and higher-order) phase transitions the two phases do not coexist. An example is the Curie point of a ferromagnet above which the magnetic moment of a material vanishes. Below the Curie temperature T_c we can observe only the ferromagnetic phase which continuously disappears at T_c. Above T_c we can observe only the paramagnetic phase. Some phase transitions are not in accord with the naively applied classification rules. Thus, the Bose-Einstein condensation in an ideal Bose gas is accompanied by a kink in the temperature dependence of specific heat at the Bose-Einstein condensation temperature but is viewed as a first-order phase transition.[1] In what follows our focus will be on the continuous phase transitions which were studied very intensively in the last century, especially in the last four decades.

Statistical mechanics provides some microscopic models of the continuous phase transitions. One of such models was invented by E. Ising[2] about

80 years ago. It became especially well known after L. Onsager[3] had found an exact solution of the model in two dimensions. Let me introduce the Ising model and fix the notation. The model consists of magnetic moments or spins which may have two values $-\frac{1}{2}$ and $\frac{1}{2}$ and which interact with the nearest neighbours. The Hamiltonian of the model on a square lattice of $N_x N_y = N$ sites can be written in the form

$$H = -\sum_{i_x=1}^{N_x}\sum_{i_y=1}^{N_y}\left(J_h s^z_{i_x,i_y} s^z_{i_x+1,i_y} + J_v s^z_{i_x,i_y} s^z_{i_x,i_y+1}\right), \tag{1}$$

where $s^z_{i_x,i_y}$ is the spin variable attached to the site i_x, i_y, and J_h and J_v are the exchange interactions in horizontal and vertical directions, respectively. If the exchange interaction in (1) is positive, the same value of spin variables at neighbouring sites is favourable, i.e. the exchange interaction is ferromagnetic. The spin variable s^z may be presented by a half of the Pauli matrix

$$\begin{pmatrix} 1 & 0 \\ 0 & -1 \end{pmatrix}$$

and the canonical partition function which determines the thermodynamics of the model reads

$$Z = \sum_{\{s^z_{i_x,i_y}=\pm\frac{1}{2}\}} \exp(-\beta H) = \mathrm{Tr}\exp\left(-\beta H\right), \tag{2}$$

where $\beta = 1/(kT)$ is the inverse temperature. We are also interested in the spin correlation functions $\langle s^z_{i_x,i_y} s^z_{j_x,j_y}\rangle$, where the canonical average means

$$\langle(\cdots)\rangle = \frac{1}{Z}\mathrm{Tr}(\exp(-\beta H)(\cdots)).$$

The spin correlation functions in the limit of infinitely large intersite distances yield the magnetization per site

$$m^z = \frac{1}{N_x N_y}\sum_{i_x=1}^{N_x}\sum_{i_y=1}^{N_y}\langle s^z_{i_x,i_y}\rangle, \tag{3}$$

which plays the role of the order parameter. Due to the seminal study by L. Onsager we understand in great detail the properties of the two-dimensional Ising model.

At zero temperature $T = 0$ all spins have the same value, say, $\frac{1}{2}$, and $m^z = \frac{1}{2}$. As the temperature becomes nonzero some of spin variables due to temperature fluctuations have the value $-\frac{1}{2}$, and thus m^z becomes

smaller than $\frac{1}{2}$. Quantitatively the temperature fluctuations of the magnetic moment can be characterized by

$$\left\langle \left(\sum_{i_x=1}^{N_x} \sum_{i_y=1}^{N_y} \left(s^z_{i_x,i_y} - m^z \right) \right)^2 \right\rangle .$$

At the critical temperature T_c the temperature fluctuations completely destroy the order: the average numbers of spins having the values $\frac{1}{2}$ and $-\frac{1}{2}$ are the same and $m^z = 0$. Above T_c the average numbers of spins having the values $\frac{1}{2}$ and $-\frac{1}{2}$ remain the same and $m^z = 0$. Analytical calculations in two dimensions predict the logarithmic singularity of the specific heat in the vicinity of T_c

$$c \sim \ln |T - T_c| , \tag{4}$$

and the vanishing of the order parameter m^z while $T_c - T \to +0$ as

$$m^z \sim (T_c - T)^{1/8} . \tag{5}$$

The correlation length ξ which characterizes the long-distance behaviour of spin correlations,

$$\langle s^z_{\mathbf{i}} s^z_{\mathbf{j}} \rangle \sim \exp\left(-\frac{|\mathbf{i} - \mathbf{j}|}{\xi} \right), \quad |\mathbf{i} - \mathbf{j}| \to \infty, \tag{6}$$

diverges in the vicinity of T_c as

$$\xi \sim |T - T_c|^{-1} . \tag{7}$$

In one dimension $T_c = 0$. At any infinitesimally small temperature the temperature fluctuations destroy the long-range order which exists only at zero temperature. The exact solution[4] for the two-point spin correlation functions reads

$$\begin{aligned} &\langle s^z_j s^z_{j+n} \rangle = \frac{1}{4} \left(\tanh \frac{\beta J}{4} \right)^n = \frac{1}{4} \exp\left(-\frac{n}{\xi} \right), \\ &\frac{1}{\xi} = \ln \coth \frac{\beta J}{4}, \end{aligned} \tag{8}$$

and hence the correlation length ξ diverges while $T \to T_c = 0$ as

$$\xi \sim \exp \frac{J}{2kT}. \tag{9}$$

We do not know the exact solution of the Ising model in three dimensions although qualitatively the briefly sketched picture for a two-dimensional case remains valid.

Numerous experimental studies of different substances in the vicinity of the continuous phase transition points show that the critical behaviour is characterized by a set of exponents which may be identical for different substances. This remarkable result of universality urged the researchers to proceed elaborating scaling concepts, establishing scaling relations and developing renormalization ideas and many systematic renormalization-group schemes in order to calculate critical exponents. These issues constitute a basic course in the theory of classical (i.e. temperature-driven) continuous phase transitions.[5,6]

In what follows I shall not speak about temperature-driven continuous phase transitions. I wish to focus on the quantum continuous phase transitions. Let me start from a brief discussion of the experiment performed by D. Bitko, T. F. Rosenbaum and G. Aeppli[7] which demonstrates how a phase transition may be driven by entirely quantum rather than temperature fluctuations. D. Bitko *et al.* carried out their measurements for a model magnet lithium holmium fluoride $LiHoF_4$ in the external field H^t, which turns out to be the experimental realization of the Ising magnet in a transverse magnetic field. At low temperatures (below 2 K), the magnetic properties arise owing to the magnetic dipolar interaction of the spins of neighbouring holmium ions Ho^{3+}. These spins prefer to be directed either up or down with respect to a certain crystalline axis and present the three-dimensional ferromagnetic Ising model. D. Bitko *et al.* investigated the behaviour of $LiHoF_4$ as a function of temperature T and an external magnetic field H^t applied normally to the Ising axis. For this purpose they measured the real and the imaginary parts of the magnetic susceptibility along the Ising axis at different temperatures establishing T_c or H_c^t. Their findings are summarized in Fig. 1.

Let us discuss the experimentally measured phase diagram (Fig. 1) of the system which is described by the Hamiltonian of the Ising magnet in a transverse magnetic field

$$H = \sum_{i,j} J_{ij} s_i^z s_j^z - \Omega \sum_i s_i^x, \tag{10}$$

where s^α, $\alpha = x, y, z$ are halves of the Pauli matrices

$$\sigma^x = \begin{pmatrix} 0 & 1 \\ 1 & 0 \end{pmatrix}, \qquad \sigma^y = \begin{pmatrix} 0 & -i \\ i & 0 \end{pmatrix}, \qquad \sigma^z = \begin{pmatrix} 1 & 0 \\ 0 & -1 \end{pmatrix}, \tag{11}$$

the J_{ij} are the Ising exchange couplings and Ω is a transverse field which mimics H^t. Consider the behaviour of the system as the temperature increases at $H^t = 0$ (the horizontal axis in Fig. 1). At $T = 0$, all spins

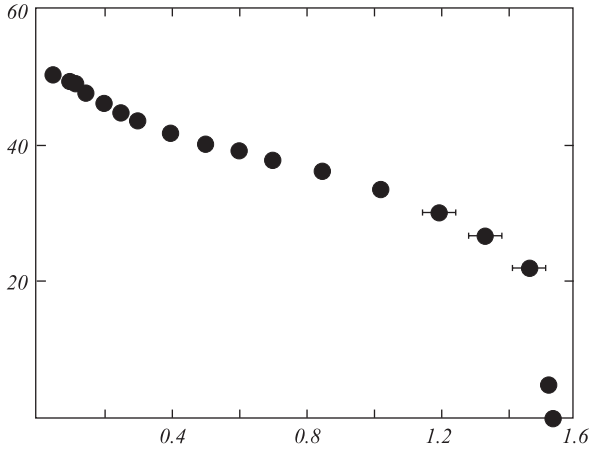

Fig. 1. The temperature–transverse field phase diagram of $LiHoF_4$. The temperature T (the horizontal axis) is measured in K, the (transverse) magnetic field H^t (the vertical axis) is measured in kOe. Experimental data for the ferromagnetic transition (filled circles) that separates the ferromagnet (lower region) from the paramagnet (upper region) are obtained via magnetic susceptibility measurements.

are pointed, say, up (i.e., fully polarized ferromagnetic state). As the temperature becomes nonzero, the temperature fluctuations cause some spins of the ground-state configuration to flip, i.e. some spins become pointed down. As the temperature increases, the number of flipped spins increases and, at $T_c = 1.53$ K, the numbers of up and down spins become equal. The numbers of spin up and spin down are the same for all temperatures above T_c. This is a scenario of the conventional temperature-driven continuous phase transition from the ferromagnetic to the paramagnetic phase with the Curie temperature $T_c = 1.53$ K.

Consider further what happens while we are moving along the vertical axis in Fig. 1, i.e. while we increase the transverse field H^t at zero temperature $T = 0$. We immediately observe that the existing order at zero temperature may be destroyed in a completely different manner even at $T = 0$. Applying the transverse field H^t we allow tunneling between spin-down and spin-up states. And if $H^t > H^t_c$, the ground state becomes paramagnetic even at $T = 0$. Hence, the quantum fluctuations destroy the order. In other words, the phase transition between ferromagnetic and paramagnetic phases described by the order parameter $\frac{1}{N}\sum_i \langle s^z_i \rangle$ is driven entirely by quantum fluctuations. For both T and H^t nonzero, D. Bitko *et al.* found experimentally a line of continuous phase transitions which separates the ferromagnetic phase (lower region in Fig. 1) from the

paramagnetic phase (upper region in Fig. 1). For example, at $T = 0.100$ K they found $H_c^t = 49.3$ kOe. Thus, the classical phase transition at $H^t = 0$ and the quantum phase transition at $T = 0$ are connected by a line of continuous phase transitions. To develop a correct theoretical description of the equally important quantum and temperature fluctuations in this region has been a focus of many recent studies.

For further discussions on this issue as well as for other examples of quantum phase transitions see the review article for a general science audience[8] and the book[9] of S. Sachdev.

2. Spin-$\frac{1}{2}$ Ising Chain in a Transverse Field as the Simplest Model for the Quantum Phase Transition Theory

In early sixties of the last century E. Lieb, T. Schultz and D. Mattis[10] (see also the paper by S. Katsura[11]) suggested a new exactly solvable model, the so-called, spin-$\frac{1}{2}$ XY chain. In a particular case it transforms into the one-dimensional spin-$\frac{1}{2}$ Ising model in a transverse field; this case was examined in detail several years later by P. Pfeuty.[12] The long-known results for the Ising chain in a transverse field may be viewed in the context of the quantum phase transition theory. The transverse Ising chain is apparently the simplest model exhibiting the continuous quantum phase transition which can be studied in much detail since many statistical mechanics quantities for that model are amenable for rigorous calculations.

I begin to discuss these results introducing the model. It consists of $N \to \infty$ spins $\frac{1}{2}$ (which are represented by halves of the Pauli matrices) which are arranged in a row. Only the neighbouring spins interact *via* the Ising exchange interaction. Moreover, the spins interact with an external transverse field. The Hamiltonian of the model may be written as

$$H = \sum_{n=1}^{N} \Omega s_n^z + \sum_{n=1}^{N} J s_n^x s_{n+1}^x. \tag{12}$$

We may impose periodic (cyclic) boundary conditions assuming $s_{N+1}^{\alpha} = s_1^{\alpha}$ or open (free) boundary conditions assuming the last term in the second sum in (12) to be zero. The Ising chain without transverse field, $\Omega = 0$, exhibits the long-range order at zero temperature $T = 0$ with the order parameter $\langle s^x \rangle = \frac{1}{N} \sum_i \langle s_i^x \rangle$ which equals, say, $\frac{1}{2}$ [we assume the exchange interaction in (12) to be ferromagnetic, $J < 0$]. The long-range order is immediately destroyed, i.e. $\langle s^x \rangle = 0$, for any nonzero temperature $T > 0$. However, the Ising magnetization $\langle s^x \rangle$ can be destroyed at $T = 0$ by

quantum fluctuations, when we switch on in (12) the transverse field $\Omega \neq 0$. Small values of Ω reduce the transverse magnetizations $\langle s^x \rangle$ and after Ω exceeds the critical value $\Omega_c = |J|/2$ the Ising magnetization becomes zero. That is the scenario which was discussed above in connection with the low-temperature properties of $LiHoF_4$. The advantage of the introduced model (12) is a possibility to follow in great detail the quantum phase transition tuned by Ω.

Just after introducing the spin-$\frac{1}{2}$ XY-chains it was recognized that there was an intimate connection between the transverse Ising chain and the square-lattice Ising model (see, for example, a rederivation of the Onsager solution using the Jordan–Wigner fermionization[13]). The relationship between these models was demonstrated explicitly by M. Suzuki.[14,15] Consider the square-lattice Ising model (1) with the strength of horizontal interactions $J_h > 0$ and with the strength of vertical interactions $J_v > 0$ and the transverse Ising chain (12) with the exchange interaction $J < 0$ and with the transverse field Ω. The thermodynamic properties of the square-lattice Ising model are equivalent to the ground-state properties of the transverse Ising chain under the relations[14–16]

$$\frac{\exp\left(-J_v/2kT\right)}{J_h/2kT} = \frac{\Omega}{|J|}, \qquad J_h \to 0, \;\; J_v \to \infty. \tag{13}$$

Moreover, the temperature-driven continuous phase transition in the square-lattice Ising model corresponds to the transverse field-driven continuous phase transition at $T = 0$ in the transverse Ising chain. The critical temperature T_c corresponds to the critical transverse field Ω_c. The functions such as the Helmholtz free energy, entropy, and specific heat of temperature T correspond to the functions such as the ground-state energy, transverse magnetization, and static transverse susceptibility of the transverse field Ω. Finally, the correlation length ξ corresponds to the inverse energy gap Δ, $\xi \sim \Delta^{-1}$. The behaviour of some ground-state quantities found by P. Pfeuty[12] is reported in Table 1 and Fig. 2.

Table 1. Towards the correspondence between thermodynamic properties of the square-lattice Ising model and the ground-state properties of the transverse Ising chain.

Square-lattice Ising model	Transverse Ising chain
$m^z \sim (T_c - T)^{1/8}$	$\langle s^x \rangle \sim (\Omega_c - \Omega)^{1/8}$
$c \sim \ln \lvert T - T_c \rvert$	$\chi^z \sim \ln \lvert \Omega - \Omega_c \rvert$
$\xi \sim \lvert T - T_c \rvert^{-1}$	$\Delta \sim \lvert \Omega - \Omega_c \rvert$

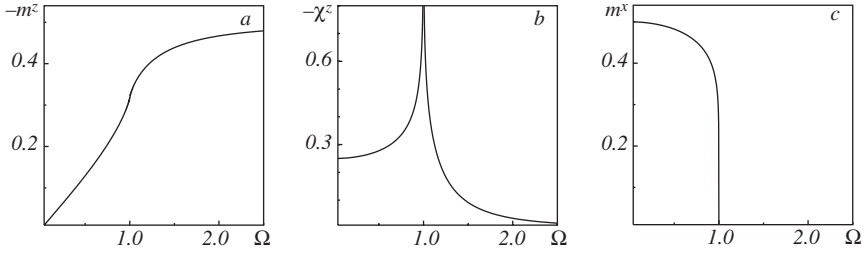

Fig. 2. The ground-state dependences of the transverse magnetization m^z (a), the static transverse susceptibility χ^z (b), and the longitudinal magnetization m^x (c) on the transverse field Ω for the transverse Ising chain (12) ($J = -2$).

Now I wish to explain briefly how the statistical mechanics calculations for the transverse Ising chain can be carried out without making any approximation. In terms of the spin raising and lowering operators $s_n^{\pm} = s_n^x \pm i s_n^y$ the Hamiltonian of the transverse Ising chain becomes

$$H = \sum_n \Omega_n \left(s_n^+ s_n^- - \frac{1}{2} \right) + \sum_n \frac{1}{2} I_n \left(s_n^+ s_{n+1}^+ + s_n^+ s_{n+1}^- + s_n^- s_{n+1}^+ + s_n^- s_{n+1}^- \right). \tag{14}$$

Bearing in mind the case of a regularly alternating chain we consider a model more general than (12) assuming that the Hamiltonian parameters are site-dependent, $\Omega \to \Omega_n$, $J \to J_n = 2I_n$. Although (14) is a bilinear form in terms of $s^{\pm}$ operators, further calculations appear to be complicated because of the commutation relations which are of the Fermi type at the same site,

$$\left\{ s_n^-, s_n^+ \right\} = 1, \qquad \left\{ s_n^-, s_n^- \right\} = \left\{ s_n^+, s_n^+ \right\} = 0 \tag{15}$$

and of the Bose type at different sites,

$$\left[s_n^-, s_m^+ \right] = \left[s_n^-, s_m^- \right] = \left[s_n^+, s_m^+ \right] = 0, \quad n \neq m. \tag{16}$$

We may use the Jordan–Wigner transformation[j] to introduce the Fermi operators according to the formulae,

$$c_n = \left(-2s_1^z\right)\left(-2s_2^z\right) \cdots \left(-2s_{n-1}^z\right) s_n^-, \tag{17}$$

$$c_n^+ = \left(-2s_1^z\right)\left(-2s_2^z\right) \cdots \left(-2s_{n-1}^z\right) s_n^+. \tag{18}$$

[j]The Jordan–Wigner transformation of the spin operators to spinless fermions is also described in Chapter 2 [see Eq. (3) of that Chapter].

Really, the introduced operators always satisfy the Fermi commutation relations

$$\left\{c_n, c_m^+\right\} = \delta_{nm}, \qquad \{c_n, c_m\} = \left\{c_n^+, c_m^+\right\} = 0. \tag{19}$$

Moreover, the Hamiltonian (14) in terms of the Fermi operators (17) and (18) remains a bilinear form, namely,

$$\begin{aligned} H &= \sum_n \Omega_n \left(c_n^+ c_n - \frac{1}{2}\right) \\ &\quad + \sum_n \frac{1}{2} I_n \left(c_n^+ c_{n+1}^+ + c_n^+ c_{n+1} - c_n c_{n+1}^+ - c_n c_{n+1}\right) \\ &= -\frac{1}{2}\sum_n \Omega_n + \sum_{n,m}\left[c_n^+ A_{nm} c_m + \frac{1}{2}\left(c_n^+ B_{nm} c_m^+ - c_n B_{nm} c_m\right)\right], \end{aligned} \tag{20}$$

where

$$A_{nm} = \Omega_n \delta_{nm} + \frac{1}{2} I_n \delta_{m,n+1} + \frac{1}{2} I_{n-1}\delta_{m,n-1} = A_{mn}, \tag{21}$$

$$B_{nm} = \frac{1}{2} I_n \delta_{m,n+1} - \frac{1}{2} I_{n-1}\delta_{m,n-1} = -B_{mn}. \tag{22}$$

For periodic boundary conditions imposed on (14), the transformed Hamiltonian (20) should also contain the so-called boundary term which is omitted since we send N to infinity.

We perform the linear canonical transformation with real coefficients to diagonalize a bilinear form (20) in Fermi operators

$$\eta_k = \sum_n \left(g_{kn} c_n + h_{kn} c_n^+\right), \qquad \eta_k^+ = \sum_n \left(g_{kn} c_n^+ + h_{kn} c_n\right). \tag{23}$$

The resulting Hamiltonian becomes

$$\begin{aligned} H &= \sum_{k=1}^{N} \Lambda_k \left(\eta_k^+ \eta_k - \frac{1}{2}\right), \\ &\left\{\eta_{k'}, \eta_{k''}^+\right\} = \delta_{k'k''}, \qquad \left\{\eta_{k'}, \eta_{k''}\right\} = \left\{\eta_{k'}^+, \eta_{k''}^+\right\} = 0, \end{aligned} \tag{24}$$

if the coefficients g_{kn}, h_{kn} or, more precisely, their linear combinations,

$$\Phi_{kn} = g_{kn} + h_{kn}, \qquad \Psi_{kn} = g_{kn} - h_{kn}, \tag{25}$$

satisfy the set of equations

$$\begin{aligned} \Lambda_k^2 \Phi_{kn} &= \sum_j \Phi_{kj} \left((\mathbf{A} - \mathbf{B})(\mathbf{A} + \mathbf{B})\right)_{jn}, \\ \Lambda_k^2 \Psi_{kn} &= \sum_j \Psi_{kj} \left((\mathbf{A} + \mathbf{B})(\mathbf{A} - \mathbf{B})\right)_{jn}. \end{aligned} \tag{26}$$

Eqs. (26) explicitly read

$$\begin{aligned}\Omega_{n-1}I_{n-1}\Phi_{k,n-1} + \left(I_{n-1}^2 + \Omega_n^2 - \Lambda_k^2\right)\Phi_{kn} + \Omega_n I_n \Phi_{k,n+1} = 0,\\ \Omega_n I_{n-1}\Psi_{k,n-1} + \left(I_n^2 + \Omega_n^2 - \Lambda_k^2\right)\Psi_{kn} + \Omega_{n+1} I_n \Psi_{k,n+1} = 0,\end{aligned} \tag{27}$$

with periodic or open boundary conditions implied. Equations (27) and (25) determine the coefficients g_{kn} and h_{kn} in (23) and the elementary excitation energies Λ_k in (24).

For the uniform transverse Ising chain, $\Omega_n = \Omega$, $I_n = I$, the bilinear form (20) in Fermi operators becomes diagonal after performing:

(i) the Fourier transformation

$$c_j = \frac{1}{\sqrt{N}}\sum_\kappa \exp\left(-i\kappa j\right) c_\kappa, \qquad c_j^+ = \frac{1}{\sqrt{N}}\sum_\kappa \exp\left(i\kappa j\right) c_\kappa^+ \tag{28}$$

with $\kappa = (2\pi/N)n$ and $n = -\frac{1}{2}N, -\frac{1}{2}N+1, \ldots, \frac{1}{2}N-1$ if N is even or $n = -\frac{1}{2}(N-1), -\frac{1}{2}(N-1)+1, \ldots, \frac{1}{2}(N-1)$ if N is odd, and

(ii) the Bogolyubov transformation

$$\eta_\kappa = x_\kappa c_\kappa + y_\kappa c_{-\kappa}^+, \qquad \eta_{-\kappa}^+ = y_{-\kappa}^* c_\kappa + x_{-\kappa}^* c_{-\kappa}^+ \tag{29}$$

with

$$x_\kappa = \frac{iI\sin\kappa}{\sqrt{2\Lambda_\kappa\left(\Lambda_\kappa - \epsilon_\kappa\right)}}, \qquad y_\kappa = \sqrt{\frac{\Lambda_\kappa - \epsilon_\kappa}{2\Lambda_\kappa}}, \tag{30}$$

$$\Lambda_\kappa = \sqrt{\epsilon_\kappa^2 + I^2\sin^2\kappa}, \qquad \epsilon_\kappa = \Omega + I\cos\kappa. \tag{31}$$

Knowing the energies of the noninteracting fermions Λ_k in (24) we immediately obtain the Helmholtz free energy per site (and hence all thermodynamic quantities),

$$\begin{aligned} f &= -\frac{1}{N\beta}\ln \mathrm{Tr}\exp\left(-\beta H\right)\\ &= -\frac{1}{N\beta}\ln\prod_{k=1}^{N}\left[\exp\left(\frac{\beta\Lambda_k}{2}\right) + \exp\left(-\frac{\beta\Lambda_k}{2}\right)\right]\\ &= -\frac{1}{N\beta}\sum_{k=1}^{N}\ln\left(2\cosh\frac{\beta\Lambda_k}{2}\right)\\ &= -\frac{1}{2\pi\beta}\int_{-\pi}^{\pi} d\kappa \ln\left(2\cosh\frac{\beta\Lambda_\kappa}{2}\right)\end{aligned} \tag{32}$$

[the last line in (32) refers to the uniform case (31)]. Note, that we can obtain all thermodynamic quantities knowing the distributions of the

energies of elementary excitations,

$$\rho(E) = \frac{1}{N}\sum_{k=1}^{N} \delta\left(E - \Lambda_k\right), \qquad \int_{-\infty}^{\infty} dE\ \rho(E) = 1, \tag{33}$$

or the distribution of the squared energies of elementary excitations

$$R(E^2) = \frac{1}{N}\sum_{k=1}^{N} \delta\left(E^2 - \Lambda_k^2\right), \qquad \int_{0}^{\infty} dE^2 R(E^2) = 1. \tag{34}$$

Really, the density of states $\rho(E)$ (33) or the density of states $R(E^2)$ (34) immediately yields

$$\begin{aligned} f &= -\frac{1}{\beta}\int_{-\infty}^{\infty} dE\ \rho(E) \ln\left(2\cosh\frac{\beta E}{2}\right) \\ &= -\frac{2}{\beta}\int_{0}^{\infty} dE\ ER(E^2) \ln\left(2\cosh\frac{\beta E}{2}\right). \end{aligned} \tag{35}$$

The calculation of the spin correlation functions in the fermionic picture looks as follows. First we write down the relations between the spin and Fermi operators. We have

$$s_n^z = c_n^+ c_n - \frac{1}{2} = -\frac{1}{2}(c_n^+ + c_n)(c_n^+ - c_n) = -\frac{1}{2}\varphi_n^+\varphi_n^-, \tag{36}$$

where we have introduced the operators $\varphi_n^{\pm} = c_n^+ \pm c_n$[k]. Further,

$$s_n^x = \frac{1}{2}\varphi_1^+\varphi_1^- \ldots \varphi_{n-1}^+\varphi_{n-1}^-\varphi_n^+, \tag{37}$$

$$s_n^y = \frac{1}{2i}\varphi_1^+\varphi_1^- \ldots \varphi_{n-1}^+\varphi_{n-1}^-\varphi_n^-. \tag{38}$$

Note that the relations between the operators s_n^x, s_n^y and the Fermi operators are nonlocal since the r.h.s. in Eqs. (37) and (38) involve the Fermi operators attached to all previous sites. That is in contrast to the similar relation (36) for the operator s_n^z, the r.h.s. of which contains only the Fermi operators attached to the same site n.

[k]The operators $\varphi^{\pm}$ are related to the Clifford operators Γ^1, Γ^2 [Chapter 2, Eq. (5)] as follows: $\varphi_n^+ = \Gamma_n^1$, $\varphi_n^- = -i\Gamma_n^2$.

Now we can rewrite the spin correlation functions in fermionic language. For example,

$$\langle s_n^z s_{n+m}^z \rangle = \frac{1}{4} \langle \varphi_n^+ \varphi_n^- \varphi_{n+m}^+ \varphi_{n+m}^- \rangle, \tag{39}$$

$$\langle s_n^x s_{n+m}^x \rangle = \frac{1}{4} \langle \varphi_n^- \varphi_{n+1}^+ \varphi_{n+1}^- \cdots \varphi_{n+m-1}^+ \varphi_{n+m-1}^- \varphi_{n+m}^+ \rangle. \tag{40}$$

To get the latter result we use the relations

$$\left\{ \varphi_n^+, \varphi_m^+ \right\} = - \left\{ \varphi_n^-, \varphi_m^- \right\} = 2\delta_{nm}, \qquad \left\{ \varphi_n^+, \varphi_m^- \right\} = 0. \tag{41}$$

The operators $\varphi_n^\pm$ are linear combinations of operators η_k, η_k^+ involved in (24),

$$\varphi_n^+ = \sum_{p=1}^{N} \Phi_{pn} \left(\eta_p^+ + \eta_p \right), \qquad \varphi_n^- = \sum_{p=1}^{N} \Psi_{pn} \left(\eta_p^+ - \eta_p \right), \tag{42}$$

or for the uniform chain

$$\begin{aligned} \varphi_n^+ &= \frac{1}{\sqrt{N}} \sum_\kappa \exp\left(i\kappa n\right) \left(x_\kappa + y_\kappa \right) \left(\eta_\kappa^+ + \eta_{-\kappa} \right), \\ \varphi_n^- &= \frac{1}{\sqrt{N}} \sum_\kappa \exp\left(i\kappa n\right) \left(x_\kappa - y_\kappa \right) \left(\eta_\kappa^+ - \eta_{-\kappa} \right). \end{aligned} \tag{43}$$

Therefore, we calculate (39), (40) using the Wick–Bloch–de Dominicis theorem,[1] namely,

$$\begin{aligned} 4\langle s_n^z s_{n+m}^z \rangle &= \langle \varphi_n^+ \varphi_n^- \varphi_{n+m}^+ \varphi_{n+m}^- \rangle \\ &= \langle \varphi_n^+ \varphi_n^- \rangle \langle \varphi_{n+m}^+ \varphi_{n+m}^- \rangle - \langle \varphi_n^+ \varphi_{n+m}^+ \rangle \langle \varphi_n^- \varphi_{n+m}^- \rangle \\ &\quad + \langle \varphi_n^+ \varphi_{n+m}^- \rangle \langle \varphi_n^- \varphi_{n+m}^+ \rangle. \end{aligned} \tag{44}$$

The r.h.s. of Eq. (44) may be compactly written as the Pfaffian of the 4×4 antisymmetric matrix

$$4\langle s_n^z s_{n+m}^z \rangle = \mathrm{Pf} \begin{pmatrix} 0 & \langle \varphi_n^+ \varphi_n^- \rangle & \langle \varphi_n^+ \varphi_{n+m}^+ \rangle & \langle \varphi_n^+ \varphi_{n+m}^- \rangle \\ -\langle \varphi_n^+ \varphi_n^- \rangle & 0 & \langle \varphi_n^- \varphi_{n+m}^+ \rangle & \langle \varphi_n^- \varphi_{n+m}^- \rangle \\ -\langle \varphi_n^+ \varphi_{n+m}^+ \rangle & -\langle \varphi_n^- \varphi_{n+m}^+ \rangle & 0 & \langle \varphi_{n+m}^+ \varphi_{n+m}^- \rangle \\ -\langle \varphi_n^+ \varphi_{n+m}^- \rangle & -\langle \varphi_n^- \varphi_{n+m}^- \rangle & -\langle \varphi_{n+m}^+ \varphi_{n+m}^- \rangle & 0 \end{pmatrix}. \tag{45}$$

[1] See also Section 3.1.2 in Chapter 2.

Similarly,

$$4\langle s_n^x s_{n+m}^x\rangle = \mathrm{Pf}\begin{pmatrix} 0 & \langle\varphi_n^-\varphi_{n+1}^+\rangle & \langle\varphi_n^-\varphi_{n+1}^-\rangle & \dots & \langle\varphi_n^-\varphi_{n+m}^+\rangle \\ -\langle\varphi_n^-\varphi_{n+1}^+\rangle & 0 & \langle\varphi_{n+1}^+\varphi_{n+1}^-\rangle & \dots & \langle\varphi_{n+1}^+\varphi_{n+m}^+\rangle \\ -\langle\varphi_n^-\varphi_{n+1}^-\rangle & -\langle\varphi_{n+1}^+\varphi_{n+1}^-\rangle & 0 & \dots & \langle\varphi_{n+1}^-\varphi_{n+m}^+\rangle \\ \vdots & \vdots & \vdots & \dots & \vdots \\ -\langle\varphi_n^-\varphi_{n+m}^+\rangle & -\langle\varphi_{n+1}^+\varphi_{n+m}^+\rangle & -\langle\varphi_{n+1}^-\varphi_{n+m}^+\rangle & \dots & 0 \end{pmatrix}. \tag{46}$$

The elementary contractions involved into (45) and (46) read

$$\begin{aligned} \langle\varphi_n^+\varphi_m^+\rangle &= \sum_{k=1}^N \Phi_{kn}\Phi_{km} = \delta_{nm}, \\ \langle\varphi_n^+\varphi_m^-\rangle &= \sum_{k=1}^N \Phi_{kn}\Psi_{km}\tanh\frac{1}{2}\beta\Lambda_p, \\ \langle\varphi_n^-\varphi_m^+\rangle &= -\sum_{k=1}^N \Psi_{kn}\Phi_{km}\tanh\frac{1}{2}\beta\Lambda_p, \\ \langle\varphi_n^-\varphi_m^-\rangle &= -\sum_{k=1}^N \Psi_{kn}\Psi_{km} = -\delta_{nm}. \end{aligned} \tag{47}$$

In the uniform case, instead of (47) we have

$$\begin{aligned} &\langle\varphi_n^+\varphi_m^+\rangle = -\langle\varphi_n^-\varphi_m^-\rangle = \delta_{nm}, \\ &\langle\varphi_n^+\varphi_m^-\rangle = \frac{1}{N}\sum_\kappa \exp(i\kappa(n-m))\frac{\Omega + I\exp(-i\kappa)}{\Lambda_\kappa}\tanh\frac{\beta\Lambda_\kappa}{2}, \\ &\langle\varphi_n^-\varphi_m^+\rangle = -\frac{1}{N}\sum_\kappa \exp(-i\kappa(n-m))\frac{\Omega + I\exp(-i\kappa)}{\Lambda_\kappa}\tanh\frac{\beta\Lambda_\kappa}{2}. \end{aligned} \tag{48}$$

It is worth recalling some properties of the Pfaffians which are used in calculating them. In the first numerical studies the authors used the relation

$$(\mathrm{Pf}\mathbf{A})^2 = \det\mathbf{A} \tag{49}$$

and computed numerically the determinants which gave the values of Pfaffians. On the other hand, the Pfaffian may be computed directly,[17,18]

noting that

$$\mathrm{Pf}\left(\mathbf{U}^T\mathbf{A}\mathbf{U}\right) = \det\mathbf{U}\ \mathrm{Pf}\mathbf{A} \tag{50}$$

and that

$$\mathrm{Pf}\begin{pmatrix} 0 & R_{12} & 0 & 0 & \dots & 0 \\ -R_{12} & 0 & 0 & 0 & \dots & 0 \\ 0 & 0 & 0 & R_{34} & \dots & 0 \\ 0 & 0 & -R_{34} & 0 & \dots & 0 \\ \vdots & \vdots & \vdots & \vdots & \dots & \vdots \\ 0 & 0 & 0 & 0 & \dots & 0 \end{pmatrix} = R_{12}R_{34}\cdots . \tag{51}$$

Let me finally show how the results for the transverse Ising chain obtained by P. Pfeuty[12] arise in the described approach. Recalling Eq. (24) [or Eq. (32)] it is not hard to see that the ground-state energy per site can be written as

$$\begin{aligned} e_0 &= \frac{1}{2\pi}\int_{-\pi}^{\pi} d\kappa \left(-\frac{\Lambda_\kappa}{2}\right) \\ &= -\frac{1}{4\pi}\int_{-\pi}^{\pi} d\kappa\ \sqrt{\Omega^2 + 2\Omega I\cos\kappa + I^2} \\ &= -\frac{I}{4\pi}\int_{-\pi}^{\pi} d\kappa \sqrt{\lambda^2 + 2\lambda\cos\kappa + 1} \\ &= -\frac{I\,(1+\lambda)}{\pi}\int_0^{\pi/2} d\phi \sqrt{1 - \left(\frac{2\sqrt{\lambda}}{1+\lambda}\right)^2 \sin^2\phi} \\ &= -\frac{I\,(1+\lambda)}{\pi} E\left(\frac{\pi}{2}, \frac{2\sqrt{\lambda}}{1+\lambda}\right), \end{aligned} \tag{52}$$

where $\lambda = \Omega/I$ and

$$E\left(\frac{\pi}{2}, a\right) = \int_0^{\pi/2} d\phi\ \sqrt{1 - a^2\sin^2\phi}$$

is the complete elliptic integral of the second kind.[19] In the vicinity of $a = 1$

$$E\left(\frac{\pi}{2}, a\right) \sim 1 + \frac{1-a^2}{4}\ln\frac{16}{1-a^2} \tag{53}$$

(see Refs. 20 and 4) and therefore in the vicinity of $\lambda_c = 1$ the ground-state energy (52) contains the nonanalytic contribution

$$e_0 \sim (\lambda - \lambda_c)^2 \ln|\lambda - \lambda_c| . \tag{54}$$

As a result the ground-state transverse magnetization contains the nonanalytic contribution

$$m^z \sim (\lambda - \lambda_c) \ln |\lambda - \lambda_c| \tag{55}$$

and the ground-state static transverse susceptibility exhibits a logarithmic singularity

$$\chi^z \sim \ln |\lambda - \lambda_c| \,. \tag{56}$$

At $\lambda_c = 1$ the energy spectrum is gapless, i.e. there is a zero-energy elementary excitation. In the vicinity of $\lambda_c = 1$ the energy gap Δ is given by the smallest value of $\Lambda_\kappa = \sqrt{\Omega^2 + 2\Omega I \cos\kappa + I^2}$ and hence

$$\Delta \sim |\lambda - \lambda_c| \,. \tag{57}$$

To end up the discussion of the ground-state properties of the transverse Ising chain, let me emphasize that the quantum phase transition appears since the spin variables are the q-numbers rather than the c-numbers. To demonstrate this explicitly we may consider the spin-vector (instead of spin-matrix) transverse Ising chain. The model consists of $N \to \infty$ 3-component vectors

$$\mathbf{s} = (s^x, s^y, s^z) = (s \sin\theta \cos\phi, s \sin\theta \sin\phi, s \cos\theta),$$

which are governed by the Hamiltonian

$$H = \sum_n \Omega s \cos\theta_n + \sum_n 2I s^2 \sin\theta_n \sin\theta_{n+1} \cos\phi_n \cos\phi_{n+1}. \tag{58}$$

Here θ and ϕ are the spherical coordinates of the spin and s is the value of the spin which plays only a quantitative role and further we have set $s = \frac{1}{2}$. To obtain the ground-state energy we should place all spins in the xz plane putting $\phi_n = 0$ ($I < 0$). Moreover, the angles θ_n must minimize the sum of contributions due to the interaction with the field and due to the intersite interaction. Thus, the ground-state energy ansatz reads

$$E_0(\theta) = \frac{1}{2} N \Omega \cos\theta - \frac{1}{2} N |I| \sin^2\theta, \tag{59}$$

where θ is determined to minimize $E_0(\theta)$ (59). Obviously

$$\cos\theta = \begin{cases} 1 & \text{if } \Omega < -2|I|, \\ -\dfrac{\Omega}{2|I|} & \text{if } -2|I| \le \Omega < 2|I|, \\ -1 & \text{if } 2|I| \le \Omega. \end{cases} \tag{60}$$

As a result, we find that the ground-state energy per site is given by

$$e_0 = \begin{cases} \dfrac{1}{2}\Omega & \text{if } \Omega < -2|I|, \\ -\dfrac{|I|}{2}\left(1 + \dfrac{\Omega^2}{4I^2}\right) & \text{if } -2|I| \le \Omega < 2|I|, \\ -\dfrac{1}{2}\Omega & \text{if } 2|I| \le \Omega. \end{cases} \tag{61}$$

Moreover, the x- and z-magnetizations which can be obtained after inserting (60) into the formulas $m^x = s\sin\theta$ and $m^z = s\cos\theta$, respectively, behave as

$$m^x = \begin{cases} 0 & \text{if } \Omega < -2|I|, \\ \dfrac{1}{2}\sqrt{1 - \dfrac{\Omega^2}{4I^2}} & \text{if } -2|I| \le \Omega < 2|I|, \\ 0 & \text{if } 2|I| \le \Omega, \end{cases} \tag{62}$$

and

$$m^z = \begin{cases} \dfrac{1}{2} & \text{if } \Omega < -2|I|, \\ -\dfrac{\Omega}{4|I|} & \text{if } -2|I| \le \Omega < 2|I|, \\ -\dfrac{1}{2} & \text{if } 2|I| \le \Omega, \end{cases} \tag{63}$$

respectively. Evidently, there is no singularity in the ground-state dependence of the static transverse susceptibility $\chi^z = \partial m^z/\partial\Omega$ on the transverse field Ω. As the transverse field increases from zero to $2|I|$, the on-site magnetic moments smoothly change their direction from the x- to the z-axis. The quantum phase transition appears only due to the quantum fluctuations, which arise when the spin components do not commute and no phase transition occurs when the spin components are classical variables (cf. Fig. 2 and Fig. 3).

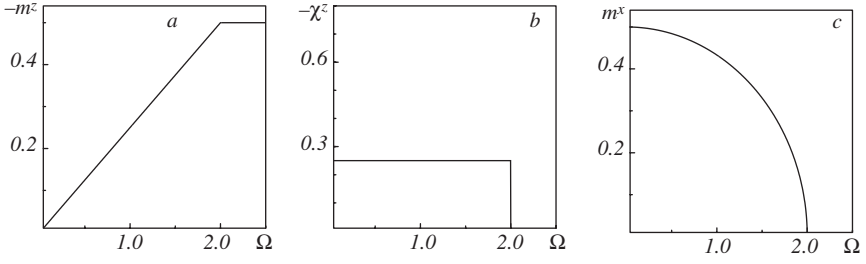

Fig. 3. The same as in Fig. 2 for the classical transverse Ising chain (58) ($s = \frac{1}{2}$, $I = -1$).

3. Spin-$\frac{1}{2}$ Ising Chain in a Transverse Field with Regularly Alternating Hamiltonian Parameters: Continued Fraction Approach

We are turning to a discussion of the effects of regularly alternating exchange interactions and fields on the quantum phase transition inherent in the transverse Ising chain. Note that there has been a great deal of work done examining the effects of different modifications of the skeleton model on the quantum phase transition. Thus, J. M. Luck[21] analysed the critical behaviour of the chain with an aperiodic sequence of interactions, D. S. Fisher[22] performed an extensive real-space renormalization group study of random chains, F. Iglói *et al.*[23] reported a renormalization-group study of aperiodic chains. However, a simpler case of regularly alternating transverse Ising chain still contains a good deal of unexplored physics. It appears possible to obtain analytically exact results for thermodynamic quantities of such models using the Jordan–Wigner fermionization and the continued fraction approach.[24,25] Moreover, for certain sets of the Hamiltonian parameters the exact results may be obtained for the spin correlation functions.[26] In all other cases, spin correlations may be explored numerically at a high precision level considering sufficiently long chains up to a few thousand sites.[26,27] It is appropriate to mention here the old studies[28,29] referring to the chains of period 2 which were extended further to the one-dimensional anisotropic XY model on superlattices.[30,31] The quantum critical points in the anisotropic XY chains in a transverse field with periodically varying intersite interactions (having periods 2 and 3) have been determined recently[32] using the transfer matrix method.

I begin with explaining how the thermodynamic quantities can be derived using continued fractions. For this purpose let me recall that the energies of the Jordan–Wigner fermions which determine the thermodynamic properties of a spin chain are involved into Eqs. (27). Consider, for example, the first set of equations in (27) which can be rewritten in the matrix form as follows:

$$\left(\mathbf{H} - \Lambda_k^2 \mathbf{1}\right) \begin{pmatrix} \Phi_{k1} \\ \Phi_{k2} \\ \Phi_{k3} \\ \vdots \\ \Phi_{kN} \end{pmatrix} = 0, \tag{64}$$

where

$$\mathbf{H} = \begin{pmatrix} \vdots & \vdots & \vdots & \vdots & \vdots & \vdots & \vdots \\ \dots & \Omega_{n-2} I_{n-2} & I_{n-2}^2 + \Omega_{n-1}^2 & \Omega_{n-1} I_{n-1} & 0 & 0 & \dots \\ \dots & 0 & \Omega_{n-1} I_{n-1} & I_{n-1}^2 + \Omega_n^2 & \Omega_n I_n & 0 & \dots \\ \dots & 0 & 0 & \Omega_n I_n & I_n^2 + \Omega_{n+1}^2 & \Omega_{n+1} I_{n+1} & \dots \\ \vdots & \vdots & \vdots & \vdots & \vdots & \vdots & \vdots \end{pmatrix} \tag{65}$$

and $\mathbf{1}$ denotes the unit matrix. Thus, all Λ_k^2 are the eigenvalues of the $N \times N$ matrix (65) entering (64). To find their distribution $R(E^2)$ (34) we may use the Green function approach. Consider a matrix $\mathbf{G}$ composed of the elements $G_{nm} = G_{nm}(E^2)$ which is introduced by the equation

$$\left(E^2 \mathbf{1} - \mathbf{H}\right) \mathbf{G} = \mathbf{1}. \tag{66}$$

Having composed a matrix $\mathbf{U}^+$ of the eigenvectors of the matrix $\mathbf{H}$ (65), i.e.

$$\mathbf{U}\mathbf{H}\mathbf{U}^+ = \begin{pmatrix} \Lambda_1^2 & 0 & \dots & 0 \\ 0 & \Lambda_2^2 & \dots & 0 \\ \vdots & \vdots & \vdots & \vdots \\ 0 & 0 & \dots & \Lambda_N^2 \end{pmatrix}, \tag{67}$$

one finds

$$\begin{pmatrix} E^2 - \Lambda_1^2 & 0 & \dots & 0 \\ 0 & E^2 - \Lambda_2^2 & \dots & 0 \\ \vdots & \vdots & \vdots & \vdots \\ 0 & 0 & \dots & E^2 - \Lambda_N^2 \end{pmatrix} \mathbf{U}\mathbf{G}\mathbf{U}^+ = \mathbf{1}. \tag{68}$$

As a result

$$\mathrm{Tr}\mathbf{G} = \sum_{k=1}^{N} \left(\mathbf{U}\mathbf{G}\mathbf{U}^+\right)_{kk} = \sum_{k=1}^{N} \frac{1}{E^2 - \Lambda_k^2}. \tag{69}$$

Making the substitution

$$E^2 \to E^2 \pm i\epsilon, \quad \epsilon \to +0 \tag{70}$$

and using the symbolic identity

$$\frac{1}{E^2 - \Lambda_k^2 \pm i\epsilon} = \mathcal{P} \frac{1}{E^2 - \Lambda_k^2} \mp i\pi\delta\left(E^2 - \Lambda_k^2\right), \quad \epsilon \to +0 \tag{71}$$

one arrives at the relation

$$\mp\frac{1}{N\pi}\sum_{n=1}^{N}\Im G_{nn}(E^2\pm i\epsilon)=\frac{1}{N}\sum_{n=1}^{N}\delta(E^2-\Lambda_n^2)=R(E^2). \qquad (72)$$

Thus, our task is to find the diagonal Green functions G_{nn} defined by Eqs. (66) and (65).

Considering the equation for G_{nn},

$$\left(E^2-\Omega_n^2-I_{n-1}^2\right)G_{nn}-\Omega_{n-1}I_{n-1}G_{n-1,n}-\Omega_nI_nG_{n+1,n}=1, \qquad (73)$$

and then the equations

$$\begin{aligned}\left(E^2-\Omega_{n-1}^2-I_{n-2}^2\right)G_{n-1,n}-\Omega_{n-2}I_{n-2}G_{n-2,n}-\Omega_{n-1}I_{n-1}G_{nn}=0,\\ \left(E^2-\Omega_{n-2}^2-I_{n-3}^2\right)G_{n-2,n}-\Omega_{n-3}I_{n-3}G_{n-3,n}-\Omega_{n-2}I_{n-2}G_{n-1,n}=0,\end{aligned} \qquad (74)$$

etc. to determine $G_{n-1,n}/G_{nn}$, $G_{n-2,n}/G_{n-1,n}$ etc., and the equations

$$\begin{aligned}\left(E^2-\Omega_{n+1}^2-I_n^2\right)G_{n+1,n}-\Omega_nI_nG_{nn}-\Omega_{n+1}I_{n+1}G_{n+2,n}=0,\\ \left(E^2-\Omega_{n+2}^2-I_{n+1}^2\right)G_{n+2,n}-\Omega_{n+1}I_{n+1}G_{n+1,n}-\Omega_{n+2}I_{n+2}G_{n+3,n}=0,\end{aligned} \qquad (75)$$

etc. to determine $G_{n+1,n}/G_{nn}$, $G_{n+2,n}/G_{n+1,n}$ etc., we easily find the following continued fraction representation for the diagonal Green functions:

$$\begin{aligned}G_{nn}&=\frac{1}{E^2-\Omega_n^2-I_{n-1}^2-\Delta_n^--\Delta_n^+},\\ \Delta_n^-&=\cfrac{\Omega_{n-1}^2I_{n-1}^2}{E^2-\Omega_{n-1}^2-I_{n-2}^2-\cfrac{\Omega_{n-2}^2I_{n-2}^2}{E^2-\Omega_{n-2}^2-I_{n-3}^2-\ddots}},\\ \Delta_n^+&=\cfrac{\Omega_n^2I_n^2}{E^2-\Omega_{n+1}^2-I_n^2-\cfrac{\Omega_{n+1}^2I_{n+1}^2}{E^2-\Omega_{n+2}^2-I_{n+1}^2-\ddots}}.\end{aligned} \qquad (76)$$

A crucial simplification occurs if a sequence of the Hamiltonian parameters is periodic,

$$\Omega_1I_1\Omega_2I_2\cdots\Omega_pI_p\Omega_1I_1\Omega_2I_2\cdots\Omega_pI_p\cdots .$$

Then the continued fractions in (76) become periodic and can be evaluated exactly by solving a square equation. Consider, for example, the case $p=1$,

i.e. the uniform chain. Then $\Delta_n^- = \Delta_n^+ = \Delta$ (not to be confused with the energy gap Δ) and Δ satisfies the following equation

$$\Delta = \frac{\Omega^2 I^2}{E^2 - \Omega^2 - I^2 - \Delta}. \tag{77}$$

The solution of Eq. (77),

$$\Delta = \frac{1}{2}(E^2 - \Omega^2 - I^2 \pm \sqrt{(E^2 - \Omega^2 - I^2)^2 - 4\Omega^2 I^2}), \tag{78}$$

yields

$$G_{nn} = \mp \frac{1}{\sqrt{(E^2 - \Omega^2 - I^2)^2 - 4\Omega^2 I^2}} \tag{79}$$

and hence in accordance with (72)

$$R(E^2) = \begin{cases} \frac{1}{\pi\sqrt{4\Omega^2 I^2 - (E^2 - \Omega^2 - I^2)^2}} & \text{if } (\Omega - I)^2 < E^2 < (\Omega + I)^2, \\ 0 & \text{otherwise.} \end{cases} \tag{80}$$

We may easily repeat the calculations for $p = 2$ or $p = 3$. The desired density of states in these cases is given by

$$R(E^2) = \begin{cases} \frac{|\mathcal{Z}_{p-1}(E^2)|}{p\pi\sqrt{\mathcal{A}_{2p}(E^2)}} & \text{if } \mathcal{A}_{2p}(E^2) > 0, \\ 0 & \text{otherwise,} \end{cases} \tag{81}$$

where $\mathcal{Z}_{p-1}(E^2)$ and $\mathcal{A}_{2p}(E^2) = -\prod_{j=1}^{2p}\left(E^2 - a_j\right)$ are polynomials of the order $p-1$ and $2p$, respectively, and $a_j \geq 0$ are the roots of $\mathcal{A}_{2p}(E^2)$. Explicitly,

$$\begin{aligned} \mathcal{Z}_1(E^2) &= 2E^2 - \Omega_1^2 - \Omega_2^2 - I_1^2 - I_2^2, \\ \mathcal{A}_4(E^2) &= 4\Omega_1^2\Omega_2^2 I_1^2 I_2^2 \\ &\quad - \left(E^4 - \left(\Omega_1^2 + \Omega_2^2 + I_1^2 + I_2^2\right) E^2 + \Omega_1^2\Omega_2^2 + I_1^2 I_2^2\right)^2 \\ &= -(E^2 - a_1)(E^2 - a_2)(E^2 - a_3)(E^2 - a_4), \\ \{a_j\} &= \Big\{\frac{1}{2}\Big[\Omega_1^2 + \Omega_2^2 + I_1^2 + I_2^2 \\ &\quad \pm\sqrt{(\Omega_1^2 + \Omega_2^2 + I_1^2 + I_2^2)^2 - 4(\Omega_1\Omega_2 \pm I_1 I_2)^2}\Big]\Big\}; \end{aligned} \tag{82}$$

$$\begin{aligned}\mathcal{Z}_2(E^2) &= 3E^4 - 2\left(\Omega_1^2+\Omega_2^2+\Omega_3^2+I_1^2+I_2^2+I_3^2\right)E^2 \\ &\quad +\Omega_1^2\Omega_2^2+\Omega_1^2I_2^2+I_1^2I_2^2+\Omega_2^2\Omega_3^2+\Omega_2^2I_3^2+I_2^2I_3^2 \\ &\quad +\Omega_3^2\Omega_1^2+\Omega_3^2I_1^2+I_3^2I_1^2,\end{aligned}$$

$$\begin{aligned}\mathcal{A}_6(E^2) &= 4\Omega_1^2\Omega_2^2\Omega_3^2I_1^2I_2^2I_3^2 \\ &\quad -\big[E^6-\left(\Omega_1^2+\Omega_2^2+\Omega_3^2+I_1^2+I_2^2+I_3^2\right)E^4 \\ &\quad +\left(\Omega_1^2\Omega_2^2+\Omega_1^2I_2^2+I_1^2I_2^2+\Omega_2^2\Omega_3^2+\Omega_2^2I_3^2+I_2^2I_3^2\right. \\ &\quad \left.+\Omega_3^2\Omega_1^2+\Omega_3^2I_1^2+I_3^2I_1^2\right)E^2-\Omega_1^2\Omega_2^2\Omega_3^2-I_1^2I_2^2I_3^2\big]^2 \\ &= -(E^2-a_1)(E^2-a_2)(E^2-a_3)(E^2-a_4)(E^2-a_5)(E^2-a_6),\end{aligned} \tag{83}$$

where $a_1,\ldots,a_6$ are the solutions of two cubic equations which follow from the equation $\mathcal{A}_6(E^2)=0$.

Knowing the density of states $R(E^2)$ (81) we immediately obtain all quantities of interest. Thus, the gap in the energy spectrum of the spin model is given by the square root of the smallest root of the polynomial $\mathcal{A}_{2p}(E^2)$. Further, the ground-state energy per site is given by

$$e_0 = -\int_0^\infty dE\ E^2R(E^2). \tag{84}$$

Recalling Eq. (35) for the Helmholtz free energy per site we find that the specific heat per site is given by

$$\frac{c}{k} = 2\int_0^\infty dE\ ER(E^2)\left(\frac{\frac{1}{2}\beta E}{\cosh\frac{1}{2}\beta E}\right)^2. \tag{85}$$

We assume that $\Omega_n=\Omega+\Delta\Omega_n$ and define the transverse magnetization per site and the static transverse susceptibility per site as follows:

$$\begin{aligned}m^z &= \partial f/\partial\Omega \\ &= -\frac{2}{\beta}\int_0^\infty dE\ E\frac{\partial R(E^2)}{\partial\Omega}\ln\left(2\cosh\frac{\beta E}{2}\right),\end{aligned} \tag{86}$$

$$\begin{aligned}\chi^z &= \partial m^z/\partial\Omega \\ &= -\frac{2}{\beta}\int_0^\infty dE\ E\frac{\partial^2 R(E^2)}{\partial\Omega^2}\ln\left(2\cosh\frac{\beta E}{2}\right).\end{aligned} \tag{87}$$

Unfortunately, the elaborate approach yields only the density of states (34) and thus is restricted to the thermodynamic quantities. To obtain the spin correlation functions $\langle s_j^\alpha s_{j+n}^\alpha\rangle$, $\alpha=x,z$ of the regularly alternating transverse Ising chain (45), (46) and (47) we use a numerical

approach.[17,18,26,27] The on-site magnetizations can be calculated from the spin correlation functions using the relation

$$m_{j_1}^{\alpha} m_{j_2}^{\alpha} = \lim_{r\to\infty} \langle s_{j_1}^{\alpha} s_{j_2+rp}^{\alpha} \rangle, \tag{88}$$

where $1 \ll j_1 \ll N$ is one of the p consecutive numbers taken sufficiently far from the ends of the chain and $j_2 - j_1 = 0, 1, \ldots, p-1$. Assuming that

$$\langle s_j^{\alpha} s_{j+rp}^{\alpha} \rangle - \langle s_j^{\alpha} \rangle \langle s_{j+rp}^{\alpha} \rangle \sim \exp\left(-rp/\xi^{\alpha}\right) \tag{89}$$

for large r ($1 \ll j, j+rp \ll N$) we can determine the correlation length ξ^{α}.

4. Effects of Regularly Alternating Bonds/Fields on the Quantum Phase Transition

Now we shall use the analytical results for the ground-state and thermodynamic quantities and the numerical data for the spin correlation functions to discuss the effects of regularly alternating Hamiltonian parameters on the quantum phase transition inherent in the transverse Ising chain.

We start with the energy gap Δ. The quantum phase transition point is determined by the condition $\Delta = 0$. The density of states $R(E^2)$ permits us to find the energy gap Δ since, as has already been mentioned, the smallest root of the polynomial $\mathcal{A}_{2p}(E^2)$ [see (81)] is the smallest elementary excitation energy squared. Therefore, the energy spectrum becomes gapless when

$$\mathcal{A}_{2p}(0) = 0. \tag{90}$$

In the case of period 2 the condition (90), $\mathcal{A}_4(0) = 0$, yields

$$\Omega_1 \Omega_2 = \pm I_1 I_2. \tag{91}$$

In the case of period 3 the condition (90), $\mathcal{A}_6(0) = 0$, yields

$$\Omega_1 \Omega_2 \Omega_3 = \pm I_1 I_2 I_3. \tag{92}$$

It should be emphasized here that we have rederived the long-known condition of the zero-energy elementary excitations obtained by P. Pfeuty.[33] P. Pfeuty showed that a nonuniform transverse Ising chain becomes gapless if

$$\Omega_1 \Omega_2 \Omega_3 \cdots \Omega_N = \pm I_1 I_2 I_3 \cdots I_N. \tag{93}$$

[In fact, Eq. (6) of the P. Pfeuty's paper[33] does not contain two signs; minus immediately follows from symmetry arguments (after performing simple rotations of spin axes) and is important for what follows.]

Analysing the conditions for quantum phase transition points (91), (92) we immediately observe that a number of quantum phase transition points for a given period of nonuniformity is strongly conditioned by specific values of the Hamiltonian parameters. Consider, for example, the case $p = 2$ and assume $\Omega_{1,2} = \Omega \pm \Delta\Omega$, $\Delta\Omega > 0$. Then, for a small strength of transverse-field nonuniformity $\Delta\Omega < (|I_1 I_2|)^{1/2}$ the system exhibits two quantum phase transition points $\Omega_c = \pm(\Delta\Omega^2 + |I_1 I_2|)^{1/2}$. Moreover, the ferromagnetic phase occurs for $|\Omega| < (\Delta\Omega^2 + |I_1 I_2|)^{1/2}$ whereas the paramagnetic phase occurs for $(\Delta\Omega^2 + |I_1 I_2|)^{1/2} < |\Omega|$. If a strength of transverse-field nonuniformity is large enough, $\Delta\Omega > (|I_1 I_2|)^{1/2}$, the system exhibits four quantum phase transition points $\Omega_c = \pm(\Delta\Omega^2 \pm |I_1 I_2|)^{1/2}$. Moreover, the ferromagnetic phase occurs for $(\Delta\Omega^2 - |I_1 I_2|)^{1/2} < |\Omega| < (\Delta\Omega^2 + |I_1 I_2|)^{1/2}$ whereas the paramagnetic phase occurs for low fields, $|\Omega| < (\Delta\Omega^2 - |I_1 I_2|)^{1/2}$, and for strong fields, $(\Delta\Omega^2 + |I_1 I_2|)^{1/2} < |\Omega|$. In the case $\Delta\Omega = (|I_1 I_2|)^{1/2}$ we get three quantum phase transition points, $\Omega_c = \pm\sqrt{2}|I_1 I_2|, 0$. The fields $\pm\sqrt{2}|I_1 I_2|$ correspond to the transition between ferromagnetic and paramagnetic phases. At $\Omega = 0$ only a weak singularity occurs. We shall motivate the statements about the phases which occur as Ω varies considering the dependence of the ground-state Ising magnetization on Ω (see below). The important message which follows from this simple analysis is that the number of quantum phase transitions in the regularly alternating transverse Ising chain of a certain period strongly depends on a specific set of the Hamiltonian parameters.

Let us note that in our treatment we assume $\Omega_n = \Omega + \Delta\Omega_n$, fix $\Delta\Omega_n$ and I_n, and consider the changes in the ground-state properties as Ω varies, thus, breaking a symmetry between the transverse fields and the exchange interactions. Alternatively, we may assume $I_n = I + \Delta I_n$, fix Ω_n and ΔI_n, and assume I to be a free parameter. In this case the quantum phase transition is tuned by varying I. Naturally, in general, the quantum phase transition conditions (91), (92) may be tuned by some parameter(s) effecting the on-site fields and the intersite interactions.

Let us consider a critical behaviour of the system in question. To get the behaviour of the ground-state properties in the vicinity of the critical fields we start with expanding the smallest root of the polynomial $\mathcal{A}_{2p}(E^2)$ with respect to deviation of the field from its critical value $\epsilon = \Omega - \Omega_c$.

For $p = 2$ with $\Omega_{1,2} = \Omega \pm \Delta\Omega$ and $\Omega_c = \pm(\Delta\Omega^2 \pm |I_1 I_2|)^{1/2}$ we have

$$\begin{aligned} a_1 &= \Omega^2 + \Delta\Omega^2 + \frac{1}{2}(I_1^2 + I_2^2) \\ &\quad - \sqrt{[\Omega^2 + \Delta\Omega^2 + \frac{1}{2}(I_1^2 + I_2^2)]^2 - (\Omega^2 - \Omega_c^2)^2} \\ &\approx \frac{(\Omega^2 - \Omega_c^2)^2}{2[\Omega^2 + \Delta\Omega^2 + \frac{1}{2}(I_1^2 + I_2^2)]}. \end{aligned} \tag{94}$$

As a result, the energy gap $\Delta = \sqrt{a_1}$ decays linearly

$$\Delta \sim |\epsilon| \tag{95}$$

if $\Omega_c \neq 0$ and as

$$\Delta \sim \epsilon^2 \tag{96}$$

if $\Omega_c = 0$. The latter case occurs when $\Delta\Omega = (|I_1 I_2|)^{1/2}$.

Now we can evaluate the ground-state energy (84) in the vicinity of the critical point. The nonanalytic contribution in the r.h.s. of Eq. (84) is coming from the energy interval between $\sqrt{a_1}$ (which is proportional either to $|\epsilon|$ or to ϵ^2) and $\sqrt{a_2}$ ($a_1 < a_2 < a_3 < \cdots$); all the other intervals of energies yield only analytical contributions to the ground-state energy e_0 with respect to ϵ. Therefore, we have

$$\begin{aligned} e_0 &= -\frac{1}{2\pi} \int_{\sqrt{a_1}}^{\sqrt{a_2}} dE \; \frac{E^2 f(E^2)}{\sqrt{E^2 - a_1}} + \text{analytical with respect to } \epsilon^2 \text{ terms} \\ &\sim \epsilon^2 \ln|\epsilon| + \text{analytical with respect to } \epsilon^2 \text{ terms.} \end{aligned} \tag{97}$$

[Here $f(E^2)$, $f(0) \neq 0$ is some function the explicit expression of which is not important for deriving the asymptotic behaviour.] Eq. (97) is valid for $\Omega_c \neq 0$ when $\sqrt{a_1} \sim |\epsilon|$. As a result

$$m^z \sim \epsilon \ln|\epsilon| + \text{analytical terms}, \tag{98}$$

$$\chi^z \sim \ln|\epsilon| + \text{analytical terms}. \tag{99}$$

Thus, the critical behaviour remains unchanged in comparison with that of the uniform chain; (cf. Eqs. (54)–(57)). This can be also nicely seen in Fig. 4 where some results referring to the chains of period 2 with $I_1 = I_2 = 1$ and $\Delta\Omega = 0.5$ and $\Delta\Omega = 1.5$ are collected.

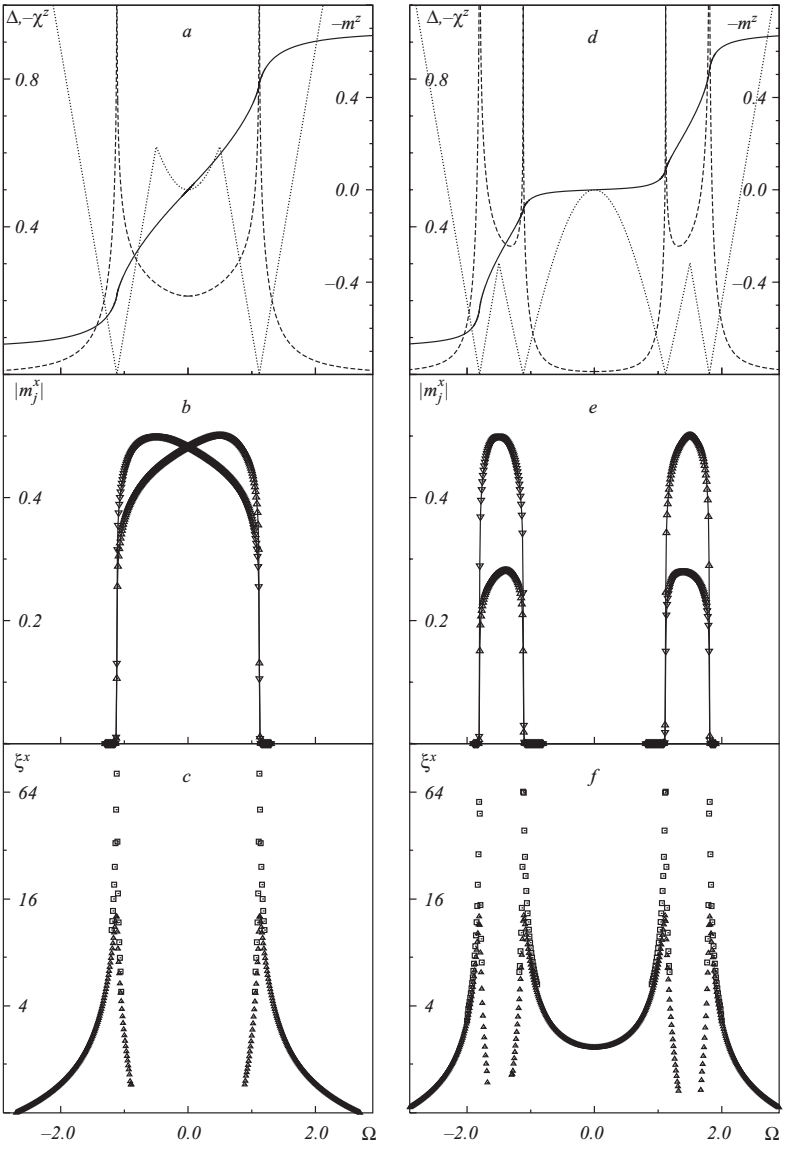

Fig. 4. Towards the ground-state properties of the transverse Ising chain of period 2, $I_1 = I_2 = 1$, $\Omega_{1,2} = \Omega \pm \Delta\Omega$, $\Delta\Omega = 0.5$ ($\Omega_c = \pm\sqrt{1.25}$) (a–c), $\Delta\Omega = 1.5$ ($\Omega_c = \pm\sqrt{1.25}, \pm\sqrt{3.25}$) (d–f). The dependences of the energy gap [dotted curves in (a) and (d)], transverse magnetization m^z [solid curves in (a) and (d)], static transverse susceptibility χ^z [dashed curves in (a) and (d)], longitudinal sublattice magnetizations $|m_j^x|$ [solid curves with up and down triangles in (b) and (e) which are obtained from the data for $N = 600$], and correlation length ξ^x [triangles and squares in (c) and (f) correspond to the data for $N = 300$ and $N = 600$, respectively] on the transverse field Ω.

Let us turn now to the case $\Omega_c = 0$ which occurs for the chain of period 2 with $\Delta\Omega = (|I_1 I_2|)^{1/2}$. In this case the smallest root a_1 tends to zero proportionally to ϵ^4 as Ω approaches Ω_c and as a result

$$e_0 \sim \epsilon^4 \ln|\epsilon| + \text{analytical terms} \tag{100}$$

and, therefore,

$$m^z \sim \epsilon^3 \ln|\epsilon| + \text{analytical terms}, \tag{101}$$

$$\chi^z \sim \epsilon^2 \ln|\epsilon| + \text{analytical terms}. \tag{102}$$

Thus, the transverse susceptibility χ^z is finite at the critical point $\Omega_c = 0$ and only its second derivative with respect to the field $\partial^2\chi^z/\partial\Omega^2$ exhibits a logarithmic singularity. This weak singularity may be called the fourth-order quantum phase transition in the Ehrenfest sense.

I proceed with exact analytical results for a regularly alternating transverse Ising chain showing how the ground-state wave function $|\mathrm{GS}\rangle$ can be obtained exactly for special sets of the Hamiltonian parameters. Let us consider the chain of period 2 with $\Omega_{1,2} = \Omega \pm \Delta\Omega$. It is obvious that

$$|\mathrm{GS}\rangle = \cdots |\uparrow\rangle_j |\uparrow\rangle_{j+1} \cdots \tag{103}$$

as $\Omega \to -\infty$ and

$$|\mathrm{GS}\rangle = \cdots |\downarrow\rangle_j |\downarrow\rangle_{j+1} \cdots \tag{104}$$

as $\Omega \to \infty$. We can also expect that at $\Omega = 0$

$$|\mathrm{GS}\rangle = \cdots |\downarrow\rangle_j |\uparrow\rangle_{j+1} \cdots \tag{105}$$

if $\Delta\Omega \gg |I_1|, |I_2|$ and

$$|\mathrm{GS}\rangle = \cdots \frac{1}{\sqrt{2}} \left(|\downarrow\rangle_j \pm |\uparrow\rangle_j\right) \frac{1}{\sqrt{2}} \left(|\downarrow\rangle_{j+1} \pm |\uparrow\rangle_{j+1}\right) \cdots \tag{106}$$

if $\Delta\Omega = 0$. Less evident is the ground-state wave function $|\mathrm{GS}\rangle$ for $\Omega = \mp\Delta\Omega$ when $\Omega_1 = 0$, $\Omega_2 = -2\Delta\Omega$ or $\Omega_1 = 2\Delta\Omega$, $\Omega_2 = 0$. To obtain the ground-state wave functions for these values of the transverse field let us note that after performing the unitary transformations

$$U = \cdots \exp\left(i\pi s_n^x s_{n+1}^y\right) \exp\left(i\pi s_{n+1}^x s_{n+2}^y\right) \cdots, \tag{107}$$

$$R^z = \cdots \exp\left(i\frac{1}{2}\pi s_n^z\right) \exp\left(i\frac{1}{2}\pi s_{n+1}^z\right) \cdots, \tag{108}$$

the Hamiltonian of the transverse Ising chains with the fields $\Omega_1\Omega_2\cdots$ and the interactions $I_1 I_2 \cdots$ transforms (with the accuracy to the boundary

terms) into the Hamiltonian of the transverse Ising chains with the fields $I_1 I_2 \cdots$ and the interactions $\Omega_1 \Omega_2 \cdots$,

$$R^z U H U^+ R^{z+} = \sum_j I_j s_j^z + \sum_j 2\Omega_{j+1} s_j^x s_{j+1}^x. \tag{109}$$

For $\Omega = \mp\Delta\Omega$ the Hamiltonian $R^z U H U^+ R^{z+}$ represents a system of noninteracting clusters which consist of two sites. We can easily find the ground-state of a two-site cluster with the Hamiltonian ($\Omega = -\Delta\Omega$)

$$H_{12} = I_1 s_1^z + I_2 s_2^z - 4\Delta\Omega s_1^x s_2^x. \tag{110}$$

It reads ($I_1 I_2 > 0$)

$$\begin{aligned} |\mathrm{GS}\rangle_{12} &= c_1 |\downarrow\rangle_1 |\downarrow\rangle_2 + c_2 |\uparrow\rangle_1 |\uparrow\rangle_2, \\ c_1 &= \frac{1}{\sqrt{2}} \frac{I + \sqrt{I^2 + \Delta\Omega^2}}{\sqrt{I^2 + I\sqrt{I^2 + \Delta\Omega^2} + \Delta\Omega^2}}, \\ c_2 &= \frac{1}{\sqrt{2}} \frac{\Delta\Omega}{\sqrt{I^2 + I\sqrt{I^2 + \Delta\Omega^2} + \Delta\Omega^2}}, \\ I &= \frac{1}{2}(I_1 + I_2). \end{aligned} \tag{111}$$

As a result, the desired ground-state wave function reads

$$\begin{aligned} |\mathrm{GS}\rangle = U^+ R^{z+} \cdots (c_1 |\downarrow\rangle_{n+1} |\downarrow\rangle_{n+2} + c_2 |\uparrow\rangle_{n+1} |\uparrow\rangle_{n+2}) \\ \times (c_1 |\downarrow\rangle_{n+3} |\downarrow\rangle_{n+4} + c_2 |\uparrow\rangle_{n+3} |\uparrow\rangle_{n+4}) \cdots . \end{aligned} \tag{112}$$

For $\Omega = \Delta\Omega$, the ground state is again given by (112) and (111) with the change $n \to n-1$, $\Delta\Omega \to -\Delta\Omega$.

Knowing the ground-state wave function we can easily calculate different spin correlation functions. For example, for $\Omega = -\Delta\Omega$ according to Eq. (112) we get

$$\begin{aligned} \langle s_{n+1}^x s_{n+2}^x \rangle = \langle s_{n+1}^x s_{n+4}^x \rangle = \cdots = \langle s_{n+2}^x s_{n+3}^x \rangle \\ = \langle s_{n+2}^x s_{n+5}^x \rangle = \cdots = \frac{1}{4}(c_2^2 - c_1^2), \\ \langle s_{n+1}^x s_{n+3}^x \rangle = \langle s_{n+1}^x s_{n+5}^x \rangle = \cdots = \frac{1}{4}(c_2^2 - c_1^2)^2, \\ \langle s_{n+2}^x s_{n+4}^x \rangle = \langle s_{n+2}^x s_{n+6}^x \rangle = \cdots = \frac{1}{4}; \end{aligned} \tag{113}$$

$$\begin{aligned} \langle s_{n+1}^z s_{n+2}^z \rangle = \langle s_{n+1}^z s_{n+4}^z \rangle = \cdots = \langle s_{n+2}^z s_{n+3}^z \rangle \\ = \langle s_{n+2}^z s_{n+5}^z \rangle = \cdots = \langle s_{n+2}^z s_{n+4}^z \rangle = \langle s_{n+2}^z s_{n+6}^z \rangle = \cdots = 0, \\ \langle s_{n+1}^z s_{n+3}^z \rangle = \langle s_{n+1}^z s_{n+5}^z \rangle = \cdots = (c_1 c_2)^2 . \end{aligned} \tag{114}$$

For $\Omega = \Delta\Omega$, the correlation functions follow from (113), (114) after the change $n \to n - 1$.

Now we discuss the exact numerical results for finite chains (up to a few thousand sites) some of which are presented in Figs. 4 and 5. The ground-state Ising (longitudinal) sublattice magnetizations $|m_j^x|$ indicate different phases and phase transitions between them. Their dependence on the transverse field Ω are shown in Figs. 4 and 5 for $\Delta\Omega < (|I_1 I_2|)^{1/2}$ [Fig. 4b and Fig. 5a (open symbols)] and $\Delta\Omega > (|I_1 I_2|)^{1/2}$ [Fig. 4e and Fig. 5a (filled symbols)]. In accordance with the analytical results for Δ, m^z

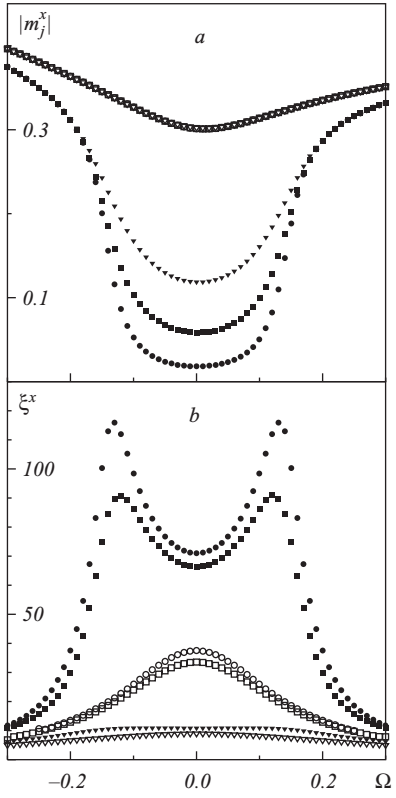

Fig. 5. Towards the ground-state properties of the transverse Ising chain of period 2, $I_1 = I_2 = 1$, $\Omega_{1,2} = \Omega \pm \Delta\Omega$, $\Delta\Omega = 0.99$ (open symbols), $\Delta\Omega = 1.01$ (filled symbols). The longitudinal sublattice magnetization $|m_j^x|$ (a) and the correlation length ξ^x (b) against the transverse field Ω for chains having 300, 600 and 900 sites (triangles, squares and circles).

and χ^z the numerical data show the existence of either two phases (quantum Ising (ferromagnetic) phase for $|\Omega| < (\Delta\Omega^2 + |I_1 I_2|)^{1/2}$ and strong-field quantum paramagnetic phase otherwise) or three phases (low-field quantum paramagnetic phase for $|\Omega| < (\Delta\Omega^2 - |I_1 I_2|)^{1/2}$, quantum Ising (ferromagnetic) phase for $(\Delta\Omega^2 - |I_1 I_2|)^{1/2} < |\Omega| < (\Delta\Omega^2 + |I_1 I_2|)^{1/2}$ and strong-field quantum paramagnetic phase otherwise). The longitudinal on-site magnetizations m_j^x are nonzero in quantum Ising phases and become strictly zero in quantum paramagnetic phases. The transverse magnetization m^z in quantum paramagnetic phases is almost constant, being in the vicinity of zero in the low-field phase and of saturation value in the strong-field phase, thus producing plateau-like steps in the dependence m^z *versus* Ω (see the solid curve in Fig. 4d). The correlation length ξ^x [Figs. 4c, 4f, 5b (filled symbols)] illustrates that the transition between different phases is accompanied by the divergency of ξ^x. Comparing the data for $N = 600$ and $N = 900$ reported in Fig. 5b one observes a strong size-dependence of the correlation length value ξ^x about the critical fields (filled squares and circles in Fig. 5b) and a weak size-dependence of ξ^x for other values of Ω (for example, open squares and circles in Fig. 5b). It is interesting to note that short chains ($N = 20$) are already sufficient to reproduce a correct order-parameter behaviour in the quantum Ising phase away from the quantum critical point, but not in the quantum paramagnetic phases.[26] The chain length of up to $N = 900$ sites is clearly sufficient to see a sharp transition in the order parameter (Figs. 4b, 4e) and even to extract reliable results for ξ^x from the long-distance behaviour of $\langle s_j^x s_{j+n}^x \rangle$ as can be seen from the data presented in Figs. 4c, 4f and in Fig. 5b. We also note that the numerical data for $|m_j^x|$ and ξ^x at $\Omega = \mp\Delta\Omega$ coincide with the exact expression (113). In particular, the values of the longitudinal sublattice magnetizations for these fields are $\frac{1}{2}$ and $\frac{1}{2}|c_2^2 - c_1^2|$.

Finally, the low-temperature dependence of the specific heat c at different Ω (≥ 0) obtained from the exact analytical expression (85) confirms the existence of either two phase transitions (Fig. 6a) or four phase transitions (Fig. 6b) depending on the relationship between $\Delta\Omega$ and $\sqrt{|I_1 I_2|}$. At the quantum phase transition points the spin chain becomes gapless and c depends linearly on T. Really, at the quantum phase transition point as T tends to zero

$$\frac{c}{k} = 2\int_0^{kT} dE\ E\frac{C}{\sqrt{E^2}}\left(\frac{E}{2kT}\right)^2 + 2\int_{kT}^{\infty} dE\ ER(E^2)\left(\frac{\frac{E}{2kT}}{\cosh\frac{E}{2kT}}\right)^2. \tag{115}$$

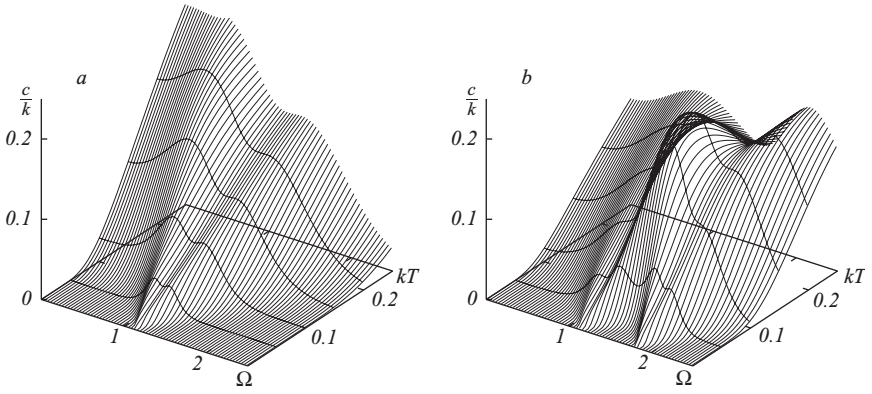

Fig. 6. The low-temperature dependence of the specific heat for the transverse Ising chain of period 2, $I_1 = I_2 = 1$, $\Omega_{1,2} = \Omega \pm \Delta\Omega$, $\Delta\Omega = 0.5$ (a), $\Delta\Omega = 1.5$ (b).

(Here C is some constant the value of which is not important for deriving the asymptotic behaviour.) The second term in (115) disappears in the limit $T \to 0$ ($E > kT$) and as a result

$$c \sim T. \tag{116}$$

The ridges seen in Figs. 6a, 6b correspond to the maxima in the dependence c versus Ω as T varies. They single out the boundaries of quantum critical regions.[9] These boundaries correspond to a relation $\Delta \sim kT$ that can be checked by comparison with the data for Δ versus Ω reported in Figs. 4a, 4d. As can be seen from Fig. 6 the $c(T)$ behaviour for Ω slightly above or below Ω_c changes crossing the boundaries of quantum critical regions. Furthermore, we notice that for $\Delta\Omega = 1.5$ (Fig. 6b) an additional low-temperature peak appears in the temperature dependence of the specific heat.

To end up, let us turn to a chain of period 3 for which the analytical and the numerical calculations presented above can be repeated. The quantum phase transition points follow from the condition (92). Depending on the parameters, either two, four, or six quantum phase transitions are possible. This behaviour is illustrated in Fig. 7 for a chain of period 3 with $I_1 = I_2 = I_3 = 1$, $\Omega_n = \Omega + \Delta\Omega_n$, $\Delta\Omega_1 + \Delta\Omega_2 + \Delta\Omega_3 = 0$. Moreover, such chains may exhibit weak singularities. For example, for the set of parameters at the boundary between dark and grey regions there are three critical fields; at one of them a weak singularity occurs.

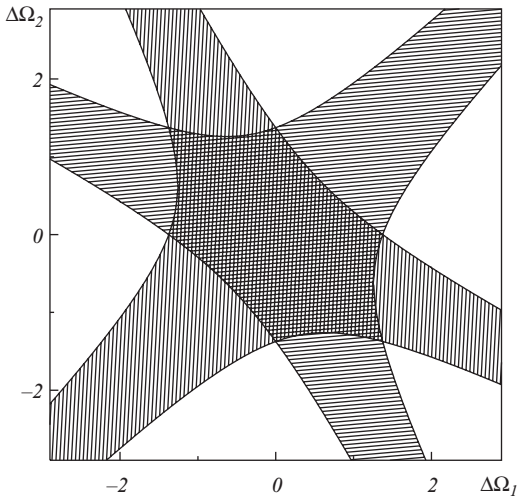

Fig. 7. Towards the number of quantum phase transitions present in the transverse Ising chain of period 3, $I_1 = I_2 = I_3 = 1$, $\Omega_{1,2,3} = \Omega + \Delta\Omega_{1,2,3}$, $\Delta\Omega_1 + \Delta\Omega_2 + \Delta\Omega_3 = 0$. The dark, grey, or light regions correspond to parameters for which the system exhibits two, four, or six quantum phase transitions, respectively. At the boundaries between different regions weak singularities occur.

To summarize, I have shown how the exact results for the thermodynamics of a regularly alternating spin-$\frac{1}{2}$ Ising chain in a transverse field can be derived using the Jordan–Wigner transformation and continued fractions. Furthermore, for special parameter values the exact ground-state wave function and spin correlation functions can be obtained as well. For parameters for which the correlation functions are not accessible for rigorous analytical analysis they can be obtained from exact numerical results for finite but large systems. From these numerical data we can extract the order parameter and the correlation length in high precision. We have found, that the quantum phase transition occurring in the uniform transverse Ising chain is not suppressed by deviation from uniformity in the form of a regular alternation of bonds and fields. On the contrary, field alternation may lead to the appearance of additional quantum phase transitions tuned by the field. The number of phase transitions for a given period of alternation strongly depends on the precise values of the parameters of the model. We have examined the critical behaviour of the energy gap Δ, the ground-state energy e_0, the transverse magnetization m^z, and the static transverse susceptibility χ^z and have found the same critical indices for

both a nonuniform and a uniform chain. For some sets of the Hamiltonian parameters, the ground-state quantities may exhibit a weak singularity.

5. Related models

In the remainder of this chapter I shall discuss other simple models which, apart from the transverse Ising chain, exhibit a quantum phase transition. Namely, I consider the spin-$\frac{1}{2}$ isotropic XY (i.e. XX) chain in a transverse field and the spin-$\frac{1}{2}$ XYZ chain in an external magnetic field directed along the z axis focusing on the effects of regularly alternating Hamiltonian parameters on the dependence of the ground-state quantities on the external field.

The uniform transverse XX chain described by the Hamiltonian

$$H = \sum_{n=1}^{N} \Omega s_n^z + \sum_{n=1}^{N} 2I \left(s_n^x s_{n+1}^x + s_n^y s_{n+1}^y \right) \tag{117}$$

by employing the Jordan–Wigner transformation (17) and (18) can be mapped onto the system of noninteracting spinless fermions with the Hamiltonian

$$H = \sum_{\kappa=1}^{N} \Lambda_\kappa \left(c_\kappa^+ c_\kappa - \frac{1}{2} \right), \tag{118}$$

where the elementary excitation energies Λ_κ are given by

$$\Lambda_\kappa = \Omega + 2I \cos \kappa. \tag{119}$$

Alternatively, we may find the density of states $\rho(E)$ (33) which is given by

$$\rho(E) = \begin{cases} \frac{1}{\pi \sqrt{4I^2 - (E-\Omega)^2}} & \text{if } 4I^2 - (E-\Omega)^2 > 0, \\ 0 & \text{otherwise.} \end{cases} \tag{120}$$

As a result, the thermodynamic properties of the spin chain (117) can be easily analysed.

In contrast to the transverse Ising chain (and to any chain with anisotropic XY interaction in a transverse field) $\sum_{n=1}^{N} s_n^z$ commutes with the Hamiltonian describing the isotropic XY interspin interaction and, therefore, a change in the transverse field Ω has a different effect on the ground-state quantities of the spin chain (117). As can be seen from (118), (119) the transverse field plays a role of the chemical potential controlling a filling of the fermion band. The transverse XX chain remains gapless until $|\Omega| \leq 2|I|$. If $|\Omega|$ exceeds $2|I|$, the energy gap Δ opens linearly. This

produces singularities in the ground-state quantities. For example, a square-root singularity in the zero-temperature dependence of the static transverse susceptibility χ^z on the transverse field Ω.

After introducing a regular alternation, i.e. after making a substitution in (117) $\Omega \to \Omega_n$, $I \to I_n$ with a periodic sequence of parameters

$$\Omega_1 I_1 \Omega_2 I_2 \cdots \Omega_p I_p \Omega_1 I_1 \Omega_2 I_2 \cdots \Omega_p I_p \cdots ,$$

we can easily obtain with the help of continued fractions the density of states $\rho(E)$ of the Jordan–Wigner fermions which represent the regularly alternating transverse XX chain, and hence analyse the effects of regularly alternating Hamiltonian parameters on the thermodynamic properties of the considered spin system[34] (for another approach see Refs. 35 and 36). The main consequence of the introduced periodic nonuniformity is a splitting of the initial fermion band into several subbands the number of which does not exceed the period of the chain p [for special (symmetric) values of the Hamiltonian parameters one may observe a smaller number of subbands than p]. The transverse field Ω ($\Omega_n = \Omega + \Delta\Omega_n$) controls a filling of the fermion subbands. Again the energy gap Δ disappears/appears linearly with varying Ω and the critical behaviour remains the same as for the uniform chain. Note, that the ground-state dependence of the transverse magnetization

$$m^z = -\frac{1}{2} \int\limits_{-\infty}^{\infty} dE \; \rho(E) \tanh \frac{E}{2kT} \tag{121}$$

on Ω is composed of sharply increasing parts separated by horizontal parts (plateaus) in accordance with a famous conjecture of M. Oshikawa, M. Yamanaka and I. Affleck (see Ref. 37).

A more general situation is the case of regularly alternating XYZ chain in a magnetic field. Let us consider the Hamiltonian

$$H = \sum_n \Omega s_n^z + \sum_n \left(I_n^x s_n^x s_{n+1}^x + I_n^y s_n^y s_{n+1}^y + I^z s_n^z s_{n+1}^z \right) ,$$
$$I_n^x = 1 + \gamma + (-1)^n \delta, \qquad I_n^y = 1 - \gamma + (-1)^n \delta, \tag{122}$$

which captures the interplay between an exchange interaction anisotropy (γ, I^z), exchange interaction modulation or, more precisely, exchange interaction dimerization (δ), and the uniform magnetic field (Ω). Such a model has been studied recently in some detail[38] using the bosonization approach[39–41] and the Lanczos diagonalization technique. Let us first discuss the free fermion case $I^z = 0$. After the Jordan–Wigner transformation

(17), (18) the Hamiltonian can be readily diagonalized (see Refs. 28, 29, 38 and 42). The critical field values at which the spin system (122) becomes gapless are given by

$$\Omega_c = \pm\sqrt{\delta^2 - \gamma^2}. \tag{123}$$

At the critical field the (transverse) magnetization behaves as

$$m^z - m_c^z \sim (\Omega - \Omega_c)\,(\ln|\Omega - \Omega_c| - 1) \tag{124}$$

and the static (transverse) susceptibility χ^z exhibits a logarithmic singularity [cf. Eqs. (98) and (99)]. The bosonization approach results[38] show that the same picture is valid for an arbitrary $I^z \neq 0$ provided δ and γ are suitably renormalized. The results of the bosonization approach elaborated for small γ and δ may be compared with numerical findings within non-perturbative regimes.[38] From this analysis ($0 \leq I^z \leq 1$) it was found that the critical line for $\Omega = 0$ is given by

$$\delta \sim \gamma, \tag{125}$$

in accord with (123). For the behaviour of the magnetization curves near the critical fields Ω_c ($I^z = 1$) a fair regime (124) was obtained. These results suggest that some basic features of the fully interacting system (122) are captured by the free fermion picture.

Acknowledgments

I would like to thank Johannes Richter, Taras Krokhmalskii and Oles' Zaburannyi in collaboration with whom the study of the regularly alternating transverse Ising chains was performed. I also would like to thank the DFG for the support of my work over the past five years in a number of ways. Finally, I thank Dr. Janush Sanotsky (physician) owing to whom I was able to give a talk at the Ising Lectures, 2002.

References

1. K. Huang, *Statistical Mechanics* (John Wiley & Sons, Inc., New York – London, 1963).
2. E. Ising, *Z. Phys.* **31**, 253 (1925).
3. L. Onsager, *Phys. Rev.* **65**, 117 (1944).
4. R. J. Baxter F. R. S., *Exactly Solved Models in Statistical Mechanics* (Academic Press, London, New York, Paris, San Diego, San Francisco, São Paulo, Sydney, Tokyo, Toronto, 1982).
5. S.-k. Ma, *Modern Theory of Critical Phenomena* (W. A. Benjamin, Inc., Reading, 1976).

6. J. Cardy, *Scaling and Renormalization in Statistical Physics* (Cambridge University Press, Cambridge, 1996).
7. D. Bitko, T. F. Rosenbaum and G. Aeppli, *Phys. Rev. Lett.* **77**, 940 (1996).
8. S. Sachdev, *Physics World* **12**, 33 (1999).
9. S. Sachdev, *Quantum Phase Transitions* (Cambridge University Press, Cambridge, 1999).
10. E. Lieb, T. Schultz and D. Mattis, *Ann. Phys. (N.Y.)* **16**, 407 (1961).
11. S. Katsura, *Phys. Rev.* **127**, 1508 (1962);
    S. Katsura, *Phys. Rev.* **129**, 2835 (1963).
12. P. Pfeuty, *Ann. Phys. (N.Y.)* **57**, 79 (1970).
13. T. D. Schultz, D. C. Mattis and E. H. Lieb, *Rev. Mod. Phys.* **36**, 856 (1964).
14. M. Suzuki, *Prog. Teor. Phys.* **46**, 1337 (1971).
15. M. Suzuki, *Prog. Teor. Phys.* **56**, 1454 (1976).
16. B. K. Chakrabarti, A. Dutta and P. Sen, *Quantum Ising Phases and Transitions in Transverse Ising Models* (Springer-Verlag, Berlin Heidelberg, 1996).
17. O. Derzhko and T. Krokhmalskii, *Phys. Rev.* **B56**, 11659 (1997).
18. O. Derzhko and T. Krokhmalskii, *phys. stat. sol. (b)* **208**, 221 (1998).
19. M. Abramowitz and I. A. Stegun, Eds., *Handbook of Mathematical Functions with Formulas, Graphs and Mathematical Tables* (National Bureau of Standards, 1964).
20. I. S. Gradshtein and I. M. Ryzhyk, *Tablitsy integralov, sum, ryadov i proizvedenii* (Fizmatgiz, Moscow, 1962).
21. J. M. Luck, *J. Stat. Phys.* **72**, 417 (1993).
22. D. S. Fisher, *Phys. Rev.* **B51**, 6411 (1995).
23. F. Iglói, L. Turban, D. Karevski and F. Szalma, *Phys. Rev.* **B56**, 11031 (1997).
24. O. Derzhko, *J. Phys.* **A33**, 8627 (2000).
25. O. Derzhko, J. Richter and O. Zaburannyi, *J. Magn. Magn. Mater.* **242–245**, 1044 (2002).
26. O. Derzhko, J. Richter, T. Krokhmalskii and O. Zaburannyi, *Phys. Rev.* **B66**, 144401 (2002).
27. O. Derzhko, J. Richter, T. Krokhmalskii and O. Zaburannyi, *Acta Physica Polonica* **B34**, 1387 (2003).
28. Jong-Won Lieh, *J. Math. Phys.* **11**, 2114 (1970).
29. J. H. H. Perk, H. W. Capel, M. J. Zuilhof and Th. J. Siskens, *Physica* **A81**, 319 (1975).
30. L. L. Gonçalves and J. P. de Lima, *J. Phys.: Condens. Matter* **9**, 3447 (1997).
31. F. F. B. Filho, J. P. de Lima and L. L. Gonçalves, *J. Magn. Magn. Mater.* **226–230**, 638 (2001).
32. P. Tong and M. Zhong, *Physica* **B304**, 91 (2001).
33. P. Pfeuty, *Phys. Lett.* **A72**, 245 (1979).
34. O. Derzhko, J. Richter and O. Zaburannyi, *Physica* **A282**, 495 (2000).
35. J. P. de Lima and L. L. Gonçalves, *J. Magn. Magn. Mater.* **206**, 135 (1999).
36. J. P. de Lima and L. L. Gonçalves, *Physica* **A311**, 458 (2002).

37. M. Oshikawa, M. Yamanaka and I. Affleck, *Phys. Rev. Lett.* **78**, 1984 (1997).
38. M. Arlego, D. C. Cabra, J. E. Drut and M. D. Grynberg, *Phys. Rev.* **B67**, 144426 (2003).
39. I. Affleck, in: *Fields, Strings and Critical Phenomena*, Ed. E. Brézin and J. Zinn-Justin, (Elsevier Science Publishers B.V., Amsterdam, 1989), p. 563.
40. J. von Delft and H. Schoeller, *Ann. Phys. (Leipzig)* **7**, 225 (1998).
41. S. Rao and D. Sen, cond-mat/0005492.
42. F. Ye, G.-H. Ding and B.-W. Xu, cond-mat/0105584.

This page intentionally left blank

CHAPTER 4

PHASE TRANSITIONS IN TWO-DIMENSIONAL RANDOM POTTS MODELS

Bertrand Berche and Christophe Chatelain

Laboratoire de Physique des Matériaux
Université Henri Poincaré, Nancy 1
BP 239, F-54506 Vandœuvre les Nancy, France
E-mail: berche@lpm.u-nancy.fr

The influence of uncorrelated, quenched disorder on the phase transition of two-dimensional Potts models will be reviewed. After an introduction where the conditions of relevance of quenched randomness on phase transitions are exemplified by experimental measurements, the results of perturbative and numerical investigations in the case of the Potts model will be presented. The Potts model is of particular interest, since it can have in the pure case a second-order or a first-order transition, depending on the number of states per spin. In 2D, transfer matrix calculations and Monte Carlo simulations have been used in order to check the validity of conformal invariance methods in disordered systems. These techniques were then used to investigate the universality class of the disordered Potts model, in both regimes of the pure model phase transitions. A test of replica symmetry becomes possible through a study of multiscaling properties and also a detailed analysis of the probability distribution of the correlation functions becomes possible.

1. Introduction

Quenched disorder has been the subject of an intensive activity in statistical physics during the past decades. The qualitative influence of disorder coupled to the energy-density at *second order* phase transitions is well understood since Harris proposed a celebrated relevance criterion.[1] At *first order* transitions, randomness obviously softens the transitions, and, under some circumstances may even induce second order transitions according to a picture first proposed by Imry and Wortis[2] and then stated on more

rigorous grounds by Aizenman and Wehr,[3,4] implying in particular that an infinitesimal disorder induces continuous transitions in 2D. Reviews can be found in the books of S.K. Ma, J.L. Cardy or Vik. Dotsenko.[5–7]

In spin models, the influence of quenched disorder strongly depends on the nature of randomness, i.e. to which quantity the perturbation is coupled in the Hamiltonian. Consider for example a very general model with spins $\mathbf{s}_i$ on a lattice and define the Hamiltonian

$$-\beta\mathcal{H} = \sum_{(ij)} K_{ij}\mathbf{s}_i\mathbf{s}_j + \sum_i \mathbf{H}_i\mathbf{s}_i + \sum_i D(\mathbf{s}_i\mathbf{n}_i)^2 + \cdots,$$

where K_{ij}, $\mathbf{H}_i$, or $\mathbf{n}_i$ are independent random quenched variables drawn from some probability distributions $P[K_{ij}]$, $P[\mathbf{H}_i]$, or $P[\mathbf{n}_i]$, and which respectively describe random-bond or dilute problems,[8] random fields,[9–13] and random anisotropy models.[14,15] As usual, the sum over (ij) is supposed to be restricted to nearest neighbours. Usually, we decide to work with uncorrelated quenched random variables, for example $\overline{K_{ij}} \equiv \int KP[K]\,dK = K_0$, and $\overline{K_{ij}K_{kl}} = \Delta\delta_{ik}\delta_{jl}$ and we will here only concentrate on the first category, namely random-bond systems where disorder is coupled to the energy density. Special cases of probability distributions of interest are for example listed below (all written here in the bond version of the problem):

(i) *dilution problems*, where non magnetic impurities are randomly distributed on the bonds or sites of the lattice, e.g. in the bond case

$$\mathcal{P}[K_{ij}] = \prod_{(ij)} [p\delta(K_{ij} - K) + (1-p)\delta(K_{ij})], \tag{1}$$

(ii) *binary distributions*, where we can imagine for example a disordered alloy of two magnetic species

$$\mathcal{P}[K_{ij}] = \prod_{(ij)} [p\delta(K_{ij} - K) + (1-p)\delta(K_{ij} - Kr)], \tag{2}$$

(iii) *Gaussian distributions* which are of particular interest to perform Gaussian integration in analytic approaches

$$\mathcal{P}[K_{ij}] = \prod_{(ij)} \frac{1}{\sqrt{2\pi\sigma^2}} \exp\left(-(K_{ij} - K)^2/2\sigma^2\right), \tag{3}$$

(iv) *Continuous self-dual distributions* (to be discussed later)

$$\mathcal{P}[y_{ij}] = \prod_{(ij)} (\cosh y_{ij}/\lambda)^{-1}, \qquad e^{y_{ij}} = \frac{1}{\sqrt{q}}(e^{K_{ij}} - 1). \tag{4}$$

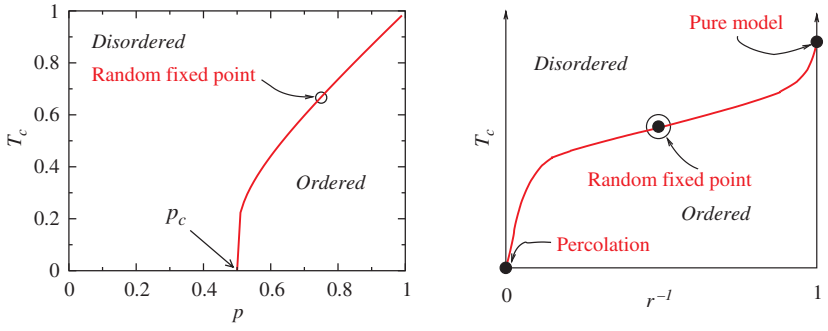

Fig. 1. Phase diagram of the dilution (left) and binary problems (right).

In each case, there is a control parameter (p, r, σ or λ) which determines the strength of the disorder. The phase diagram is sketched in Fig. 1 for dilution and binary distribution. We expect a transition line between ordered and disordered phases along which the transition is continuous in 2D. For dilute problems, there exists a percolation threshold where the transition temperature vanishes and below which long range order cannot exist. In the bimodal case, the percolation fixed point at finite q is reached in the limit $r \to \infty$. On the transition line, there should be some particular strength of disorder corresponding to the location of the random fixed point, where corrections to scaling should be small.

The q-state Potts model[16] is the natural candidate for the investigations of influence of disorder, since the pure model exhibits two different regimes (see Fig. 2): a second order phase transition when $q \leq 4$ and a first order one for $q > 4$ in two dimensions (2D). In 3D, ordering is easier and the transition becomes weakly first order even at $q = 3$.

The 2-dimensional q-state Potts model is defined by the Hamiltonian

$$-\beta\mathcal{H} = \sum_{(i,j)} K_{ij}\delta_{\sigma_i,\sigma_j}, \tag{5}$$

where the sum is restricted to nearest neighbours (here on a square lattice), the degrees of freedom $\{\sigma_i\}$ can take q values and the exchange couplings $K_{ij} = J_{ij}/k_{\mathrm{B}}T$ are quenched independent random variables chosen according to some distribution $\{K_{ij}\}$ to be specified later.

Many results were obtained for quenched randomness in this model in the last ten years, including:

(i) *Perturbative expansions* for $2 \leq q \leq 4$.[17–27] This work was initiated in a series of papers by A.W.W. Ludwig and J.L. Cardy.[17–19] A systematic study of energy-energy and spin-spin correlators in random bond Ising and

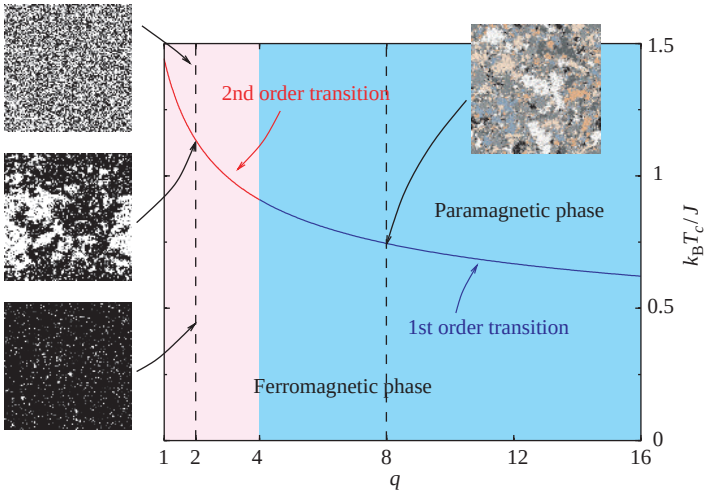

Fig. 2. Phase diagram of the 2D pure Potts model as a function of the number of states per spin. The transition is of second order when $q \leq 4$ and becomes of first order above. Insets show Monte Carlo snapshots of typical spin configurations.

Potts models, including tests of replica symmetry, was then performed by a group around Vl.S. Dotsenko,[20–26] with M. Picco, P. Pujol, Vik. Dotsenko, J.L. Jacobsen, and M.-A. Lewis.

(ii) *Monte Carlo simulations* in both regimes $2 \leq q \leq 4$ and $q > 4$.[28–35] In the second order regime, simulations were first performed by S. Wiseman and E. Domany in the case of the Ashkin–Teller model[36] (which exhibits a critical line and for a given set of couplings belongs to the 4-state Potts model universality class) and in the 3-state Potts model by J.K. Kim.[37] In the case $q = 8$, the first Monte Carlo simulations were reported by S. Chen, A.M. Ferrenberg and D.P. Landau in Refs. 38 and 39, but then in both regimes, more accurate results were obtained by different groups, like M. Picco,[28] T. Olson and P. Young,[34] or the present authors.[29,30]

(iii) *Transfer matrices* in both regimes.[40–48] This technique was used to study random Potts models very early by U. Glaus, then more refined computations were reported, for example by J.L. Cardy and J.L. Jacobsen[41,43] or in Ref. 46.

(iv) *High-temperature series expansions*, initially used in the random Ising model[49,50] to show the logarithmic corrections, then extended to $q = 3$ in 3D,[51] were also shortly applied to the two-dimensional case.[52]

(v) *Short-time dynamic scaling*.[53–57]

We also notice that dynamical properties (in order to discriminate between conventional or activated dynamics) linked to non self-averaging have been recently studied also[58] and that the interesting limit $q \to \infty$ was carefully investigated in Refs. 45 and 59. Reviews on selective parts of the subject were reported in Ph.D dissertations in Refs. 60–63.

Although closely related, the random-bond Ising model will not be discussed here, since it has already been the subject of many reviews, e.g. in Refs. 64–66. We will only remind here that in the pure 2D Ising model, the exponent α of the specific heat vanishes and further investigation is needed, since the Harris criterion becomes inconclusive. It is now generally believed that uncorrelated quenched randomness is a marginally irrelevant perturbation which does not modify the universal critical behaviour, but produces logarithmic corrections. For example the singular part of the specific heat exhibits the following behaviour,

$$\begin{aligned} C_s(t) &\sim \ln(1/|t|) && \theta \ll |t| \ll 1, \\ C_s(t) &\sim \ln\ln(1/|t|) && |t| \ll \theta, \end{aligned}$$

$$\theta \sim e^{-\pi/g^2},$$

where t is a reduced distance to the critical point and g is the amplitude of disorder, linked to the impurity concentration. The behaviour of the main physical quantities in the neighbourhood of the random fixed point is given in Table 2. It was confirmed unambiguously by Monte Carlo simulations[67–70] as shown in the same table. We also note that conformal mappings associated to Monte Carlo simulations were initially used in the random-bond Ising problem by A. Talapov and Vl.S. Dotsenko.[71]

The numerical studies of disordered models showed many difficulties, like the lack of self averaging[72–75] or varying effective exponents due to crossover phenomena. Averaging physical quantities over the samples with

Table 2. Critical behaviour of the random-bond Ising model.

	Random-bond Ising model	
	Analytical results	Numerical results
Correlation function	$\langle\sigma_0\sigma_R\rangle \sim R^{-1/4}(\ln R)^{1/8}$	$\eta = 0.2493 \pm 0.0014$
Correlation length	$\xi(t) \sim \lvert t\rvert^{-1}[\ln(1/\lvert t\rvert)]^{1/2}$	
Magnetisation	$m(t) \sim \lvert t\rvert^{1/8}[\ln(1/\lvert t\rvert)]^{1/16}$	$\beta/\nu = 0.1245 \pm 0.0009$
Susceptibility	$\chi(t) \sim \lvert t\rvert^{-7/4}[\ln(1/\lvert t\rvert)]^{7/8}$	$\gamma/\nu = 1.7507 \pm 0.0014$
Specific heat	$C(t) \sim \ln\ln(1/\lvert t\rvert)$	

a poor statistics may thus lead to erroneous determinations of the critical exponents. Almost all the studies mentioned here were reported in the case of the random bond system with self-dual probability distributions of the coupling strengths in order to preserve the exact knowledge of the transition line, which is an important simplification when one wants to use finite-size-scaling techniques or conformal mappings which hold at criticality only.

In real experiments on the other hand, disorder is inherent to the working-out process and may result e.g. from the presence of impurities or vacancies. For the description of such a disordered system, dilution is thus more realistic than for example a random distribution of non-vanishing couplings (the so-called random-bond problem). Since universality is expected to hold, the detailed structure of the Hamiltonian should not play any determining role in universal quantities like critical exponents, but crossover phenomena may alter the determination of the universality class. Experimentally, the role of disorder in 2D systems has been investigated in several systems. Illustrating the influence of random defects in the case of the 2D Ising model universality class, samples made of thin magnetic amorphous layers of $(Tb_{0.27}Dy_{0.73})_{0.32}Fe_{0.68}$ of 10 Å width, separated by non magnetic spacers of 100 Å Nb in order to decouple the magnetic layers were produced using sputtering techniques. A structural analysis (high resolution transmission electron microscopy and X-ray analysis) was performed to characterise the defects inherent to such amorphous structures, and in spite of these random defects separated on average by a distance of a few nm, the samples were shown to exhibit Ising-like singularities with critical exponents[76]

$$\beta = 0.126(20), \qquad \gamma = 1.75(3), \qquad \delta = 15.1(10).$$

This is compatible with the fact that disorder does not change the universality class of the 2D Ising model, apart from logarithmic corrections which are probably impossible to observe experimentally, since their role becomes prominent only in the close neighbourhood of the critical point. A beautiful experimental confirmation of the Harris criterion – which predicts a modification of the critical behaviour in random systems when the exponent α of the specific heat is positive for the pure system – was reported in a low energy electron diffraction (LEED) investigation of a 2D order disorder transition[77] belonging to the 4-state Potts model universality class. Order–disorder transitions of adsorbed atomic layers are known to belong to different two-dimensional universality classes depending on the type of superstructures in the ordered phase of the ad-layer.[78,79] The substrate plays a major role in ad-atom ordering, as well as the coverage

(defined as the number of ad-atoms per surface atom) which determines the possible superstructures of the over-layer. For example, sulfur chemisorbed on Ru(001) exhibits four-state or three-state Potts critical singularities for the $p(2 \times 2)$ and the $(\sqrt{3} \times \sqrt{3})R30°$ respectively[80] (at coverages $\frac{1}{4}$ and $\frac{1}{2}$). The case of the (2×2)-2H/Ni(111) order–disorder transition of hydrogen adsorbed on the (111) surface of Ni thus belongs to the 2D four-state Potts model universality class, since the ground state, stable at low temperatures, has a four-fold degenaracy due to the four possible coverings of the ad-atoms at the (111) surface (see Fig. 3).

The expected exponents are thus close to theoretical values of $\beta = \frac{1}{12} \simeq 0.083$, $\gamma = \frac{7}{6} \simeq 1.167$ and $\nu = \frac{2}{3} \simeq 0.667$ for example.

Low energy electron diffraction (LEED) enables one to measure these exponents through the diffracted intensity $I(\mathbf{q})$ or structure factor. This is the two-dimensional Fourier transform of the pair correlation function of ad-atom density. Long range correlations produce an isotropic Lorentzian centered at the superstructure spot position $\mathbf{q}_0$ with a peak intensity given by the susceptibility and a width determined by the inverse correlation length, while long range order gives a background signal proportional to the order parameter squared:

$$I(\mathbf{q}) = \langle m^2 \rangle \delta(\mathbf{q} - \mathbf{q}_0) + \frac{\chi}{1 + \xi^2 (\mathbf{q} - \mathbf{q}_0)^2}.$$

The following exponents were thus measured[77,81,82]

$$\beta = 0.11 \pm 0.01, \qquad \gamma = 1.2 \pm 0.1, \qquad \nu = 0.68 \pm 0.05$$

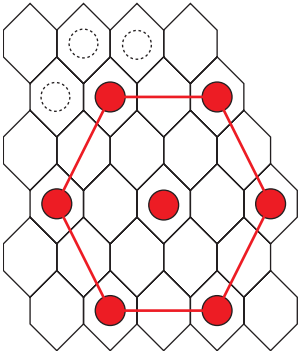

Fig. 3. (2×2)-2H/Ni(111) order–disorder transition of hydrogen. The ground state has a four-fold degenaracy due to the four possible covering of the (111) surface of Ni by H ad-atoms.

in correct agreement with 4-state Potts values (the small deviation, especially for the exponent β, is attributed to the logarithmic corrections to scaling of the pure 4-state Potts model[83]). The same experiments were then reproduced in the presence of intentionally added oxygen impurities, at a temperature which is above the ordering temperature of pure oxygen adsorbed on the same substrate. The mobility of these oxygen atoms is furthermore considered to be low enough at the hydrogen order–disorder transition critical temperature that they essentially represent quenched impurities randomly distributed in the hydrogen layer (see Fig. 4). The exponents become

$$\beta = 0.135 \pm 0.010, \qquad \gamma = 1.68 \pm 0.15, \qquad \nu = 1.03 \pm 0.08,$$

which definitely supports the modification of the universality class in the presence of quenched disorder, in agreement with Harris' criterion ($\alpha = 2/3$ for the 4-state Potts model).

The aim of this chapter is to provide a review of both perturbative and numerical studies of the disordered Potts model for several values of the number of states per spin (in order to cover the two different regimes of the phase transitions in the pure system). In Section 2, the perturbative approach is discussed and the essential results are summarised in the 2D case with $2 \leq q \leq 4$. The details of the numerical techniques used in two dimensions are presented in Sections 3 and 4, while the comparison between numerical and analytical results is made in Section 5.

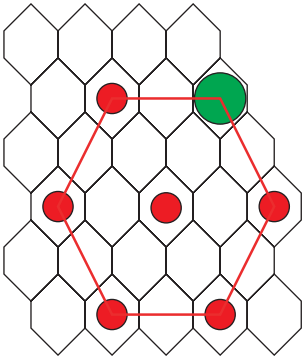

Fig. 4. (2×2)-2H/Ni(111) order–disorder transition of hydrogen with oxygen impurities randomly chemisorbed on the surface, and occupying some of the lattice sites.

2. Perturbative Approach in 2D

2.1. *Replicas and Relevance Criterion*

For a specific disorder realization $[K_{ij}]$, the Hamiltonian $\mathcal{H}[K_{ij}, \sigma_i]$ is written as

$$-\beta\mathcal{H}[K_{ij}, \sigma_i] = \sum_{(ij)} (K_0 + \delta K_{ij})\delta_{\sigma_i,\sigma_j}. \tag{6}$$

The corresponding partition function and free energy are given by

$$Z[K_{ij}] = \int \mathcal{D}[\sigma_i]\, e^{-\beta\mathcal{H}[K_{ij},\sigma_i]}, \qquad F[K_{ij}] = -k_{\mathrm{B}}T \ln Z[K_{ij}].$$

To get the quantities of interest, for example the average free energy, we have to perform an average over the distribution $\mathcal{P}[K_{ij}]$,[m]

$$F = \overline{F[K_{ij}]} = -k_{\mathrm{B}}T \int \mathcal{D}[K_{ij}]\mathcal{P}[K_{ij}] \ln Z[K_{ij}]. \tag{7}$$

Averaging the logarithm of the partition function is possible through the identity

$$\ln Z = \lim_{n\to\infty} \frac{1}{n}(Z^n - 1),$$

which requires, before averaging, to produce n copies or replicas (with labels α) of the system with the same disorder configuration,

$$(Z[K_{ij}])^n = \int \left(\prod_{\alpha=1}^{n} \mathcal{D}[\sigma_i^{(\alpha)}] \right) \exp\left(-\beta \sum_{\alpha} \mathcal{H}[K_{ij}, \sigma_i^{(\alpha)}] \right),$$

and then to perform integrations over $\mathcal{P}[K_{ij}]$,

$$\overline{e^{-X}} = e^{-\bar{X} + \frac{1}{2}(\overline{X^2} - \bar{X}^2) + \cdots},$$

[m] In the case of an annealed disorder the impurities are thermalized (this would only be possible if the relaxation time of randomness is small compared to the time scale of the experiment) and their probability distribution $\mathcal{P}[K_{ij}]$ depends strongly on the spins (and vice-versa); since it is the equilibrium distribution $\mathcal{P}[K_{ij}] = \int \mathcal{D}[\sigma_i] Z^{-1} e^{-\beta\mathcal{H}[K_{ij},\sigma_i]}$, where Z no longer depends on the disorder realization, but is obtained through $Z = \int \mathcal{D}[K_{ij}]\mathcal{D}[\sigma_i] e^{-\beta\mathcal{H}[K_{ij},\sigma_i]}$. In the annealed case, if the impurity concentration is kept constant, there is a 'Fisher's renormalization' of the exponents if the specific heat of the pure system is diverging.[84]

leading to

$$\overline{(Z[K_{ij}])^n} = \int \left(\prod_{\alpha=1}^{n} \mathcal{D}[\sigma_i^{(\alpha)}] \right) \exp\left(-\sum_{\alpha} (K_0 + \overline{\delta K}) \sum_{(ij)} \delta_{\sigma_i^{(\alpha)}, \sigma_j^{(\alpha)}} \right)$$
$$\times \exp\left(\sum_{\alpha \neq \beta} (\overline{\delta K^2} - \overline{\delta K}^2) \sum_{(ij)} \delta_{\sigma_i^{(\alpha)}, \sigma_j^{(\alpha)}} \delta_{\sigma_i^{(\beta)}, \sigma_j^{(\beta)}} + \cdots \right). \quad (8)$$

In the leading term, $\overline{\delta K_{ij}}$ has Renormalization Group (RG) eigenvalue $y_t = d - x_\varepsilon$ (x_ε is the energy density scaling dimension) and corresponds to a simple shift of the transition temperature (which is obviously a relevant effect). In the next term, the second moment of the distribution, $\overline{\delta K^2} - \overline{\delta K}^2$, has RG eigenvalue $y_H = d - 2x_\varepsilon$,[n] and all the following terms are irrelevant.[o] Using the hyperscaling relation, the Harris scaling dimension of disorder is rewritten

$$y_H = \alpha/\nu. \quad (9)$$

It implies that at second-order transitions, disorder is a relevant perturbation which modifies the critical behaviour when the specific heat exponent α of the pure system is positive, while it is irrelevant (and universal properties are thus unaffected by randomness) when α is negative. In the borderline case $\alpha = 0$, randomness is marginal to leading order. This is the case for example of the 2D Ising model discussed in the introduction, where quenched disorder is eventually marginally irrelevant and produces only logarithmic corrections to the unchanged leading critical behaviour.

The case of first-order transitions was considered later, by Imry and Wortis, by Aizenman and Wehr, then by Hui and Berker.[2–4] It can be intuitively understood from the above results simply by noticing that the existence of a latent heat at first-order transition corresponds to a discontinuity of the energy density and can be described by a vanishing energy density scaling dimension, so that disorder is always relevant in this sense.

[n] In this review, we use the notation y_H for the Harris eigenvalue which has nothing to do with the magnetic field RG eigenvalue $y_h = d - x_\sigma$.

[o] The leading (unperturbed) term is written in the continuum limit as $-\beta\mathcal{H}_c = m_0 \int \sum_\alpha \varepsilon_\alpha(\mathbf{r}) d^2r$ where m_0 stands for $K_0 + \overline{\delta K}$ while the perturbation is written $g_0 \int \sum_{\alpha \neq \beta} \varepsilon_\alpha(\mathbf{r}) \varepsilon_\beta(\mathbf{r}) d^2r$ with g_0 corresponding to $\overline{\delta K^2} - \overline{\delta K}^2$.

2.2. *Perturbation Techniques*

2.2.1. *Average Correlation Functions*

Many results were obtained in the 2D random Potts model using RG perturbations, mainly around Ludwig and Vl. Dotsenko. In Eq. (8), it appears that $\overline{Z^n}$ couples the replicas via energy–energy interactions

$$\sum_{\alpha\neq\beta}(\overline{\delta K^2}-\overline{\delta K}^2)\sum_{\mathbf{r}}\varepsilon_\alpha(\mathbf{r})\varepsilon_\beta(\mathbf{r})$$

which have to be treated as a perturbation around the pure fixed point. Here, $\varepsilon_\alpha(\mathbf{r})$ is a short notation for $\delta_{\sigma_i^{(\alpha)},\sigma_j^{(\alpha)}}$, and $\mathbf{r}$ stands for the lattice vectors. The second cumulant of the coupling distribution will be denoted by g_0 in the following. Two different schemes have been considered in the literature,[25,60]

(i) *replica symmetric scenario*, where all the replicas are coupled through the same interaction strength,

$$\sum_{\alpha\neq\beta}g_0\sum_{\mathbf{r}}\varepsilon_\alpha(\mathbf{r})\varepsilon_\beta(\mathbf{r}), \tag{10}$$

(ii) *replica symmetry breaking scenario*, where the couplings between replicas are replica-dependent,

$$\sum_{\alpha\neq\beta}g_{\alpha\beta}\sum_{\mathbf{r}}\varepsilon_\alpha(\mathbf{r})\varepsilon_\beta(\mathbf{r}). \tag{11}$$

The program is thus to consider the 2D Potts model with weak bond randomness, to compute the scaling dimensions $x'_\sigma(n)$ of the order parameter and $x'_\varepsilon(n)$ of the energy-density perturbatively[p] around the Ising model conformal field theory, and then take the replica limit $n\to 0$. Expansions are performed around the pure model fixed point (weak disorder) in terms of the disorder strength $\overline{\delta K_{ij}^2}-\overline{\delta K_{ij}}^2$, and the exponents are given in powers of $y_H=\alpha/\nu$.

Different expansion parameters can be found in the literature, and it is worth collecting the main notation. The Potts models can be identified to minimal conformal models[85] which are parametrised by an integer m determining the central charge and critical behaviour of the model. The

[p]The primes denote the scaling dimensions at the random fixed point.

correspondence is given by

$$m = \frac{\pi}{\cos^{-1}(\sqrt{q}/2)} - 1$$

and the central charge and the exponents follow from

$$c = 1 - \frac{6}{m(m+1)}, \qquad x_\varepsilon = \frac{m+3}{2m}, \qquad x_\sigma = \frac{(m+3)(m-1)}{8m(m+1)}.$$

We note that $m = 3$ for the Ising model, $m = 5$ for the 3-state Potts model and $m \to \infty$ for the 4-state Potts model. The scaling dimension of disorder becomes

$$y_H = (m-3)/m,$$

which is proportional to $q-2$ to linear order (q being the number of states per spin of the Potts model):

$$y_H = \frac{4}{3\pi}(q-2) - \frac{4}{9\pi^2}(q-2)^2 + O[(q-2)^3]. \tag{12}$$

Using a Coulomb gas representation, a natural expansion parameter ϵ is defined through

$$\alpha_+^2 = \frac{m+1}{m} = \frac{4}{3} + \epsilon,$$

and it is linked to y_H by $\epsilon = -\frac{1}{3} y_H$.

(i) *The replica symmetric case* is based on the assumption that replica symmetry is not broken initially, and is then preserved by the renormalization group. The renormalization of the coupling constant g_0 is determined by perturbative calculation using the operator algebra. For any scaling operator ϕ, the perturbed two-point correlation function $\langle \phi(0)\phi(\mathbf{R})\rangle_g$ corresponds, in the limit $n \to 0$, to the average correlator $\overline{\langle \phi(0)\phi(\mathbf{R})\rangle}$. We can write

$$\langle \phi(0)\phi(\mathbf{R})\rangle_g = \frac{\operatorname{Tr} \phi(0)\phi(\mathbf{R})\, e^{-\beta(\mathcal{H}_c + \mathcal{H}_g)}}{\operatorname{Tr} e^{-\beta(\mathcal{H}_c+\mathcal{H}_g)}}$$

where the perturbation term

$$-\beta \mathcal{H}_g = g_0 \int \sum_{\alpha \neq \beta} \varepsilon_\alpha(\mathbf{r}) \varepsilon_\beta(\mathbf{r}) d^2 r$$

acts on the 'critical' Hamiltonian

$$-\beta \mathcal{H}_c = m_0 \int \sum_\alpha \varepsilon_\alpha(\mathbf{r}) d^2 r + h_0 \int \sum_\alpha \sigma_\alpha(\mathbf{r}) d^2 r,$$

the last term being included in order to compute the renormalization of the spin operator.

When expanded in terms of unperturbed correlators, it yields the expansion[86,87]

$$\langle\phi(0)\phi(\mathbf{R})\rangle_g = \langle\phi(0)\phi(\mathbf{R})\rangle_0 - \beta\langle\mathcal{H}_g\phi(0)\phi(\mathbf{R})\rangle_0 + \frac{1}{2}\beta^2\langle\mathcal{H}_g^2\phi(0)\phi(\mathbf{R})\rangle_0 + \cdots .$$

The renormalization of the coupling constant follows from the expansion[20–23]

$$\begin{aligned} & g_0 \int \sum_{\alpha\neq\beta} \varepsilon_\alpha(\mathbf{r})\varepsilon_\beta(\mathbf{r})d^2r \\ & \quad + \frac{1}{2}g_0^2 \int \sum_{\alpha\neq\beta} \varepsilon_\alpha(\mathbf{r})\varepsilon_\beta(\mathbf{r})d^2r \int \sum_{\gamma\neq\delta} \varepsilon_\gamma(\mathbf{r}')\varepsilon_\delta(\mathbf{r}')d^2r' + \cdots \\ & = g \int \sum_{\alpha\neq\beta} \varepsilon_\alpha(\mathbf{r})\varepsilon_\beta(\mathbf{r})d^2r, \end{aligned} \tag{13}$$

leading to $g = g_0(1 + A_1 g_0 + A_2 g_0^2 + \cdots)$. The successive terms are obtained from operator product expansions. In the first-order term, the dominant contribution to A_1 follows from contraction of neighbouring pairs, $\varepsilon(\mathbf{r})\varepsilon(\mathbf{r}') \sim |\mathbf{r} - \mathbf{r}'|^{-2x_\varepsilon}$, in the same replica ($\beta = \gamma \neq \alpha, \delta$ and $\alpha \neq \delta$). Such an expression has to be understood inside unperturbed correlators. Including combinatorial factors [there are $2(n-2)$ such factors], integration over space up to an infrared cutoff, $b > |\mathbf{r} - \mathbf{r}'|$, leads to $\frac{1}{2}g_0^2 A_1 \int \sum_{\alpha\neq\delta} \varepsilon_\alpha(\mathbf{r})\varepsilon_\delta(\mathbf{r})d^2r$, where A_1 is dominated by

$$A_1 = 2(n-2) \int\limits_{|\mathbf{r}-\mathbf{r}'|<b} |\mathbf{r} - \mathbf{r}'|^{-2x_\varepsilon} d^2r' = 4\pi(n-2)\frac{b^{2-2x_\varepsilon}}{2-2x_\varepsilon}.$$

Since $y_H = 2 - 2x_\varepsilon$, one recovers the Harris criterion. Up to the first order, we get the following expression for g in terms of the bare coupling constant g_0:

$$g = g_0 \left[1 + 2\pi(n-2)\frac{1}{y_H} b^{y_H} g_0 + O(g_0^2)\right].$$

Following Dotsenko and co-workers,[20–22] the coupling constants are multiplied by a factor b^{y_H} in order to get dimensionless coupling constants $g(b)$.

The β-function up to the second order in the $n \to 0$ limit is finally given by

$$\beta(g) = \frac{dg(b)}{d\ln b} = y_H g(b) - 8\pi g^2(b) + 32\pi^2 g^3(b) + O(g^4(b)). \qquad (14)$$

It leads to a nontrivial IR (infrared stable) fixed point (which determines the long distance physics) $g_c = (1/8\pi)y_H + (1/16\pi)y_H^2 + O(y_H^3)$. Renormalization of the energy and of the order parameter density operators follows from the same analysis, e.g.

$$\begin{aligned} m_0 \int \sum_\alpha \varepsilon_\alpha(\mathbf{r}) d^2r \Bigg(1 + g_0 \int \sum_{\beta\neq\gamma} \varepsilon_\beta(\mathbf{r}')\varepsilon_\gamma(\mathbf{r}') d^2r' \\ + \frac{1}{2} g_0^2 \int \sum_{\beta\neq\gamma} \varepsilon_\beta(\mathbf{r}')\varepsilon_\gamma(\mathbf{r}') d^2r' \int \sum_{\delta\neq\eta} \varepsilon_\delta(\mathbf{r}'')\varepsilon_\eta(\mathbf{r}'')\, d^2r'' + \cdots \Bigg) \\ = m \int \sum_\alpha \varepsilon_\alpha(\mathbf{r})\, d^2r, \end{aligned} \qquad (15)$$

and provides the expansions (details of the calculation of the integrals, using a Coulomb gas representation, can be found e.g. in Ref. 20)

$$\begin{aligned} m &= m_0(1 + B_1 g_0 + B_2 g_0^2 + \cdots) = Z_\varepsilon m_0, \\ h &= h_0(1 + C_1 g_0 + C_2 g_0^2 + \cdots) = Z_\sigma h_0, \end{aligned}$$

leading when $n \to 0$ to

$$\begin{aligned} \gamma_\varepsilon(g) &= \frac{d\ln Z_\varepsilon}{d\ln b} = -4\pi g(b) + 8\pi^2 g^2(b), \\ \gamma_\sigma(g) &= \frac{d\ln Z_\sigma}{d\ln b} = -\pi^2 y_H g^2(b) \left(1 + 2\frac{\Gamma^2(-\frac{2}{3})\Gamma^2(\frac{1}{6})}{\Gamma^2(-\frac{1}{3})\Gamma^2(-\frac{1}{6})} \right) + 8\pi^2 g^3(b). \end{aligned} \qquad (16)$$

For the correlators themselves, the renormalization equations can be written

$$\langle \phi(0)\phi(s\mathbf{R})\rangle = \frac{Z_\phi^2(g(bs))}{Z_\phi^2(g(b))} s^{-2x_\phi} \langle \phi(0)\phi(\mathbf{R})\rangle,$$

where s is the scaling factor. Using now

$$\gamma_\phi(g) = \frac{d\ln Z_\phi}{d\ln b},$$

or $\ln Z_\phi = \int \gamma_\phi(g)\, d\ln b$, the ratio $Z_\phi^2(g(bs))/Z_\phi^2(g(b))$ can be rewritten

$$\frac{Z_\phi^2(bs)}{Z_\phi^2(b)} = \exp\left(2\int_b^{bs} \gamma_\phi(g)\, d\ln b \right),$$

which is dominated at long distances by $g \simeq g_c$, such that $\int_b^{bs} \gamma_\phi(g)\, d\ln b \simeq \gamma_\phi(g_c) \ln s$. The homogeneity equation thus becomes

$$\langle \phi(0)\phi(s\mathbf{R})\rangle = s^{-2(x_\phi - \gamma_\phi(g_c))} \langle \phi(0)\phi(\mathbf{R})\rangle,$$

and choosing a rescaling factor $s = R^{-1}$, the two-point correlator decays as

$$\langle \phi(0)\phi(\mathbf{R})\rangle \simeq R^{-2(x_\phi - \gamma_\phi(g_c))}. \tag{17}$$

The corresponding scaling dimension is modified according to

$$x'_\phi = x_\phi - \gamma_\phi(g_c). \tag{18}$$

Collecting the results of Dotsenko and co-workers, we give the new thermal and magnetic scaling dimensions (primed quantities) in terms of the original ones (unprimed):[20–23]

$$\begin{aligned} x'_\varepsilon &= x_\varepsilon - \gamma_\varepsilon(g_c) \\ &= x_\varepsilon + \frac{1}{2} y_H + \frac{1}{8} y_H^2 + O(y_H^3), \end{aligned} \tag{19}$$

$$\begin{aligned} x'_\sigma &= x_\sigma - \gamma_\sigma(g_c) \\ &= x_\sigma + \frac{1}{32} \frac{\Gamma^2(-\frac{2}{3})\Gamma^2(\frac{1}{6})}{\Gamma^2(-\frac{1}{3})\Gamma^2(-\frac{1}{6})} y_H^3 + O(y_H^4). \end{aligned} \tag{20}$$

(ii) *The other assumption of a broken replica symmetry* leads to a different fixed point structure. The coupling between replicas, $g_{\alpha\beta}$, is now dependent on the pair indices, and it is generalised to a continuous variable x instead of pair indices, $g_{\alpha\beta} \to g(\alpha - \beta) = g(x)$. It is found that there is only one marginally attractive solution for the coupling $g(x)$ which then enables one to compute $\gamma_\varepsilon(g)$ and $\gamma_\sigma(g)$, leading to a modified thermal exponent

$$x''_\varepsilon = x_\varepsilon + \frac{1}{2} y_H + O(y_H^3), \tag{21}$$

while to y_H^3 order, the magnetic scaling index remains the same as in the replica symmetric scenario.[22]

2.2.2. *Multiscaling and Higher Order Moments of the Correlators*

In order to measure some other differences between the replica symmetric and the replica symmetry breaking cases, the moments of the correlators can also be helpful. For any scaling field $\phi(\mathbf{r})$, multiscaling arises when

the scaling dimensions associated to the moments of the correlators do not follow a simple linear law:

$$\overline{\langle\phi(0)\phi(\mathbf{R})\rangle^p} \sim R^{-2px_{\phi^p}}, \quad x_{\phi^p} \neq x_\phi. \tag{22}$$

In the magnetic sector, a difference between the two cases occurs to y_H^2 order for the second moment:[25]

$$RS \quad x'_{\sigma^2} = x_\sigma - \frac{1}{16}y_H + \frac{1}{32}\left(4\ln 2 - \frac{11}{12}\right)y_H^2 + O(y_H^3), \tag{23}$$

$$RSB\ x''_{\sigma^2} = x_\sigma - \frac{1}{16}y_H + \frac{1}{32}\left(4\ln 2 - \frac{5}{12}\right)y_H^2 + O(y_H^3). \tag{24}$$

For higher order moments, the computation was only performed in the replica symmetric case,[19,26,27] leading to

$$x'_{\varepsilon^p} = 1 - \frac{2}{9\pi^2}(3p-4)(q-2)^2 + O[(q-2)^3], \tag{25}$$

$$x'_{\sigma^p} = 1 - \frac{1}{16}(p-1)y_H^2 - \frac{1}{32}(p-1)\left[\frac{11}{12} - 4\ln 2 + \frac{1}{24}(33 - 29\sqrt{3}\pi/3)(p-2)\right]y_H^3 + O(y_H^4). \tag{26}$$

2.2.3. *Are these Effects Measurable?*

The question is now to try to detect numerically the effects discussed above. These are perturbative expansions around $q = 2$, so that a natural choice of system to measure the scaling dimensions in the presence of quenched disorder is the 3-state Potts model. At $q = 3$ we have $x_\varepsilon = \frac{4}{5}$ and $y_H = \frac{2}{5}$ from which the perturbed scaling dimensions in the energy and magnetic sectors can be obtained. The values are given in Table 3. The numerical data clearly

Table 3. Comparison between pure 3-state Potts model critical exponents and the expected values obtained from perturbation expansions. The notation x_{σ^2} corresponds to the second moment of the spin–spin correlation function, while x_{σ^0} and x_{ε^0} are associated to the typical correlations.

Scheme	Scaling dimensions				
	x_σ	x_ε	x_{σ^2}	x_{σ^0}	x_{ε^0}
Pure system	0.13333	0.800	0.13333	0.13333	0.800
RS	0.13465	1.000	0.11761	0.18303	1.090
RSB	0.13465	1.020	0.12011	–	–

show that the expected variations are quite small and accurate numerical techniques are needed to discriminate between RS and RSB schemes.

3. Numerical Techniques in 2D

3.1. *Monte Carlo Simulations*

3.1.1. *Cluster Algorithms*

For the simulation of spin systems, standard Metropolis algorithms based on local updates of single spins suffer from the well known critical slowing down. As the second-order phase transition is approached, the correlation length becomes larger and the system contains larger and larger clusters in which all the spins are in the same state. Statistically independent configurations can be obtained by local iteration rules only after a long dynamical evolution which needs a huge number of MC steps. This makes this type of algorithm inefficient close to a critical point.

Since the transition of the disordered Potts model is always expected to be on average a second-order one, the resort to cluster update algorithms is more convenient.[88,89] The main recipe of cluster algorithms is the identification of clusters of sites using a bond percolation process connected to the spin configuration. The spins of the clusters are then independently flipped. A cluster algorithm is particularly efficient if the percolation threshold coincides with the transition point of the spin model, which guarantees that clusters of all sizes will be updated in a single MC sweep.

In the case of the Potts model, the percolation process involved is obtained through the mapping onto the random graph model. These algorithms are based on the Fortuin–Kasteleyn representation[90] where bond variables are introduced. In the Swendsen–Wang algorithm,[91] a cluster update sweep consists of three steps: depending on the nearest neighbour exchange interactions, assign values to the bond variables, then identify clusters of spins connected by active bonds, and eventually assign a random value to all the spins in a given cluster. The Wolff algorithm[92] is a simpler variant in which only a single cluster is flipped at a time. A spin is randomly chosen, then the cluster connected with this spin is constructed and all the spins in the cluster are updated. Both algorithms considerably improve the efficiency close to the critical point and their performances are comparable in two dimensions, so in principle one can equally choose either one of them. Nevertheless, when one uses particular boundary conditions, with fixed spins along some surface for example, the Wolff algorithm is less efficient, since close to criticality the unique cluster will often reach the boundary and no update is made in this case.

3.1.2. *Definition of the Physical Quantities*

For each disorder strength, many samples ($N_{\rm rdm}$) from the same probability distribution are studied at a given temperature. Each sample, initialised from the low-temperature phase, is thermalized during $N_{\rm th}$ Monte Carlo sweeps and the physical quantities are then measured during $N_{\rm MC}$ sweeps. Different quantities, averaged over the MC sweeps denoted by $\langle \cdots \rangle$, are stored for each sample. Many physical quantities can be measured:

(i) *The order parameter density* follows from the standard definition for the Potts model:

$$M = \langle \sigma \rangle, \quad \sigma = \frac{q\rho_{\max} - 1}{q - 1},$$

where $\rho_{\max}$ is the fraction of spins in the majority orientation

$$\rho_{\max} = {\rm Max}_\alpha(\rho_\alpha), \quad \rho_\alpha = \frac{1}{L^2} \sum_j \delta_{\sigma_j,\alpha}.$$

Thermal average is understood in the notation M. To obtain the local order parameter $\langle \sigma(i) \rangle$ at site i, it is counted 1 when the spin at site i is in the majority state and 0 otherwise.

(ii) *The susceptibility* is given by the fluctuation–dissipation theorem

$$k_B T \chi = \langle \sigma^2 \rangle - \langle \sigma \rangle^2.$$

(iii) *Energy density:*

$$E = \langle \varepsilon \rangle, \quad \varepsilon = \frac{1}{2L^2} \sum_{(i,j)} K_{ij} \delta_{\sigma_i,\sigma_j}.$$

(iv) *Specific heat:*

$$C/k_B = \langle \varepsilon^2 \rangle - \langle \varepsilon \rangle^2.$$

(v) *Energy Binder cumulant:*

$$U_E = 1 - \langle \varepsilon^4 \rangle / 3 \langle \varepsilon^2 \rangle^2.$$

(vi) *Correlation functions:* the connected spin–spin correlation function $G_\sigma(i,j) = \langle \sigma(i)\sigma(j) \rangle - \langle \sigma^2 \rangle$ at criticality is obtained by the estimator of

the paramagnetic phase,

$$\frac{q\langle\delta_{\sigma_i,\sigma_j}\rangle - 1}{q-1},$$

given by the probability that spins at sites i and j belong to the same finite cluster.

All these quantities are then averaged over the disorder realisations

$$\overline{\langle\cdots\rangle} = \int \langle\cdots\rangle \mathcal{P}[\langle K\rangle]\, \mathcal{D}\langle K\rangle.$$

3.2. *Transfer Matrix Technique*

The disordered Potts model can be studied using the transfer matrix method introduced by Blöte and Nightingale,[93] which takes advantage of the Fortuin–Kasteleyn representation[90] in terms of graphs of the partition function of the Potts model in order to reduce the dimension of the Hilbert space.[q] In the Fortuin–Kasteleyn representation, the partition function (with no magnetic field) is

$$Z = \mathrm{Tr} \prod_{(i,j)} (1 + \delta_{\sigma_i,\sigma_j} u_{ij}),$$

where $u_{ij} = e^{K_{ij}} - 1$, is expanded as a sum over all the possible graphs $\mathcal{G}$ (with s sites and $l(\mathcal{G})$ loops) leading to the random cluster model:

$$Z = q^s \sum_{\mathcal{G}} q^{l(\mathcal{G})} \prod_{(i,j)/b_{ij}=1} \left(\frac{u_{ij}}{q}\right),$$

the $b_{ij} \in \{0;1\}$ being the bond variables. Blöte and Nightingale suggested to introduce a set of connectivity states which contain the information about which sites on a given row belong to the same cluster when they are interconnected through a part of the lattice previously built. A unique connectivity label $\eta_i = \eta$ is attributed to all the sites i of such a cluster. In the connectivity space, $|Z(m)\rangle$ is a vector whose components are given by the partial partition function $Z(m, \{\eta_i\}_m)$ of a strip of length m whose connectivity on the last row is given by $\{\eta_i\}_m$. The connectivity transfer matrix is then defined according to $|Z(m+1)\rangle = \mathbf{T}_m |Z(m)\rangle$ and the partition function of a strip of length m becomes $|Z(m)\rangle = \prod_{k=1}^{m-1} \mathbf{T}_k |Z(1)\rangle$, where $|Z(1)\rangle$ is the statistics of uncorrelated spins (Fig. 5).

[q] A refined algorithm based on a loop representation of the partition function was proposed in Ref. 94.

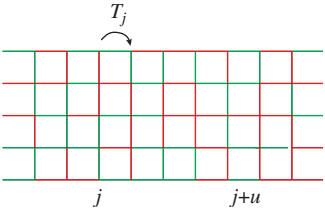

Fig. 5. Transfer matrix along the disordered strip.

The following physical quantities are measured:

(i) *The quenched free energy density* is given (up to a $k_{\mathrm{B}}T$ factor) by the Lyapunov exponent of the product of an infinite number of transfer matrices $\mathbf{T}_k$[95]

$$\overline{f_L} = -L^{-1}\Lambda_0(L), \tag{27}$$

$$\Lambda_0(L) = \lim_{m\to\infty} \frac{1}{m} \ln \left\| \left(\prod_{k=1}^{m} \mathbf{T}_k \right) |\, v_0\rangle \right\|, \tag{28}$$

where $|\, v_0\rangle$ is a unit initial vector.

For a pure system, the central charge c is defined as the universal coefficient in the lowest-order correction to scaling of the free energy density f_L of a strip of width L:

$$f_L = f_\infty - \frac{\pi c}{6L^2} + O\left(\frac{1}{L^4}\right), \tag{29}$$

where the regular contribution is $f_\infty = \lim_{L\to+\infty} f_L$. For a disordered system, c is defined in the same way from the finite-size behaviour of the quenched average free energy density $\overline{f_L}$, and numerically, since the strip widths available are small, we can only expect to measure effective central charges which depend on the disorder strength, $c_{\mathrm{eff}}(g)$, and which would converge towards the true value c in the thermodynamic limit.[45,94]

$$\overline{f_L} = f_\infty - \frac{\pi c_{\mathrm{eff}}}{6L^2} + a_4 L^{-4}. \tag{30}$$

(ii) *The spin–spin correlation functions* in the time-direction (u) of the strip are calculated using an extension of the Hilbert space that allows one to keep track of the connectivity with a given spin. For a specific disorder

realisation, the spin–spin correlation function along the strip,

$$G_\sigma(u) = \frac{q\langle\delta_{\sigma_j,\sigma_{j+u}}\rangle - 1}{q-1}, \tag{31}$$

is given by the probability that the spins along some row, at columns j and $j+u$, are in the same state, and is expressed, in the absence of long-range order, in terms of a product of non-commuting transfer matrices:

$$\langle\delta_{\sigma_j,\sigma_{j+u}}\rangle \sim \langle\Lambda_0|\,\mathbf{g}_j \left(\prod_{k=j}^{j+u-1} \mathbf{T}'_k\right) \mathbf{d}_{j+u}\,|\Lambda_0\rangle, \tag{32}$$

where $|\Lambda_0\rangle$ is the ground state eigenvector and $\mathbf{T}'_k$ is the transfer matrix in the extended Hilbert space. The operators $\mathbf{g}_j$ and $\mathbf{d}_{j+u}$ realise the mapping between the two connectivity spaces. The correlations are computed on strips of varying widths and then averaged over many disorder realisations.

4. Analysis of Numerical Data in 2D

4.1. *Location of the Random Fixed Point*

The transition line between ordered and disordered phases in the phase diagram starts at some point corresponding to the pure system and ends at another point where the critical properties are governed by the percolation universality class. Somewhere in between, the random fixed point governs the critical behaviour of quenched randomness. Although this random fixed point is attractive, its precise location is an important preliminary step. Indeed, if the assumption of the existence of a unique stable random fixed point holds, one expects that the critical behaviour is asymptotically the same as when the system is moved along the transition line. However, in finite systems, one generically has to deal with strong crossover effects due to the competition between the disordered fixed point and the pure and percolation fixed points, or due to corrections to scaling linked to the appearance of irrelevant scaling variables. These latter effects are generally important in random systems and the corresponding corrections to scaling can be substantially reduced when one measures the critical exponents in the regime of the random fixed point, expected to be reached in the vicinity of the maximum of the effective central charge.

Let us consider the finite-size behaviour of an observable Q measured at a deviation $t = K - K_c(g)$ from the critical point on some system of characteristic size L, in the presence of disorder whose strength is measured by an amplitude g (ratio r between strong and weak interactions,

probability p of non-vanishing bond, ...). The variables t and L^{-1} play the role of relevant scaling fields (with positive RG eigenvalues $y_t = 1/\nu$ and $y_L = 1$ respectively), while close to the fixed point, disorder is supposed to be related to some irrelevant scaling variable with eigenvalue $y_g = -\omega < 0$. At the fixed point there is no need for the irrelevant scaling field to vanish, so that one can write g^* for the corresponding disorder strength at the fixed point, and the observable Q obeys the following homogeneity assumption in the scaling region:

$$Q(t, L^{-1}, g) = L^{-x_Q} f(L^{1/\nu} t, L^{-\omega}(g - g^*)).$$

An expansion of the last variable (keeping the leading term only) along the critical line (i.e. varying g in $K_c(g)$) gives

$$Q(0, L^{-1}, g) = \Gamma_Q L^{-x_Q}(1 + \Gamma_Q^{(2)}(g - g^*)L^{-\omega} + \cdots),$$

where the Γ's are non-universal critical amplitudes. It is thus possible to fix $g = g^*$ in order to minimise the corrections to scaling (see Fig. 6).

From a finite-size scaling analysis (see Section 4.3), the optimal disorder strength g^* is reached when a given quantity seems to be well fitted by a simple power law (i.e. no bending in the log–log plot). In the strip

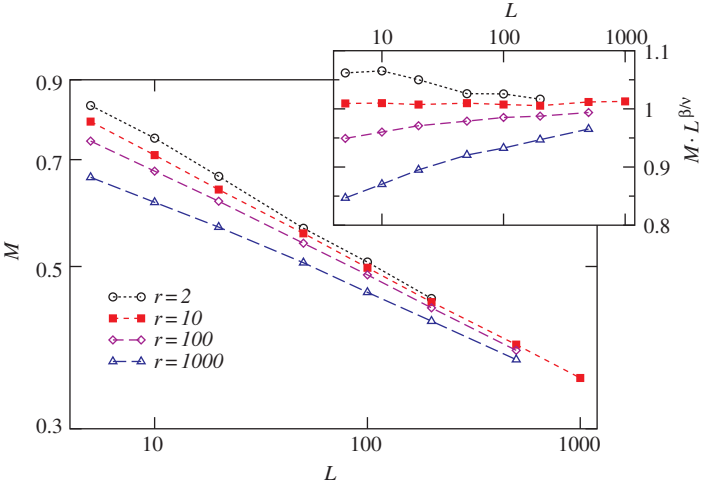

Fig. 6. Finite-size scaling behaviour of the magnetisation ($q = 8$, binary disorder) for different disorder amplitudes r (binary distribution). The corrections to scaling are smaller close to $r = 10$ (taken from Picco[28]).

geometry, this value of g^* is found to coincide with the location of the maximum of the central charge along the critical line,[43,44] as a consequence of Zamolodchikov's c-theorem[96] (see Fig. 7).

In the literature, different types of disorder distributions have been considered. In the most studied case, when self-duality holds, the exact transition curve is known and the optimal disorder strength g^* has to be found while moving one parameter only, which simplifies the task. If one defines the variables y_{ij} by $e^{y_{ij}} = \frac{1}{\sqrt{q}}(e^{K_{ij}} - 1)$, the duality relation can be written[16]

$$e^{y^*_{ij}} = \frac{e^{K^*_{ij}} - 1}{\sqrt{q}} = \frac{\sqrt{q}}{e^{K_{ij}} - 1} = e^{-y_{ij}},$$

and self-duality is satisfied when the probability of each coupling equals the probability of its dual coupling,

$$\mathcal{P}(y_{ij})\, dy_{ij} = \mathcal{P}(y^*_{ij})\, dy^*_{ij}, \tag{33}$$

that is if the distribution $\mathcal{P}(y_{ij})$ is even. In the case of the bimodal distribution, the self-duality point

$$[\exp(K_c(r)) - 1][\exp(rK_c(r)) - 1] = q\,, \tag{34}$$

corresponds to the critical point of the model if only one phase transition takes place in the system, as shown rigorously in Ref. 97.

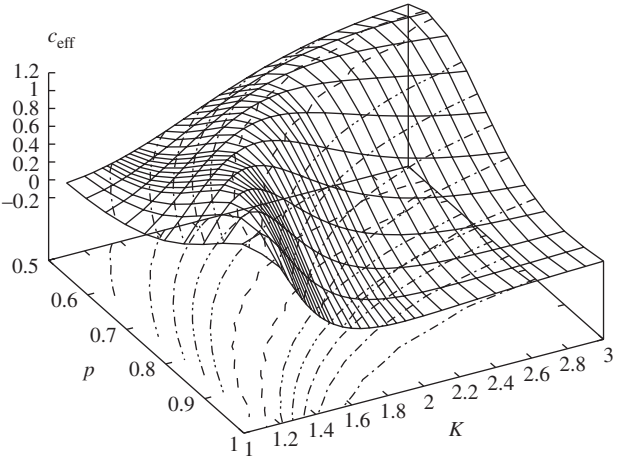

Fig. 7. Dependence of the effective central charge c_{eff} on the exchange coupling K and the bond probability p (diluted problem) for the 4-state Potts model. The maximum gives the location of the transition line and the absolute maximum corresponds to the optimal disorder strength.

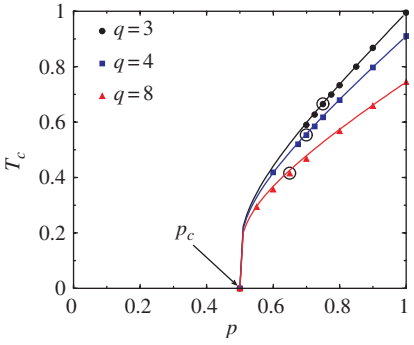

Fig. 8. Phase diagram obtained from the condition of a maximum of the central charge for the dilute Potts model ($q = 3$, 4, and 8). The optimal disorder strength (here p^*) is denoted by a larger circle and the full lines correspond to the single-bond effective medium approximation.[98–100]

In the case of dilution, self-duality does not work and the transition line has to be found numerically. The condition of a maximum of the central charge is again used as illustrated in Figs. 7 and 8. The result is in fair agreement with the effective medium approximation.[98–100]

4.2. *Temperature Dependence*

According to their definition, the critical exponents can be obtained from a temperature-dependence study. Using for example the case of the order parameter in the low temperature phase, one can write

$$M(t) = B_-|t|^\beta(1 + \cdots), \quad t = K_c - K < 0.$$

The dots indicate the correction terms the importance of which depends on the size of the system and on the distance from the transition temperature. Technically, one uses the definition of an effective temperature-dependent exponent, as illustrated in Figs. 9 and 10,

$$\beta_{\text{eff}}(t) = \frac{d \ln M(t)}{d \ln t}, \quad \beta = \lim_{t \to 0} \beta_{\text{eff}}(t).$$

The precise value of the disorder strength g of course also influences the value of $\beta_{\text{eff}}(t)$ (playing a role in the corrections to scaling as mentioned above) but asymptotically the limit $t \to 0$ should be independent of the (non-zero) g, since there is only one fixed point governing the disordered system.

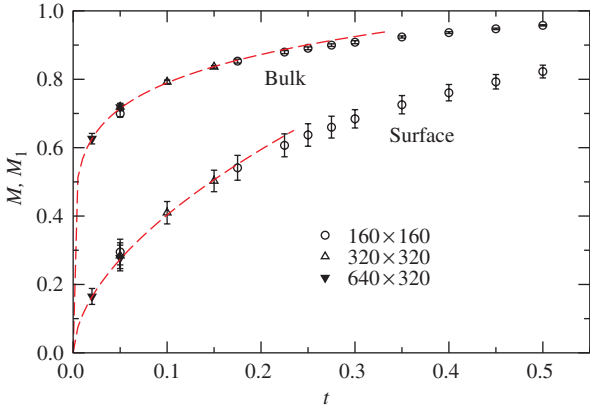

Fig. 9. Temperature dependence of the bulk and boundary magnetisation ($q = 8$, $r = 10$, binary disorder).

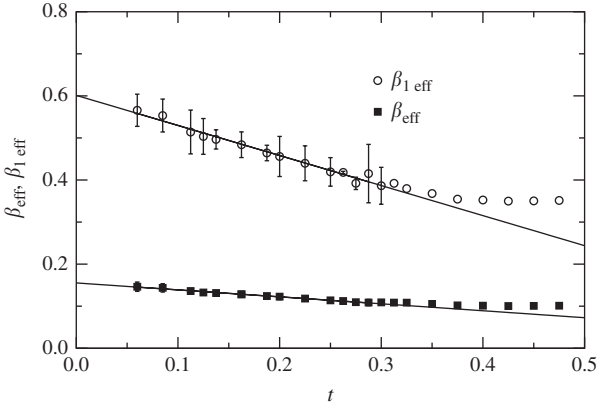

Fig. 10. Temperature dependence of the exponents associated to the bulk and boundary magnetisation ($q = 8$, $r = 10$, binary disorder).

4.3. *Finite-Size Scaling*

One of the simplest methods to extract critical exponents (once the critical temperature is known) is probably standard Finite-Size Scaling. On a finite system, the physical quantities cannot exhibit any singularity. They can be written as a singular term corrected by some scaling function which depends on the characteristic sizes of the problem, the correlation length ξ and the size of the system L. In the case of the order parameter density for example we get $M_L(T) = |K - K_c|^\beta f(L/\xi)$. The function $f(x)$ of course depends

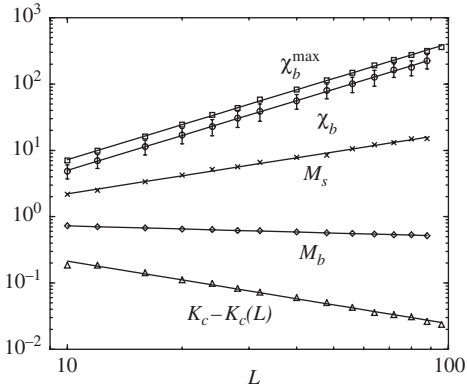

Fig. 11. Finite-size scaling analysis of magnetisation, susceptibility and effective transition temperature shift for the critical self-dual binary disordered 8-state Potts model.

on the geometry, but at the critical point K_c, the following behaviour is obtained:

$$M_L(K_c) \underset{L\to\infty}{\sim} L^{-\beta/\nu}. \tag{35}$$

Here, the ratio β/ν is precisely the magnetic scaling dimension x_σ. An example is shown in Fig. 11 for the 8-state Potts model. From the slopes of the curves, the values $\gamma/\nu = 1.686(17)$, $\beta/\nu = 0.152(4)$ and $\nu = 1.005(30)$ can be obtained.[63] The results here are interesting as reference values that we shall compare with more sophisticated techniques later.

4.4. *Short-Time Dynamics Scaling*

It is commonly believed that universality can be found only in the equilibrium stage of the long-time regime in numerical simulations. For a magnetic system far from criticality, e.g. in the high temperature phase, suddenly quenched to the critical temperature, a universal dynamic scaling behaviour emerges already within the short-time regime, according to a simple generalisation of the homogeneity assumption for the order parameter,[53–55,58]

$$M(t, \tau, L, M_0) = b^{-\beta/\nu} M(b^{1/\nu} t, b^{-z}\tau, b^{-1}L, b^{x_0} M_0), \tag{36}$$

where z is the dynamic exponent (dependent on the choice of algorithm), $t = |K - K_c|$ is the deviation from the critical point, M_0 is the initial magnetisation with the associated scaling dimension x_0, and τ is the time (measured in MC sweeps). In the thermodynamic limit, $L \to \infty$,

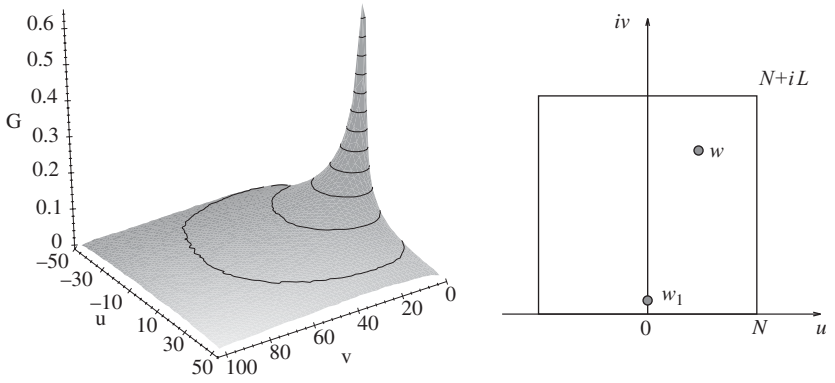

Fig. 12. Monte Carlo simulations of the 2D Ising model inside a square of 101×101 lattice sites (10^6 MCS/spin, Swendsen–Wang cluster algorithm). The figure shows the correlation function between a point close to the surface ($w_1 = i$) and all other points w in the square. The sketch on the right specifies the notation.

and at criticality, $t = 0$, the expected evolution is given by $M(\tau, M_0) = \tau^{-\beta/\nu z} f(M_0 \tau^{-x_0/z})$ and allows the computation of the critical exponents. The main interest of short-time dynamics scaling is that it is not affected by critical slowing down, since only early time stages of the simulation are involved.

4.5. *Conformal Mappings*

Monte Carlo simulations of two-dimensional spin systems are generally performed on systems of square shape while transfer matrix computations are done in strip geometries. In the following, we consider such a system of size $2N \times L$, and call u and v the corresponding directions (Fig. 12). The order parameter correlations between a point close to the surface, and a point in the bulk of the system should, in principle, lead to both surface and bulk critical exponents. Practically, it is not of great help for the accurate determination of critical exponents, since

(i) strong surface effects (shape effects) occur which modify the large distance power-law behaviour,

(ii) the universal scaling function entering the correlation function is likely to display a crossover before its asymptotic regime is reached (system-dependent effect).

One can proceed as follows: systems of increasing size are successively considered, and the correlations are computed along the u-axis (parallel to

a square edge considered as the free surface) and the v-axis (perpendicular to this edge). The order parameter correlation function for example is supposed to obey a scaling form which reproduces the expected power-law behaviour in the thermodynamic limit:

$$G_{\perp}(v) = \frac{1}{v^{x_\sigma + x_\sigma^1}} f_{\square}\left(\frac{v}{L}\right), \qquad G_{\parallel}(u) = \frac{1}{u^{2x_\sigma^1}} f'_{\square}\left(\frac{u}{N}\right), \tag{37}$$

where x_σ and x_σ^1 are, respectively, the bulk and surface order parameter scaling dimensions. The scaling functions $f_\square$ depend on the geometry, but have to satisfy asymptotic expansions including corrections to scaling, e.g. $f_\square\,(v/L) \sim 1 + \text{const}\,(v/L)^\epsilon + \cdots$ in the boundary region $v \to L$.

Equations (37) are not very useful for the determination of critical exponents, since at least five unknown quantities appear, and the correction terms in $f_\square(x)$ may have a large amplitude, resulting from the significance of finite-size corrections. Nevertheless, if the power-law fit is limited to the linear regions on a log–log scale (almost one decade in Fig. 13 top), one gets correct estimations of the critical exponents, as long as condition (ii) is fulfilled.

At a critical point, scale invariance coupled with rotation and translation invariance also implies covariance under local scale transformations, i.e. conformal transformations.[6] The conformal transformations are those general coordinate transformations which preserve the angle between any two vectors. They leave the metric invariant up to a scale change. The conformal group includes the Euclidean group as a subgroup, the dilatations and the special conformal transformations. In any dimension these conformal transformations are also called global conformal transformations because they map the infinite space onto itself. Consider a lattice model described in the continuum limit by a local theory defined by some action S. Conformal symmetry occurs when a local theory is scale invariant. In lattice systems, nearest-neighbour interactions ensure that physics is local and scale invariance holds at the critical point where a continuous limit description is allowed. For any local field (the energy density or the magnetisation for a spin system for example) the usual homogeneity assumption under a homogeneous rescaling $\mathbf{R} \to b\mathbf{R}$,

$$\langle \phi(0)\phi(b\mathbf{R})\rangle = b^{-2x_\phi}\langle \phi(0)\phi(\mathbf{R})\rangle, \tag{38}$$

is extended to local transformations with a position-dependent rescaling factor. In two dimensions conformal transformations are realized by the

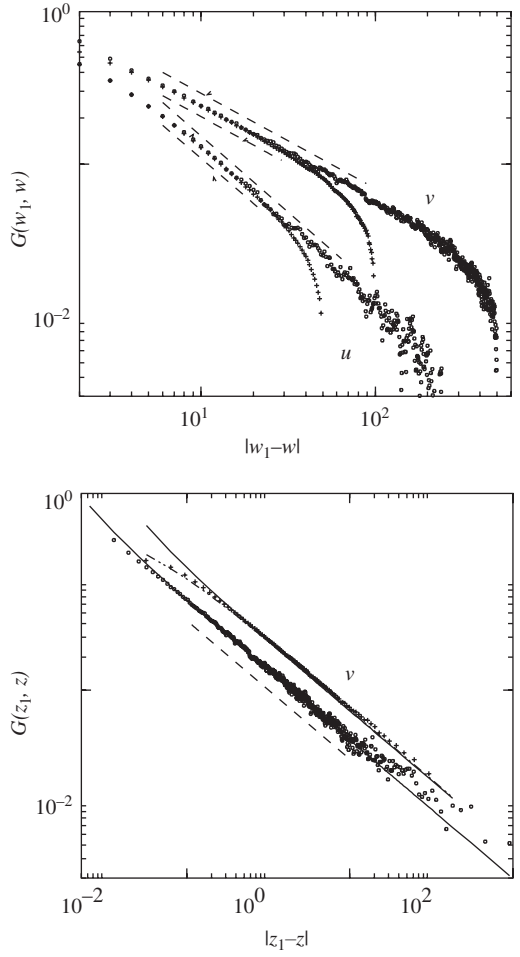

Fig. 13. Monte Carlo simulations in the case of the two-dimensional Ising model. Top: Log–log plot of the order parameter correlation function perpendicular to the surface (v-direction) and parallel to this surface (u-direction) for system sizes 101×101 ($+$, 5×10^6 MCS/spin) and 501×501 ($\circ$, 2×10^5 MCS/spin). The correlations are computed between a point $w_1 = i$ close to the surface and points $w = iv$, and $w = u + i$, respectively. The corresponding estimations for $x_\sigma + x_\sigma^1$ and $2x_\sigma^1$ are indicated by a dashed line. The figures correspond to power-law fits for the size 501×501. Bottom: Conformal rescaling of the perpendicular correlations for the two sizes (see below). The rescaled correlation function exhibits a true power-law in the whole range of variation of the new variable, and the value for $x_\sigma + x_\sigma^1$ is improved. The solid lines correspond to the theoretical asymptotic form while the dotted line is a fit.

analytic functions in the complex plane (the conformal group is thus infinite-dimensional): $z \longrightarrow w(z)$ and Eq. (38) is thus generalised to a covariance law of transformation of the (N-point) correlators under conformal mappings:

$$\langle \phi(w_1)\phi(w_2)\rangle = |w'(z_1)|^{-x_\phi} |w'(z_2)|^{-x_\phi} \langle \phi(z_1)\phi(z_2)\rangle. \tag{39}$$

Here, z_1 and z_2 are two points in the original complex plane and w_1 and w_2 are the corresponding points in the transformed complex geometry under the mapping $w(z)$. This transformation law is very helpful in numerical analysis, since simulations or numerical computations are always performed on finite systems of particular shape, depending on the technique used. The critical properties of an infinite system $\langle \phi(z_1)\phi(z_2)\rangle \sim |z_1 - z_2|^{-2x_\phi}$ can thus be obtained by fitting the numerical data to the transformed conformal expression which usually deviates significantly from a simple power law (although the algebraic decay at criticality must be recovered asymptotically in the limit of an infinite system of course). The situation is schematically sketched in Fig. 14. For a recent systematic use of such mappings applied to Monte Carlo data, see Ref. 109.

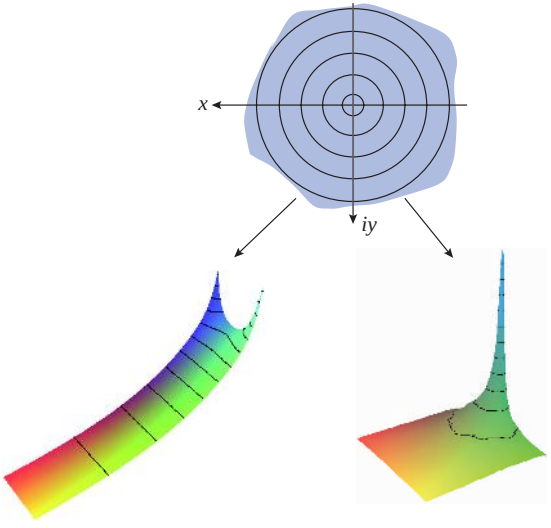

Fig. 14. Conformal mapping of the infinite plane $z = x + iy$ inside a finite square $N \times N$ with free edges or a strip of width L with periodic boundary conditions.

Among all the possible mappings, we shall here specify a few cases of interest:

(i) *Mapping onto a cylinder:* the logarithmic transformation

$$w(z) = \frac{L}{2\pi} \ln z = u + iv \tag{40}$$

is well known to map the infinite plane onto a strip of finite width L with periodic boundary conditions and infinite length. This is the limit $N \to \infty$ in the rectangular geometry described above. Using the algebraic decay of the two-point correlator in the z-plane, one gets on the strip

$$\langle \phi(0,0)\phi(u,v)\rangle = \left(\frac{2\pi}{L}\right)^{2x_\phi} \left[2\cosh\left(\frac{2\pi u}{L}\right) - 2\cos\left(\frac{2\pi v}{L}\right)\right]^{-x_\phi}. \tag{41}$$

In the long direction of the strip, at large distances it becomes an exponential decay

$$\langle \phi(0,0)\phi(u,0)\rangle_{\text{pbc}} = \left(\frac{2\pi}{L}\right)^{2x_\phi} \exp\left(-\frac{2\pi u x_\phi}{L}\right). \tag{42}$$

For sufficiently large strip widths, the transverse direction can also give some interesting results. Using the mapping $w(z) = (L/\pi)\ln z$, the half-infinite plane is mapped onto a strip with open boundaries in the transverse direction. If the boundary conditions are fixed (for example using an ordering surface field coupled to the order parameter) on one edge and free on the opposite edge (this is the meaning of the notation $+f$ below), the transverse profile (Fig. 15) of the order parameter density is given by the conformal expression

$$\langle \sigma(v)\rangle_{+f} = \text{const} \times \left[\frac{L}{\pi}\sin\left(\frac{\pi v}{L}\right)\right]^{-x_\sigma} F\left[\cos\left(\frac{\pi v}{2L}\right)\right]. \tag{43}$$

The shape of the scaling function $F(x)$ is asymptotically constrained by simple scaling, $F(x) \sim x^{x_\sigma^1}$ (here, x_σ^1 is the boundary scaling dimension of the order parameter).

(ii) *Mapping onto a square:* the Schwarz-Christoffel transformation

$$w(z) = \frac{N}{2\mathrm{K}}\mathrm{F}(z,k), \quad z = \mathrm{sn}\left(\frac{2\mathrm{K}w}{N}\right) \tag{44}$$

maps the half-infinite plane $z = x + iy$ $(0 \le y < \infty)$ inside a square $w = u + iv$ of size $N \times N$ $(-N/2 \le u \le N/2,\, 0 \le v \le N)$ with free boundary conditions along the four edges. Here, $\mathrm{F}(z,k)$ is the elliptic integral of the first kind, $\mathrm{sn}\,(2\mathrm{K}w/N)$ the Jacobian elliptic sine, $\mathrm{K} = K(k)$ the complete

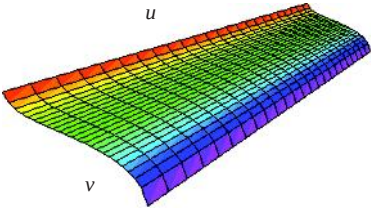

Fig. 15. Transverse profile of the order parameter in an infinitely long strip with fixed-free boundary conditions.

elliptic integral of the first kind,[102,103] and the modulus k is solution of $K(k)/K(\sqrt{1-k^2}) = \frac{1}{2}$.

In the semi-infinite geometry, the two-point correlator is fixed up to an unknown scaling function (apart from some asymptotic limits implied by scaling). Fixing one point z_1 close to the free surface ($z_1 = i$) of the half-infinite plane, and leaving the second point exploring the rest of the geometry, $z_2 = z$, the following behaviour is expected:

$$\langle \phi(z_1)\phi(z) \rangle_{\frac{1}{2}\infty} \sim y^{-x_\sigma} \psi(\omega), \tag{45}$$

where the dependence on $\omega = \frac{y_1 y}{|z_1 - z|^2}$ of the universal scaling function ψ is constrained by the special conformal transformation and its asymptotic behaviour, $\psi(\omega) \sim \omega^{x_\phi^1}$, in the limit $y \gg 1$, is implied by scaling.

Using the mapping (44), the local rescaling factor in Eq. (39) is obtained,

$$w'(z) = \frac{N}{2\mathrm{K}} [(1-z^2)(1-k^2 z^2)]^{-1/2},$$

and inside the square the two-point correlation function becomes (see Ref. 44)

$$\langle \phi(w_1)\phi(w) \rangle_{\mathrm{sq.}} \sim \underbrace{\left(\Im[z] \cdot \left(|1-z^2| \cdot |1-k^2 z^2| \right)^{-1/2} \right)^{-x_\phi}}_{\kappa(w)} \psi(\omega), \tag{46}$$

with $z(w)$ given by Eq. (44). This expression is correct up to a constant amplitude determined by $\kappa(w_1)$ which is kept fixed, but the function $\psi(\omega)$ is still varying with the location of the second point, w.

In order to eliminate the role of the unknown scaling function, it is more convenient to work with a density profile in the presence of ordering surface fields (Fig. 16). This is a one-point correlator of which the functional shape in the half-infinite geometry is determined by scaling apart from some

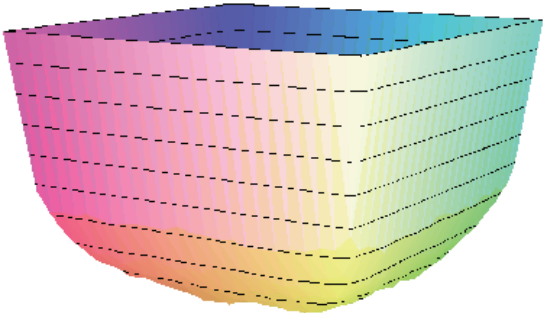

Fig. 16. Profile of the order parameter in a square with fixed boundary conditions.

amplitude:

$$\langle \sigma(z) \rangle_{\frac{1}{2}\infty} = \text{const} \times y^{-x_\sigma}, \tag{47}$$

and it maps onto

$$\langle \sigma(w) \rangle_{\text{sq.}} = \text{const} \times [\kappa(w)]^{-x_\sigma}, \tag{48}$$

where the function $\kappa(w)$ again comes from the mapping. The case of the mapping of the infinite complex plane inside a square with periodic boundary conditions was for example used in Ref. 71.

Other mappings can be convenient. Our choice here was motivated by the fact that Monte Carlo simulations are usually performed on samples of square shapes. On the other hand, the strip (with free or fixed boundary conditions) is the natural geometry generated in transfer matrix calculations.

4.6. *Impact of Rare Events and Non-Self-Averaging*

As we mentioned, the physical properties have to be averaged over many samples produced with a given probability distribution. One can typically encounter two opposite situations, depending on the quantities of interest. The average order parameter for example is defined as a sum of quantities affected by randomness,

$$\overline{\langle \sigma \rangle} = \frac{1}{N^2} \overline{\sum_i \langle \sigma_i \rangle},$$

while the correlation function

$$\langle \delta_{\sigma_j, \sigma_{j+u}} \rangle \simeq \langle \Lambda_0 | \, \mathbf{g}_j \left(\prod_{k=j}^{j+u-1} \mathbf{T}'_k \right) \mathbf{d}_{j+u} \, | \Lambda_0 \rangle,$$

essentially depends on a product of non-commuting matrices of which the elements are determined by the disorder distribution. These two types of quantities definitely exhibit different properties as functions of the number of samples used to scan the probability distribution. When computing mean values, it is clear that the accuracy of the results for a given number of disorder realizations does not have the same behaviour in the case of sums or of products of random variables. Consider as an example the sum and the product of random variables λ_i taken from a binary distribution,

$$\Sigma_\lambda = \sum_{i=1}^{n} \lambda_i, \qquad \Pi_\lambda = \prod_{i=1}^{n} \lambda_i,$$

and compute the moments (rescaled by a power $1/p$) $[\overline{(\Sigma_\lambda)^p}]^{1/p}$ and $[\overline{(\Pi_\lambda)^p}]^{1/p}$ averaged over N realizations of the λ_i (here we choose for this example $n = 50$, so there are some 10^{15} configurations). Numerical results are given in Table 4 for selected parameters.

It is particularly clear that the values obtained from the sum Σ converge rapidly (the variations between results obtained at different numbers of realizations correspond to a statistical noise). This is due to the fact that Σ is normally distributed, while in the case of the product Π, we note a continuous increase of the numerical estimate of a given moment as the number of samples increases and this effect is especially pronounced for the high moment order p. This is due to the fact that the distribution of the Π is log-normal and thus there exist some events which have a dominant role in the average, but which are so rare that they are not scanned by a poor statistics which would essentially explore the region of typical values. In order to be more precise in the distinction between typical value and average value, we rewrite $\ln \Pi$ as a sum of random variables,

Table 4. Comparison between the moments of a sum and of a product of random variables distributed according to a bimodal probability distribution, as a function of the number of realizations.

	Σ_λ				Π_λ			
N	$p=1$	$p=5$	$p=20$	$p=50$	$p=1$	$p=5$	$p=20$	$p=50$
10^1	0.990	1.060	1.228	1.305	1.054	1.529	2.042	2.188
10^3	1.014	1.049	1.156	1.298	1.060	1.292	2.143	2.630
10^5	1.010	1.047	1.161	1.327	1.054	1.303	2.480	3.467
10^7	1.010	1.047	1.160	1.322	1.055	1.301	2.511	3.857

$\ln \Pi_\lambda = \sum_i \ln \lambda_i$, which, according to the central limit theorem, has a Gaussian distribution in the limit of a large number of draws. The typical value corresponds to the maximum of the probability distribution, $\Pi_{\rm typ} = e^{\overline{\ln \Pi}}$ where the Gaussian is centered, and clearly differs from the average value $\overline{\Pi} = \overline{e^{\ln \Pi}}$.

The same situation occurs when computing the spin–spin correlation function $\overline{\langle \sigma(0)\sigma(u)\rangle}_{\rm st} = \overline{G_\sigma(u)}$. Since the probability distribution is almost log-normal (see Fig. 17), the logarithm of $G_\sigma(u)$ is self-averaging and the average $\overline{\ln G_\sigma(u)}$ as well as higher order moments are well behaved. A cumulant expansion is thus convenient for reconstructing the average $\overline{G_\sigma(u)}$ through

$$\overline{G_\sigma(u)} = \exp\left(\overline{\ln G_\sigma(u)} + \tfrac{1}{2}(\overline{\ln^2 G_\sigma(u)} - \overline{\ln G_\sigma(u)}^2) + \cdots\right). \tag{49}$$

This is a test (see Fig. 18) which proves that the probability distribution is sufficiently well scanned with the large numbers of realizations used in this run.

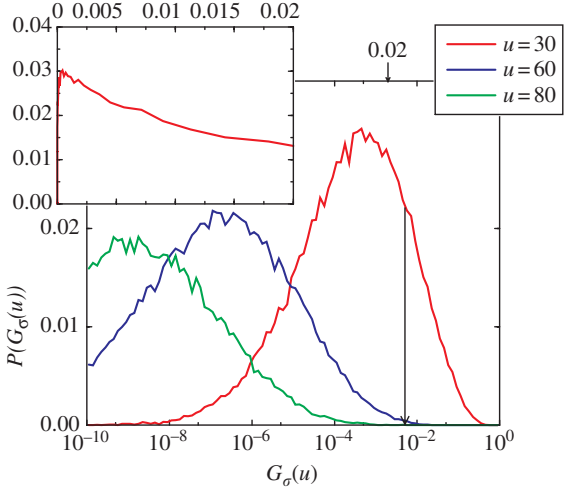

Fig. 17. Probability distribution of the spin–spin correlation function (8-state Potts model with bimodal disorder). The inset shows $\mathcal{P}(G_\sigma(u))$ (with a very long tail on the right), while it is shown on a logarithmic scale in the main frame, where one can notice the shape which is close to a log-normal distribution. The arrow at $u = 30$ marks the average value.

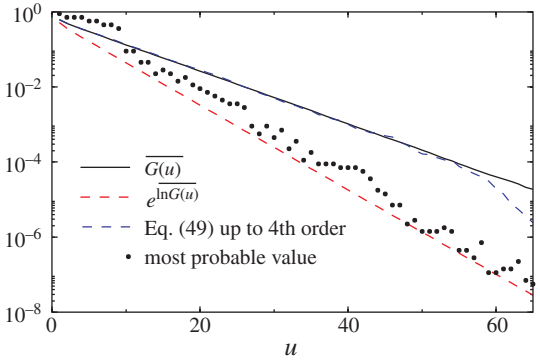

Fig. 18. Reconstruction of the correlation function from the moments of its logarithm.

5. Numerical Results and Comparison with Perturbative Expansions in 2D

5.1. *Regime $q > 4$*

5.1.1. *Randomness Induces a Second-Order Regime*

Although there is no perturbation result for $q > 4$, we shall start with the regime of first-order transition of the pure model. A first step was to prove that even for large numbers of states per spin, the transition was rounded to become continuous. That was done by different authors.[39,41] Chen *et al.* studied the free energy barrier $\Delta F(L)$, defined from the energy histogram $\mathcal{P}(E)$ in Monte Carlo simulations according to $e^{-\beta\Delta F(L)} = P_{\max}/P_{\text{well}}$, with $P_{\max}$ given by the maximum of $\mathcal{P}(E)$ and P_{well} corresponding to the value at the bottom of the well separating the two coexisting phases. They showed that the energy barrier $\Delta F(L) = -2\sigma_{\text{o.d.}} L^{d-1}$ vanishes in the thermodynamic limit (Fig. 19) where $\sigma_{\text{o.d.}}$ is the order–disorder interface tension between the two possibly coexisting phases.

The dynamics of the Monte Carlo simulations leads to compatible conclusions. The energy autocorrelation time τ_E is indeed exponentially large (with the system size) when a non vanishing order–disorder interface tension $\sigma_{\text{o.d.}}$ exists,

$$\tau_E \sim L^{d/2} e^{2\sigma_{\text{o.d.}} L^{d-1}},$$

while it is only increasing as a power law at second-order transitions,

$$\tau_E \sim L^z,$$

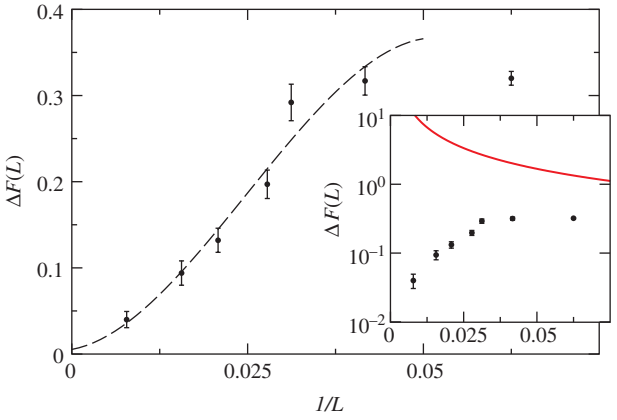

Fig. 19. Evolution of the free energy barrier with the size of the system for the 8-state Potts model with binary disorder (at small disorder strength). The dotted line is a guide for the eyes. In the inset, the line shows the case of the pure system [taken from Chen, Ferrenberg and Landau (Ref. 39)].

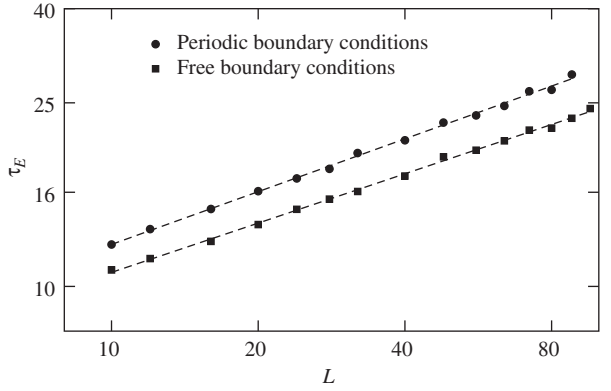

Fig. 20. Power-law behaviour of the energy autocorrelation time, averaged over the disorder realizations, in the 8-state Potts model with binary disorder.

with a dynamical exponent z which strongly depends on the algorithm used. This latter situation is indeed observed[63] in the disordered 8-state Potts model (Fig. 20).

Cardy and Jacobsen on the other hand used transfer matrix calculations,[41] measuring the free energy density $\bar{f}_L$ for which corrections to scaling behave at first-order transitions such as $\bar{f}_L \sim f_\infty + O(L^{-d} e^{-L/\xi})$. Plotting then $\lambda(L) = \ln(\bar{f}_L - f_\infty) + d \ln L$ versus the strip width L should

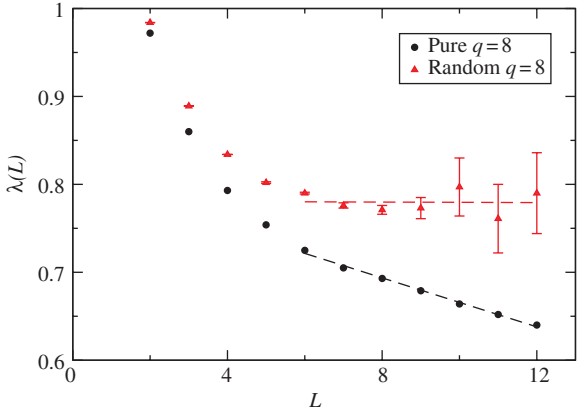

Fig. 21. Evolution of the corrections to scaling to the free energy in a strip geometry (taken from Cardy and Jacobsen[41]).

give asymptotically a straight line with a slope given by the inverse correlation length $1/\xi$. In the presence of randomness, the curve corresponding to the 8-state Potts model indicates a diverging correlation length as expected at a second-order phase transition (Fig. 21).

5.1.2. *Comparison between Finite-Size Scaling and Conformal Mappings*

Conformal mappings provide quite efficient techniques for the determination of critical exponents. The validity of such an approach is nevertheless restricted to systems where scale invariance, translation invariance and rotation invariance do hold. This requirement is not obviously fulfilled in random systems, since disorder breaks the symmetries. Hopefully, one may expect that after averaging over many disorder realizations, one is led to some effective system for which these symmetries are restored. This assumption can be checked from numerical simulations. Studying the critical behaviour using an independent technique, namely finite-size-scaling which can safely be supposed to give the correct results, we then compare the outcome to the exponents deduced from various mappings which are allowed when conformal symmetries are assumed to be restored. The comparison was performed carefully in the case of the 8-state Potts model with binary disorder, and the technique was then applied in the regime $q > 4$, and even to asymptotically large q.[45] The FSS results, which are considered here as the reference results, are shown in Fig. 11. In strip geometries, the

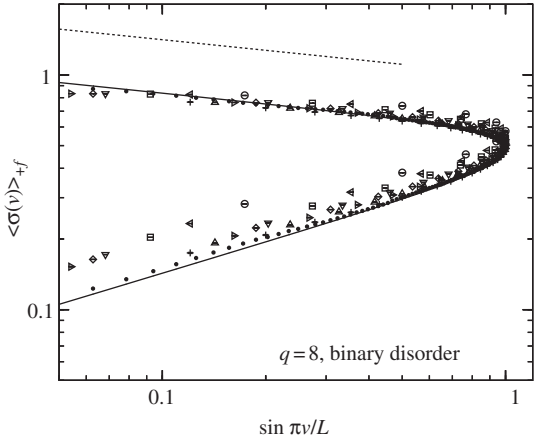

Fig. 22. Fixed-free BC order parameter critical profile for the self-dual binary disordered 8-state Potts model. The behaviour close to the fixed surface gives access to the bulk scaling dimension (the corresponding curve is shown in dotted line and the conformal expression is shown in full line while the symbols correspond to strips of various widths).

correlation functions in the long direction and the order parameter profile in the transverse direction (Fig. 22) lead to compatible results.

In the square geometry, the fit of the correlation function must be done along some curves inside the square where the scaling variable ω remains constant. This implies that the function $\psi(\omega)$ also remains constant and a simple power-law fit is then needed,

$$\overline{\langle\sigma(w_1)\sigma(w)\rangle}_{\rm sq} \sim A_\omega |\kappa(w)|^{-x'_\sigma},$$

where A_ω stands for the amplitude which contains $\psi(\omega)$ (w_1 is fixed and chosen equal to the imaginary unit $w_1 = i$). A difficulty appears due to the discretization of the lattice. Estimation of the correlation function along the continuous curve $\omega = \text{const}$ is obtained using a Taylor expansion from the data taken at four neighbour points on each plaquette. This explains the non monotonic behaviour of the error bars in Fig. 23.

The case of the density profile is more readily achieved, since it involves no unknown scaling function, but a single constant amplitude (it is a one-point correlator). All the points inside the square enter the power-law fit

$$\overline{\langle\sigma(w)\rangle}_{\rm sq} \sim \text{const} \times |\kappa(w)|^{-x'_\sigma}$$

and make the fit more accurate (since there is no need of any expansion around the lattice points). When the number of points (N^2) is large enough,

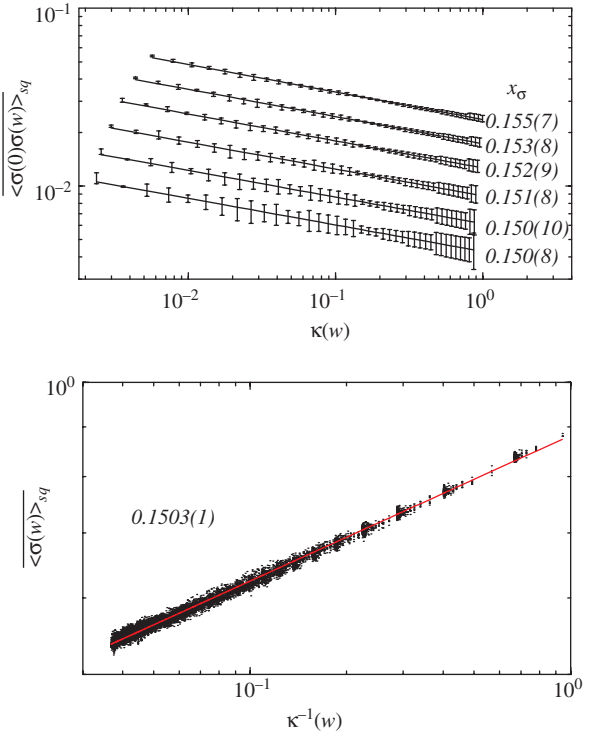

Fig. 23. Fitting the correlation function (top) and the order parameter profile (bottom) in a square geometry. The different curves (top) correspond to different values of the variable ω. This is the case $q = 8$, with a binary distribution, at the optimal disorder strength estimated by the maximum of the central charge in strip geometry.

we can even ignore the uncertainties on each point and simply take as error bar on the resulting exponent the standard deviation of the fit.

The results for the magnetic scaling dimension measured using Finite-Size Scaling techniques, compared to the mappings onto strips or square geometries, are compared in Table 5 in the case of the 8-state Potts model with a self-dual binary probability distribution of coupling strengths. First we note that the transition is second-order, even in the regime $q > 4$, as predicted by the Imry–Wortis agreement. More important for the following is the fact that the agreement between different techniques is quite fair and leads to the conclusion that conformal techniques can be applied here, in spite of the lack of the symmetry properties which should in principle be required. This is due to the fact that we are interested in *average quantities*. The system thus becomes, on average, translationally

Table 5. Comparison between temperature dependence, FSS and short-time dynamics scaling results for the magnetic exponent β'/ν' and the scaling dimension x'_σ at the random fixed point deduced from the logarithmic and the Schwarz–Christoffel mappings for the 8-state Potts model. In the first line, the exponent β' deduced from the temperature dependence is close to x'_σ, since the value of the correlation length exponent is found very close to 1 ($\nu' \simeq 1.01(1)$). We note also that in all these references but Ref. 34, a binary distribution of disorder was used.

x'_σ for the 8-state Potts model with binary disorder			
Technique	Quantity	Scaling dimension	Reference
Standard techniques			
t-dependence	$\overline{M_b(t)}$	0.151(1)	33
FSS	$\overline{M_b(K_c)}$	0.153(1)	28, 29
FSS	$\overline{\langle\sigma(0)\sigma(L/2)\rangle}$	0.159(3)	34
Short-time dynamics	$\overline{M_b(\tau)}$	0.151(3)	53
Conformal mappings			
Periodic strip	$\overline{\langle\sigma(0)\sigma(u)\rangle}_{\rm st}$	0.1505(3)	30, 44, 63
Free BC square	$\overline{\langle\sigma(0)\sigma(w)\rangle}_{\rm sq}$	0.152(3)	30, 44, 63
Fixed-free strip	$\overline{\langle\sigma(v)\rangle}_{\rm st}$	0.150(1)	33, 63
Fixed BC square	$\overline{\langle\sigma(w)\rangle}_{\rm sq}$	0.1503(1)	30, 44, 63

and rotationally invariant, as well as scale invariant at the critical point. This is an important point, because the use of conformal mappings is more accurate than standard FSS methods, and the comparison between different schemes in the $2 \leq q \leq 4$ regime will require great accuracy, as already noted in Table 3.

5.2. *Regime $q \leq 4$*

5.2.1. *Tests of Replica Symmetry*

First of all, the fitting procedure has to be validated. From the exponential decay of the average spin–spin correlation function, the exponent x'_σ is deduced and presented as a function of q for the case of a binary disorder in Fig. 24. These results were first reported by Cardy and Jacobsen in Ref. 41. The agreement with the third-order expansion in Eq. (20) is extremely good especially in the region where the expansion is supposed to be valid when q is not too far from the Ising model value $q = 2$. The quality of the data confirms the reliability of the averaging procedure (Table 6). Even close to the marginally irrelevant case of the Ising model where logarithmic corrections are known to be present for some quantities, we note that the numerical

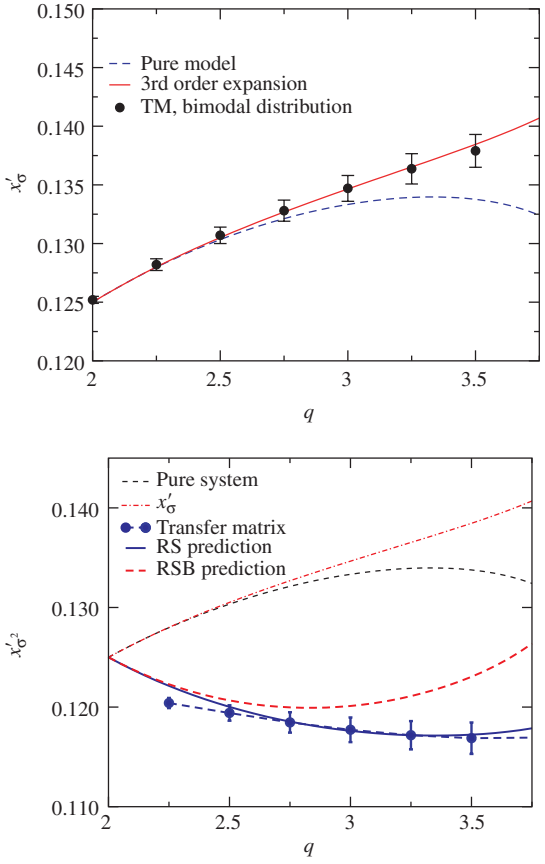

Fig. 24. Top: Scaling dimension of the order parameter (binary disorder) compared to the third-order expansion of Dotsenko and co-workers.[20] The scaling dimension corresponding to the pure model is shown for comparison. Bottom: Exponent of the second moment of the spin–spin correlation function as a function of the number of states of the disordered Potts model (binary disorder). The comparison is done with Replica Symmetry and Replica Symmetry Breaking scenarios.[25] The agreement with the RS result is quite good around $q = 3$. When q is close to 2, the discrepancy can be attributed to the weak relevance of disorder. We indeed used a simple exponential fit as can be expected at a stable disordered FP. But at $q = 2$, one knows from Ludwig's results[17] that logarithmic corrections must be added. These corrections can also influence the vicinity of $q = 2$ in a numerical approach.

data are quite satisfactorily in agreement with the perturbative results. The agreement is made better by the absence of logarithmic corrections for the *average* correlation function at $q = 2$, and we will see that this observation is no longer true in the following study of other moments.

Table 6. Comparison of the numerical results for the magnetic scaling dimension (bimodal probability distribution) x'_σ (from transfer matrix computations in Ref. 46) with the third-order expansion [Eq. (20)] of Dotsenko and co-workers.[20] The error bars systematically contain the analytical value.

q	x'_σ	
	Expansion (20)	TM result (Ref. 46)
2	0.12500	0.1252(3)
2.25	0.12800	0.1282(5)
2.5	0.13051	0.1307(7)
2.75	0.13269	0.1328(9)
3	0.13465	0.1347(11)
3.25	0.13653	0.1364(13)
3.5	0.13845	0.1379(14)

The question of a possible breaking of replica symmetry in disordered systems is very controversial and far from being settled, especially in spin glasses (see e.g., Refs. 104–108). In the context of disordered Potts ferromagnets, the question was first addressed by Dotsenko *et al.*[25] In order to test the difference between Replica Symmetry and Replica Symmetry Breaking schemes, Dotsenko *et al.* performed a second-order expansion of the exponent of the second moment of the spin–spin correlation function decay in both cases [Eqs. (23) and (24)]. MC simulations were first performed at $q = 3$ but were not completely conclusive, although in favour of Replica Symmetry: the perturbation expansion leads to $x'_{\sigma^2}(3) = 0.1176$ and $x''_{\sigma^2}(3) = 0.1201$ according to Eqs. (23) and (24), while previous numerical results lead to 0.113(1),[25] 0.1140(5),[62] 0.116(1)[33] and 0.119(2).[34]

Conclusive results for different values of q were then obtained using transfer matrices. Close to $q = 2$, the proximity of the marginally irrelevant Ising FP will surely alter the data, as a reminiscent effect of the logarithmic corrections present exactly at $q = 2$ for the second moment.[17,109] Too large values of q on the other hand are not very helpful for the purpose of checking perturbation expansions which break down when one explores higher values of the expansion parameter. One thus has to find a balance between these two extreme situations and the comparison between numerical data and perturbation results should be conclusive around or slightly below $q = 3$. The TM technique thus appears to be well adapted, since it is capable to deal with non integer values of q. The comparison is shown in Fig. 24 for the bimodal probability distribution and the results are also given in Table 7. In the convenient domain for the test, around $q = 3$, the results

Table 7. Decay exponent of the second moment of the spin–spin correlation function as obtained numerically in Ref. 46, compared to Replica Symmetry and Replica Symmetry Breaking expressions of Eqs. (23) and (24).[25] The results written in bold face correspond to the range of values of q where the agreement is particularly satisfactory. The second part of the table presents Jacobsen's results[47] for the exponent of the average energy correlation function.

q	Perturbative results		TM result
	x'_{σ^2}	x''_{σ^2}	Ref. 46
2.25	0.12213	0.12229	0.1204(5)
2.5	0.12002	0.12067	0.1194(8)
2.75	**0.11854**	0.11997	**0.1185(10)**
3.	**0.11761**	0.12011	**0.1177(12)**
3.25	**0.11718**	0.12110	**0.1172(14)**
3.5	**0.11723**	0.12304	**0.1169(16)**
	x'_{ε}	x''_{ε}	Ref. 47
2.5	**1.006**	1.000	**1.00(1)**
2.75	**1.013**	1.000	**1.01(1)**
3.	**1.023**	1.000	**1.02(1)**

are written in bold face. The agreement with Replica Symmetry is quite convincing. The results for the exponent associated to the average energy density correlations[47] confirm this conclusion (Table 8).

5.2.2. *Multiscaling*

The multiscaling behaviour of the spin–spin correlation functions is noticeable in the p-dependent set of exponents of the reduced moments

$$\overline{\langle\sigma(0)\sigma(R)\rangle^p}^{1/p}.$$

In Ref. 46, an exhaustive computation of 50 different moments in the range $0 \leq p \leq 5$ was performed in the strip geometry, and the associated scaling dimensions were derived from a semi-log fit $\ln \overline{\langle\sigma(0)\sigma(u)\rangle^p}$ vs $\ln u$, followed by an extrapolation to $L \to \infty$. The numerical results were compared to the first-order expansion of Ludwig and to the second-order expansion in the RS scheme in Eq. (26). The second-order result is clearly very good up to values of p close to 3 and then breaks down as already noticed by Lewis.[62]

An alternative presentation of the results (used e.g. by Ludwig[19]) is given by the scaling dimension of the moment of the correlation function itself, $\overline{\langle\sigma(0)\sigma(R)\rangle^p}$ $\left(\text{not the reduced function } \overline{\langle\sigma(0)\sigma(R)\rangle^p}^{1/p}\right)$. The scaling

dimension is thus simply $px'_{\sigma^p}(q)$, hereafter denoted by $X'_{\sigma^p}(q)$. An example, with $q = 3$, is shown in Fig. 25 depicting the results obtained with the bimodal and the continuous self-dual probability distributions at the optimal disorder amplitude as well as the dilution case at optimal dilution. Once again, we find a fair agreement between the numerical data and the perturbative result which confirms universality, i.e. the exponent associated to a given moment of the correlation function does not depend on the detailed probability distribution of the coupling strengths (provided that it remains uncorrelated).

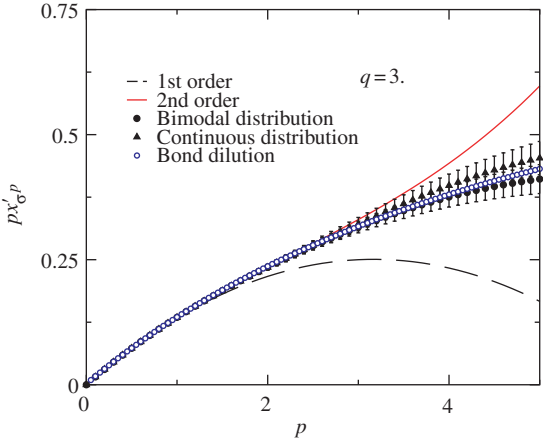

Fig. 25. Comparison of the multi-fractal exponents (moment of the correlation function $\overline{\langle\sigma(0)\sigma(u)\rangle^p}$) with the second-order expansion of Lewis in the RS scheme[26] for both the bimodal and the continuous probability distributions.

Table 8. Decay exponent of the average and typical energy–energy correlation functions: comparison between perturbative expansion from Ref. 27 and transfer matrix computation (from Jacobsen[47]).

	Average		Typical	
q	$x'_{\varepsilon 1}$	TM	$x'_{\varepsilon 0}$	TM
2.5	1.006	1.00(1)	1.023	1.02(1)
2.75	1.013	1.01(1)	1.051	1.04(2)
3	1.023	1.02(1)	1.090	1.06(3)

5.2.3. *Probability Distribution of Correlation Functions*

In Ref. 19, Ludwig presented a remarkable discussion of the spin–spin correlation function probability distribution. The relevant information on the large-distance behaviour is encoded in the multiscaling function $H(\alpha)$,[r] which is the Legendre transform of the set of independent scaling indices $X'_{\sigma^p}(q)$. Setting $dX'_{\sigma^p}(q) = \alpha dp$, this function is simply obtained by

$$H(\alpha) = X'_{\sigma^p}(q) - \alpha p.$$

The geometrical interpretation of this Legendre transform follows from the relation $\partial H/\partial\alpha = -p$ where α is defined by $\partial X'_{\sigma^p}(q)/\partial p = \alpha$. The scaling dimension $x'_{\sigma^p}(q)$ is obtained from the plot of $H(\alpha)$ by the intercept of the tangent of slope $-p$ with the abscissa. An example of a multiscaling function $H(\alpha)$ deduced from the numerical data with the bimodal probability distribution is shown in Fig. 26.

In this section, we follow Ludwig's arguments and report a numerical study of the correlation function probability distribution in the cylinder geometry.

According to the results of the previous section, the moments of the spin–spin correlation function along the strip behave asymptotically as follows:

$$\overline{G^p(u)} \equiv \overline{\langle\sigma(0)\sigma(u)\rangle^p} \sim B_p \exp\left(-\frac{2\pi u}{L} X'_{\sigma^p}\right) \tag{50}$$

and are defined in terms of the probability distribution $\mathcal{P}[G(u)]$:

$$\overline{G^p(u)} = \int_0^1 dG(u)\ \mathcal{P}[G(u)]G^p(u). \tag{51}$$

Following Ludwig, we introduce the variable $Y(u) = -\ln G(u)$ and write $G^p(u) = \mathrm{e}^{-pY(u)}$. Using the identity $\mathcal{P}[G(u)]dG = \mathcal{P}[Y(u)]dY$ and Eqs. (50) and (51), we obtain

$$\int_0^\infty dY(u)\ \mathcal{P}[Y(u)]\mathrm{e}^{-pY(u)} \sim B_p\ \exp\left(-\frac{2\pi u}{L} X'_{\sigma^p}\right)$$

which leads to the expression of the probability distribution by inverting the Laplace transform ($\delta > 0$):

$$\mathcal{P}[Y(u)] = \frac{1}{2i\pi} \lim_{\delta\to 0} \int_{\delta-i\infty}^{\delta+i\infty} dp\ B_p \exp\left[-\frac{2\pi u}{L}\left(X'_{\sigma^p} - \frac{Y(u)}{2\pi u/L} p\right)\right].$$

[r] In the context of multifractality, this function is usually denoted as $-f(\alpha)$.

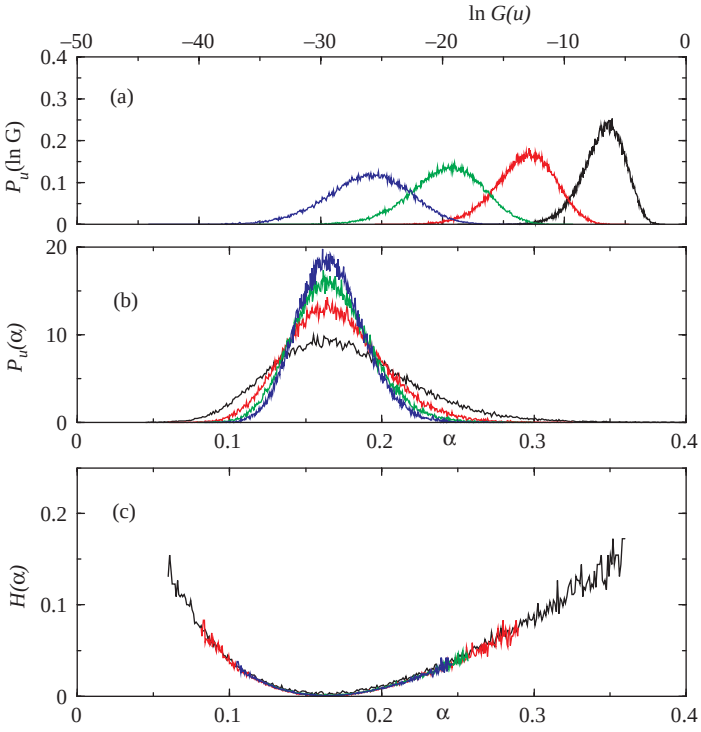

Fig. 26. Fitting the probability distribution of the spin–spin correlation function to get a collapse onto a universal multiscaling function (four different values of u are shown for a given strip width).

The amplitude B_p is assumed to be smoothly dependent on p (this can be checked numerically), and its dependence can be ignored with respect to the exponential, since it only introduces a correction when $2\pi u/L \to \infty$. Let us define the function $h(p) = X'_{\sigma^p} - \frac{Y(u)}{2\pi u/L}p$. In the large-distance limit $2\pi u/L \to \infty$, the integral can be evaluated by the saddle-point approximation at the minimum p_0 of $h(p)$:

$$\left(\frac{\partial}{\partial p}X'_{\sigma^p}\right)_{p_0} = \frac{Y(u)}{2\pi u/L}.$$

Instead of $Y(u)$, we define the scaled variable $\alpha = \frac{Y(u)}{2\pi u/L}$, and the saddle point value at p_0 only depends on this variable $h(p_0) = H(\alpha)$. We thus obtain the probability distribution

$$\mathcal{P}[Y(u)] \sim \exp\left[-\frac{2\pi u}{L}H\left(\frac{Y(u)}{2\pi u/L}\right)\right], \tag{52}$$

or, using $\mathcal{P}[Y(u)]\,dY = \mathcal{P}(\alpha)d\alpha$,

$$\mathcal{P}(\alpha) \sim \frac{2\pi u}{L}\ \exp\left[-\frac{2\pi u}{L}H(\alpha)\right]. \tag{53}$$

The multiscaling function contains the essential information on the probability distribution. A correction to the leading behaviour given by the saddle-point approximation is needed here to improve the data collapse onto a single multiscaling function. If we expand the function $h(p)$ close to p_0, $h(p) \simeq H(\alpha) + \frac{1}{2}h''(p_0)(p-p_0)^2$, with $h''(p_0) > 0$ we obtain, instead of Eq. (52), the following result for the probability distribution $\mathcal{P}[Y(u)]$:[110–112]

$$\mathcal{P}[Y(u)] \sim \left(\frac{2\pi u}{L}\right)^{-1/2} \exp\left[-\frac{2\pi u}{L}H\left(\frac{Y(u)}{2\pi u/L}\right)\right] \tag{54}$$

and a correction appears in $\mathcal{P}(\alpha)$,

$$\mathcal{P}(\alpha) \sim \left(\frac{2\pi u}{L}\right)^{1/2} \exp\left[-\frac{2\pi u}{L}H(\alpha)\right], \tag{55}$$

which enables one to extract $H(\alpha)$ at fixed α by fitting the probability distribution to the expression

$$\ln \mathcal{P}(\alpha) - \frac{1}{2}\ln\frac{2\pi u}{L} = \text{const} - \frac{2\pi u}{L}H(\alpha). \tag{56}$$

This is shown in Fig. 26 where the probability distribution of the spin–spin correlation function was obtained after collecting the results over 96 000 disorder realizations in 50 classes.[46] All the data collapse onto a single multiscaling function $H(\alpha)$ for different distances u and this is even the case, while still retaining good accuracy for different strip widths or different probability distributions.[46,48]

6. Conclusion and Summary of the Main Results

The two-dimensional Potts model is the ideal framework to test the influence of quenched randomness on phase transitions and critical behaviour. It exhibits a second-order phase transition completely characterised by conformal invariance when the number of states per spin is lower than or equal to 4, and a first-order transition above 4. The transition line is known exactly, and it is easy to construct, in the random case, probability distributions of coupling strengths which preserve the self-duality relation.

With respect to these advantages, many results concerning the effect of a weak disorder were obtained during the last decade using perturbation expansions around the pure fixed point. Different solutions were considered, first replica-symmetric solutions where the symmetry between all the replicas is supposed to be preserved in the renormalization equations, then the case of a spontaneous breaking of the replica symmetry was also studied perturbatively.

Numerical studies have also been performed from different viewpoints. First of all, Monte Carlo simulations coupled to finite-size scaling analysis; subsequently transfer matrices and sophisticated graph and loop algorithms coupled to extensive use of conformal mappings in order to extract the values of the critical exponents with fairly good accuracy. All the results were in fair agreement with the perturbative expansions close to the Ising model limit and concluded in favour of replica symmetric scenarios. The multiscaling properties of the order parameter and energy density were also analysed, and a characterisation of the probability distributions of the correlation functions was made in terms of universal multiscaling functions. The regime $q > 4$ where the pure model exhibits a first-order transition has also been extensively studied, but has not displayed any particular features compared to the regime $q \leq 4$ in the presence of quenched randomness.

The most important question which remains open up to now is the identification of the conformal field theories which could describe the random fixed point. This is a delicate program, since in the replica limit of coupled models, the theory is not unitary (with a central charge which evolves continuously with the value of q). We may hope for some progress in this direction for the near future, which would undoubtedly lead to a considerable contribution to the understanding of two-dimensional disordered systems.

Acknowledgements

Part of the material discussed here was presented at the Helsinki SPHINX ESF Conference 2002 on *Disordered systems at low temperatures and their topological properties*, and at the *Ising lectures* 2002 at Lviv. BB gratefully acknowledges the organisers of the Helsinki workshop, M. Alava and H. Rieger and of the Lviv lectures, Yu. Holovatch, I. Mryglod, and K. Tabunshchyk, for the opportunity given to present this review. This is also a pleasure to thank here the Dnipro program for French-Ukrainian cooperation, since it is the context where a collaboration with Yu. Holovatch was initiated.

References

1. A.B. Harris, *J. Phys. C* **7**, 1671 (1974).
2. Y. Imry and M. Wortis, *Phys. Rev.* **B19**, 3580 (1979).
3. M. Aizenman and J. Wehr, *Phys. Rev. Lett.* **62**, 2503 (1989).
4. K. Hui and A.N. Berker, *Phys. Rev. Lett.* **62**, 2507 (1989).
5. S.K. Ma, *Modern theory of critical phenomena*, Benjamin Inc., Reading 1976.
6. J.L. Cardy, *Scaling and renormalization in statistical physics* (Cambridge University Press, Cambridge, 1996).
7. Vik. Dotsenko, *Introduction to the replica theory of disordered statistical systems* (Cambridge University Press, Cambridge, 2001).
8. R.B. Stinchcombe, In *Phase Transitions and Critical Phenomena* vol. **7**, C. Domb and J.L. Lebowitz eds. (Academic Press, London, 1983), p. 152.
9. A. Aharony, *Phys. Rev.* **B18**, 3318 (1978).
10. Y. Imry and S.K. Ma, *Phys. Rev. Lett.* **35**, 1399 (1975).
11. G. Grinstein and S.K. Ma, *Phys. Rev. Lett.* **49**, 684 (1982).
12. J. Bricmont and A. Kupiainen, *Phys. Rev. Lett.* **59**, 1829 (1987).
13. Y.S. Shapir and A. Aharony, *J. Phys. C.* **14**, L905 (1981).
14. A. Aharony, *Phys. Rev.* **B12**, 1038 (1975).
15. M. Dudka, R. Folk and Yu. Holovatch, *Cond. Matter Phys.* **4**, 77 (2001).
16. F.Y. Wu, *Rev. Mod. Phys.* **54**, 235 (1982).
17. A.W.W. Ludwig, *Nucl. Phys.* **B285 [FS19]**, 97 (1987).
18. A.W.W. Ludwig and J.L. Cardy, *Nucl. Phys.* **B330 [FS19]**, 687 (1987).
19. A.W.W. Ludwig, *Nucl. Phys.* **B330**, 639 (1990).
20. Vl. Dotsenko, M. Picco and P. Pujol, *Nucl. Phys.* **B455 [FS]**, 701 (1995), `hep-th/9501017`.
21. Vl. Dotsenko, M. Picco and P. Pujol, *Phys. Lett.* **347B**, 113 (1995), `hep-th/9405003`.
22. Vik. Dotsenko, Vl. Dotsenko, M. Picco and P. Pujol, *Europhys. Lett.* **32**, 425 (1995), `hep-th/9502134`.
23. Vl. Dotsenko, M. Picco and P. Pujol, *Nucl. Phys. B., Proceedings-Supplements* **45A**, 145 (1996), `cond-mat/9509149`.
24. G. Jug and B.N. Shalaev, *Phys. Rev.* **B54**, 3442 (1996).
25. Vik. Dotsenko, Vl. Dotsenko and M. Picco, *Nucl. Phys.* **B250**, 633 (1998), `hep-th/9709136`.
26. M.A. Lewis, *Europhys. Lett.* **43**, 189 (1998), Erratum, *Europhys. Lett.* **47**, 129 (1999), `cond-mat/9710312`.
27. M. Jeng and A.W.W. Ludwig, *Nucl. Phys.* **B594**, 685 (2001), `cond-mat/9910181`.
28. M. Picco, e-print `cond-mat/9802092`.
29. C. Chatelain and B. Berche, *Phys. Rev. Lett.* **80**, 1670 (1998), `cond-mat/9801028`.
30. C. Chatelain and B. Berche, *Phys. Rev.* **E58**, R6899 (1998), `cond-mat/9810270`.
31. F. Yaąsar, Y. Gündüç and T. Çelik, *Phys. Rev.* **E58**, 4210 (1998).

32. B. Berche and C. Chatelain, *Comp. Phys. Comm.* **121–122**, 191 (1999).
33. G. Palágyi, C. Chatelain, B. Berche and F. Iglói, *Eur. Phys. J.* **B13**, 357 (2000), `cond-mat/9906067`.
34. T. Olson and A.P. Young, *Phys. Rev.* **B60**, 3428 (1999), `cond-mat/9903068`.
35. R. Paredes and J. Valbuena, *Phys. Rev.* **E59**, 6275 (1999).
36. S. Wiseman and E. Domany, *Phys. Rev.* **E51**, 3074 (1995), `cond-mat/9411046`.
37. J.K. Kim, *Phys. Rev.* **B53**, 3388 (1996), `cond-mat/9506117`.
38. S. Chen, A.M. Ferrenberg and D.P. Landau, *Phys. Rev. Lett.* **69**, 1213 (1992).
39. S. Chen, A.M. Ferrenberg and D.P. Landau, *Phys. Rev.* **E52**, 1377 (1995).
40. U. Glaus, *J. Phys. A* **20**, L595 (1987).
41. J.L. Cardy and J.L. Jacobsen, *Phys. Rev. Lett.* **79**, 4063 (1997), `cond-mat/9705038`.
42. M. Picco, *Phys. Rev. Lett.* **79**, 2998 (1997).
43. J.L. Jacobsen and J.L. Cardy, *Nucl. Phys.* **B515**, 701 (1998), `cond-mat/9711279`.
44. C. Chatelain and B. Berche, *Phys. Rev.* **E60**, 3853 (1999), `cond-mat/9902212`.
45. J.L. Jacobsen and M. Picco, *Phys. Rev.* **E61**, R13 (2000), `cond-mat/9910071`.
46. C. Chatelain and B. Berche, *Nucl. Phys.* **B572**, 626 (2000), `cond-mat/9911221`.
47. J.L.L. Jacobsen, *Phys. Rev.* **E61**, R6060 (2000), `cond-mat/9912304`.
48. C. Chatelain, B. Berche and L.N. Shchur, *J. Phys. A* **34**, 9593 (2001), `cond-mat/0108014`.
49. A. Roder, J. Adler, and W. Janke, *Phys. Rev. Lett.* **80**, 4697 (1998).
50. A. Roder, J. Adler, and W. Janke, *Physica* **265A**, 28 (1999).
51. M. Hellmund and W. Janke, *Nucl. Phys. B (Proc. Suppl.)* **106**, 923 (2002).
52. W. Janke, private communication.
53. H.P. Ying and K. Harada, *Phys. Rev.* **E62**, 174 (2000), `cond-mat/0001284`.
54. Z.Q. Pan, H.P. Ying and D.W. Gu, `cond-mat/0103130`.
55. H.P. Ying, B.J. Bian, D.R. Ji, H.J. Luo and L. Schuelke, `cond-mat/0103355`.
56. H.P. Ying, Z.Q. Pan, H.J. Luo, S. Marculsecu and L. Schülke, *Nucl. Phys. (Proc. Suppl.)* **106**, 920 (2002).
57. H.P. Ying, H. Ren, H.J. Luo and L. Schülke, *Phys. Lett.* **298A**, 60 (2002).
58. C. Deroulers and A.P. Young, `cond-mat/0202135`.
59. R. Juhasz, H. Rieger and F. Iglói, *Phys. Rev.* **E64**, 056122 (2001), `cond-mat/0106217`.
60. P. Pujol, *Théories conformes et systèmes désordonnés*, Ph.D dissertation, Université Pierre et Marie Curie, Paris VI, 1996, `http://thesesENligne.ccsd.cnrs.fr/`.
61. J.L. Jacobsen, *Frustration and disorder in discrete lattice models*, Ph.D dissertation, Åarhus University 1998, `http://ipnweb.in2p3.fr/~lptms/membres/jacobsen`.

62. M.-A Lewis, *Théorie des champs conformes: Systèmes désordonnés, couplés et modèle d'Ising sur variétés à bords*, Ph.D. dissertation, Université Pierre et Marie Curie, Paris VI, 1999.
63. C. Chatelain, *Influence du désordre sur les propriétés critiques du modèle de Potts*, Ph.D. dissertation, Université Henri Poincaré, Nancy 1, 2000, `http://thesesENligne.ccsd.cnrs.fr/`.
64. Vik.S. Dotsenko and Vl.S. Dotsenko, *Adv. Phys.* **32**, 129 (1983).
65. B.N. Shalaev, *Phys. Rep.* **237**, 129 (1994).
66. W. Selke, L.N. Shchur and A.L. Talapov, In *Annual Reviews of Computational Physics* vol. **1**, D. Stauffer ed. (World Scientific, Singapore, 1994), p. 17.
67. J.S. Wang, W. Selke, Vl.S. Dotsenko and V.B. Andreichenko, *Physica* **164A**, 221 (1990).
68. J.S. Wang, W. Selke, Vl.S. Dotsenko and V.B. Andreichenko, *Europhys. Lett.* **11**, 301 (1990).
69. V.B. Andreichenko, Vl.S. Dotsenko, W. Selke and J.S. Wang, *Nucl. Phys.* **B344**, 531 (1990).
70. A.L. Talapov and L.N. Shchur, *Europhys. Lett.* **27**, 193 (1994).
71. A.L. Talapov and Vl.S. Dotsenko, `cond-mat/9306027`.
72. B. Derrida, *Phys. Rep.* **103**, 29 (1984).
73. A. Aharony and A.B. Harris, *Phys. Rev. Lett.* **77**, 3700 (1996).
74. S. Wiseman and E. Domany, *Phys. Rev. Lett.* **81**, 22 (1998).
75. S. Wiseman and E. Domany, *Phys. Rev.* **E58**, 2938 (1998).
76. Ch. V. Mohan, H. Kronmüller and M. Kelsch, *Phys. Rev.* **B57**, 2701 (1998).
77. L. Schwenger, K. Budde, C. Voges and H. Pfnür, *Phys. Rev. Lett.* **73**, 296 (1994).
78. E. Domany, M. Schick, J.S. Walker and R.B. Griffiths, *Phys. Rev.* **B18**, 2209 (1978).
79. C. Rottman, *Phys. Rev.* **B24**, 14821 (1981).
80. M. Sokolowski and H. Pfnür, *Phys. Rev.* **B49**, 7716 (1994).
81. K. Budde, L. Schwenger, C. Voges, and H. Pfnür, *Phys. Rev.* **B52**, 9275 (1995).
82. C. Voges and H. Pfnür, *Phys. Rev.* **B57**, 3345 (1998).
83. J.L. Cardy, M. Nauenberg and D.J. Scalapino, *Phys. Rev.* **B22**, 2560 (1980).
84. M.E. Fisher, *Phys. Rev.* **176**, 257 (1968).
85. D. Friedan, Z. Qiu and S. Shenker, *Phys. Rev. Lett.* **52**, 1575 (1984).
86. A.Z. Patashinskii and V.L. Prokowskii, *Fluctuation theory of phase transitions* (Pergamon Press, Oxford, 1979).
87. A.M. Polyakov, *Sov. Phys. JETP* **36**, 12 (1973).
88. W. Janke, in *Computational Physics: Selected Methods–Simple Exercises–Serious Applications*, edited by K.H. Hoffmann and M. Schreiber (Springer, Berlin, 1996).
89. G.T. Barkema and M.E.J. Newmann, in *Monte Carlo Methods in Chemical Physics*, *Advances in Chemical Physics* **105,** edited by D. Ferguson, J.I. Siepmann, and D.G. Truhlar (Wiley, New York, 1999).

90. P.W. Kasteleyn and C.M. Fortuin, *J. Phys. Soc. Japan* **26 Suppl.**, 11 (1969).
91. R.H. Swendsen and J.S. Wang, *Phys. Rev. Lett.* **58**, 86 (1987).
92. U. Wolff, *Phys. Rev. Lett.* **62**, 361 (1989).
93. H.W.J. Blöte and M.P. Nightingale, *Physica* **112A**, 405 (1982).
94. V. Dotsenko, J.L. Jacobsen, M.-A. Lewis and M. Picco, *Nucl. Phys.* **B546**, 507 (1999).
95. H. Furstenberg, *Trans. Am. Math. Soc.* **108**, 377 (1963).
96. A.B. Zamolodchikov, *JETP Lett.* **43**, 730 (1986).
97. L. Chayes and K. Shtengel, `cond-mat/981103`.
98. L. Turban, *Phys. Lett.* **75A**, 307 (1980).
99. L. Turban, *J. Phys. C* **13**, L13 (1980).
100. P. Guilmin and L. Turban, *J. Phys. C* **13**, 4077 (1980).
101. B. Berche, *J. Phys. A* **36**, 585 (2003), `cond-mat/0211584`.
102. M. Lavrentiev and B. Chabat, Méthodes de la théorie des fonctions d'une variable complexe, Mir, Moscou 1972, Chap. VII.
103. M. Abramowitz and I.A. Stegun, *Handbook of mathematical functions*, (Dover Publ., New York, 1970).
104. M. Mézard, G. Parisi and M.A. Virasoro, *Spin Glass Theory and beyond*, (World Scientific, Singapore, 1987).
105. E. Marinari, G. Parisi, J. Ruiz-Lorenzo and F. Ritort, *Phys. Rev. Lett.* **76**, 843 (1996).
106. E. Marinari, C. Naitza, F. Zuliani, G. Parisi, M. Picco and F. Ritort, *Phys. Rev. Lett.* **81**, 1698 (1999).
107. H. Bokil, A.J. Bray, B. Drossel and M.A. Moore, *Phys. Rev. Lett.* **82**, 5174 (1999).
108. E. Marinari, C. Naitza, F. Zuliani, G. Parisi, M. Picco and F. Ritort, *Phys. Rev. Lett.* **82**, 5175 (1999).
109. S.L.A. de Queiroz and R.B. Stinchcombe, *Phys. Rev.* **E54**, 190 (1996), `cond-mat/9604053`.
110. N.G. De Bruijn, *Asymptotic methods in analysis* (Dover Publ., New York, 1981).
111. B. Fourcade and A.-M.S. Tremblay, *Phys. Rev.* **A36**, 2352 (1987).
112. A. Aharony and R. Blumenfeld, *Phys. Rev.* **B47**, 5756 (1993).

This page intentionally left blank

CHAPTER 5

SCALING OF MIKTOARM STAR POLYMERS

Christian von Ferber

Theoretical Polymer Physics, Freiburg University,
79104 Freiburg, Germany
E-mail: ferber@physik.uni-freiburg.de

We review results on the scaling properties of star polymers built from chains of different species, so called miktoarm star polymers. The method covered in this review is primarily the field theoretical renormalization group analysis. The results of this approach are compared with computer simulation and, for their extrapolation to two-dimensional situations, with exact results derived from conformal invariance, Coulomb gas methods and most recently from a mapping between flat and fluctuating geometries (quantum gravity). As examples of the application of the theory we present the calculation of interactions of star polymers in solution, i.e. effective pair and triplet forces, as well as the derivation of the multifractal properties of Brownian motion near absorbing polymeric structures.

1. Introduction

This lecture seems at first sight odd as part of a collection concerning spins, electrons, Ising and Potts models which primarily describe physical phenomena observed in metals and alloys. However, the success of the Ising model and related spin models is due to the fact that the critical behaviour of a physical system at a phase transition that can be described in terms of such a model, will be universal in the sense that it does not depend on the values of the specific microscopic parameters. Rather, the classification into universality classes is related to the symmetries of the system. Consequently the applicability of the Ising model is not restricted to a (magnetic) spin system but equally describes a gas of interacting particles in terms of lattice gas theory. For this the spin values are interpreted as flags for the occupation of a given site.

In polymer science the power law and scaling behaviour of observables has long been known and treated by scaling arguments following the ideas of Flory.[1] As an example, the radius of gyration of a polymer chain in a good solution varies with the molecular weight or equivalently with the number N of monomers like

$$R_g \sim aN^{\nu}, \tag{1}$$

with an exponent ν that is independent of the nature of the polymer chain and the solvent. The same behaviour on the other hand is observed for self-avoiding walks on a lattice in computer simulations. Following the theory developed by de Gennes[2] and des Cloizeaux[3] these excluded volume effects may be treated using a classical field theory. The coils formed by polymers in solution have radii R that are small in comparison with the size L of the container but large compared to the atomic scale. The thermodynamic limit of $L \to \infty$ with fixed concentration c_p of chains and fixed chain lengths N is thus well defined. The case of low monomer concentration $c = Nc_p$ is well described by a model of self-avoiding walks. In the critical limit $c \to 0$, $N \to \infty$, this system with repulsive effective interactions displays scale invariant properties which are governed by the renormalization group. A large set of experimental observations can be explained often quantitatively using the calculational tools of the field theory of critical phenomena.[6] The renormalizability and consistency of the theory have been proven by mapping the polymer system to the standard $O(m)$ Landau–Ginzburg model of the ferromagnetic phase transitions in the formal limit of a zero component ($m = 0$) spin field. The above limit can be understood in terms of the perturbation theory as a selection rule for the perturbative contributions and their graphs. This brings us back to the theory of spins that is in one way or another the topic of all contributions to this collection of lectures.

As far as some simplifications result from the zero component limit and many results may be confirmed by experiment, polymers have served as a testing ground for field theory since the early seventies.[4–6] The path integral formulation[7] allows for a direct interpretation of the paths as conformations of random walks (RWs) and self-avoiding walks (SAWs). Closed paths in this theory have a multiplicity of the number of components M of the field. The formal limit $m = 0$ excludes these loops and yields the polymer limit of field theory, that describes self and mutually interacting paths. The field theoretical description of the scaling properties of polymer chains in good solvents has been generalized to the case of multicomponent polymer

solutions[8–11] and linked polymers.[12–16] The theory is also suited to describe polymer networks of different species.[17–22] Considerable interest focusses on the relation of field theory and multifractals[23–29] and the associated multifractal dimension spectra,[30–34] as well as non-intersecting random walks, their 2D conformal theory[35–41] and their rigorous mathematical description.[42,43]

We review a model of multicomponent polymer networks that shows a common core of these topics and allows for a detailed study of the interrelations in terms of a renormalizable field theory. While a multifractal spectrum may be derived from the scaling exponents of two mutually avoiding stars of random walks,[30] a description in terms of power-of-field operators seems to be ruled out by stability considerations.[23] Nevertheless, it has been shown that already a simple product of two power-of-field operators complies with two somewhat contradictory requirements.[17,18] The concept of polymer stars may be generalized by introducing a matrix of interactions between all chains of a star-like arrangement of polymers. This way the same formalism describes homogeneous polymer stars, stars of mutually avoiding walks (MAW), and the situation of two mutually interacting stars. By studying these situations in two dimensions Duplantier[40,44,45] deduced that while scaling dimensions are additive for mutually transparent objects in a flat geometry, they are also additive for mutually avoiding objects in a fluctuating metric. Combining this with a relation between the scaling dimensions in both geometries given by Knizhnik, Polyakov and Zamolodchikov,[46] an exact algebra results for the two-dimensional exponents in all situations discussed above. We compare these and earlier exact results with the 2D-extrapolation of perturbation theory.

The present review originates from a lecture presented during the 2002 Ising Lectures at the Institute for Condensed Matter Physics in Lviv. It encompasses subjects and results previously published in particular in collaborations of the present author with Yu. Holovatch,[17,18,20,47,48] with L. Schäfer, B. Duplantier, and U. Lehr,[49] as well as with A. Jusufi, M. Watzlawek, C. N. Likos, and H. Löwen.[50,51]

1.1. *Star Polymers and Polymer Networks*

Polymers and polymer solutions are among the most intensively studied objects in condensed matter physics.[5] The behaviour of multicomponent solutions containing polymers of different species is especially rich. Systems of chemically linked polymer chains of different species like block

copolymers are of special experimental and technical interest. Linking the polymer chains of different or even contradictory properties, like hydrophilic and hydrophobic chains, one obtains systems with a qualitatively new behaviour. Here, we concentrate on systems of chains in a solvent which, in a given temperature range, differ in their respective steric interaction properties. The theory of multicomponent polymer solutions[8–11,52] is generalized for this purpose to solutions of copolymer networks, i.e. chains of different species linked at their endpoints in the form of stars or networks of any topology (see Figs. 1–3).

The scaling properties of solutions of polymer networks of a single species have been studied extensively (for a review see Ref. 15). Star polymers as the simplest polymer networks may be produced by linking together the endpoints of polymer chains at some core molecule (Fig. 1). In the same way more general networks of a given topology are formed (Fig. 2). Randomly linked polymer networks on the other hand are obtained as a result of

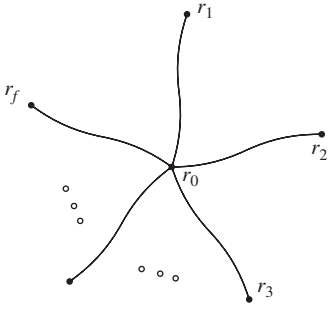

Fig. 1. Graph of a star polymer of f arms linked together at point r_0 with extremities placed at points $r_1 \dots r_f$.

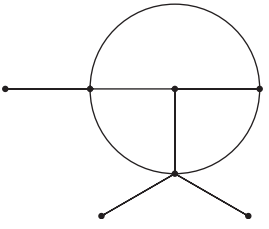

Fig. 2. Graph of a polymer network G. It is characterized by the numbers n_f of f-leg vertices. Here $n_1 = 3$, $n_3 = 2$, $n_4 = 1$, $n_5 = 1$.

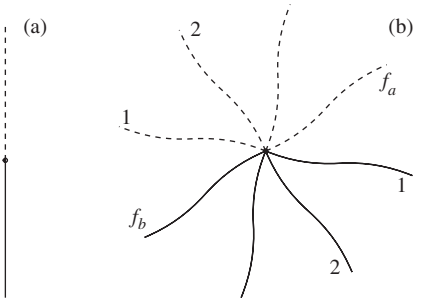

Fig. 3. (*a*) A block copolymer consisting of two polymer chains of different species (shown by solid and dashed curves) linked at their endpoints. (*b*) A miktoarm (co-)polymer star consisting of f_a arms of species a and f_b arms of species b tied together at their endpoints.

a vulcanization process by randomly linking nearby monomers of different chains to each other.

The asymptotic properties of homogeneous systems of linear chain molecules in solution are universal in the limit of long chains. A polymer solution usually exibits a so-called Θ temperature at which the two-point attractive and repulsive interactions between the different monomers compensate each other. Below this temperature the polymers collapse and precipitation occurs. Exactly at the Θ point the polymer chains may be described by random walks (up to higher-order corrections): the mean square distance between the chain endpoints $\langle R^2 \rangle$ scales with the number of monomers N like $\langle R^2 \rangle \sim N$. Above the Θ temperature one finds the "good solvent" regime where the effective interaction between the monomers is repulsive resulting in a swelling of the polymer coil which is universal in the asymptotics:

$$\langle R^2 \rangle \sim N^{2\nu} \text{ for } N \to \infty \quad \text{with} \quad \nu(d=3) \approx 0.588, \tag{2}$$

d being the dimension of space. The number of configurations $\mathcal{Z}$ of a polymer chain of N monomers scales with N like

$$\mathcal{Z} \sim e^{\mu N} N^{\gamma - 1}, \tag{3}$$

with a non-universal fugacity e^{μ}. In the early 70-ies following the work of de Gennes[2] the analogy between the asymptotic properties of long polymer chains and the long-distance correlations of a magnetic system in the vicinity of the 2nd order phase transition was recognized and elaborated in detail (see Refs. 4 and 5). This mapping allows us to obtain the above defined exponents ν and γ as $m \to 0$ limits of the correlation length exponent ν

and the magnetic susceptibility critical exponent γ of the $O(m)$-symmetric model.

On the other hand, if polymers of different species are present in the same solution, the scaling behaviour of the observables may be much richer. Let us consider a solution of two different species of polymers in some solvent, a so-called ternary polymer solution. Depending on the temperature the system may then behave as if one or more of the inter- and intra-chain interactions vanished in the sense described above.[8–11,52] This will lead to asymptotic scaling laws that differ from those observed for each species alone.[53]

Very interesting new systems are obtained when linking together polymers of different species. The simplest system of this kind is a so-called block copolymer consisting of two parts of different species. These are of some technical importance, e.g., in serving as surfactants.[54] In our context in the simplest example of a polymer star consists of chains of two different species (Fig. 3a) which is often referred to as a miktoarm or hetero-arm star polymer or copolymer star.[55–57] For the homogeneous polymer star in a good solvent the asymptotic properties are uniquely defined by the number of its constituting chains and the dimension of space.[12,15] For the number of configurations $\mathcal{Z}_f$ of a polymer star of f chains each consisting of N monomers one finds:

$$\mathcal{Z}_f \sim e^{\mu N f} N^{\gamma_f - 1}, \quad N \to \infty. \tag{4}$$

The exponents γ_f, $f = 1, 2, 3, \ldots$ constitute a family of star exponents, which depends on the number of arms f in a nontrivial way. The case of linear polymer chains is included in this family with the exponent $\gamma = \gamma_1 = \gamma_2$ defined in (3). For general numbers of arms f the star exponents γ_f have no physical counterparts in the set of exponents describing magnetic phase transitions. Nevertheless they can be related to the scaling dimensions of composite operators of traceless symmetry in the polymer limit $m \to 0$ of the $O(m)$ symmetric m vector model.[49,58] These exponents have been calculated analytically in perturbation theory,[12,16,49,59] by exact methods in two dimensions,[12,14] and by Monte Carlo (MC) simulations.[60–62]

It has been shown that the scaling properties of polymer networks of arbitrary but fixed topology are uniquely defined by its constituting stars,[15] as long as the statistical ensemble respects some conditions on chain length distribution.[49] Thus the knowledge of the set of star exponents allows one to obtain the power laws corresponding to (4) also for a general polymer network of arbitrary topology.

1.2. *Miktoarm Star Polymers and Multifractal Spectra*

In this review we also address the following somewhat more complex problem: what happens to the scaling laws if we build a polymer star or general network of chains out of different species? In view of the above introduced ternary solutions, one may thus study systems of polymer networks in which some of the intra- and inter-chain interactions vanish. For example, one may describe a copolymer star in solution consisting of say f_a chains of species a and f_b chains of species b (see Fig. 3b) in the case that there are no interactions among the chains of each individual species but only between chains of different species a and b. This situation in turn may also be interpreted as a number f_b of random walks which end at the core of a star of f_a chains with the constraint that the f_b random walks avoid the chains of the star. One may thus describe diffusion phenomena with some complicated boundary condition and find a special case of the more complex growth phenomena in a Laplacian field which gives rise to a multifractal (MF) spectrum of exponents.[18,30] The concept of multifractality developed in the last decades has proven to be a powerful tool for analyzing systems with complex statistics which otherwise appear to be intractable.[63,64] It has found direct application in a wide range of fields including turbulence, chaotic attractors, Laplacian growth phenomena, etc.[25,64–70]

Let us give a simple example of a MF phenomenon. On a possibly fractal set $X \subset \mathbb{R}^d$ of total size R a field $\varphi(r)$ is given at a microscopic scale ℓ. Then the normalized moments of this field may have a power law scaling behaviour for $\ell/R \to 0$:

$$\langle \varphi(r)^n \rangle / \langle \varphi(r) \rangle^n \sim (R/\ell)^{-\tau_n}. \tag{5}$$

Nontrivial MF scaling is found if $\tau_n \neq 0$. When the moments are averages over the sites of X, $\varphi(r)$ defines a measure on X and rigorous arguments show that the τ_n are convex from below as functions of n.[23,72] In a model formulated by Cates and Witten[30,73] the above fractal set is given by a polymer which is thought to be absorbing otherwise freely diffusing particles. The flux of particles on the polymer defines a field at each site which turns out to have multifractal properties. This idea may be generalized by deriving the corresponding MF spectrum in the framework of a field theoretical formalism, and by making use of renormalization group (RG) methods accompanied by the resummation technique. The MF spectrum is related to the spectrum of scaling dimensions of a family of composite operators of Lagrangian ϕ^4 field theory. This gives an example of the power-of-field

operators of which the scaling dimensions show the appropriate convexity for a MF spectrum.[17,18,23]

This addresses a special case of a growth process controlled by a Laplacian field. A variety of phenomena is described by this situation depending on the interpretation of the field. For diffusion limited aggregation (DLA) this field is given by the concentration of diffusing particles, in solidification processes it is given by the temperature field, in dielectric breakdown it is the electric potential, in viscous finger formation it is the pressure.[69,70] In all these processes the resulting structure appears to be of fractal nature and is characterized by appropriate fractal dimensions.[74] The growth and spatial correlations of the structure are governed by spectra of multifractal dimensions.[63,64] In general, the boundary conditions determining the field will be given on the surface of the growing aggregate itself. It is this dynamic coupling that produces the rich structure of the phenomena and seems to make the general dynamical problem intractable analytically. The scaling of the moments of the concentration near the surface of a DLA aggregate has been investigated in detail by MC methods. Simulations with high accuracy show that in $d = 3$ dimensions this scaling is described by the MF formalism while in $d = 2$ no power law scaling for higher moments occurs.[75–78]

The situation is simpler when the absorbing fractal structure is fixed, in which case one looks for the distribution of the Laplacian field $\rho(r)$ and its higher moments near the surface of the structure.[20,30,73] Following the diffusion picture, the aggregate is considered as an absorbing fractal, "the absorber". The field $\rho(r)$ gives the concentration of diffusing particles, it vanishes on the surface of the absorber, and it defines the harmonic measure of absorbtion on the absorber. More specifically, we may consider the Laplacian field $\rho(r)$ in the vicinity of an absorbing polymer, or near the core of a polymer star. Specifically, the ensembles of absorbers are characterized by either RW or SAW statistics. MF scaling is found for the n-moments $\langle \rho^n(r) \rangle$ of the field with respect to these ensembles. The two-dimensional version of this problem is under current discussion. Sets of multifractal exponents for $d = 2$ have been proposed recently with exact results from conformal field theory on random graphs[40,44] and with results extrapolated to 2D from the perturbative renormalization group approach.[18,20,48]

The formulation in terms of polymers and random walks allows one to use the polymer picture and theory developed for polymer networks and stars[12,15,16,49] together with the extension for copolymer stars.[17,18] The theory is then mapped to a Lagrangian ϕ^4 field theory with several

couplings[10,11,53] and higher-order composite operators[18,20,49] that describe the star vertices.

1.3. *Interactions of Star Polymers*

Star polymers[79] have also attracted interest in their quality as very soft colloidal particles.[80–84] As the number f of chains increases, they interpolate between linear polymers and polymeric micelles.[79,80,85] For large f, the effective repulsion between the cores of different polymer stars becomes strong enough to allow for crystalline ordering in a concentrated star polymer solution. While such a behaviour has already been predicted by early scaling arguments,[86,87] corresponding experiments with sufficiently dense star solutions have become feasible only recently. The crystallization transition occurs roughly at the overlap concentration c^* which is the number density of stars where their coronae start to touch experiencing the mutual repulsion. It is defined as $c^* = 1/(2R_g)^3$ where R_g, the radius of gyration, is the root mean square distance of the monomers from the center of mass of a single star. In addition, theory and computer simulation have refined the original estimate[86,87] for the number of chains f necessary for a freezing transition from $f \sim 100$ to $f \sim 34$, and they have predicted a rich phase diagram including stable anisotropic and diamond solid structures at high densities and high arm numbers.[83] These results were found using an effective *pair potential* between stars with a logarithmic short distance behaviour derived from scaling theory.

The effective pair and triplet interactions of star polymers in a good solvent may be derived using an analytical short-distance expansion inspired by scaling theory. These compare well with computer simulations[50,51,84] for different arm numbers f. The simulation data show good correspondence with the theoretical predictions and justify the effective pair potential picture even beyond the star polymer overlap concentration. Triplet forces, i.e. three-star forces, not forces between monomers, become relevant with respect to the pairwise forces if the typical separations between the particles are smaller than this typical length scale ℓ. This implies a triple overlap of particle coronae drawn as spheres of diameter ℓ around the particle centers. The triple overlap volume is an estimate for the magnitude of the triplet forces. Hence a three-particle configuration on an equilateral triangle is the configuration where triplet effects should be most pronounced.

In Ref. 50 a set-up of three-star polymers of which the centers are on an equilateral triangle was considered. It was found that the triplet part

is attractive but its relative contribution is small (11%) with respect to the repulsive pairwise part. This relative correction is universal, i.e., it is independent of the particle separation and of the arm number. It even persists for a collinear configuration of three-star polymers where the absolute correction is smaller than in the triangular situation for the same star–star distance. Consequently, the validity of the effective pair potential model appears to be justified even at densities above the overlap concentration. In particular, this result gives evidence that the anisotropic and diamond solids predicted by the pair theory[83] may indeed be realizable in actual samples of concentrated star polymer solutions.

1.4. *Comparison with Exact Results in 2D*

Polymer field theory usually has to be evaluated in terms of a theory of a truncated perturbation series. Obviously, it is always of special importance to compare these with the exact results if such exist. As a rule they are available for $d = 1, 2$. For the critical exponents that describe the scaling of homogeneous polymer chains and star polymers (or, more generally, homogeneous polymer networks) the perturbative approach[12,15,16,49] is in fair agreement with the exact data for $d = 2$.[12–14] For the heterogeneous case however, only perturbative results[17,18,20–22] were available until recently. An exact solution for scaling exponents has since been proposed that uses methods of conformal invariance on random graphs.[40,41] A rigorous mathematical treatment of the problem supporting this approach has been given in which a number of these exact results are proven with mathematical rigor.[42] A comparative analysis of the properties of the perturbative solution and of these exact results complemented by computer simulation data have been presented.[48] This shows the areas where the approaches agree and explains why they differ in general. In this respect some of the speculative results of Ref. 40 derived from the algebra of conformal dimensions for copolymer stars on 2D random graphs (quantum gravity) are confirmed.

2. Miktoarm Star Polymers

2.1. *Model and Notations*

Let us first take a look at the model used to describe polymers. In a first discrete version we will describe a configuration of the polymer by a set of positions of segment endpoints:

$$\text{Configuration}\{r_1, \ldots, r_N\} \in I\!R^{d\times N}.$$

Its statistical weight (Boltzmann factor) in terms of the Hamiltonian $\mathcal{H}$ divided by the product of the Boltzmann constant k_B and temperature T is given by

$$\exp\left(-\frac{1}{k_\mathrm{B}T}\mathcal{H}\right) = \exp\left(-\frac{1}{4\ell_0^2}\sum_{j=2}^{N}(r_j - r_{j-1})^2 - \beta\ell_0^d \sum_{i\neq j=1}^{N} \delta^d(r_i - r_j)\right). \tag{6}$$

The first term describes the chain connectivity, the parameter ℓ_0 governing the mean segment length. The second term describes the excluded volume interaction forbidding two segment end points to take the same position in space. The parameter β gives the strength of this interaction. The third parameter in this model is the chain length or number of segments N.

The partition sum $\mathcal{Z}_1$ is calculated as an integral over all configurations of the polymer divided by the system volume Ω, thus dividing out identical configurations just translated in space:

$$\mathcal{Z}_1(N) = \frac{1}{\Omega}\int \prod_{i=1}^{N} dr_i \exp\left(-\frac{1}{k_\mathrm{B}T}\mathcal{H}\{r_i\}\right). \tag{7}$$

The partition sum can be interpreted as giving the "number of configurations" of the polymer (3). The polymer model is mapped to a renormalizable field theory making use of well developed formalisms (see, e.g., Refs. 4 and 5). To this end, a continuous version of the model was proposed by Edwards.[88,89] This model is generalized to describe a set of f polymer chains of varying composition possibly tied together at their endpoints. The configuration of one polymer in this formulation is then given by a path $r^a(s)$ in d-dimensional space $\mathbb{R}^d$ parameterized by a surface variable $0 \leq s \leq S_a$. The relation of the "Gaussian surface" S_a of the chain a to the number of segments N_a in the discrete model is $S_a = N_a\ell_0^2$. Allowing for a symmetric matrix of excluded volume interactions u_{ab} between chains $a, b = 1, \ldots, f$, the Hamiltonian $\mathcal{H}$ reads

$$\frac{1}{k_\mathrm{B}T}\mathcal{H}(r^a) = \sum_{a=1}^{f}\int_0^{S_a} ds \left(\frac{dr^a(s)}{ds}\right)^2 + \frac{1}{6}\sum_{a,b=1}^{f} u_{ab}\int d^d r \rho_a(r)\rho_b(r), \tag{8}$$

with densities $\rho_a(r) = \int_0^{S_a} ds\ \delta^d(r - r^a(s))$. The partition sum is calculated as a functional integral:

$$\mathcal{Z}_f\{S_a\} = \frac{1}{\Omega}\int \mathcal{D}[r^a(s)] \exp\left(-\frac{1}{k_\mathrm{B}T}\mathcal{H}(r^a)\right). \tag{9}$$

Here, the symbol $\mathcal{D}[r_a(s)]$ includes normalization such that $\mathcal{Z}_f\{S_a\} = 1$ in the absence of all interactions, i.e. if all $u_{ab} = 0$. Let us note here that the continuous chains may be understood as a limit of discrete self-avoiding walks, when the length of each step is decreasing while the number of steps N_a is increasing keeping the Gaussian surface S_a of each path fixed:

$$S_a = N_a \ell_0^2. \tag{10}$$

The continuous chain model (8) is mapped to a corresponding polymer (Ginzburg–Landau) field theory by a Laplace transform in the Gaussian surfaces S_a to conjugate chemical potentials ("mass variables") μ_a

$$\tilde{\mathcal{Z}}_f\{\mu_a\} = \int_0^\infty \prod_b \mathbf{d}S_b \; e^{-\mu_b S_b} \mathcal{Z}_f\{S_a\}. \tag{11}$$

Here, the Laplace-transformed partition function $\tilde{\mathcal{Z}}_f\{\mu_a\}$ can be expressed as the $m = 0$ limit of the functional integral over the vector fields ϕ_a, $a = 1, \ldots, f$ each with m components ϕ_a^α, $\alpha = 1, \ldots, m$

$$\tilde{\mathcal{Z}}_f\{\mu_b\} = \frac{1}{\Omega} \int \mathcal{D}[\phi_a(r)] \;\; \exp[-\mathcal{L}\{\phi_b, \mu_b\}] \,|_{m=0}, \tag{12}$$

where the Landau–Ginzburg–Wilson Lagrangean $\mathcal{L}$ of f interacting fields ϕ_b each with m components reads

$$\begin{aligned} \mathcal{L}\{\phi_b, \mu_b\} = \frac{1}{2} \sum_{a=1}^{f} \int d^d r \; [\mu_a \phi_a^2 + (\nabla \phi_a(r))^2] \\ + \frac{1}{4!} \sum_{a,a'=1}^{f} u_{a,a'} \int d^d r \; \phi_a^2(r) \phi_{a'}^2(r). \end{aligned} \tag{13}$$

Here

$$\phi_a^2 = \sum_{\alpha=1}^{m} (\phi_a^\alpha)^2. \tag{14}$$

The limit $m = 0$ in (12) can be understood as a selection rule for the diagrams that appear in the perturbation theory expansions and can be checked diagrammatically. A rigorous proof based on the application of the Stratonovich–Hubbard transformation to linearize terms in (8) is given for the multicomponent case in Ref. 53.

The one-particle irreducible vertex function $\Gamma^{(L)}(q_i)$ can be defined by

$$\delta\left(\sum q_i\right)\Gamma^{(L)}(q_i) = \int e^{iq_i r_i}\; dr_1 \cdots dr_L\; \langle\phi_{a_1}(r_1)\cdots\phi_{a_L}(r_L)\rangle^{\mathcal{L}}_{1PI}. \quad (15)$$

The averaging in (15) is done with respect to the Lagrangean (13) while keeping only those contributions which correspond to one-particle irreducible graphs.

The partition function $\mathcal{Z}_{*f}\{S_a\}$ of a polymer star consisting of f polymers of different species $1,\ldots,f$ constrained to have a common end point is obtained from (9) by introducing an appropriate product of δ-functions ensuring the "star-like" structure. It reads

$$\begin{aligned}\mathcal{Z}_{*f}\{S_a\} = \frac{1}{\Omega}\int \mathcal{D}[r_a] \\ \times\exp\left[-\sum_{a=1}^{f}\int_0^{S_a} ds\left(\frac{d\vec{r}_a(s)}{ds}\right)^2 - \frac{1}{6}\sum_{a,b=1}^{f} u_{ab}\int d^d r\;\rho_a(\vec{r})\rho_b(\vec{r})\right] \\ \times\prod_{a=2}^{f}\delta^d(\vec{r}_a(0)-\vec{r}_1(0)). \quad (16)\end{aligned}$$

The vertex part of its Laplace transform may then be defined[49] by

$$\begin{aligned}&\delta\left(p+\sum q_i\right)\Gamma^{(*f)}_{a_1\cdots a_f}(p,q_1\cdots q_f) \\ &= \int e^{i(pr_0+q_i r_i)} d^d r_0 d^d r_1\cdots d^d r_f \\ &\qquad\times\langle\phi_{a_1}(r_0)\cdots\phi_{a_f}(r_0)\phi_{a_1}(r_1)\cdots\phi_{a_f}(r_f)\rangle^{\mathcal{L}}_{1PI}, \quad (17)\end{aligned}$$

where all $a_1,\ldots a_f$ are distinct. Here, the local operator product or composite operator $\prod_i \phi_{a_i}(r_0)$ that is inserted to define the vertex function governs the anomalous scaling behaviour. When only species a is present one may also define Γ^{*f} in terms of

$$\begin{aligned}&\delta\left(p+\sum q_i\right)\Gamma^{(*f)}(q,p_1\cdots p_f) \\ &= \int e^{i(qr_0+p_i r_i)} d^d r_0 d^d r_1\cdots d^d r_f \\ &\qquad\times\langle N^{\alpha_1\cdots\alpha_f}\phi_a^{\alpha_1}(r_0)\cdots\phi_a^{\alpha_f}(r_0)\phi_a^{\alpha_1}(r_1)\cdots\phi_a^{\alpha_f}(r_f)\rangle^{\mathcal{L}}_{1PI}, \quad (18)\end{aligned}$$

where α is the index of the field component and the tensor $N^{\alpha_1,\ldots,\alpha_f}$ has traceless symmetry[49,58]

$$\sum_{\alpha} N^{\alpha\alpha\alpha_3\cdots\alpha_f} = 0. \quad (19)$$

In what follows our interest is mainly focussed on the case when only two species of polymers are present, with interactions u_{11}, u_{22} between polymers of the same species and $u_{12} = u_{21}$ between polymers of different species. Thus, let us elaborate the results for the case of a ternary polymer solution. In terms of the scaling behaviour this situation is the generic case and easily generalized to the case of higher numbers of polymer species by appropriate combinatorics; as a special case of such a situation we treat a star of f mutually avoiding (but internally transparent) walks. Let us list here the expressions to the third order for those vertex functions that enter the theory. They involve the loop integrals I_k^L, J_k^L which are given in Table 1 and in Fig. 4 showing the correspondence to the graphs of perturbation theory. The bare Gamma functions read[53]

$$\frac{\partial}{\partial k^2}\Gamma^{(2)}_{(aa)} = 1 - \frac{1}{9}J_1^2 u_{aa}^2 + \frac{4}{27}J_1^3 u_{aa}^3, \quad a = 1, 2, \tag{20}$$

$$\begin{aligned}\Gamma^{(4)}_{(aaaa)} = u_{aa} &- \frac{4}{3}I_1^1 u_{aa}^2 + \left(\frac{5}{9}I_1^2 + \frac{22}{9}I_2^2\right) u_{aa}^3 \\ &- \left(\frac{2}{9}I_1^3 + \frac{28}{27}I_2^3 + \frac{8}{27}I_3^3 + \frac{40}{9}I_7^3 + \frac{58}{27}I_5^3 + \frac{14}{27}I_8^3 + \frac{22}{27}I_4^3\right) u_{aa}^4, \\ &\qquad a = 1, 2.\end{aligned} \tag{21}$$

The bare vertex function for the star vertex of a miktoarm star reads[18]

$$\begin{aligned}\Gamma^{(*f)} = 1 &+ \frac{1}{2}I_1^1 \bar{u}_{a_1a_2} + \frac{1}{8}I_1^2 \bar{u}_{a_1a_2}\bar{u}_{a_3a_4} + \bar{u}_{a_1a_2}\bar{u}_{a_1a_3}I_2^2 + \bar{u}_{a_1a_1}\bar{u}_{a_1a_2}I_2^2 \\ &+ \frac{1}{2}(I_2^2 + I_1^2)\bar{u}_{a_1a_2}^2 + \frac{1}{48}I_1^3 \bar{u}_{a_1a_2}\bar{u}_{a_3a_4}\bar{u}_{a_5a_6} \\ &+ \frac{1}{2}\bar{u}_{a_1a_2}\bar{u}_{a_1a_3}\bar{u}_{a_4a_5}I_2^3 + \bar{u}_{a_1a_2}\bar{u}_{a_1a_3}\bar{u}_{a_3a_4}I_7^3 \\ &+ \frac{1}{2}(I_5^3 + I_8^3)\bar{u}_{a_1a_2}\bar{u}_{a_1a_3}\bar{u}_{a_2a_4} + \bar{u}_{a_1a_2}\bar{u}_{a_1a_3}\bar{u}_{a_1a_4}I_7^3 \\ &+ \frac{1}{3}(3\ I_7^3 + I_4^3)\bar{u}_{a_1a_2}\bar{u}_{a_1a_3}\bar{u}_{a_2a_3} + \frac{1}{4}(I_2^3 + I_1^3)\bar{u}_{a_1a_2}^2\bar{u}_{a_3a_4} \\ &+ \left(I_2^3 + 2I_7^3 + 2I_5^3 + I_4^3\right)\bar{u}_{a_1a_2}^2\bar{u}_{a_1a_3} + \left(I_3^3 + 3I_7^3 + I_5^3\right)\bar{u}_{a_1a_1}^2\bar{u}_{a_1a_2} \\ &+ \frac{1}{2}(I_2^3 + 2\ I_7^3 + I_5^3 + I_8^3 + I_1^3)\bar{u}_{a_1a_2}^3 + \frac{1}{2}\bar{u}_{a_1a_1}\bar{u}_{a_1a_2}\bar{u}_{a_3a_4}I_2^3 \\ &+ \left(I_7^3 + I_5^3\right)\bar{u}_{a_1a_1}\bar{u}_{a_1a_2}\bar{u}_{a_2a_3} + \left(I_7^3 + I_5^3 + I_4^3\right)\bar{u}_{a_1a_1}\bar{u}_{a_1a_2}\bar{u}_{a_1a_3} \\ &+ \frac{1}{2}\bar{u}_{a_1a_1}\bar{u}_{a_1a_2}\bar{u}_{a_2a_2}I_5^3 + \left(I_2^3 + 4I_7^3 + I_8^3\right)\bar{u}_{a_1a_1}\bar{u}_{a_1a_2}^2.\end{aligned} \tag{22}$$

Table 1. Expansion in ε-poles of integrals contributing to $\Gamma^{(4)}$ and $(\partial/\partial k^2)\Gamma^{(2)}(k)$, and $\Gamma^{(*f)}$

I_1^1	$(1/\varepsilon)(1+\frac{1}{2}\varepsilon+\frac{1}{2}\varepsilon^2)$
I_1^2	$(I_1^1)^2$
I_2^2	$(1/2\varepsilon^2)(1+\frac{3}{2}\varepsilon+\frac{5}{2}\varepsilon^2-\frac{1}{2}J\varepsilon^2)$
I_1^3	$(I_1^1)^3$
I_2^3	$I_1^1 I_2^2$
I_3^3	$-(1/24\varepsilon^2)(1+\frac{15}{4}\varepsilon)$
I_4^3	$\frac{\zeta(3)}{2\varepsilon}$
I_5^3	$(1/3\varepsilon^3)(1+\frac{5}{2}\varepsilon+\frac{23}{4}\varepsilon^2-\frac{3}{2}J\varepsilon^2)$
I_6^3	I_5^3
I_7^3	$(1/6\varepsilon^3)(1+3\varepsilon+\frac{31}{4}\varepsilon^2-\frac{3}{2}J\varepsilon^2)$
I_8^3	$(1/3\varepsilon^3)(1+2\varepsilon+\frac{13}{4}\varepsilon^2)$
J_1^2	$-(1/8\varepsilon)(1+\frac{5}{4}\varepsilon)$
J_1^3	$-(1/6\varepsilon^2)(1+2\varepsilon)$

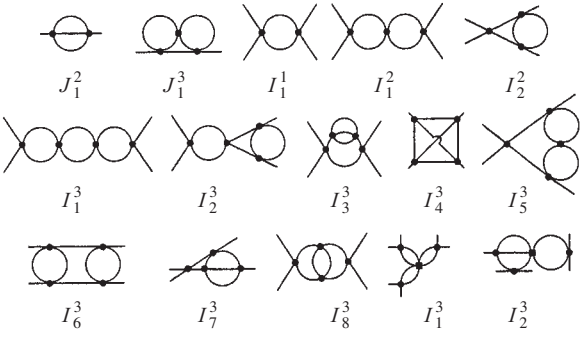

Fig. 4. Graphs of contributions to $\Gamma^{(2)}$, $\Gamma^{(4)}$ in three-loop approximation. The last two graphs represent additional contributions to $\Gamma^{(*f)}$.

Here, summation over $a_i = 1 \cdots f$ is assumed. For a star of f_1 chains of species 1 and f_2 chains of species 2 the matrix of interactions $\bar{u}_{ab}$ is given by

$$\bar{u}_{ab}^{f_1 f_2} = \begin{cases} u_{11}/3 & \text{if } \ 1 \le a, b \le f_1, \\ u_{22}/3 & \text{if } \ f_1 < a, b \le f, \\ u_{12}/3 & \text{else.} \end{cases} \tag{23}$$

Let us define

$$\Gamma^{(*f_1 f_2)} = \Gamma^{(*f)}|_{\bar{u}_{ab}=\bar{u}_{ab}^{f_1 f_2}}. \tag{24}$$

For general f_1 and f_2, the corresponding combinatorics may also be directly calculated by summation over $a_i = 1, 2$ instead. Replacing $\bar{u}$ by u, each term in the sum with indices $a_1 \cdots a_k$ then acquires a factor

$$\binom{f_1}{\mathcal{N}_1}\binom{f_2}{\mathcal{N}_2}\mathcal{N}_1!\mathcal{N}_2!. \tag{25}$$

Here $\mathcal{N}_1 = \sum_k \delta_{1,a_k}$ is the number of $a_k = 1$ whereas $\mathcal{N}_2 = \sum_k \delta_{2,a_k}$ is the number of $a_k = 2$.

As a special case we may derive the vertex function $\Gamma^{(4)}_{1122}$ for the u_{12} interaction using the relation $\Gamma^{(*22)} = (\partial/\partial u_{12})\Gamma^{(4)}_{1122}$ which is obvious from the perturbation theory (see, e.g., Ref. 53),

$$\Gamma^{(4)}_{1122} = \int du_{12}\ \Gamma^{(*22)}. \tag{26}$$

With the same formalism we can also describe a star of f mutually avoiding walks.[35,36] In this case all interactions on the same chain $\bar{u}_{aa}$ vanish and only those $\bar{u}_{ab}$ with $a \neq b$ remain,

$$\Gamma^{(*f)}_{\mathrm{MAW}} = \Gamma^{(*f)}|_{\bar{u}_{ab}=(1-\delta_{ab})u_{12}}. \tag{27}$$

Here, each term with indices $a_1 \cdots a_k$ acquires a factor $\binom{f}{k}k!$.

As well known, ultraviolet divergences occur when the vertex functions (20)–(22) are evaluated naively.[90] In the next section the field theoretical renormalization group approach is to be applied to study this problem.

2.2. *Renormalization*

Renormalization group (RG) theory is employed to utilize the scaling symmetry of the systems in the asymptotic limit, in order to extract the universal content and at the same time remove divergences which occur for the evaluation of the bare functions in this limit.[90–92] One passes from the theory in terms of the initial bare variables to a renormalized theory. This can be achieved by a controlled rearrangement of the series for the vertex functions. Several asymptotically equivalent procedures serve for this purpose. In our presentation of the renormalization procedure we here restrict ourselves to the zero mass renormalization (see, e.g., Ref. 91) with successive ε-expansion.[93] When presenting numerical results for the exponents we will nevertheless compare them with those of the fixed dimension RG

approach.[94] In the present context both approaches have been exploited in Refs. 18, 20 and 47. The zero mass renormalization is defined directly for the critical point but has to make use of the $\varepsilon = 4 - d$ expansion in order to give results for critical exponents at the physically interesting dimensions $d = 2$ and $d = 3$.[93,95–97] The fixed dimension approach renormalizes for nonzero mass and leads to results[98,99] for critical exponents directly in space dimensions $d = 2$ and $d = 3$. However, it cannot be performed at the critical point itself, although it leads to quantitative results for the preasymptotic critical behaviour.[100,101] Most authors tend to prefer one method and to exclude the other for non-obvious reasons. Having at hand the results of both approaches allows for a check of the consistency of the approximations and the accuracy of the results obtained.

Let us formulate the relations to obtain a renormalized theory in terms of corresponding renormalization conditions. Note that the polymer limit of zero component fields leads to an essential simplification. Each field ϕ_a, mass m_a and coupling u_{aa} renormalizes as if the other fields were absent, in so far as any coupling terms are only present for non-zero numbers of the field components. Renormalized couplings g_{ab} may be introduced by

$$u_{aa} = \mu^\varepsilon Z_{\phi_a}^2 Z_{aa} g_{aa}, \quad a = 1, 2, \tag{28}$$

$$u_{12} = \mu^\varepsilon Z_{\phi_1} Z_{\phi_2} Z_{12} g_{12}. \tag{29}$$

Here, μ is a scale parameter giving the scale of external momenta in the massless scheme. The renormalization factors Z_{ϕ_a}, Z_{ab} are defined as power series in the renormalized coupling which fulfill the following RG conditions:

$$Z_{\phi_a}(g_{aa}) \frac{\partial}{\partial k^2} \Gamma^{(2)}_{aa}(u_{aa}(g_{aa})) = 1, \tag{30}$$

$$Z_{aa}(g_{aa}) \Gamma^{(4)}_{aaaa}(u_{aa}(g_{aa})) = \mu^\varepsilon g_{aa}, \tag{31}$$

$$Z_{12}(g_{ab}) \Gamma^{(4)}_{1122}(u_{ab}(g_{ab})) = \mu^\varepsilon g_{12}. \tag{32}$$

Evaluating these formulas perturbatively, the corresponding loop integrals are evaluated in the massless approach for external momenta at the scale of μ. The RG condition for the vertex function $\Gamma^{(2)}$ reads for massless renormalization

$$\Gamma^{(2)}_{aa}(u_{aa}(g_{aa}))|_{k^2=\mu^2} = 0, \quad a = 1, 2. \tag{33}$$

In order to renormalize the (dimensionless) star vertex functions we introduce renormalization factors Z_{*f_1,f_2} by

$$Z_{\phi_1}^{f_1/2} Z_{\phi_2}^{f_2/2} Z_{*f_1,f_2} \Gamma^{(*f_1 f_2)}(u_{ab}(g_{ab})) = 1. \tag{34}$$

In the same way we define the appropriate renormalization of the mutually avoiding walks (MAWs) vertex function

$$Z_{\phi_1}^{f/2} Z_{(\mathrm{MAW}f)} \Gamma^{*f}_{\mathrm{MAW}}(u_{12}(g_{ab})) = 1. \tag{35}$$

The renormalized couplings g_{ab} defined by the relations (28) and (29) depend on the scale parameter μ. By their dependence on g_{ab} also the renormalization Z factors depend implicitly on μ. This dependence is expressed by the renormalization group functions defined by the following relations:

$$\mu \frac{d}{d\mu} g_{ab} = \beta_{ab}(g_{a'b'}), \tag{36}$$

$$\mu \frac{d}{d\mu} \ln Z_{\phi_a} = \eta_{\phi_a}(g_{aa}), \tag{37}$$

$$\mu \frac{d}{d\mu} \ln Z_{*f_1 f_2} = \eta_{*f_1 f_2}(g_{ab}), \tag{38}$$

$$\mu \frac{d}{d\mu} \ln Z_{\mathrm{MAW}f} = \eta_f^{\mathrm{MAW}}(g_{ab}). \tag{39}$$

The function η_{ϕ_a} describes the pair correlation critical exponent, while the functions $\eta_{*f_1 f_2}$ and $\eta_f^{\mathrm{MAW}}(g_{ab})$ define the set of anomalous dimensions for copolymer stars and stars of MAWs. Explicit expressions for the β and η functions are given in the next section together with a study of the RG flow and the fixed points of the theory.

2.3. *Renormalization Group Flow and the Fixed Points*

We now discuss the RG flow of the theory. In particular we want to find appropriate representations for the fixed points of the flow for both approaches used here. In a study devoted to ternary polymer solutions the RG flow was calculated[53] in the frames of massless renormalization and given to third loop order in the ε-expansion. Note that for the diagonal coupling g_{aa} the corresponding expressions are also found in the polymer limit $m = 0$ of the $O(m)$-symmetrical ϕ^4 model. They are known in even higher orders of perturbation theory [see, e.g., formula (9.8) of Ref. 91]. To third loop order the expressions read[53]

$$\beta^{\varepsilon}_{g_{aa}} = -\varepsilon g_{aa} + \frac{1}{3}(4 + 2\varepsilon + 2\varepsilon^2) g_{aa}^2 - \frac{1}{9}\left(\frac{21}{2} + \frac{215}{8}\varepsilon - 11J\varepsilon\right) g_{aa}^3$$

$$+ \frac{1}{27}[79 - 22J + 33\zeta(3)] g_{aa}^4 + O(g_{aa}^5), \quad a = 1, 2. \tag{40}$$

$$\beta^{\varepsilon}_{g_{12}} = -\varepsilon g_{12} + \frac{1}{3}\left(1 + \frac{1}{2}\varepsilon + \frac{1}{2}\varepsilon^2\right)(g_{11} + g_{22})g_{12} + \frac{1}{3}(2 + \varepsilon + \varepsilon^2)g_{12}^2$$
$$-\frac{1}{9}\left(\frac{5}{4} + \frac{55}{16}\varepsilon - \frac{3}{2}J\varepsilon\right)(g_{11}^2 + g_{22}^2)g_{12}$$
$$-\frac{1}{9}\left(3 + \frac{15}{2}\varepsilon - 3J\varepsilon\right)(g_{11} + g_{22})g_{12}^2 - \frac{1}{9}(2 + 5\varepsilon - 2J\varepsilon)g_{12}^3$$
$$+\frac{1}{54}(15 - J)(g_{11}^3 + g_{22}^3)g_{12} + \frac{1}{27}\left[\frac{27}{2} + 9\zeta(3) - 6J\right](g_{11}^2 + g_{22}^2)g_{12}^2$$
$$+\frac{1}{27}(7 - 3J)g_{11}g_{22}g_{12}^2 + \frac{1}{27}[12 + 6\zeta(3) - 2J](g_{11} + g_{22})g_{12}^3$$
$$+\frac{1}{27}[6 + 3\zeta(3) - 2J]g_{12}^4 + O(g^5). \tag{41}$$

Here the Riemann ζ-function with $\zeta(3) \approx 1.202$ and the constant $J \approx 0.7494$ occur. The index ε at β^{ε} is used to indicate that the β-functions are obtained in the massless renormalization scheme with successive ε-expansion.

The equations for the fixed points $\{g_{11}^*, g_{22}^*, g_{12}^*\}$ of the functions β^{ε} as obtained in the massless renormalization,

$$\beta^{\varepsilon}_{g_{aa}}(g_{aa}^*) = 0, \quad a = 1, 2; \qquad \beta^{\varepsilon}_{g_{12}}(g_{11}^*, g_{22}^*, g_{12}^*) = 0, \tag{42}$$

have 8 different solutions, corresponding to the different cases of interacting and non-interacting chains. In the case when the interaction between the chains of different species is absent ($g_{12}^* = 0$) one finds the following fixed points: $G_0\,(g_{11}^* = 0,\, g_{22}^* = 0)$, $U_0\,(g_{11}^* \neq 0,\, g_{22}^* = 0)$, $U_0'\,(g_{11}^* = 0,\, g_{22}^* \neq 0)$, $S_0\,(g_{11}^* \neq 0,\, g_{22}^* \neq 0)$.

It is clear from expressions (40) for the β-functions that the non-zero solutions for g_{11}^* and g_{22}^* in (42) correspond to the fixed points describing SAWs (zero solutions correspond to RWs). More interesting are the fixed points corresponding to the case of mutually interacting chains ($g_{12}^* \neq 0$). Keeping the notation of Ref. 53 they are: $G\,(g_{11}^* = 0,\, g_{22}^* = 0)$, $U\,(g_{11}^* \neq 0,\, g_{22}^* = 0)$, $U'\,(g_{11}^* = 0,\, g_{22}^* \neq 0)$ and $S\,(g_{11}^* \neq 0,\, g_{22}^* \neq 0)$. In the three-dimensional space of the couplings g_{11}, g_{22}, g_{12} the above discussed fixed points of the renormalization group flow show up in a corresponding flow diagram at the corners of a cube deformed in the g_{12} direction (see Fig. 5). Their ε-expansions are[53]

$$g_G^* = \frac{3}{2}\varepsilon - \left[J + \frac{3}{2}\zeta(3)\right]\frac{3}{8}\varepsilon^3, \tag{43}$$

$$g_U^* = \frac{9}{8}\varepsilon + \frac{39}{256}\varepsilon^2 + \left[\frac{267}{4096} - \frac{693}{1024}\zeta(3) - \frac{189}{512}J\right]\varepsilon^3, \tag{44}$$

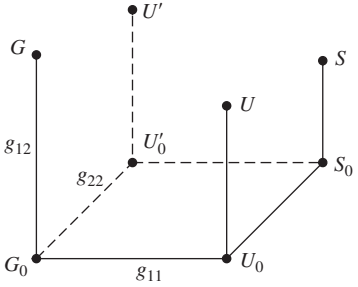

Fig. 5. Fixed points of the RG flow for ternary polymer systems. See text for discussion.

$$g_S^* = \frac{3}{4}\varepsilon + \frac{15}{128}\varepsilon^2 + \left[\frac{111}{2048} - \frac{99}{256}\zeta(3) - \frac{33}{128}J\right]\varepsilon^3. \tag{45}$$

Expressions (43)–(45) give the fixed point values of ternary solutions in the massless renormalization scheme and are used in the subsequent discussion.

Looking for the stability of the above described fixed points one finds that only the fixed point S is stable and thus in the excluded volume limit of infinitely long chains the behaviour of a system of two polymer species is described by the same scaling laws as a solution of only one polymer species. Nevertheless while studying polymer mixtures at different temperatures and also taking into account that real polymer chains are not infinitely long, one may also study crossover phenomena which are governed by the unstable fixed points. The knowledge of the total flow allows for a description of the crossover phenomena in the entire region.[53]

However, here we restrict the present discussion to the fixed point behaviour and the properties of the star vertex functions at these fixed points.

2.4. *Results for the Exponents*

For homogeneous stars of polymer chains of a single species, several sets of star exponents have been defined, each describing either the scaling properties of the configurational number [see Eq. (4)], or the anomalous dimensions of star vertices, *etc.* Due to scaling relations these exponents can be expressed in terms of each other.[15] In this sense each set of star exponents forms a complete basis. For the copolymer and MAW stars considered here we choose to present all results in terms of the exponents $\eta_{f_1 f_2}$ and η_f^{MAW} given by fixed point values of the functions $\eta_{* f_1 f_2}(g_{ab})$ (38) and

$\eta_f^{\mathrm{MAW}}(g_{ab})$ (39). We denote the asymptotic values of the copolymer star exponents and MAW star exponents by:

$$\eta^G_{f_1f_2} = \eta_{*f_1f_2}(g_{ab})|_G, \tag{46}$$

$$\eta^U_{f_1f_2} = \eta_{*f_1f_2}(g_{ab})|_U = \eta_{*f_2f_1}(g_{ab})|_{U'}, \tag{47}$$

$$\eta^S_f = \eta^U_{f,0}, \tag{48}$$

$$\eta^{\mathrm{MAW}}_f = \eta^{\mathrm{MAW}}_f(g_{ab})|_G. \tag{49}$$

In the case of the symmetric fixed point S where we reproduce the results for homogeneous polymer stars[49] we can relate the exponent η^S_f to the configurational number star exponent γ_f introduced by (4),

$$\gamma^S_f - 1 = \nu\eta^S_f + (\nu(2-\eta_\phi)-1)f = \nu(\eta^S_f - f\eta^S_2). \tag{50}$$

Note, that η^S_2 is not to be confused with η_ϕ. In the asymmetric case, when one set of chains is self-avoiding and the other is not, the corresponding exponents $\gamma_{f_1f_2}$ are not well defined. This can be seen from Eq. (50) as it is not clear what should be the value of ν in the first term of its right hand side. On the other hand, the scaling law of the number of configurations on the basis of the number of monomers will also be ill-defined. The set of SAWs will fill a much larger volume for the same number of monomers than the non-self-avoiding walks. These two sets will not interact along the full length of SAWs. In this case the exponent describes rather the power law scaling of the partition function of a (miktoarm) copolymer star with a common radius R of all arms (e.g. common end-to-end distance):

$$\mathcal{Z}^U_{f_1f_2}(R) \sim R^{\eta^U_{f_1f_2} - f_1\eta^U_{2,0}}. \tag{51}$$

In the same way the power law scaling of the partition function for two mutually avoiding sets of f_1 and f_2 otherwise transparent RWs, as well as for f mutually avoiding walks, may be written in terms of their common radius R

$$\mathcal{Z}^G_{f_1f_2}(R) \sim R^{\eta^G_{f_1f_2}}, \tag{52}$$

$$\mathcal{Z}^{\mathrm{MAW}}_f(R) \sim R^{\eta^{\mathrm{MAW}}_f}. \tag{53}$$

In the case that some of the chains are much shorter than the others with radii $R_1 \ll R_2$ a short chain expansion for polymer networks shows that a power law scaling will prevail on the shorter scale with[102]

$$\mathcal{Z}_*(R_1 \ll R_2) \sim R_1^{\eta_* - \hat{\eta}_*}, \tag{54}$$

where $\hat{\eta}_*$ is the corresponding exponent of the polymer star with all short chains removed i.e. on the scale R_2.

Now, from the expressions for the fixed points given in the previous section and the relations (48) and (49) the series for the appropriate star exponents can be derived. The ε-expansions of the exponents $\eta_{f_1 f_2}$ read

$$\eta^G_{f_1 f_2}(\varepsilon) = -\frac{1}{2} f_1\, f_2 \varepsilon + \frac{1}{8} f_1\, f_2 (f_2 - 3 + f_1)\varepsilon^2 - \frac{1}{16} f_1\, f_2 (f_2 - 3 + f_1)(f_1 + f_2 + 3\,\zeta(3) - 3)\varepsilon^3, \tag{55}$$

$$\begin{aligned}\eta^U_{f_1 f_2}(\varepsilon) = {} & \frac{1}{8} f_1 (1 - f_1 - 3 f_2)\varepsilon \\ & + \frac{1}{256} f_1 (25 - 33 f_1 + 8 {f_1}^2 - 91 f_2 + 42 f_1 f_2 + 18 {f_2}^2)\varepsilon^2 \\ & + \frac{1}{4096} f_1 [577 - 969 f_1 + 456 {f_1}^2 - 64 {f_1}^3 - 2463 f_2 \\ & + 2290 f_1 f_2 - 492 {f_1}^2 f_2 + 1050 {f_2}^2 - 504 f_1 {f_2}^2 - 108 {f_2}^3 \\ & - 712\zeta(3) + 936 f_1 \zeta(3) - 224 {f_1}^2 \zeta(3) + 2652 f_2 \zeta(3) \\ & - 1188 f_1 f_2 \zeta(3) - 540 {f_2}^2 \zeta(3)]\varepsilon^3,\end{aligned} \tag{56}$$

$$\eta^{\mathrm{MAW}}_f(\varepsilon) = -\frac{1}{4}(f-1) f \varepsilon + \frac{1}{16} f (f-1)(2f-5)\varepsilon^2 - \frac{1}{32}(f-1) f [4f^2 - 20 f + 8 f \zeta(3) - 19\zeta(3) + 25]\varepsilon^3. \tag{57}$$

For the sake of completeness we give also the ε-expansions for the exponents ν and η_ϕ that appear in relation (50)

$$\eta_\phi(\varepsilon) = \frac{1}{64}\varepsilon^2 + \frac{17}{1024}\varepsilon^3, \tag{58}$$

$$\nu(\varepsilon) = \frac{1}{2} + \frac{1}{16}\varepsilon + \frac{15}{512}\varepsilon^2 + \left[\frac{135}{8192} - \frac{33}{1024}\zeta(3)\right]\varepsilon^3. \tag{59}$$

2.5. *Resummation*

The series of the perturbation theory of the field theoretic RG scheme is not convergent. The growth of the coefficients of perturbation theory series may

be estimated using information such as the growth of the combinatorial multiplicity of diagrams. The series for the β function of the $O(m)$ symmetric ϕ^4 model with one coupling g has the following asymptotic behaviour:[103,104]

$$\beta(g) = \sum_k A_k g^k, \tag{60}$$

$$A_k = ck^{b_0}(-a)^k k![1 + O(1/k)], \quad k \to \infty. \tag{61}$$

The quantities a, b_0, c were calculated in Refs. 103 and 105. Such a behaviour is also expected and may be proven for the critical exponents as series in terms of the coupling. These results also show the divergence of the ε-expansions of the η-exponents and indicate their Borel summability.[106] This procedure of resummation takes into account the asymptotic growth of the coefficients and allows one to map the asymptotic series to a convergent series with the same limiting value. The function β_{aa} considered here (36) coincides with the $O(m)$ symmetric β function (60) in the polymer limit $m = 0$. Thus, its asymptotic behaviour is known. The asymptotic behaviour of the off diagonal β function β_{12} has been investigated[53] by an instanton analysis.[107,108]

Let us introduce the techniques for resummation of the series based on the knowledge of the asymptotic behaviour. Here, we make use of Padé–Borel resummation and a resummation extended by a conformal mapping. The first way of resummation is applicable only for alternating series, while the second is more universal.

The resummation procedures are as follows. For the asymptotic series for an exponent γ given as a series in the expansion parameter ε

$$\gamma(\varepsilon) = \sum_j \gamma^{(j)} \varepsilon^j, \tag{62}$$

one defines the Borel–Leroy transform $\gamma^B(\varepsilon)$ of the series by

$$\gamma^B(\varepsilon) = \sum_j \frac{\gamma^{(j)}}{\Gamma(j + b + 1)} (\varepsilon)^j, \tag{63}$$

b being the fit parameter. Then the value of the initial series may be calculated from

$$\gamma(\varepsilon) = \int_0^\infty dt\ t^b e^{-t} \gamma^B(\varepsilon t). \tag{64}$$

Evaluating this for the truncated series as calculated from the perturbation theory and substituting for $\gamma^B(\varepsilon t)$ in (64) its analytic continuation

in the form of Padé approximant this procedure constitutes the Padé–Borel resummation.

The conformal mapping technique postulates in addition the knowledge of the constant a entering (61). Assuming the behaviour (61) holds also for the expansion of $\gamma(\varepsilon)$ in ε, one concludes that the singularity of the transformed series $\gamma^B(\varepsilon)$ closest to the origin is located at the point $(-1/a)$ and one can map the ε plane onto a circle with a conformal map that leaves the origin invariant:

$$w = \frac{(1+a\varepsilon)^{1/2}-1}{(1+a\varepsilon)^{1/2}+1}, \quad \varepsilon = \frac{4}{a}\frac{w}{(1-w)^2}. \tag{65}$$

Thus one obtains an expression for $\gamma^B(\varepsilon)$ convergent in the whole cut plane and, as a result, the expression for the resummed function γ^{res}. In order to weaken a possible singularity on the w-plane the corresponding expression may be multiplied by $(1-w)^\alpha$ introducing a parameter α. In the resummation procedure the value of a is taken from the known large-order behaviour of the ε-expansion series, while in calculations α is chosen as a fit parameter defined by the condition of minimal difference between resummed 2nd order and 3rd order results. The resummation procedure is seen to be quite insensitive to the parameter b introduced by the Borel–Leroy transformation (63).

For the resummation of the exponents $\eta_{f_1 f_2}$ one can take into account in addition the knowledge of the combinatorial factors which multiply each contribution according to the numbers of chains f_1 and f_2. This leads to an additional factor $(f_1+f_2)^k$ for the kth order contributions. It may be introduced into the resummation procedure by multiplying the constant a by (f_1+f_2). To resum the series at the fixed points S, G and U the following values of $a = a^S, a^G, a^U$ have been derived:[53,103]

$$a^S = a^G = \frac{3}{8} \quad \text{and} \quad a^U = \frac{27}{64}. \tag{66}$$

2.6. *Numerical Results*

We present numerical results for the exponents $\eta^G_{f_1 f_2}$, $\eta^U_{f_1 f_2}$ and η_f^{MAW} as calculated in Ref. 18. Results for the symmetric case $\eta_f^S = \eta^U_{f,0}$ have been calculated using the ε-expansion in Ref. 49 and the pseudo-ε expansion in Ref. 47.

Even though the non-resummed results of different RG approaches differ to great extent for higher numbers of arms, resummation shows the consistency of the approaches on the numerical level. Further applying the

Table 2. Values of the copolymer star exponent $\eta^G_{f_1 f_2}$ at $d = 3$ obtained by ε-expansion (η^G_ε) compared with those obtained by the fixed dimension technique[18] (η^G_{3d}).

f_1	f_2	η^G_ε	η^G_{3d}	f_1	f_2	η^G_ε	η^G_{3d}
1	1	−0.56	−0.58	3	3	−3.38	−3.57
1	2	−0.99	−1.00	3	4	−4.21	−4.50
1	3	−1.33	−1.35	3	5	−4.94	−5.36
1	4	−1.63	−1.69	3	6	−5.62	−6.15
1	5	−1.88	−1.98	4	4	−5.27	−5.71
1	6	−2.10	−2.24	4	5	−6.24	−6.84
2	2	−1.77	−1.81	4	6	−7.12	−7.90
2	3	−2.45	−2.53	5	5	−7.42	−8.24
2	4	−3.01	−3.17	5	6	−8.50	−9.54
2	5	−3.51	−3.75	6	6	−9.78	−11.07
2	6	−3.95	−4.28				

resummation procedure based on the conformal mapping technique as described in the previous section we find the results given in Tables 2–4. Comparing the numerical values listed in the above tables it is convincing that the two approaches and the different resummation procedures all lead to results which lie within a bandwidth of consistency, which is broadening for larger values of the number of chains. This is not surprising as we have seen in Section 2.4 that our expansion parameters are multiplied by the number of chains. It is rather remarkable that even for a total number of chains of the order of 10 (see Tables 2 and 3) we still obtain results comparing well with each other.

3. Multifractal Spectra for the Polymer Absorber Model

Here, we show how to describe the diffusion of particles in the presence of an absorbing polymer using a "polymer" formalism that represents both the RWs of the diffusing particles and the absorber itself in the same way.[30,66,73,109–111] We first formulate this problem in terms of the diffusion of particles in time. The probability to find a diffusing particle at point r_1 at time t if it started at point r_0 at time $t = 0$ can be described by the following normalized path integral:

$$G^0(r_0, r_1, t) = \langle \delta(r^{(1)}(0) - r_0)\delta(r^{(1)}(t) - r_1)\rangle_{\mathcal{H}_0(r^{(1)},t)}. \tag{67}$$

The angular brackets in Eq. (67) stand for the following average:

$$\langle \cdots \rangle_{\mathcal{H}_0(r^{(1)},t)} = \frac{\int (\cdots) \exp(-\mathcal{H}_0(r^{(1)}, t))\ d\{r^{(1)}\}}{\int \exp(-\mathcal{H}_0(r^{(1)}, t))\ d\{r^{(1)}\}}, \tag{68}$$

Table 3. Values of the copolymer star exponent $\eta^U_{f_1 f_2}$ at $d = 3$ obtained by ε-expansion (η^U_ε) and by fixed dimension technique (η^U_{3d}).

f_1	f_2	η^U_ε	η^U_{3d}	f_1	f_2	η^U_ε	η^U_{3d}
1	1	−0.43	−0.45	4	1	−2.39	−2.47
1	2	−0.79	−0.81	4	2	−3.33	−3.50
1	3	−1.09	−1.09	4	3	−4.20	−4.48
1	4	−1.35	−1.37	4	4	−5.02	−5.40
1	5	−1.60	−1.64	4	5	−5.80	−6.30
1	6	−1.81	−1.89	4	6	−6.53	−7.15
2	1	−0.98	−0.98	5	1	−3.21	−3.38
2	2	−1.58	−1.60	5	2	−4.28	−4.57
2	3	−2.13	−2.19	5	3	−5.28	−5.71
2	4	−2.61	−2.71	5	4	−6.24	−6.81
2	5	−3.05	−3.21	5	5	−7.15	−7.89
2	6	−3.46	−3.68	5	6	−8.02	−8.92
3	1	−1.64	−1.67	6	1	−4.11	−4.40
3	2	−2.44	−2.52	6	2	−5.29	−5.73
3	3	−3.16	−3.30	6	3	−6.41	−7.03
3	4	−3.82	−4.04	6	4	−7.48	−8.28
3	5	−4.44	−4.75	6	5	−8.51	−9.50
3	6	−5.01	−5.42	6	6	−9.50	−10.69

Table 4. Values of η^{MAW}_f exponents of star of mutually avoiding walks at $d = 2$, $d = 3$ obtained by ε-expansion ($\eta^{\mathrm{MAW}}_\varepsilon$) and by fixed dimension technique[18] (η^{MAW}_{3d}, η^{MAW}_{2d}). The last column gives the exact conjecture[35,36] $\eta^{\mathrm{MAW}}_{\mathrm{exact}}$ for $d = 2$.

	$d = 3$		$d = 2$		
f	$\eta^{\mathrm{MAW}}_\varepsilon$	η^{MAW}_{3d}	$\eta^{\mathrm{MAW}}_\varepsilon$	η^{MAW}_{2d}	$\eta^{\mathrm{MAW}}_{\mathrm{exact}}$
1	0	0	0	0	−0.250
2	−0.56	−0.56	−1.20	−1.19	−1.250
3	−1.38	−1.36	−2.71	−2.60	$-2.91\bar{6}$
4	−2.36	−2.34	−4.36	−4.07	−5.250
5	−3.43	−3.43	−6.04	−5.61	−8.250
6	−4.58	−4.64	−7.78	−7.17	$-11.91\bar{6}$
7	−5.81	−5.93	−9.57	−8.75	−16.250
8	−7.09	−7.30	−11.42	−10.36	−21.250
9	−8.42	−8.74	−13.31	−11.97	$-26.91\bar{6}$
10	−9.81	−10.24	−15.25	−13.60	−33.250

which is performed with the Hamiltonian:

$$\mathcal{H}_0(r^{(1)}, t) = \int_0^t \left(\frac{dr^{(1)}(\tau)}{2\, d\tau} \right)^2 d\tau. \tag{69}$$

The integration in Eq. (67) is over all paths $r^{(1)}(\tau)$ with $0 \leq \tau \leq t$. Here, the diffusion constant is absorbed by a re-definition of time. The unit of the dimensionless Hamiltonian $\mathcal{H}_0$ is the product $k_{\mathrm{B}}T$ of the Boltzmann constant and temperature while that of time t is the square microscopic length ℓ^2. Spatial boundaries may be included in Eq. (67) by restricting the path integral to a subspace. The path integrals in Eq. (68) are Gaussian and may be performed with the boundary conditions of Eq. (67) and shown to be equivalent to the solution of the following harmonic differential equation:[7]

$$\Big(\Delta_{r_0} - \frac{\partial}{\partial t}\Big) G^0(r_0, r_1, t) = 0, \qquad G^0(r_0, r_1, 0) = \delta(r_1 - r_0). \tag{70}$$

Let us introduce the absorbing polymer into the system volume. The latter is assumed to be of much larger size than the absorber itself. The probability to diffuse from r_0 to r_1 is now $G(r_0, r_1, t)$. Walks that touch the absorber cannot contribute to this probability. The absorber itself is again described by a path $r^{(2)}(s)$, $0 \leq s \leq S_2$. The boundary condition is implemented by an avoidance interaction u_{12} punishing any coincidence of the path $r^{(1)}$ of the RW and the path $r^{(2)}$ of the absorber. The correlation function of a RW in the presence of an absorbing path $r^{(2)}(s)$ with $0 \leq s \leq S_2$ may then be written as

$$\begin{aligned} &G(r_0, r_1, S_1) \\ &= \Bigg\langle \delta(r^{(1)}(0) - r_0)\delta(r^{(1)}(S_1) - r_1) \\ &\quad \times \exp\left(-\frac{u_{12}}{3!}\int_0^{S_1} ds_1 \int_0^{S_2} ds_2 \; \delta(r^{(1)}(s_1) - r^{(2)}(s_2)\right)\Bigg\rangle_{\mathcal{H}_0(r^{(1)}, S_1)}, \end{aligned} \tag{71}$$

where we have adopted the notation $t = S_1$. Obviously this is symmetric in r_0 and r_1. The probability to find a particle at $t = 0$ in r_0 if it was launched at time $t = -\infty$ at any point r_1 in the volume is then described by the field

$$\rho(r_0) = \lim_{S_1 \to \infty} \frac{1}{V} \int dr_1 \; G(r_0, r_1, S_1). \tag{72}$$

Due to Eq. (70) which is not perturbed in the volume outside the absorber, $\rho(r_0)$ obeys the Laplace equation:

$$\Delta\rho(r) = 0, \tag{73}$$

with the following boundary conditions. Because of the avoidance condition ρ vanishes on the absorber. If the integration volume boundary ∂V is far

enough from the absorber we may at least in 3D assume a steady state situation with a constant concentration $\rho = \rho_\infty$ on ∂V.

The central object of interest in the present context is the ensemble averaged moment $\langle \rho^n(r_0+\xi)\rangle$ of the field in the vicinity of the absorber, i.e. with microscopic ξ. For the RW ensemble the average is performed with respect to the Hamiltonian $\mathcal{H}_0(r^{(2)}, S_2)$, for the SAW ensemble an additional interaction has to be included. The moments we calculate as an ensemble average over all configurations of the absorbing polymer choosing the site r_0 in the middle of the polymer. This redefinition leads to some peculiarities in the MF spectrum as discussed in Refs. 30 and 73 and as we will see later. Formally we write these moments for $\xi \to 0$ as

$$\lim_{|\xi|\to 0} \langle \rho^n(r_0+\xi)\rangle = \lim_{S_{a>m}\to\infty} \frac{1}{\mathcal{Z}^0_{*m0}} \int \prod_{a=1}^{m+n} dr_a \, G^*_{mn}(r_0, r_1, \ldots, r_{m+n}, S_1, \ldots, S_{m+n}). \quad (74)$$

The normalization $\mathcal{Z}^0_{*m0}$ takes care of the configurations of the absorber, as explained in the next section, whereas the correlation function G^*_{mn} is defined as

$$\begin{aligned} &G^*_{mn}(r_0, r_1, \ldots, r_{m+n}, S_1, \ldots, S_{m+n}) \\ &\quad = \left\langle \prod_{a=1}^{m+n} \delta(r^{(a)}(0) - r_0)\delta(r^{(a)}(S_a) - r_a) \exp\left(-\sum_{a,b=1}^{m+n} \frac{\bar{u}_{ab}}{3!} \right.\right. \\ &\qquad \left.\left. \times \int_0^{S_a} ds_a \int_0^{S_b} ds_b \; \delta(r^{(a)}(s_a) - r^{(b)}(s_b)) \right) \right\rangle_{\mathcal{H}_0^{mn}}, \\ &\mathcal{H}_0^{mn} = \sum_{a=1}^{m+n} \mathcal{H}_0(r^{(a)}, S_a). \end{aligned} \quad (75)$$

Here, the absorbing walk is represented by $m = 2$ paths and $r^{(1)}$, $r^{(2)}$, while the remaining n paths represent n RWs, as shown in Fig. 6. The interaction matrix $\bar{u}_{ab}$ is in this case given by $\bar{u}_{ab} = \{0$ if $a, b \le m$ or $a, b > m$; u_{12} else$\}$.

The limits in Eq. (74) look rather ill-defined at first sight, and indeed they should not be taken naively. Also the evaluation of the functional integral (75) is not defined in this bare form. Having at hand the polymer field theory elaborated in the previous sections, the problems of evaluating these formal expressions are solved by mapping the situation to a renormalizable

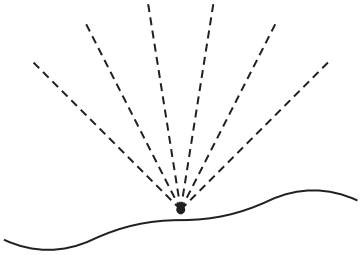

Fig. 6. Sketch of a set of RWs of particles that are absorbed on a polymer chain.

$O(m)$ symmetric field theory in terms of which the limits and a perturbative expansion of (75) make sense. For instance the limit $|\xi| \to 0$ may be interpreted as a short-distance limit defining a composite operator, while the limit $S_{a>m} \to \infty$, with $S_{b\leq m}$ staying finite corresponds to a short-chain limit[102] as given in Eq. (54). In the frames of the polymer picture $G^*_{mn}(r_0, r_1, \ldots, r_{m+n}, S_1, \ldots, S_{m+n})$ is the correlation function of $m+n$ interacting walks all starting at point r_0 with endpoints at $r_1, \ldots, r_{m+n}$ describing a corresponding polymer star. The normalized partition function of this star of $m+n$ polymer chains with chain lengths parameterized by S_a is related to G^*_{mn} by[12,15,20,49]

$$\mathcal{Z}_{*mn}\{S_a\} = \frac{1}{\mathcal{N}_{mn}} \int \prod_{a=1}^{m+n} dr_a \, G^*_{mn}(r_0, r_1, \ldots, r_{m+n}, S_1, \ldots, S_{m+n}). \quad (76)$$

The normalization $\mathcal{N}_{mn}$ is chosen such that $\mathcal{Z}_{*mn}\{S_a\}|_{\bar{u}_{ab}=0} = 1$ for vanishing interactions and the point r_0 is arbitrary. This allows us to think of the absorbing paths $r^{(1)}, \ldots, r^{(m)}$ as being either of a RW ($u_{11} = 0$) or of a SAW ($u_{11} \neq 0$) ensemble. The moments of the diffusion field near the core of a polymer star are described for $m > 2$.

The scaling may be formulated in terms of the size R of the absorbing walks while the RWs of the diffusing particles are taken infinitely long corresponding to the short-chain expansion,[102] see Eq. (54). The partition function is normalized by the number of configurations of the absorber given by $\mathcal{Z}_{*m0}$ and by the nth power of the first moment [see Eq. (5)]. For large R on the microscopic scale ℓ, the moments of $\rho(r_0)$ at point r_0 in the vicinity of the core of the star scale like

$$\frac{\langle \rho(r_0)^n \rangle}{\langle \rho(r_0) \rangle^n} = \mathcal{Z}_{*mn}/\mathcal{Z}_{*m0}(\mathcal{Z}_{*m1}/\mathcal{Z}_{*m0})^{-n} \sim \left(\frac{R}{\ell}\right)^{-\tau_{mn}}. \quad (77)$$

Here $R = S^{\nu}_{a\leq m}$ is the radius of the absorbing polymer (star) which is much smaller than the radii of the RWs describing diffusing particles. Matching (77) with Eqs. (51)–(53) the exponents τ_{mn} are then given by either of

$$\tau^{G}_{mn} = -\eta^{G}_{mn} + n\eta^{G}_{m1}, \tag{78}$$

$$\tau^{U}_{mn} = -\eta^{U}_{mn} + n\eta^{U}_{m1} - (n-1)\eta^{U}_{m0}. \tag{79}$$

Here, the τ^U exponents correspond to the case of a SAW absorber and $\nu \simeq 0.588$ for SAWs at $d = 3$ while a τ^G exponent corresponds a RW absorber and $\nu = \frac{1}{2}$.

3.1. *Multifractal Spectrum*

A widely used characterization for the MF spectrum is the so-called spectral function $f_m(\alpha)$.[64] To obtain this function for the absorption process at the center of a star with m legs we analytically continue the set of exponents τ_{mn} in the variable n and calculate the following Legendre transform

$$f_m(\alpha_{mn}) = -\tau_{mn} + n\alpha_{mn} + D_m \quad \text{with} \quad \alpha_{mn} = \frac{d\tau_{mn}}{dn} + D_m. \tag{80}$$

Following the standard definition, the fractal dimension D_m of the absorber is included into Eq. (80). In particular, this gives the maximal value of the spectral function $f_m(\alpha_{mn})$ to be equal to the dimension D_m. An absorbing chain is described by the case $m = 2$ where $D_2 = 2$ if the chain is a random walk, and $D_2 = 1.71$ if it is self-avoiding. In this special case the mid point of the chain corresponding to the "core" of the 2-star is equivalent to any other point along the chain as far as the MF scaling of the moments of concentration is concerned. This excludes the endpoint regions which are described by the $m = 1$ case. D_2 thus corresponds to the fractal dimension of this set of equivalent points. There appears to be no natural generalization of D_m to arbitrary m where only the moments of concentration near a special point of the absorbing structure (the core of the star) are of interest. In any case D_m only shifts the curve of the spectral function $f(\alpha)$ in the f–α plane by a constant offset. In our presentation we have chosen this offset in such a way that for all m the maximal point of the spectral curve coincides with that of the case $m = 2$. This corresponds to the fact that the fractal dimension of a polymer star is equal to that of a linear chain.

In the $m = 2$ case the moments of concentration may also be defined by an average over all the sites along the chain. For a very long chain one may expect this average to be equivalent to an average of the moments of

concentration at the mid point site using an ensemble average over all configurations of the chain.[30,73] The site average has been the original approach to multifractality also due to its easier application in MC simulations. For general m new interesting behaviour occurs only in the vicinity of the core of the star. Here, only an ensemble average can be used to define the moments of concentration near this point. The same approach is used here for all values of m. Note that some features of MF spectra that are defined using site averages do not hold for those based on ensemble averages. This is discussed below.

Expressions for the spectral function have been derived using the perturbation expansions for the η-exponents given to third order both in massless and massive renormalization.[17,18] Starting from the relations for τ_{mn} (79) and the spectral function (80) some algebra results in the following ε-expansions of the MF spectra for absorption on stars of RWs and SAWs are:[20]

$$\alpha_{mn}^{\mathrm{RW}}(\varepsilon) = -m(2n-1)\frac{1}{8}\varepsilon^2 + m[4mn + 6n\zeta(3) - 12n + 3n^2 + 5 - 2m - 3\zeta(3)]\frac{1}{16}\varepsilon^3, \quad (81)$$

$$f_m^{\mathrm{RW}}(\alpha) = -mn^2\frac{1}{8}\varepsilon^2 + mn^2\frac{1}{16}[-6 + 2n + 2m + 3\zeta(3)]\varepsilon^3, \quad (82)$$

$$\alpha_{mn}^{\mathrm{SAW}}(\varepsilon) = -9m(2n-1)\frac{1}{128}\varepsilon^2 + 3m[168mn + 54n^2 + 157 + 180n\zeta(3) - 350n - 84m - 90\zeta(3)]\frac{\varepsilon^3}{2048}, \quad (83)$$

$$f_m^{\mathrm{SAW}}(\alpha) = -\frac{9mn^2\varepsilon^2}{128} + \frac{3mn^2\varepsilon^3}{2048}[-175 + 36n + 84m + 90\zeta(3)], \quad (84)$$

Here, $\zeta(3) \simeq 1.202$ is the value of the Riemann zeta function.

3.2. *Resummation and Results*

To extract numerical results, the series in Eqs. (81)–(84) must be treated by resummation as explained in Section 2.5. Numerical results for the spectral functions calculated in Ref. 20 are presented in Fig. 7. Each point marked by a symbol corresponds to the resummation of both $f_m(\alpha_{mn})$ and α_{mn} for a given pair (m, n) in half-integer spacing for the values of n. Note that the right wings of the curves correspond to negative $n < 0$. In this region reliable resummations are feasible only for sufficiently large m.

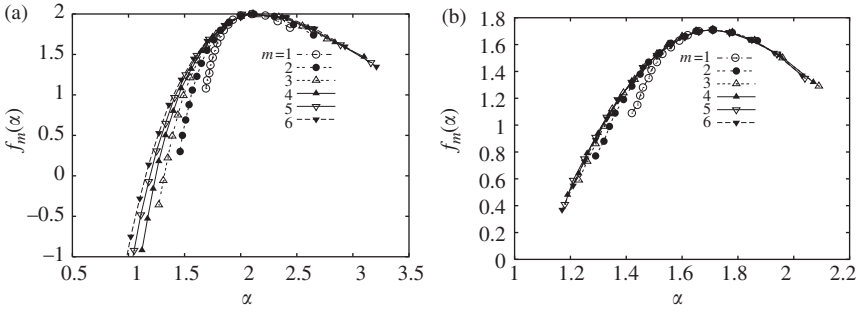

Fig. 7. The multifractal spectrum governing the harmonic measure of diffusion near an absorbing (a) star of RWs or (b) a star polymer.

Figures 7a and 7b present the resummed MF spectra $f_m(\alpha)$ of Brownian motion near general m-leg polymer stars in $d = 3$ dimensions. The family of curves $f_m(\alpha)$ appears to approach some limiting envelope for increasing m in both cases. This behaviour is more pronounced in the case of Brownian motion near an absorbing SAW star. This provides evidence that the MF spectrum catches rather general properties of the phenomena under consideration. Here, for the absorption of diffusing particles on a polymer star the spectrum only slightly varies with the number of legs m of the star even in the vicinity of the core of the star. Only the absorption on an endpoint ($m = 1$) proves to be an exception.

The behaviour of the maximum of the spectra may also be studied in terms of a series expansion. The original position of the maximum is given by its α-coordinate in the ε-expansion in the following form:

$$\alpha_{m,0} = \eta_{m,1} - \eta'_{m,0}, \tag{85}$$

$$\alpha_{\max}^{\mathrm{RW}} = \frac{1}{8} m\varepsilon + \cdots, \tag{86}$$

$$\alpha_{\max}^{\mathrm{SAW}} = \frac{1}{8} m(1-m)\varepsilon + \cdots. \tag{87}$$

For $m > 1$ the position of the SAW maximum is shifted in the opposite direction to that of the RW maximum. In the ε-expansion the curvature at the maximum is:

$$\frac{1}{f''_m}(\alpha) = -\eta''_{m,0}, \tag{88}$$

$$\frac{1}{f''^{\mathrm{RW}}_m}(\alpha) = -m\frac{\varepsilon^2}{4}\left\{1 - \frac{\varepsilon}{2}[2m - 6 + 3\zeta(3)] + \cdots\right\}, \tag{89}$$

$$\frac{1}{f_m''^{\mathrm{SAW}}}(\alpha) = -9m\frac{\varepsilon^2}{64} + \cdots . \tag{90}$$

Here, the notation

$$f_m'(\alpha) = (d/d\alpha) f_m(\alpha_{m,n})|_{n=0}, \qquad \eta_{m,n}' = (d/dn)\eta_{m,n}|_{n=0}$$

and correspondingly for higher derivatives, is used. As can be seen also in the plots, the radius $\mathcal{R}_m \sim |1/f_m''(\alpha)|$ of the curvature increases with m for both the RW and the SAW star. Some asymmetry is also present in the curves. It may be more explicitly extracted from the series by considering

$$\frac{f_m''(\alpha)}{f_m'''(\alpha)} = \frac{(\eta_{m,0}'')^2}{\eta_{0,m}'''}, \tag{91}$$

$$\frac{f_m''^{\mathrm{RW}}(\alpha)}{f_m'''^{\mathrm{RW}}(\alpha)} = \frac{m\varepsilon}{12}\{1 - \varepsilon[2m - 6 + 3\zeta(3)] + \cdots\}, \tag{92}$$

$$\frac{f_m''^{\mathrm{SAW}}(\alpha)}{f_m'''^{\mathrm{SAW}}(\alpha)} = \frac{m\varepsilon}{16}\left\{1 - \varepsilon\left[\frac{7}{2}m - \frac{175}{24} + \frac{15}{64}\zeta(3)\right] + \cdots\right\}. \tag{93}$$

This shows that the asymmetry at the maximum decreases slightly with m. The plots seem to indicate that it approaches some limiting value.

From the plots we present here, in general one may deduce that the series for the MF spectra for diffusion near an absorbing polymer star possess stable resummations and that the shape of the resulting curves is robust against the change of the number of legs m of the polymer star, while a limiting curve appears to be approached with increasing m.

4. Comparison with 2D Exact Results

While star polymers are difficult to realize experimentally, their study is of some theoretical interest and they may be related to 2D diffusion processes corresponding to the situations described in Section 3. The scaling dimensions of two-dimensional uniform polymer stars belong to a limiting case of the so-called conformal Kac table of conformally invariant theories.[112–114] They have also been calculated exactly by Coulomb gas techniques.[12,14] Exact relations have also been proposed for stars of mutually avoiding walks[35,36] and for the copolymer star system.[40,44]

Exact results for exponents of two-dimensional systems which are described by a conformally invariant field theory with central charge $c < 1$

may be taken from the Kac table of scaling dimensions:

$$h_{p,q}(m) = \frac{[(m+1)p - mq]^2 - 1}{4m(m+1)}\,, \tag{94}$$

where p, q are integers in the minimal block

$$1 \le p \le m-1, \quad 1 \le q \le p \tag{95}$$

and m is connected with the central charge c by

$$c = 1 - 6/m(m+1), \quad m \ge 3. \tag{96}$$

The exact result for the star exponents of uniform stars in two dimensions is obtained in the limiting case of $m = 2$ (which means central charge $c = 0$) for half-integer values of p,

$$x_f = 2h_{f/2,0}(2) = (9f^2 - 4)/48. \tag{97}$$

The scaling dimension x_f is related to the exponent η_f^S by

$$x_f = -\eta_f^S + \frac{1}{2}(d - 2 + \eta_\phi)f\,, \tag{98}$$

with $\eta_\phi = \frac{5}{24}$ for $d = 2$. For the 2D exponents of the star of MAW the following result has been conjectured:[35,36]

$$\eta_f^{\mathrm{MAW}} = -x_f^{\mathrm{MAW}} = -2h_{0,f}(2) = \frac{1 - 4f^2}{12}\,. \tag{99}$$

These values are shown in the last column of Table 4. Plotting the resummed data for η_f^{MAW} from Table 4 with respect to f^2 one finds good agreement with the conjectured slope of $-1/3$.

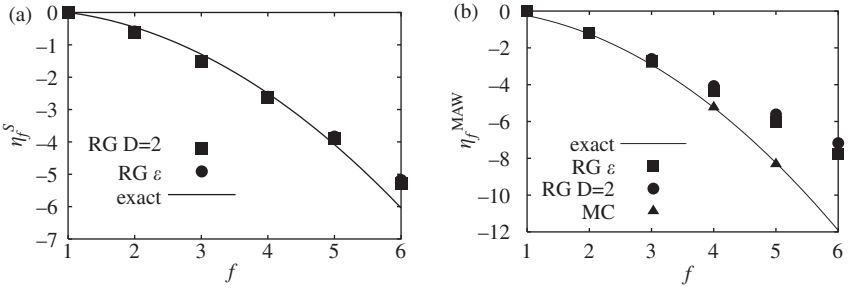

Fig. 8. 2D exponents η_f^S and η_f^{MAW} obtained in the ε-expansion and in the fixed $d = 2$ RG scheme, in comparison with exact results and MC simulations.[12,36]

The behaviour of the exponents η_f^S and η_f^{MAW} is shown in Fig. 8 comparing the results of the extrapolation of the perturbative approach to $d = 2$ dimensions with the exact prediction, as well as with an MC simulation for the MAW case. In Ref. 40 exact results for the $d = 2$ copolymer star of two or more mutually avoiding bunches of SAWs and RWs are proposed. In the following, exact expressions for the corresponding exponents are derived from Ref. 40, where relations between exponents in fluctuating geometry (quantum gravity) and flat 2D geometry are used to extract the exact 2D exponents. We note that at least for the RW case (i.e. exponents η^G) these results have been rigorously confirmed by probabilistic mathematical methods.[42] The relations read

$$\eta^G_{f_1,f_2} = \frac{1}{48}\{4 - [\sqrt{24f_1+1} + \sqrt{24f_2+1} - 2]^2\}, \tag{100}$$

$$\eta^U_{f_1,f_2} = \frac{1}{48}\{4 + 5f_1 - [3f_1 + \sqrt{24f_2+1} - 1]^2\}. \tag{101}$$

The starting point in both cases is the 2D boundary scaling dimensions for a polymer (SAW) and for Brownian walks (RW) with one extremity at a Dirichlet boundary in the flat geometry which read[12,115]

$$\tilde{\Delta}_P^{(0)}(1) = \frac{5}{8}, \qquad \tilde{\Delta}_B^{(0)}(1) = 1, \qquad \tilde{\Delta}_B^{(0)}(f) = f, \tag{102}$$

for a single polymer, a single RW and a set of f transparent RWs, respectively. The last equation reflects the fact that the scaling dimensions of transparent, i.e. noninteracting, walks are additive in planar geometry. Mapping these situations to the boundary of a random surface, the following remarkable relation of the corresponding random boundary dimensions to the planar boundary ones, given by Knizhnik *et al.,* applies:[46]

$$\tilde{\Delta} = U^{-1}(\tilde{\Delta}^{(0)}), \qquad U^{-1}(x) = \frac{1}{4}(\sqrt{24x+1} - 1)\,. \tag{103}$$

With these relations one finds for the above cases

$$\tilde{\Delta}_P(1) = \frac{3}{4}, \tag{104}$$

$$\tilde{\Delta}_B(1) = 1, \tag{105}$$

$$\tilde{\Delta}_B(f) = \frac{1}{4}(\sqrt{24f+1} - 1). \tag{106}$$

Note that while the dimensions of the transparent RWs are additive at the planar boundary, they are coupled at the random boundary. On the other hand, as shown by Duplantier[40,44] *interacting* sets of walks will

decouple at the random boundary rendering their scaling dimensions additive. This means that for a set of f_1 interacting polymers with one extremity at a common point at the random boundary one finds

$$\tilde{\Delta}_P(f_1) = \frac{3}{4} f_1. \tag{107}$$

When this set of polymers is interacting with a second set of mutually transparent RWs f_2, or when two sets of f_1 and f_2 transparent RWs are mutually avoiding, the corresponding random boundary dimensions are, respectively,

$$\tilde{\Delta}^U(f_1, f_2) = \frac{3}{4} f_1 + \frac{1}{4}(\sqrt{24 f_2 + 1} - 1), \tag{108}$$

$$\tilde{\Delta}^G(f_1, f_2) = \frac{1}{4}(\sqrt{24 f_2 + 1} - 1) + \frac{1}{4}(\sqrt{24 f_2 + 1} - 1). \tag{109}$$

Again, using the relations of Knizhnik *et al.,* we can now map to the bulk random and bulk planar situations with scaling dimensions

$$\Delta = \frac{1}{2}(\tilde{\Delta} + \gamma_{\rm str}), \qquad \gamma_{\rm str} = -\frac{1}{2}, \tag{110}$$

$$\Delta^{(0)} = U(\Delta) = V(\tilde{\Delta}), \quad V(x) = \frac{1}{24}(4x^2 - 1), \tag{111}$$

where the string suseptibility exponent[116] $\gamma_{\rm str}$ is evaluated for the sphere. For the above situations we thus find the planar bulk dimensions

$$\Delta^{(0)G}(f_1, f_2) = \frac{1}{96}\{[\sqrt{24 f_1 + 1} + \sqrt{24 f_2 + 1} - 2]^2 - 4\}, \tag{112}$$

$$\Delta^{(0)U}(f_1, f_2) = \frac{1}{96}\{[3 f_1 + \sqrt{24 f_2 + 1} - 1]^2 - 4\}. \tag{113}$$

Finally we note the relations between these bulk dimensions with the exponents η used throughout this review,

$$\eta^G_{f_1, f_2} = -2\Delta^{(0)G}(f_1, f_2), \tag{114}$$

$$\eta^U_{f_1, f_2} = -2\Delta^{(0)U}(f_1, f_2) + f_1 \frac{1}{2}\eta_\phi, \qquad \eta_\phi(2D) = \frac{5}{24}. \tag{115}$$

Note a mismatch between Eqs. (51)–(53) and the discussion of Eq. (3) in Ref. 40 where one should read $x_{P,1} = \eta_2^S - \eta_\phi/2$ instead of $x_{P,1} = \eta_\phi/2$.

These exact 2D results have been compared to the 2D extrapolation of the perturbation theory as well as checked by a MC simulation for the simplest case when the copolymer star consists of RWs only. In these simulations[48] the stars are grown on a square lattice until a non-allowed intersection occurs. The number of stars $C(N)$ generated during the growing process is accumulated for all chain lengths N. Exponents are

extracted assuming a power law $C(N) \sim N^{-\nu_0 \lambda_{f_1,f_2}}$. For stars up to a maximum chain length $N_{\max} = 10^3$ these configurations are accumulated until $C(N_{\max}) = 10^5$. The number of successful attempts to grow stars with longer chains decreases rapidly for higher $f_1 + f_2$, which increases the simulation time drastically. While for the case $1+1$ a total of 10^6 attempts are needed, this number rises to 5×10^9 for $5+1$. Therefore, results in Table 5 are given only for $f_1 + f_2 \leq 6$ together with the statistical error in the lines marked "MC" and "$\pm\Delta$", and compared with the exact numbers according to Eq. (100). The results are in fair agreement despite a slightly growing discrepancy as the number of RWs f_2 increases. Note that only after restoring convergence of the ε-expansion by resummation may reliable exponent values be extracted. The same resummation is applied for the renormalization group expansions at fixed $d = 2$, also reported in Table 5. For $\eta^G_{1,2}$ also perturbation theory gives the exact result at first order with all higher orders vanishing.[117]

In the perturbative treatment (which starts from the upper critical dimension[5,6] $d = 4$) the order of the chains in the star does not matter for the scaling laws: there is always a possibility for every chain to interact with any other chain constituting a star. On the other hand, in $d = 2$ the order of chains does matter: each chain of the star will interact only with its direct neighbours. This topological restriction has to be taken into account when comparing exact and perturbative results for $d = 2$ linked polymers.

The data of Table 5 convince us that perturbation theory series for low numbers of chains f_2 is reliable even for $d = 2$. Also, we note that the $d = 2$ copolymers with $f_1 = 2$ are less well described by perturbation theory than those with $f_1 = 1$ where the topological restriction is not present, due to the symmetry of ordering.

Table 5. 2D exponents $-\eta^G_{f_1,f_2}$ (f_1 RWs and f_2 RWs) calculated by different techniques.

$f_1; f_2$	1;1	1;2	1;3	1;4	1;5	2;2	2;3	2;4	2;5
Exact	1.25	2	2.693	3.356	4	2.916	3.738	4.510	5.25
MC	1.251	1.986	2.662	3.295	3.908	2.913	3.703	4.506	
$\pm\Delta$	0.004	0.004	0.005	0.015	0.022	0.005	0.030	0.039	
$d = 2$	1.22	2.00	2.58	3.04	3.43	3.45	4.59	5.52	6.34
ε^3	1.20	2.00	2.56	2.99	3.36	3.41	4.49	5.37	6.13

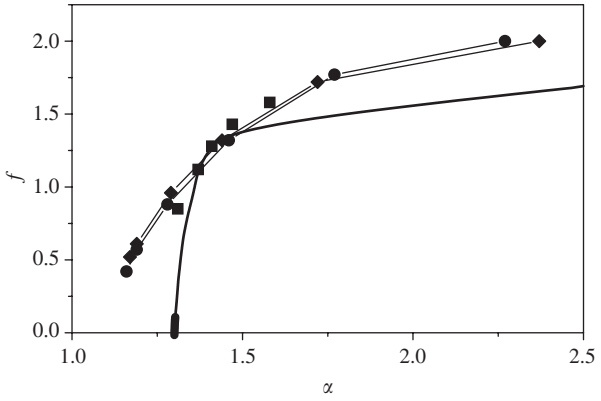

Fig. 9. The spectral function for the absorption at a RW end. Bold line: exact. Symbols: MC (■, size is larger than error bars); the resummed ε^3 (●), and $d = 2$ data (♦) are connected by thin lines.

4.1. *Multifractal Spectrum in 2D*

For the diffusion of freely moving particles in the presence of a polymer absorber we have seen in Section 3 that the moments of particle density display universal scaling laws in the vicinity of the absorbing polymer. According to the standard definition[30] we have included into (80) the fractal dimension D_m of the absorber. In particular, this gives the maximal value of the spectral function to be equal to D_m. There appears to be no natural generalization of D_m for arbitrary m. In our presentation we use a fractal dimension for a polymer star, which equals to that of a polymer chain ($d = 2$ for a RW and $d = \frac{4}{3}$ for a SAW in $d = 2$, correspondingly). Another way to define the multifractal spectrum is chosen in Ref. 40 where the nth moments (77) are normalized not by $\langle\phi\rangle^n$ but by $\langle\phi\rangle$. This choice has the remarkable feature that without introducing an additional dimension d in (80) the maximum of $f(\alpha)$ is $d = 4/3$ for both the SAW and the RW absorbers with $f_1 = 2$. However, this definition is not valid for $d = 3$, where it does not lead to the correct location of the spectral function maximum.

We display the spectral function for the case of the absorption at a RW end in Fig. 9. The spectral function is negative for some values of α. This behaviour has already been observed in the perturbative studies of Ref. 30 and related to the ensemble average in formula (77), in contrast to the usual site average over the support of the measure. Comparing the perturbative, the MC and the exact results, we note that the region of $1 < n < 5$ in

which reasonable agreement for the dimension spectra λ and τ is found corresponds to a rather small region in terms of the parameter α in the left wing of the spectral functions.

5. Scaling Theory of Forces between Star Polymers

5.1. *Two-Star Polymers*

We now turn to the effective interaction between the cores of two star polymers at small distances r that are small on the scale of the size R_g of the stars. For the moment we consider a more general case of two star polymers with f_1 and f_2 arms respectively. The cores of the two stars are at a distance r from each other. We assume all chains involved to be of the same length. The power law for the partition sum $\mathcal{Z}^{(2)}_{f_1 f_2}(r)$ of two star polymers may then be derived from a short-distance expansion. This expansion is originally established in the field theoretic formulation of the n-component spin model. While we do not intend to give any details of these considerations here, applications to polymer theory may be found in Refs. 15 and 102. The relevant result on the other hand is simple enough: the partition sum of the two stars $\mathcal{Z}^{(2)}_{f_1 f_2}(N, r)$ at a small distance r factorizes into a function $C_{f_1 f_2}(r)$ of r alone and the partition function $\mathcal{Z}_{f_1+f_2}(N)$ of the star with $f_1 + f_2$ arms that is formed when the cores of the two stars coincide,

$$\mathcal{Z}^{(2)}_{f_1 f_2}(N, r) \sim C_{f_1 f_2}(r) \mathcal{Z}_{f_1+f_2}(N). \tag{116}$$

For the function $C_{f_1 f_2}(r)$ one may show that power-law scaling for small r holds in the form

$$C_{f_1 f_2}(r) \sim r^{\Theta^{(2)}_{f_1 f_2}}, \tag{117}$$

with the contact exponent $\Theta^{(2)}_{f_1 f_2}$. To find the scaling relation for this power law we change the length scale in (116) in an invariant way by letting $r \to \lambda r$ and $N \to \lambda^{1/\nu} N$. The scaling of the partition function $\mathcal{Z}^{(2)}_{f_1 f_2}$ may be shown to factorize into the contributions for the two stars. This transforms (116) to

$$\begin{aligned} &\lambda^{-1/\nu(\gamma_{f_1}-1)} \lambda^{-1/\nu(\gamma_{f_2}-1)} \mathcal{Z}^{(2)}_{f_1 f_2}(\lambda^{1/\nu} N, \lambda r) \\ &\quad \sim \lambda^{-\Theta^{(2)}_{f_1 f_2}} C_{f_1 f_2}(\lambda r) \lambda^{-1/\nu(\gamma_{f_1+f_2}-1)} \mathcal{Z}_{f_1+f_2}(\lambda^{1/\nu} N)\,. \end{aligned} \tag{118}$$

Collecting powers of λ provides the scaling relation

$$\begin{aligned} \nu \Theta^{(2)}_{f_1 f_2} &= (\gamma_{f_1} - 1) + (\gamma_{f_2} - 1) - (\gamma_{f_1+f_2} - 1)\,, \\ \Theta^{(2)}_{f_1 f_2} &= \eta^S_{f_1} + \eta^S_{f_2} - \eta^S_{f_1+f_2}\,. \end{aligned} \tag{119}$$

We now specialize our consideration to the interaction between two stars of equal numbers of arms $f_1 = f_2 = f$. The mean force $F_{ff}^{(2)}(r)$ between the two star polymers at short distance r is then easily derived from the effective potential $V^{\rm eff}(r) = -k_{\rm B}T \log[\mathcal{Z}_{ff}^{(2)}(r)/(\mathcal{Z}_f)^2]$ with $k_{\rm B}T$ denoting the thermal energy. For the force this results in

$$\frac{1}{k_{\rm B}T} F_{ff}^{(2)}(r) = \frac{\Theta_{ff}^{(2)}}{r}. \tag{120}$$

For large f the leading coefficient of the kth order term ε^k in Eq. (56) is multiplied by f^{k+1}. This is due to combinatorial reasons. It limits the use of the series to low values of f.

Another possibility to estimate the values of the star polymer scaling exponents γ_f is to consider the limiting case of many arm star polymers. For large f each chain of the star is restricted approximately to a cone of solid angle $\Omega_f = 4\pi/f$. In this cone approximation one finds[118] for large f

$$\gamma_f \sim -f^{3/2}. \tag{121}$$

The cone approximation for the contact exponents[3] $\Theta_{ff}^{(2)}$ may be matched to the known values for $f = 1, 2$ (see Table 1), fixing the otherwise unknown prefactor. Assuming that the behaviour of the $\Theta_{ff}^{(2)}$ may be described by the cone approximation for all f, one finds:

$$F_{ff}^{(2)}(r) \approx \frac{5}{18} \frac{f^{3/2}}{r}. \tag{122}$$

This matching in turn suggests an approximate value for the η_f exponents,

$$\eta_f^S \approx -\frac{5}{18}(2^{3/2} - 2)^{-1}(f^{3/2} - f), \tag{123}$$

consistent with the exact result $\eta_1 = 0$. This approximation works well for $\Theta_{ff}^{(2)}$ in the range $f = 1, \ldots, 6$ where we have calculated the corresponding values from the perturbation theory results as well as according to the cone approximation. Our results, displayed in the second part of Table 6, show good correspondence of the cone approximation with the resummation values.

5.2. *Three Stars*

The idea of the short-distance expansion has been extended to derive the triplet interaction of three star polymers at close distance.[50] One considers a symmetric situation in which the three cores of the polymer stars are located on the corners of an equilateral triangle (see Fig. 10). The distance

Table 6. Calculation of the exponents that govern the pair and triplet interactions. The labels (a) and (b) stand for the two complementary renormalization group approaches (expansion in $\varepsilon = 4 - d$ and massive renormalization at $d = 3$) used to calculate the exponents η_f. The difference between the two results may be taken as an estimation of the error of the method. Label (c) stands for the cone approximation result with matching to $f = 1, 2$ as explained in the text.

f	1	2	3	4	5	6
a η_f	0	−0.28	−0.75	−1.36	−2.07	−2.88
b	0	−0.28	−0.76	−1.38	−2.14	−3.01
f		8	9	10	12	15
a η_f		−4.71	−5.72	−6.80	−9.12	−12.98
b		−5.06	−6.22	−7.48	−10.23	−14.93
f	1	2	3	4	5	6
a $\Theta^{(2)}_{ff}$	0.28	0.80	1.38	1.99	2.66	3.36
b	0.28	0.82	1.49	2.30	3.20	4.21
c	0.28	0.79	1.44	2.22	3.11	4.08
a $\Theta^{(3)}_{fff}$	0.75	2.04	3.47	5.04	6.77	
b	0.76	2.17	3.94	6.09	8.51	
c	0.74	2.08	3.83	5.89	10.82	
a $\Delta F/F$	−0.11	−0.15	−0.16	−0.16	−0.15	
b	−0.09	−0.12	−0.12	−0.12	−0.11	
c	−0.11	−0.11	−0.11	−0.11	−0.11	

between the cores is r while their distance to the center of the triangle is R. We assume that the radius of gyration R_g of the star polymers is much larger than their mutual distance $R_g \gg r$.

To make the argument more transparent let us treat the slightly more general case of three stars with f_1, f_2 and f_3 arms, respectively. Shrinking the outer radius R of the triangle on which the cores are located, the partition function of this configuration of three stars will scale with R according to

$$\mathcal{Z}_{f_1 f_2 f_3}(R) \sim R^{\Theta^{(3)}_{f_1 f_2 f_3}}, \tag{124}$$

$$\Theta^{(3)}_{f_1 f_2 f_3} = \eta^S_{f_1} + \eta^S_{f_2} + \eta^S_{f_3} - \eta^S_{f_1+f_2+f_3}. \tag{125}$$

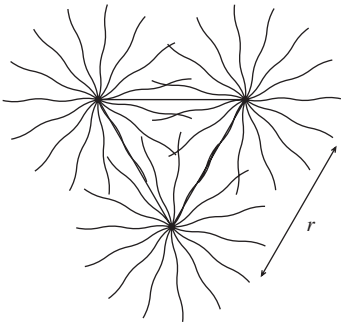

Fig. 10. Three star polymers at mutual distance r. The cores of the stars (with radius R_d) are located at the corners of an equilateral triangle. The distance from the center is R. The mean radius of gyration of a single star is R_g.

Now, the scaling exponent $\eta^S_{f_1+f_2+f_3}$ of the star that results by collapsing the cores of the three stars at one point has to be taken into account as follows from an argument analogous to the above consideration for two stars.

Let us specify the result for the symmetric situation of three equivalent stars $f_1 = f_2 = f_3 = f$. Furthermore, we assume that the large f approximation (123) is valid for the exponents η^S_f. Then the three-star contact exponent may be written as

$$\Theta^{(3)}_{fff} = \frac{3^{3/2}-3}{2^{3/2}-2} \cdot \frac{5}{18} f^{3/2}. \tag{126}$$

An effective potential of the system of the three stars at small distance R from the center may then be defined by

$$V^{(3)\mathrm{eff}}_{fff}(R) = -k_{\mathrm{B}}T\Theta^{(3)}_{fff} \ln(R/R_g). \tag{127}$$

We now derive the corresponding three-body force underlying this effective potential. Note that the absolute value of the force is the same for all three stars. The relation of the potential to the force on the core of one star is then

$$V^{(3)\mathrm{eff}}_{fff}(R+dR) - V^{(3)\mathrm{eff}}_{fff}(R) = \sum_{i=1}^{3} \vec{F}_i \, d\vec{R}_i = 3F^{(3)}_{fff}(R)dR. \tag{128}$$

The final result for the total force on each of the stars that includes any three-body forces is therefore

$$F^{(3)}_{fff}(R) = -k_{\mathrm{B}}T\Theta^{(3)}_{fff}/(3R). \tag{129}$$

If one starts instead from a sum of two-body forces, then one star experiences the sum of the two forces calculated for the star–star interaction. With the given geometry of the equilateral triangle this is easily calculated to give

$$F^{(2)}_{fff}(r) = |\hat{r}_{12}\Theta^{(2)}_{ff}/r_{12} + \hat{r}_{13}\Theta^{(2)}_{ff}/r_{13}| = -k_{\mathrm{B}}T\Theta^{(2)}_{ff}/R. \tag{130}$$

Here, $r = r_{12} = r_{13} = R\sqrt{3}$ denotes the distance between two of the stars, while the $\hat{r}_{ij}$ are the unit vectors along the edges of the triangle (see Fig. 1). The relative deviation from the pair potential picture is then given by

$$\frac{\Delta F}{F^{(2)}_{fff}} = \frac{F^{(3)}_{fff}(r) - F^{(2)}_{fff}(r)}{F^{(2)}_{fff}(r)} = \frac{\Theta^{(3)}_{fff} - 3\Theta^{(2)}_{ff}}{3\Theta^{(2)}_{ff}}. \tag{131}$$

Using the cone approximation for the contact exponent one obtains for the relative deviation caused by triplet forces alone

$$\frac{\Delta F}{F^{(2)}_{fff}} = \frac{3^{1/2} - 1}{2^{3/2} - 2} - 1 \approx -0.11. \tag{132}$$

This result is independent of the number of arms and valid in the full region that is described by the logarithmic potential. In Table 6 the exponents as derived from the perturbation expansion of polymer field theory[17,18] are listed confirming the relation Eq. (132). Taking into account the error that may be estimated from the difference in the results obtained using η-exponents from two complementary RG approaches, the results are in good agreement with the cone approximation even for low f values. The fair coincidence is rather surprising as additional numerical errors might be introduced by the derivation of the contact exponents from the original star exponents. It confirms our estimate of the relative deviation caused by triplet forces to be of the order of not more than 11% for all analytic approaches followed in Table 6. Let us note that the analogous calculation for a symmetric linear configuration of three stars yields the same relative deviation Eq. (132). The absolute triplet forces for the linear configuration are smaller than for the triangular configuration with the same star–star distance by a factor $\frac{\sqrt{3}}{2}$. We note that with the same methods arbitrary higher-order many-body forces can be investigated assuming a cluster of M stars. Such a calculation is given in Ref. 50. As a result, the deviations from the pair potential picture increase with the number M and even diverge for $M \to \infty$. This implies that the pair potential picture breaks

down for very high concentrations. This is expected, as for high concentrations a star polymer solution is mainly a semi-dilute solution of linear chains where it is irrelevant at which center they are attached to.[86]

5.3. *Computer Simulation*

In Refs. 50, 51 and 84 molecular dynamics (MD) simulations were performed to test the effective pair and triplet potential using a method originally proposed to study single-star polymers.[119,120] In this model the configuration of star polymer $i = 1, 2, 3$ is given by the coordinates $\vec{r}_m^{(i,j)}$ of the N monomers $m = 1, \ldots, N$ of the f chains $j = 1, \ldots, f$ and the position of its core $r_0^{(i)}$. The main features of this model are the following: (1) A purely repulsive truncated Lennard-Jones like potential acts between all monomers $m = 0, \ldots, N$ on all chains. (2) An attractive FENE-potential[119,120] that preserves the chain connectivity and acts only between consecutive monomers $m, m+1$ along each chain. (3) These potentials have to be slightly modified for the interaction between the first monomer $m = 1$ and the core $m = 0$ of the star to allow the core to have a radius R_d that is sufficiently large to place f monomers in its vicinity.

Results of the computer simulation are compared to the theory in Figs. 11a and 11b. The reduced averaged force on a single star is shown versus the reduced triangle length for different arm numbers. As a reference case, also the corresponding results in a pair potential picture are shown, both within theory and simulation. For technical reasons a small core radius

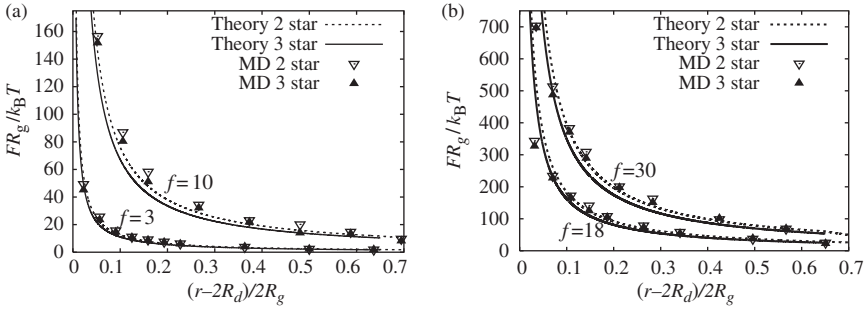

Fig. 11. Comparison of the force F measured in the three-star MD with that calculated from a corresponding two-star MD simulation for (a) $f = 3$ and $f = 10$ with $N = 100$, and (b) for $f = 18$ and $f = 30$ with $N = 50$. Also the results predicted by the theory are plotted as a continuous line (only pair forces) and a broken line (including triplet forces).[50]

R_d is kept in the simulation, which is roughly 10% of the radius of gyration of the whole star. In the theory, on the other hand, the core size was zero. Hence, to compare properly,[84] a shift $r - 2R_d$ has to be performed.

As expected, in both theory and simulation, the triplet forces become relevant only within the coronae. A comparison with pure pairwise forces leads to the first important observation that the triplet force is smaller, i.e. the pure triplet contribution is *attractive*. (Note that one has to multiply the pure two-star force by a factor of $\sqrt{3}$ for simple geometrical reasons.) The relative magnitude of the triplet term, however, is small. A quantitative comparison with theory and simulation leads to good overall agreement.

In order to check this in more detail, one may extract the prefactors $\Theta_{ff}, \Theta_{fff}$ from appropriate fits to all simulation data and again calculate the relative differences between the pair and triplet cases. While the theory predicts a constant value of 0.11, see Eq. (130), the simulation data scatter a lot in the range between 0.05 and 0.15 due to the large statistical error but the theoretical value falls reasonably within the data.[50] Consequently, the triplet contributions are found to be attractive and small even for nearly touching cores where the triplet overlap of the coronae is substantial. As far as further simulational work is concerned, there are many open problems left. Apart from the investigation for arbitrary triplet configurations and their extensions to an arbitrary number of stars, the most challenging problem is a full "ab initio" simulation of many stars including many-body forces from the very beginning. This is in analogy to Car–Parrinello simulations[121] which were also applied to colloidal suspensions.[122] A first attempt has been made,[123] but certainly more work is needed here.

6. Summary

6.1. *Miktoarm Star Polymers*

We reviewed studies of the spectrum of exponents governing the scaling properties of stars of walks. The self and mutual interactions of a linked system of two species of polymers have been treated in the frames of field theoretical RG theory and perturbation expansions[16,18,20,35,48,49,59] as well as by using methods of conformal field theory and quantum gravity.[36,40,124] The problem of finding the scaling exponents of star polymers is formulated in terms of the determination of the scaling dimensions of composite field operators of Lagrangean field theory. On the one hand this allows for the application of well developed formalisms and methods for analyzing the scaling properties. On the other hand it defines these new families of

exponents which extend previous sets in the framework of Lagrangean field theory. The results agree with previous studies of special cases which were in part done only to 2nd order of the ε-expansion.[35,36] Here the generic case of a star of two mutually avoiding sets of walks, the walks of each set being either interacting or transparent, is considered, as well as the case of a star of mutually interacting walks. Calculations so far have been performed to third order of perturbation theory. A recent approach extends the calculation to the fourth loop order.[125] The three loop ε-expansions of the exponents are given in Eqs. (55)–(57). Numerical values produced by careful resummation of the asymptotic series using the results of an instanton analysis of the three coupling problem[53] are presented in Tables 2–6.

Remarkable consistency and stability of the results in $d = 2$ and $d = 3$ is found with the expected growth of deviations for a large number of arms belonging to one star. Results for homogeneous star polymers[47,49] are in good agreement with MC simulations.[60–62]

6.2. *Multifractality*

The theory of miktoarm star polymers also applies to the multifractal behaviour of Brownian motion in the vicinity of an absorbing polymer structure. This extends ideas by Cates and Witten[30,73] to map this problem to a problem of interacting walks. These authors used a Fixman expansion technique to extract the exponents governing the MF scaling. This approach is equivalent to a direct renormalization method and unique to dimensional renormalization with ε-expansion. The Fixman expansion assumes the renormalizability of the quantities corresponding to higher moments of the Laplacian field of Brownian motion. Mapping the problem to an $O(M)$-symmetric ϕ^4-field theory relates the above quantities to corresponding composite operators for which renormalizability has been proven.[49] Furthermore, the scaling exponents of these operators may be retrieved from Refs. 17 and 18, showing that the resulting spectra of scaling dimensions of these operators display the convexity properties which are necessarily found for multifractal scaling but are unusual for power of field operators in field theory.[18,23]

Using the three-loop results of Refs. 17 and 18, the general case of Brownian motion near the core of a star polymer with m legs is tractable. The higher order calculations are improved by resummation giving reliable estimates for the families of MF spectra that describe the multi-scaling of Brownian motion near absorbing RW or SAW stars.

The results plotted in Fig. 7 indicate some independence of the spectral function from the number of legs of the absorbing polymer star. For a higher number of legs the spectrum seems to approach a limiting curve. The MF spectra show most of the common features shared by spectral functions that describe a variety of MF phenomena. However, unlike the common definition of the underlying scaling exponents based on site averages, one here relies on ensemble averages for the moments of the Laplacian field of Brownian motion. The average is over the configurational ensembles of absorbing polymer stars. Only for the case of $m = 2$ legs of the absorbing star, could a site average definition be also used. As has been noted, also in Refs. 30, 34 and 73 the ensemble average leads to the possibility of negative values of the spectral function (see Fig. 7).

Experimentally such absorbing systems are realized in diffusion controlled reactions with traps or reaction sites attached to polymer chains. This is described by the irreversible reaction $A + B \to B$ with freely diffusing particles A and traps B attached along the polymer chain.[109–111] The higher nth moments of the field at some special trap might then describe the reaction rate for $A^n + C \to C$. If C is located at the core of a polymer star this system realizes all aspects of the studies presented. While extensive MC studies exist for many problems in the field of DLA a MC simulation to the present problem is lacking.

6.3. *2D Exact Results and Extensions*

The field-theoretical description of a polymer network of different species has been derived by means of renormalization group perturbation theory in the form of a series that can be extrapolated to $d = 2$ dimensions. These perturbation expansion results for $d = 2$ are compared with subsequently published exact results[40,42] and MC simulations.[48] The series, when appropriately resummed, gives a reliable description of the scaling of copolymer stars with not too many chains even for the $d = 2$ dimensional case. Not only does the increase of the expansion parameter forbid application of the perturbative results for higher numbers of chains: in $d = 2$ topological restrictions appear that are not taken into account by field theory.

Analyzing the MF properties of the resulting spectra of exponents one finds that the spectrum $\tau(n)$ is in much closer coincidence with the exact counterpart than the spectral function $f(\alpha)$. In the latter case the perturbative approach gives comparable results only for a narrow region in the left wing of the spectral function. Note however, that the right wing corresponds

to negative values of n, where obviously the analytic continuation of the perturbative expansions as well as of the exact results is speculative.

We note that the notion of MF spectra has recently been extended to describe the higher MF structure encountered in 2D.[41] In particular, the double MF spectrum of the harmonic measure of absorption on a polymer simultaneously from the right and from the left hand sides may be derived in this formalism.

Acknowledgments

The author has enjoyed fruitful collaboration and discussions on the subject with Yurij Holovatch in Lviv, with Ulrike Lehr and Lothar Schäfer in Essen, Bertrand Duplantier in Saclay, with Arben Jusufi, Joachim Dzubiella, Christos N. Likos, Martin Watzlawek and Hartmut Löwen in Düsseldorf, and most recently with Verena Schulte-Frohlinde and Alexander Blumen in Freiburg. This work was supported in part by the Deutsche Forschungsgemeinschaft.

References

1. P. J. Flory, *Principles of Polymer Chemistry* (Cornell University Press, Ithaca, NY, 1970).
2. P. G. de Gennes, *Phys. Lett.* **A38**, 3390 (1972).
3. J. des Cloizeaux, *J. Phys. (Paris)* **36**, 281 (1975).
4. P.-G. de Gennes, *Scaling Concepts in Polymer Physics* (Cornell University Press, Ithaca and London, 1979).
5. J. des Cloizeaux and G. Jannink, *Polymers in Solution* (Clarendon Press, Oxford, 1990).
6. L. Schäfer, *Excluded Volume Effects in Polymer Solutions as Explained by the Renormalization Group* (Springer, Berlin, 1999).
7. H. Kleinert, *Path Integrals in Quantum Mechanics, Statistics and Polymer Physics* (World Scientific Publishing Co., Singapore, 1995).
8. J.-F. Joanny, L. Leibler and R. Ball, *J. Chem. Phys.* **81**, 4640 (1984).
9. J. F. Douglas and K. F. Freed, *J. Comput. Phys.* **86**, 4280 (1987).
10. L. Schäfer and Ch. Kappeler, *J. Phys. (Paris)* **46**, 1853 (1985).
11. L. Schäfer and C. Kappeler, *Colloid Polym. Sci.* **268**, 995 (1990).
12. B. Duplantier, *Phys. Rev. Lett.* **57**, 941 (1986).
13. B. Duplantier and H. Saleur, *Phys. Rev. Lett.* **57**, 3179 (1986).
14. H. Saleur, *J. Phys.* **A19**, L807 (1986).
15. B. Duplantier, *J. Stat. Phys.* **54**, 581 (1989).
16. K. Ohno and K. Binder, *J. Phys. (Paris)* **49**, 1329 (1988).
17. C. von Ferber and Yu. Holovatch, *Europhys. Lett.* **39**, 31 (1997).
18. C. von Ferber and Yu. Holovatch, *Phys. Rev.* **E56**, 6370 (1997).
19. C. von Ferber and Yu. Holovatch, *Physica* **A249**, 327 (1998).
20. C. von Ferber and Yu. Holovatch, *Phys. Rev.* **E59**, 6914 (1999).

21. C. von Ferber, Yu. Holovatch, A. Jusufi, C. N. Likos, H. Löwen and M. Watzlawek, *J. Mol. Liq.* **93**, 151 (2001).
22. C. von Ferber and Yu. Holovatch, *J. Mol. Liq.* **93**, 155 (2001).
23. B. Duplantier and A. W. W. Ludwig, *Phys. Rev. Lett.* **66**, 247 (1991).
24. A. W. W. Ludwig, *Nucl. Phys.* **B330** (1990).
25. J. M. Deutsch and R. A. Zacher, *Phys. Rev.* **E49**, R8 (1994).
26. M. Janssen, *Int. J. Mod. Phys.* **B8**, 943 (1994).
27. O. Stenull and H. K. Janssen, *Europhys. Lett.* **51**, 539 (2000).
28. O. Stenull and H. K. Janssen, *Phys. Rev.* **E65**, 036124 (2002).
29. H. Hinrichsen, O. Stenull and H. K. Janssen, *Phys. Rev.* **E65**, 045104(R) (2002).
30. M. E. Cates and T. A. Witten, *Phys. Rev.* **A35**, 1809 (1987).
31. B. Fourcade and A. M. S. Tremblay, *Phys. Rev.* **A36**, 2352 (1987).
32. A. B. Chabra and K. R. Screenivasan, *Phys. Rev.* **A43**, R1114 (1991).
33. T. C. Halsey and M. Leibig, *Phys. Rev.* **A46**, 7793 (1992).
34. T. C. Halsey, K. Honda and B. Duplantier, *J. Stat. Phys.* **85**, 681 (1996).
35. B. Duplantier, *Commun. Math. Phys.* **117**, 279 (1988).
36. B. Duplantier and K.-H. Kwon, *Phys. Rev. Lett.* **61**, 2514 (1988).
37. B. Li and A. D. Sokal, *J. Stat. Phys.* **61**, 723 (1990).
38. H. Saleur, *Nucl. Phys.* **B382**, 486 (1992).
39. B. Duplantier, *Bull. Sci. Math.* **117**, 91 (1993).
40. B. Duplantier, *Phys. Rev. Lett.* **82**, 880 (1999).
41. B. Duplantier, *J. Stat. Phys.* **110**, 691 (2003).
42. G. F. Lawler, O. Schramm and W. Werner, *Acta Math. Djursholm* **187**, 275 (2001).
43. G. F. Lawler, O. Schramm and W. Werner, *Acta Math. Djursholm* **189**, 179 (2002).
44. B. Duplantier, *Phys. Rev. Lett.* **81**, 5489 (1998).
45. B. Duplantier, *Physica* **A263**, 452 (1999).
46. V. G. Knizhnik, A. M. Polyakov and A. B. Zamolodchikov, *Mod. Phys. Lett.* **A3**, 819 (1988).
47. C. von Ferber and Yu. Holovatch, *Theor. Math. Physics* **109**, 1274 (1996).
48. C. von Ferber and Yu. Holovatch, *Phys. Rev.* **E65**, 042801 (2002).
49. L. Schäfer, C. von Ferber, U. Lehr and B. Duplantier, *Nucl. Phys.* **B374**, 473 (1992).
50. C. von Ferber, A. Jusufi, C. N. Likos, H. Löwen and M. Watzlawek, *Eur. Phys. J.* **E2**, 311 (2000).
51. C. von Ferber, A. Jusufi, M. Watzlawek, C. N. Likos and H. Löwen, *Phys. Rev.* **E62**, 6949 (2000).
52. J. Roovers, J. F. Douglas and K. F. Freed, *Macromolecules* **23**, 4168 (1990).
53. L. Schäfer, U. Lehr and C. Kappeler, *J. Phys. (Paris) I* **1**, 211 (1991).
54. F. S. Bates and G. H. Fredrickson, *Annu. Rev. Phys. Chem.* **41**, 525 (1990).
55. C. H. Vlahos, A. Horta and J. J. Freire, *Macromolecules* **25**, 5974 (1992).
56. H. Iatru and N. Hadjichistidis, *Macromolecules* **25**, 4649 (1992).
57. A. M. Rubio, P. Brea, J. J. Freire and C. Vlahos, *Macromolecules* **33**, 207 (2000).

58. D. J. Wallace and R. K. P. Zia, *J. Phys.* **C8**, 839 (1975).
59. A. Miyake and K. F. Freed, *Macromolecules* **16**, 1228 (1983).
60. A. J. Barrett and D. L. Tremain, *Macromolecules* **20**, 1687 (1987).
61. J. Batoulis and K. Kremer, *Macromolecules* **22**, 4277 (1989).
62. P. Grassberger, *J. Phys.* **A27**, L721 (1994).
63. H. G. E. Hentschel and I. Procaccia, *Physica* **D8**, 435 (1983).
64. T. C. Halsey, M. H. Jensen, L. P. Kadanoff, I. Procaccia and B. I. Shraiman, *Phys. Rev.* **A33**, 1141 (1986).
65. B. B. Mandelbrot, *J. Fluid. Mech.* **62**, 331 (1974).
66. T. A. Witten and M. E. Cates, *Science* **232**, 1607 (1986).
67. M. Marsili and L. Pietronero, *Physica* **A175**, 9 (1991).
68. G. Eyink and N. Goldenfeld, *Phys. Rev.* **E50**, 4679 (1994).
69. P. Meakin, in Landau *et al.* (Ref. 71).
70. F. Family, in Landau *et al.* (Ref. 71).
71. D. P. Landau, K. K. Mon and H.-B. Schüttler, eds. *Springer Proceedings in Physics. Computer Simulation Studies in Condensed Matter Physics* (Springer-Verlag, Berlin Heidelberg, 1988).
72. W. Feller, *An Introduction to Probability Theory* (Wiley, New York, 1966).
73. M. E. Cates and T. A. Witten, *Phys. Rev. Lett.* **56**, 2497 (1986).
74. B. B. Mandelbrot, *The fractal geometry of nature* (W. H. Freeman and Company, New York, 1983).
75. J. Lee and H. E. Stanley, *Phys. Rev. Lett.* **61**, 2945 (1988).
76. P. Meakin, *Phys. Rev.* **A35**, 2234 (1987).
77. A. Block, W. von Bloh and H. J. Schellnhuber, *Phys. Rev.* **A42**, 1869 (1990).
78. S. Schwarzer, M. Wolf, S. Havlin, P. Meakin and H. E. Stanley, *Phys. Rev.* **A46**, R3016 (1992).
79. G. S. Grest, L. J. Fetters and J. S. Huang, *Adv. Chem. Phys.* **XCIV**, 67 (1996).
80. A. P. Gast, *Langmuir* **12**, 4060 (1996).
81. R. Seghrouchni, G. Petekidis, G. Fytas, A. N. Semenov, J. Roovers and G. Fleischer, *Europhys. Lett.* **42**, 271 (1998).
82. C. N. Likos, H. Löwen, M. Watzlawek, B. Abbas, O. Jucknischke, J. Allgaier and D. Richter, *Phys. Rev. Lett.* **80**, 4450 (1998).
83. M. Watzlawek, C. N. Likos and H. Löwen, *Phys. Rev. Lett.* **82**, 5289 (1999).
84. A. Jusufi, M. Watzlawek and H. Löwen, *Macromol.* **32**, 4470 (1999).
85. G. Fleischer, F. Rittig, J. Kärger, C. M. Papadakis, K. Mortensen, K. Almdal and P. Stepanek, *J. Chem. Phys.* **111**, 2789 (1999).
86. T. A. Witten and P. A. Pincus, *Macromolecules* **19**, 2509 (1986).
87. T. A. Witten and P. A. Pincus, *Europhys. Lett.* **2**, 137 (1986).
88. S. F. Edwards, *Proc. Phys. Soc.* **85**, 613 (1965).
89. S. F. Edwards, *Proc. Phys. Soc.* **88**, 265 (1966).
90. N. N. Bogoliubov and D. V. Shirkov, *Introduction to the theory of quantized fields* (Wiley, New York, 1959).
91. E. Brezin, J. C. Le Guillou and J. Zinn-Justin, *Field theoretical approach to critical phenomena*, In C. Domb and M. S. Green, eds., *Phase transitions and critical phenomena* **6**, 125 (Academic Press, New York, 1976).

92. D. J. Amit, *Field Theory, the Renormalization Group, and Critical Phenomena* (World Scientific, Singapore, 2nd ed. 1984).
93. K. G. Wilson and M. E. Fisher, *Phys. Rev. Lett.* **28**, 240 (1972).
94. G. Parisi, *J. Stat. Phys.* **23**, 49 (1980).
95. E. Brézin, J. C. Le Guillou, J. Zinn-Justin and B. G. Nickel, *Phys. Lett.* **A44**, 227 (1973).
96. A. A. Vladimirov, D. I. Kazakov and O. V. Tarasov, *Sov. Phys. JETP* **77**, 1035 (1979).
97. S. G. Gorishny, S. A. Larin and F. V. Tkachov, *Phys. Lett.* **A101**, 120 (1984).
98. B. G. Nickel, G. A. Baker Jr. and D. I. Meiron, *Phys. Rev.* **B17**, 1365 (1978).
99. J. C. Le Guillou and J. Zinn-Justin, *Phys. Rev.* **B21**, 3976 (1980).
100. C. Bagnuls and C. Bervillier, *Phys. Rev.* **B32**, 7209 (1985).
101. C. Bagnuls and C. Bervillier, *Phys. Rev.* **B35**, 3585 (1987).
102. C. von Ferber, *Nucl. Phys.* **B490**, 511 (1997).
103. E. Brézin, J. C. Le Guillou and J. Zinn-Justin, *Phys. Rev.* **D15**, 1544 (1977).
104. L. N. Lipatov, *Sov. Phys. JETP* **45**, 216 (1977).
105. E. Brezin and G. Parisi, *J. Stat. Phys.* **19**, 269 (1978).
106. G.H. Hardy, *Divergent Series* (Oxford University, Oxford, 1948).
107. J. Zinn-Justin, *Euclidean Field Theory and Critical Phenomena* (Oxford University Press, New York, 1989).
108. C. Itzykson and J. B. Zuber, *Quantum Field Theory* (McGraw-Hill, New York, 1980).
109. S. F. Burlatsky and G. S. Oshanin, *Phys. Lett.* **A145**, 61 (1990).
110. S. F. Burlatsky, G. S. Oshanin and V. N. Likhachev, *Sov. J. Chem. Phys.* **7**, 1680 (1991).
111. G. Oshanin, M. Moreau and S. Burlatsky, *Adv. Coll. Int. Sci.* **49**, 1 (1994).
112. V. G. Kac, In *Lecture Notes in Physics* **94**, 441 (Springer Verlag, Heidelberg, New York, 1979).
113. A. A. Belavin, A. M. Polyakov and A. B. Zamolodchikov, *Nucl. Phys.* **B241**, 333 (1984).
114. D. Friedan, Z. Qiu and S. Shenker, *Phys. Rev. Lett.* **52**, 1575 (1984).
115. J. Cardy, *Nucl. Phys.* **B240**, 514 (1984).
116. I. K. Kostov and M. L. Mehta, *Phys. Lett.* **B189**, 118 (1987).
117. A. N. Semenov, *J. Phys. France* **49**, 1353 (1988).
118. K. Ohno, *Phys. Rev.* **A40**, 1524 (1989).
119. G. S. Grest, K. Kremer and T. A. Witten, *Macromol.* **20**, 1376 (1987).
120. G. S. Grest, *Macromol.* **27**, 3493 (1994).
121. R. Car and M. Parinello, *Phys. Rev. Lett.* **55**, 2471 (1985).
122. H. Löwen, J.-P. Hansen and P. A. Madden, *J. Chem. Phys.* **98**, 3275 (1992).
123. T. Pakula, D. Vlassopoulos, G. Fytas and J. Roovers, *Macromolecules* **31**, 8931 (1998)
124. B. Duplantier, *Phys. Rev.* **B35**, 5290 (1987).
125. V. Schulte-Frohlinde, Yu. Holovatch, C. von Ferber and A. Blumen, (to be published) (2003).

This page intentionally left blank

CHAPTER 6

FIELD THEORETIC APPROACHES TO THE SUPERCONDUCTING PHASE TRANSITION

Flavio S. Nogueira and Hagen Kleinert

Institut für Theoretische Physik, Freie Universität Berlin, Arnimallee 14, D-14195 Berlin, Germany
E-mail: nogueira@physik.fu-berlin.de

Several field theoretic approaches to the superconducting phase transition are discussed. Emphasis is given to theories of scaling and renormalization group in the context of the Ginzburg–Landau theory and its variants. Also discussed is the duality approach, which allows one to access the strong-coupling limit of the Ginzburg–Landau theory.

1. Introduction

The Ginzburg–Landau (GL) phenomenological theory of superconductivity[1] was proposed long before the famous Bardeen–Cooper–Schrieffer (BCS) microscopic theory of superconductivity.[2] A few years after the BCS theory, Gorkov[3] derived the GL theory from the BCS theory. This was done by deriving an effective theory for the Cooper pairs valid in the neighborhood of the critical temperature T_c. The modern derivation proceeds most elegantly via functional integrals, introducing a collective quantum field $\Delta(\mathbf{x}, t)$ for the Cooper pairs via a Hubbard–Stratonovich transformation and integrating out the fermions in the partition function.[4]

Amazingly, the GL theory has kept great actuality up to now. It is highly relevant for the description of high-T_c superconductors, even though the original BCS theory is inadequate to treat these materials. The success of the GL theory in the study of modern problems of superconductivity lies on its universal effective character, the details of the microscopic model being unimportant. In the neighborhood of the critical point the GL theory covers a wide range of applications, many of them outside the field of superconductivity. Perhaps the most famous example in condensed matter

physics is an application to the smectic-A to nematic phase transition in liquid crystals.[5] In elementary particle physics, Gorkov's derivation of the GL theory has been imitated starting out from a four-dimensional relativistic version of the BCS model, the so-called Nambu–Jona–Lasinio model. The GL field in the resulting GL theory describes quark–antiquark bound states, the mesons π, σ, ρ, and A_1.[6] This model is still of wide use in nuclear physics. Another relativistic GL model is needed to generate the masses of the vector bosons W and Z in the unified theory of electromagnetic and weak interactions in a renormalizable way.[7] This is done by a nonabelian analog of the *Meissner effect*, which in this context is called the *Higgs mechanism*.

In 1973 Coleman and Weinberg[8] showed that the four-dimensional abelian GL model (or scalar electrodynamics, in the language of elementary particle physics) exhibits a spontaneous mass generation in an initially massless theory. In the language of statistical mechanics, this implies a first-order transition if the mass of the scalar field passes through zero. One year later, Halperin, Lubensky and Ma (HLM) observed a similar phenomenon in the three-dimensional GL theory of superconductivity.[9] These papers inaugurated a new era in the study of the GL model. It was the first time that renormalization group (RG) methods were used to study the superconducting phase transition.

At the mean-field level, the GL model exhibits a second-order phase transition. The HLM analysis, however, concludes that fluctuations change the order of the transition to first. The phase transition would be of second order only if the number of complex components of the order parameter is absurdly high. If the number of complex components is $N/2$, the one-loop RG analysis of HLM gave the lower bound $N > N_c = 365$ for a second-order transition. No infrared stable charged fixed point was found for $N \leq N_c$. However, years later Dasgupta and Halperin[10] raised doubts on this result by using duality arguments and a Monte Carlo simulation of a lattice model in the London limit, to demonstrate that the transition for $N = 2$ in the type II regime is of second order. The RG result that the phase transition is always of first order seems therefore to be an artifact of the ε-expansion. Shortly after this, Kleinert[11] performed a quantitative duality on the lattice and found a disorder field theory[12] which clarified the discrepancy between the HLM RG result and the numerical simulations of Dasgupta and Halperin. He showed that there exists a tricritical point in the phase diagram of the superconductor on the separation line between first- and second-order regimes. This result and the numerical prediction[11]

were fully confirmed only recently by large scale Monte Carlo simulations of Mo *et al.*[13]

In the last ten years the RG approach to the GL model was revisited by several groups.[14–18] The aim was to improve the RG analysis in such a way as to obtain the charged fixed point for $N = 2$ predicted by the duality scenario. Despite considerable progress, our understanding of this problem is far from satisfactory.

In this paper we shall review the basic field theoretic ideas relevant for the understanding of the superconducting phase transition. The reader is supposed to have some familiarity with RG theory and duality transformations. For a recent review on the RG approach to the GL model which focus more on resummation of ε-expansion results, including calculations of amplitude ratios, see Ref. 19.

2. Review of the HLM Theory

The GL Hamiltonian is given by

$$\mathcal{H} = \frac{1}{2}(\boldsymbol{\nabla} \times \mathbf{A})^2 + |(\boldsymbol{\nabla} - ie\mathbf{A})\psi|^2 + m^2|\psi|^2 + \frac{1}{2}u|\psi|^4, \tag{1}$$

where ψ is the order field and $\mathbf{A}$ is the fluctuating vector potential. The partition function is written in the form of a functional integral as

$$Z = \int \mathcal{D}\mathbf{A}\mathcal{D}\psi^\dagger\mathcal{D}\psi \det(-\boldsymbol{\nabla}^2)\delta(\boldsymbol{\nabla}\cdot\mathbf{A}) \exp\left(-\int d^3r\mathcal{H}\right), \tag{2}$$

where a delta functional in the measure of integration enforces the Coulomb gauge $\boldsymbol{\nabla}\cdot\mathbf{A} = 0$. The factor $\det(-\boldsymbol{\nabla}^2)$ is the associated Faddeev–Popov determinant.[7] The above Hamiltonian coincides with the Euclidian version of the Abelian Higgs model in particle physics. The Coulomb gauge is the Euclidian counterpart of the relativistic Lorentz gauge. The Faddeev–Popov determinant should be included in order to cancel a contribution $1/\det(-\boldsymbol{\nabla}^2)$ that arises upon integration over $\mathbf{A}$ taking into account the constraint $\boldsymbol{\nabla}\cdot\mathbf{A} = 0$.[7,30]

2.1. *HLM Mean-Field Theory*

Let us make the following change of variables in the partition function (2):

$$\psi = \frac{1}{\sqrt{2}}\rho\, e^{i\theta}, \qquad \mathbf{A} = \mathbf{a} + \frac{1}{e}\boldsymbol{\nabla}\theta, \tag{3}$$

which brings the partition function to the form

$$Z = \int \mathcal{D}\mathbf{a}\, \mathcal{D}\rho\, \mathcal{D}\theta\ \rho\ \det(-\boldsymbol{\nabla}^2)\delta(\boldsymbol{\nabla}\cdot\mathbf{a}+e^{-1}\boldsymbol{\nabla}^2\theta)\exp\left(-\int d^3r\ \mathcal{H}\right), \quad (4)$$

with

$$\mathcal{H} = \frac{1}{2}(\boldsymbol{\nabla}\times\mathbf{a})^2 + \frac{1}{2}e^2\rho^2\mathbf{a}^2 + \frac{1}{2}(\boldsymbol{\nabla}\rho)^2 + \frac{1}{2}m^2\rho^2 + \frac{1}{8}u\rho^4. \quad (5)$$

In these variables, the Hamiltonian does not depend on θ. This change of variables is allowed only in a region where the system has few vortex lines, since otherwise the cyclic nature of the θ-field becomes relevant, and $\boldsymbol{\nabla}\, e^{i\theta}$ is no longer equal to $i\boldsymbol{\nabla}\theta\, e^{i\theta}$, as assumed in going from (1) to (5), but equal to $i(\boldsymbol{\nabla}\theta - 2\pi\mathbf{n})e^{i\theta}$, where $\mathbf{n}$ is a vortex gauge field.[12,20] This problem of the Hamiltonian (5) which is said to be in the *unitary gauge* will need special attention.

Now we can use the delta function to integrate out θ. The result of this integration cancels out the Faddeev–Popov determinant.

Next we assume that ρ is uniform, say $\rho = \bar{\rho} = \text{const}$. Since the Hamiltonian is quadratic in $\mathbf{a}$, the $\mathbf{a}$ integration can be done straightforwardly to obtain the free energy density:

$$\mathcal{F} = \frac{1}{2V}\mathrm{Tr}\ln[(-\boldsymbol{\nabla}^2 + e^2\bar{\rho}^2)\delta_{\mu\nu} + \partial_\mu\partial_\nu] - \frac{1}{2V}\delta^3(0)\mathrm{Tr}\ln(e^2\bar{\rho}^2) + \frac{m^2}{2}\bar{\rho}^2 + \frac{u}{8}\bar{\rho}^4, \quad (6)$$

where V is the (infinite) volume and the term $\delta^3(0)\mathrm{Tr}\ln(e^2\bar{\rho}^2)/2V$ comes from the exponentiation of the functional Jacobian in Eq. (4). In order to evaluate the Tr ln in Eq. (6) we have to use the Fourier transform of the operator

$$M(\mathbf{r},\mathbf{r}') = [(-\boldsymbol{\nabla}^2 + e^2\bar{\rho}^2)\delta_{\mu\nu} + \partial_\mu\partial_\nu]\delta^3(\mathbf{r}-\mathbf{r}'). \quad (7)$$

The operator $M(\mathbf{r},\mathbf{r}')$ is diagonal in momentum space. Indeed, we can write

$$M(\mathbf{r},\mathbf{r}') = \int \frac{d^3p}{(2\pi)^3}\ e^{i\mathbf{p}\cdot(\mathbf{r}-\mathbf{r}')}\hat{M}(\mathbf{p}), \quad (8)$$

$$\hat{M}(\mathbf{p}) = (\mathbf{p}^2 + e^2\bar{\rho}^2)P^T_{\mu\nu}(\mathbf{p}) + e^2\bar{\rho}^2 P^L_{\mu\nu}(\mathbf{p}), \quad (9)$$

where $P^T_{\mu\nu}(\mathbf{p}) = \delta_{\mu\nu} - p_\mu p_\nu/\mathbf{p}^2$ and $P^L_{\mu\nu}(\mathbf{p}) = p_\mu p_\nu/\mathbf{p}^2$ are the transverse and longitudinal projectors, respectively. Now, the $\mathrm{Tr}\ln M(\mathbf{r},\mathbf{r}')$ is obtained first by taking the logarithm of the transversal and longitudinal parts of $\hat{M}(\mathbf{p})$ and tracing over the vector indices. The second step is to trace out the coordinates by integrating over $\mathbf{r}$ for $\mathbf{r} = \mathbf{r}'$. This produces an overall volume factor V which cancels out exactly the $1/V$ factor in Eq. (6). Note

that the term proportional to $\delta^3(0)\ln(e^2\bar{\rho}^2)$ drops out in the calculations. If we write $\bar{\rho} = |\bar{\psi}|$, the end result is the celebrated HLM mean field free energy:

$$\mathcal{F}_{\rm HLM} = -\frac{e^3|\bar{\psi}|^3}{6\pi} + \frac{m^2}{2}|\bar{\psi}|^2 + \frac{u}{8}|\bar{\psi}|^4. \tag{10}$$

Due to the cubic term in Eq. (10), the transition is of first order. The basic problem with this argument was pointed out in Ref. 11. In the critical regime of a type-II superconductor, the order field contains numerous lines of zeros which make it impossible to use the uniformity assumption $\rho = \bar{\rho} = \text{const}$.

2.2. *Renormalization Group in $d = 4 - \epsilon$ Dimensions*

In the original HLM work, the RG calculations were performed using the Wilson version of the renormalization group,[21] where fast modes are integrated out to obtain an effective theory in terms of the slow modes. The field theoretical approach using the Callan–Symanzik equation gives an equivalent result in a perturbative setting. We shall discuss the RG calculation in $d = 4 - \epsilon$ dimensions in this context.

The dimensionless renormalized couplings are defined by

$$f \equiv \mu^{-\epsilon} Z_A e_0^2, \qquad g \equiv \mu^{-\epsilon} Z_\psi^2 Z_g^{-1} u_0, \tag{11}$$

where μ gives the mass scale of the problem. Note that in Eq. (11) we have denoted the bare couplings by a zero subindex. The bare fields are denoted by ψ_0 and $\mathbf{A}_0$. Accordingly, the bare mass is denoted by m_0. We shall use this notation from now on.

The renormalization constants are defined such that the "renormalized Hamiltonian" $\mathcal{H}_r$ is given by the following rewriting of the bare Hamiltonian:

$$\begin{aligned}&\mathcal{H}_r(\mathbf{A}, \psi; m^2, u, e)\\ &\quad = \mathcal{H}(Z_A^{1/2}\mathbf{A}, Z_\psi^{1/2}\psi; Z_m Z_\psi^{-1} m^2, Z_g Z_\psi^{-2} u, Z_A^{-1/2} e).\end{aligned} \tag{12}$$

From Eq. (12) we see that the renormalized fields are given by $\psi = Z_\psi^{-1/2}\psi_0$ and $\mathbf{A} = Z_A^{-1/2}\mathbf{A}_0$.

The calculations are more easily done if we set $m = 0$ and evaluate the Feynman graphs at nonzero external momenta to avoid infrared divergences. The external momenta in a four-leg graph will be taken at the

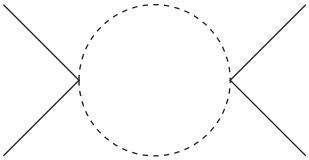

Fig. 1. Feynman graph contributing to the f^2 term in β_g. The dashed lines represent the vector potential propagator, while the external lines represent the order parameter.

symmetry point

$$\mathbf{p}_i \cdot \mathbf{p}_j = \frac{1}{4}\mu^2(4\delta_{ij} - 1). \tag{13}$$

Even if $m \neq 0$ we have to face severe infrared divergences in this problem. This is due to the masslessness of the vector potential field. The free $\mathbf{A}$ propagator is given in the Coulomb gauge by

$$D_{\mu\nu}(\mathbf{p}) = \frac{1}{\mathbf{p}^2}\left(\delta_{\mu\nu} - \frac{p_\mu p_\nu}{\mathbf{p}^2}\right). \tag{14}$$

Thus, the graph in Fig. 1 is proportional to the integral

$$\int \frac{d^dk}{(2\pi)^d}\,\frac{1}{\mathbf{k}^2(\mathbf{p}-\mathbf{k})^2}\bigg|_{\rm SP} = \frac{\pi^{d/2}}{(2\pi)^d}\,\frac{\Gamma(2-d/2)\Gamma^2(d/2-1)}{\Gamma(d-2)}\mu^{d-4}, \tag{15}$$

evaluated at the symmetry point (SP) as prescribed in Eq. (13).

The β-functions are defined by

$$\beta_f \equiv \mu\frac{\partial f}{\partial \mu}, \qquad \beta_g \equiv \mu\frac{\partial g}{\partial \mu}. \tag{16}$$

These β-functions are defined for the dimension d in the interval $(2, 4]$. For $d > 4$ the theory is no longer renormalizable and the β-functions are not defined. At $d = 2$ the infrared divergences are very strong and require a special treatment.

Let us assume that the order parameter field has $N/2$ complex components. Then, for any dimension $d \in (2, 4]$ the β-functions are given at one-loop order by

$$\beta_f = (4-d)[-f + NA(d)f^2], \tag{17}$$

$$\beta_g = (4-d)\left\{-g + B(d)\left[-2(d-1)fg + \frac{(N+8)}{2}g^2 + 2(d-1)f^2\right]\right\}, \tag{18}$$

where

$$A(d) = -\frac{\Gamma(1-d/2)\Gamma^2(d/2)}{(4\pi)^{d/2}\Gamma(d)}, \tag{19}$$

$$B(d) = \frac{\Gamma(2-d/2)\Gamma^2(d/2-1)}{(4\pi)^{d/2}\Gamma(d-2)}. \tag{20}$$

If we set $d = 4 - \epsilon$ and expand to first order in ϵ, we obtain[9,44]

$$\beta_f = -\epsilon f + \frac{N}{48\pi^2} f^2, \tag{21}$$

$$\beta_g = -\epsilon g - \frac{3fg}{4\pi^2} + \frac{N+8}{8\pi^2} g^2 + \frac{3}{8\pi^2} f^2. \tag{22}$$

From Eqs. (21) and (22) we see easily that *charged* fixed points exist only if $N > N_c = 365.9$. Thus, if N is large enough to allow for the existence of charged fixed points we obtain the flow diagram shown schematically in Fig. 2. In the figure the arrows correspond to $\mu \to 0$. There are four fixed points. The Gaussian fixed point is trivial and corresponds to $f_* = g_* = 0$. It governs the ordinary mean-field behavior. There is one non-trivial uncharged fixed point, labeled "Heisenberg" in the figure, which governs the N-component Heisenberg model universality class. For $N = 2$ the superfluid ^{4}He belongs to this universality class (in this case we speak of an XY universality class). The Heisenberg fixed point is unstable for non-zero charge. There are two charged fixed points. The one labeled SC in the figure is infrared stable and governs the superconducting phase transition. Its infrared stability ensures that the phase transition is second order. The second charged fixed point is labeled with a T and is called the tricritical

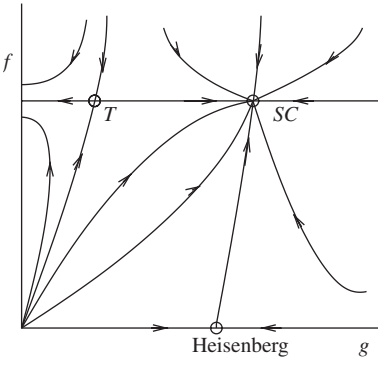

Fig. 2. Schematic flow diagram for the GL model for $N > N_c$.

fixed point. It is infrared stable along the line starting in the Gaussian fixed point and unstable along the g-direction. The line of stability of the tricritical fixed point is called the tricritical line. The tricritical line separates the regions in the flow diagram corresponding to first- and second-order phase transition.

As we shall see later on in these lectures, the flow diagram shown in Fig. 2 should also be valid for $N = 2$.[s] For the moment let us remark that if we use the β-functions in fixed dimension as given in Eqs. (17) and (18) the value of N_c is considerably smaller at $d = 3$. Indeed, by setting $d = 3$ in Eqs. (17) and (18), we obtain that charged fixed points exist for $N > N_c = 103.4$.

2.3. *Critical Exponents*

The critical exponents can be evaluated using standard methods.[22] The η exponent is obtained as the value of the RG function

$$\gamma_\psi = \mu \frac{\partial \ln Z_\psi}{\partial \mu}, \tag{23}$$

at the infrared stable fixed point. The η exponent governs the large distance behavior of the order field correlation function at the critical point:

$$\langle \psi(\mathbf{r}) \psi^\dagger(\mathbf{r}') \rangle \sim \frac{1}{|\mathbf{r} - \mathbf{r}'|^{d-2+\eta}}. \tag{24}$$

The critical exponent ν, governing the scaling of the correlation length $\xi = m^{-1} \sim t^{-\nu}$, with t being the reduced temperature, is obtained as the infrared stable fixed point value of the RG function ν_ψ defined by the equation

$$\frac{1}{\nu_\psi} - 2 = \gamma_m, \tag{25}$$

$$\gamma_m = \mu \frac{\partial}{\partial \mu} \ln \left(\frac{Z_m}{Z_\psi} \right). \tag{26}$$

In an approach where the correlation functions are computed at the critical point the mass renormalization Z_m must be computed through $|\psi|^2$ insertions in the 2-point function.[7,22] For any dimension $d \in (2, 4]$, we obtain

[s] In the context of the ϵ-expansion, see for example the two-loops resummed RG analysis by Folk and Holovatch.[15,19]

the one-loop result

$$\gamma_\psi = (1-d)(4-d)B(d)f, \tag{27}$$

$$\gamma_m = (N+2)(d-4)B(d)g/2 - \gamma_\psi. \tag{28}$$

Once the critical exponents η and ν are evaluated, all the other critical exponents can be obtained using the standard scaling relations. We shall prove later that the standard scaling relations apply also in the case of the GL model.

2.4. $1/N$ *Expansion*

The $1/N$ expansion is one of the most popular non-perturbative methods in the field theoretical and statistical physics literature. The critical exponents of the GL model at $\mathcal{O}(1/N)$ were calculated at $d = 3$ by HLM. Since the original paper does not contain any detail of the calculation, we shall outline it here. The large N limit in the GL model is taken at Nu and Ne^2 fixed.

Let us calculate the critical exponent η. The relevant graphs are shown in Fig. 3. The idea is to pick up the $\mathbf{p}^2 \ln|\mathbf{p}|$ contribution of $\Gamma^{(2)}(\mathbf{p}) = G^{-1}(\mathbf{p})$, where G is the order field propagator. To keep the theory massless, we have to subtract the $\mathbf{p} = 0$ contribution of the self-energy. The subtracted

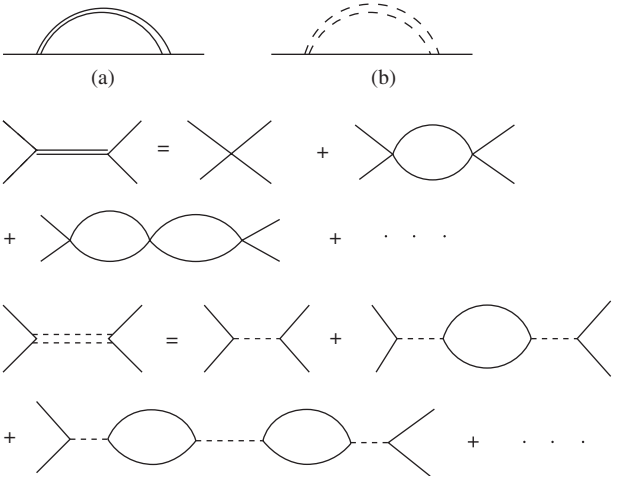

Fig. 3. Feynman graph contributing to the momentum dependent part of the self-energy of the order field propagator. The double lines represent dressed propagators. The graphs (a) and (b) contain effective vertices given by an infinite sum of a chain of bubbles.

contribution coming from the graph (a) in Fig. 3 is

$$\Sigma_a(\mathbf{p}) = \int \frac{d^3k}{(2\pi)^3}\, V(\mathbf{k}) \left(\frac{1}{(\mathbf{p}-\mathbf{k})^2} - \frac{1}{\mathbf{k}^2} \right), \tag{29}$$

where

$$V(\mathbf{k}) = \frac{2u}{1 + uN\Pi(\mathbf{k})}, \tag{30}$$

and $\Pi(\mathbf{k})$ is the polarization bubble

$$\Pi(\mathbf{p}) = \int \frac{d^3k}{(2\pi)^3}\, G_0(\mathbf{p}-\mathbf{k}) G_0(\mathbf{k}), \tag{31}$$

where G_0 is the free scalar propagator. In the massless case we have simply

$$\Pi(\mathbf{p}) = \frac{1}{8|\mathbf{p}|}. \tag{32}$$

When $e = 0$, Eq. (30) gives the effective interaction of the $O(N)$ model.[7] The $-\eta_a \mathbf{p}^2 \ln|\mathbf{p}|$ contribution from Eq. (29) gives

$$\eta_a = \frac{8}{3\pi^2 N}, \tag{33}$$

which is just the η-exponent of the $O(N)$ model at $\mathcal{O}(1/N)$.[7]

In order to compute the contribution from the graph (b) of Fig. 3, we need to calculate the *dressed* vector potential propagator. The dressed propagator is obtained by summing the chain of bubbles shown in Fig. 3. The result is

$$D_{\mu\nu}(\mathbf{p}) = \frac{1}{\mathbf{p}^2 + \Sigma_A(\mathbf{p})} \left(\delta_{\mu\nu} - \frac{p_\mu p_\nu}{\mathbf{p}^2} \right), \tag{34}$$

where in the massless case

$$\Sigma_A(\mathbf{p}) = \frac{1}{32} N e^2 |\mathbf{p}|. \tag{35}$$

The self-energy contribution from graph (b) is then

$$\Sigma_b(\mathbf{p}) = -e^2 \int \frac{d^3k}{(2\pi)^3}\, \frac{(2p_\mu - k_\mu)(2p_\nu - k_\nu)}{(\mathbf{p}-\mathbf{k})^2} D_{\mu\nu}(\mathbf{k}). \tag{36}$$

Thus, we obtain the contribution $-\eta_b \mathbf{p}^2 \ln|\mathbf{p}|$, where

$$\eta_b = -\frac{128}{3\pi^2 N}. \tag{37}$$

The η-exponent of the GL model at $\mathcal{O}(1/N)$ is obtained by adding the contributions from Eqs. (33) and (37),

$$\eta = \eta_a + \eta_b = -\frac{40}{\pi^2 N}. \tag{38}$$

The critical exponent ν at $\mathcal{O}(1/N)$ can be computed through similar calculations, except that one needs to consider massive propagators for the order field. Instead of picking up the contribution $\mathbf{p}^2 \ln|\mathbf{p}|$, we take the $m^2 \ln m$ one from the self-energy at zero momentum. This gives in fact the critical exponent γ. The critical exponent ν is obtained straightforwardly by using the scaling relation $\gamma = \nu(2-\eta)$. The end result is:

$$\nu = 1 - \frac{96}{\pi^2 N}. \tag{39}$$

Note that in the $1/N$ expansion no tricritical fixed point is generated at $\mathcal{O}(1/N)$. The reason for that comes from the fact that the graph in Fig. 1 is $\mathcal{O}(1/N^2)$ and does not contribute to the above calculations. This graph is the main obstacle against attaining the charged fixed point.

3. Existence of the Charged Fixed Point

3.1. *Scaling near the Charged Fixed Point*

By assuming the existence of the charged fixed point, it is possible to derive exact scaling relations for the GL theory.[23] For example, it is easy to prove that if a charged fixed point exists then $\nu' = \nu$, where ν' is the exponent of the penetration depth λ. To this end, it is necessary to consider the GL model in the ordered phase, that is, at $T < T_c$. In this situation the vector potential becomes massive through the Higgs mechanism,[7] with a mass $m_A = \lambda^{-1}$. The Higgs mechanism implies that there are no massless modes in the superconductor in the ordered phase. This shows a fundamental difference between a superconductor and a superfluid: The ordered phase of a superfluid contains a massless mode or Goldstone boson. The Ginzburg parameter κ is defined by the ratio between the Higgs mass and the vector potential mass: $\kappa = m/m_A$. It can be shown that $m^2 = u\rho_s/2$ and $m_A^2 = e^2\rho_s$, with ρ_s being the superfluid density. These formulas are easily obtained in a tree level analysis of the Higgs mechanism. Their application in the renormalized case follows from imposing suitable renormalization conditions and the Ward identities.[18,24] Thus, $\kappa^2 = u/2e^2 = g/2f$. Since both f and g tend to a nonzero fixed point value in the infrared ($m \to 0$), it follows that the Ginzburg parameter $\kappa^2 = \lambda^2/\xi^2 = g/2f \to$ const as $m \to 0$. As a consequence, the scaling relation $\lambda \sim \xi$ holds and therefore the equality between the corresponding critical exponents.

In the following it will be useful to use m as the running RG scale. Thus, $f = m^{d-4} Z_A e_0^2$ and $g = m^{d-4} Z_\psi^2 Z_g^{-1} u_0$. Therefore,

$$\beta_f \equiv m \frac{\partial f}{\partial m} = (\gamma_A + d - 4) f, \tag{40}$$

$$\gamma_A \equiv m \frac{\partial \ln Z_A}{\partial m}. \tag{41}$$

Thus, under the assumption of existence of the charged fixed point we obtain that

$$\eta_A \equiv \gamma_A(f_*, g_*) = 4 - d. \tag{42}$$

The above equation gives the *exact* anomalous dimension of the vector potential.[17] This means that the large distance behavior at the critical point,

$$\langle A_\mu(\mathbf{r}) A_\mu(\mathbf{r}') \rangle \sim \frac{1}{|\mathbf{r} - \mathbf{r}'|^{d-2+\eta_A}} \sim \frac{1}{|\mathbf{r} - \mathbf{r}'|^2}, \tag{43}$$

holds for all $d \in (2, 4]$.

It is instructive and experimentally relevant to compare the scaling near a charged fixed point with the one governed by the XY fixed point. To this end, let us first note that the flow equation for κ^2 is written exactly as[23]

$$m \frac{\partial \kappa^2}{\partial m} = \kappa^2 \left(\frac{\beta_g}{g} + 4 - d - \gamma_A \right). \tag{44}$$

Since $\kappa^2 = m^2 / m_A^2$, the following exact evolution equation holds for m_A^2:[23]

$$m \frac{\partial m_A^2}{\partial m} = m_A^2 \left(d - 2 + \gamma_A - \frac{\beta_g}{g} \right). \tag{45}$$

From Eq. (45) we obtain that near a fixed point m_A behaves as

$$m_A \sim m^{(d-2+\eta_A)/2}. \tag{46}$$

The above constitutes a rederivation of a result due to Herbut and Tesanovic.[17] For the charged fixed point $\eta_A = 4 - d$ and we obtain once more that $\nu' = \nu$ (remember: $m = \xi^{-1}$ and $m_A = \lambda^{-1}$). For the XY fixed point, on the other hand, $\eta_A = 0$ and we obtain from Eq. (46) the scaling relation for the superconducting XY universality class:[25]

$$\nu' = \frac{\nu(d-2)}{2}. \tag{47}$$

A further interesting consequence of the scaling relation (46) is the following. The vector potential mass is given in terms of the superfluid density

ρ_s as $m_A^2 = e^2\rho_s$. Equation (40) implies the scaling $e^2 \sim m^{\eta_A}$ near the charged fixed point. Therefore, from Eq. (46) we obtain[23]

$$\rho_s \sim m^{d-2} \sim |t|^{\nu(d-2)}, \tag{48}$$

where t is the reduced temperature. Equation (48) is just the Josephson relation[26] and we have thus shown that it is also valid near the charged fixed point. In his original paper, Josephson has obtained the above relation for the superfluid in the form $\rho_s \sim t^{2\beta-\nu\eta}$.[26] Then he derived the result (48) by assuming that hyperscaling holds, that is, $d\nu = 2-\alpha$, which together with the scaling relations $\alpha+2\beta+\gamma = 2$ and $\gamma = \nu(2-\eta)$ imply $2\beta-\nu\eta = \nu(d-2)$. *We have obtained the result (48) without using these supplementary scaling relations.* Our result follows from the exact evolution equation for the vector potential mass, Eq. (45). The form $\rho_s \sim t^{2\beta-\nu\eta}$ can be proven without any reference to the charge and is therefore valid also for the superconductor. From this statement and Eq. (48) we prove

$$2\beta - \nu\eta = \nu(d-2) \tag{49}$$

for the superconductor.

Experiments in high quality crystals of $YBa_2Cu_3O_{7-\delta}$ (YBCO) performed at zero field verify very well Eq. (47) for the $d = 3$ case.[27] Most experiments are unable to probe the *charged* critical region. However, in experiments involving critical dynamics the situation is not clear. In this case we have again that different scaling relations are obtained near the charged fixed point. In general the AC conductivity scales as $\sigma(\omega) \sim e^2\rho_s/(-i\omega)$. Since $\rho_s \sim \xi^{2-d}$, $e^2 \sim \xi^{-\eta_A}$, and $\omega \sim \xi^{-z}$, where z is the dynamical critical exponent, we derive the scaling relation[28]

$$\sigma(\omega) \sim \xi^{2-d+z-\eta_A} \sim |t|^{\nu(d-2-z-\eta_A)}. \tag{50}$$

For the XY universality class where $\eta_A = 0$ we have $\sigma(\omega) \sim \xi^{2-d+z}$.[25] Near the charged fixed point, however, we obtain $\sigma(\omega) \sim |t|^{\nu(2-z)}$.[28,29]

3.2. *Duality*

Duality is a powerful tool in physics.[30] It allows the mapping of a weak-coupling problem on a strong-coupling one. In the context of statistical physics, it maps the low temperature expansion into a high temperature expansion. In some cases, duality allows one to obtain exact information on the physical system. The classical example is the two-dimensional Ising model, where the exact critical temperature was obtained[31] before the exact solution appeared.[32] The exact determination of the critical temperature

was possible because the Ising model has the self-duality property, that is, the duality transformation has a fixed point. The self-duality property is also verified in other systems and for $d > 3$, as in the Z_2 lattice gauge theories. However, the discreteness of the gauge group makes these theories very similar from the point of view of duality to the two-dimensional Ising model. Self-duality is more difficult to find in continuous gauge groups. The GL model, for example, has no such property, but as we shall see, it is nevertheless almost self-dual.

In this section we shall discuss the field theoretic approach to duality in the GL model. We shall show in detail how scaling works in a disorder field theory (DFT) for the superconducting phase transition. The DFT to be discussed here was proposed first by Kleinert nearly twenty years ago.[11] This formulation allows one to demonstrate that tricritical point exists in the phase diagram of the superconductor. The existence of this tricritical point allows one to build a consistent picture where the strong-coupling limit – which exhibits a second-order phase transition[10] – and the weak coupling limit, with its weak first order scenario, coexist with the normal phase, meeting at the tricritical point. On the basis of the DFT, the estimated value of κ at the tricritical point was $\kappa_t \approx 0.8/\sqrt{2}$.[11] Early Monte Carlo simulations[33] give, on the other hand, the estimate $\kappa_t \approx 0.42/\sqrt{2}$. Remarkably, Kleinert's estimate agrees within 5% with a recent, more precise, Monte Carlo simulation by Mo, Hove and Sudbø.[13]

The first scaling analysis of the DFT was made by Kiometzis, Kleinert, and Schakel.[14] From the analysis in Ref. 14, it is possible to establish the value of the critical exponent ν as having a XY value, $\nu \simeq 0.67$. However, as we shall see, the scaling analysis of the DFT contains some ambiguities which are not yet completely resolved.

3.2.1. *Duality in the Lattice Ginzburg–Landau Model*

A lattice version of the GL model has the Hamiltonian

$$H = -\beta \sum_{i,\mu} \cos(\boldsymbol{\nabla}_\mu \theta_i - eA_{i\mu}) + \frac{1}{2} \sum_i (\boldsymbol{\nabla} \times \mathbf{A}_i)^2, \tag{51}$$

where ∇_μ is the lattice derivative, $\nabla_\mu f_i \equiv f_{i+\hat{\mu}} - f_i$, and $\beta = 1/T$. The partition function is then given by

$$Z = \int_{-\pi}^{\pi} \left(\prod_i \frac{d\theta_i}{2\pi} \right) \int_{-\infty}^{\infty} \left(\prod_{i,\mu} dA_{i\mu} \right) \exp(-H). \tag{52}$$

The duality transformation can be done exactly when the Villain form of the Hamiltonian is used. The Villain approximation[34] corresponds to the replacement

$$\exp(\beta\cos x) \to \sum_{n=-\infty}^{\infty} \exp\left(-\frac{\beta}{2}(x-2\pi n)^2\right), \tag{53}$$

which turns out to be very accurate near the critical region.[35]

Assuming from now on the Villain approximation, we introduce an auxiliary integer field $m_{i\mu}$ such that

$$\sum_{\{n_{i\mu}\}} \exp\left(-\frac{\beta}{2}(\nabla_\mu\theta_i - eA_{i\mu} - 2\pi n_{i\mu})^2\right)$$
$$\propto \sum_{\{m_{i\mu}\}} \exp\left(-\frac{1}{2\beta}m_{i\mu}^2 + i(\nabla_\mu\theta_i - eA_{i\mu})m_{i\mu}\right). \tag{54}$$

The proportionality factor above is not important in the following. All such proportionality factors in the foregoing manipulations will be neglected. They correspond to smooth factors in the temperature. Equation (54) was obtained using the identity

$$\sum_{m=-\infty}^{\infty} \exp[(-t/2)m^2 + ixm] = \sqrt{\frac{2\pi}{t}} \sum_{n=-\infty}^{\infty} \exp[(-1/2t)(x-2\pi n)^2]. \tag{55}$$

The summation notation in Eq. (54) with a $\{n_{i\mu}\}$ means a *multiple* summation, analogous to multiple integration.

By integrating out the angular variables θ_i we obtain the partition function

$$Z = \int_{-\infty}^{\infty} \left[\prod_{i,\mu} dA_{i\mu}\right] \sum_{\{\mathbf{m}_i\}} \delta_{\boldsymbol{\nabla}\cdot\mathbf{m}_i,0}$$
$$\times \exp\left\{\sum_i \left[-\frac{1}{2\beta}\mathbf{m}_i^2 + ie\mathbf{A}_i\cdot\mathbf{m}_i - \frac{1}{2}(\boldsymbol{\nabla}\times\mathbf{A}_i)^2\right]\right\}. \tag{56}$$

The Kronecker delta constraint $\boldsymbol{\nabla}\cdot\mathbf{m}_i = 0$ generated by the θ_i integrations implies that the link variables $m_{i\mu}$ form closed loops. These closed loops are interpreted as magnetic vortices.[30] When $e = 0$ the vector potential decouples and we have, up to a proportionality factor, the partition function

for the XY model in terms of link variables,

$$Z_{XY} = \sum_{\{\mathbf{m}_i\}} (\delta_{\boldsymbol{\nabla}\cdot\mathbf{m}_i,0}) \exp\left(-\frac{1}{2\beta}\sum_i \mathbf{m}_i^2\right). \tag{57}$$

We can solve the constraint on $\mathbf{m}_i$ by introducing a new integer link variable through $\mathbf{m}_i = \boldsymbol{\nabla}\times\mathbf{l}_i$. After integrating out $\mathbf{A}_i$ and using the Poisson formula

$$\sum_{n=-\infty}^{\infty} F(n) = \sum_{m=-\infty}^{\infty} \int_{-\infty}^{\infty} dx\ F(x) e^{2\pi i m x}, \tag{58}$$

to go from the integer variables $\mathbf{l}_i$ to continuum variables $\mathbf{h}_i$, we obtain

$$Z = \int_{-\infty}^{\infty} \left[\prod_{i,\mu} dh_{i\mu}\right] \sum_{\{\mathbf{m}_i\}} \delta_{\boldsymbol{\nabla}\cdot\mathbf{m}_i,0} \times \exp\left[\sum_i \left(-\frac{1}{2\beta}(\boldsymbol{\nabla}\mathbf{h}_i)^2 - \frac{e^2}{2}\mathbf{h}_i^2 + 2\pi i \mathbf{m}_i\cdot\mathbf{h}_i\right)\right]. \tag{59}$$

Equation (59) corresponds to the dually transformed lattice GL model.

By performing the $\mathbf{h}_i$ integration in Eq. (59) we obtain

$$Z = \sum_{\{\mathbf{m}_i\}} (\delta_{\boldsymbol{\nabla}\cdot\mathbf{m}_i,0}) \exp\left(-2\pi^2\beta \sum_{i,j,\mu} m_{i\mu} G(\mathbf{r}_i - \mathbf{r}_j) m_{j\mu}\right), \tag{60}$$

where the Green function G has the following behavior at large distances:

$$G(\mathbf{r}_i - \mathbf{r}_j) \sim \frac{e^{-\sqrt{\beta}e|\mathbf{r}_i - \mathbf{r}_j|}}{4\pi|\mathbf{r}_i - \mathbf{r}_j|}. \tag{61}$$

Thus, in the superconductor the magnetic vortex loops interact with a screened long range interaction.

Let us consider now the "frozen" superconductor limit[36] of the dual representation (59). The "frozen" superconductor corresponds to the zero

temperature limit, $T \to 0$. In this case, after integrating out $\mathbf{h}_i$, we obtain

$$Z_{\text{frozen}} = \sum_{\{\mathbf{m}_i\}} (\delta_{\boldsymbol{\nabla}\cdot\mathbf{m}_i,0}) \exp\left(-\frac{2\pi^2}{e^2}\sum_i \mathbf{m}_i^2\right). \tag{62}$$

Equation (62) has the same form as Eq. (57). Thus, the "frozen" superconductor is the same as a XY model provided we identify

$$e^2 = \frac{4\pi^2}{T}. \tag{63}$$

The above result allows us to localize a critical point on the e^2-axis in the phase diagram in the e^2–T-plane. Using Eq. (63) and the fact that $T_c \approx 3$ for the XY model in the Villain approximation,[30] we obtain $e_c^2 = 4\pi^2/T_c \approx 13.159$ on the e^2-axis. Thus, we can locate two limiting critical points in the phase diagram, since we have in the T-axis the Villain-XY critical point at $T_c \approx 3$.

The vortex–vortex interaction in Eq. (60) is singular at short distances. Therefore, it is natural to introduce a vortex core term with energy ϵ_0 in the dual lattice Hamiltonian,

$$H_{\text{dual}} = \sum_i \left(\frac{1}{2\beta}(\boldsymbol{\nabla}\times\mathbf{h}_i)^2 + \frac{e^2}{2}\mathbf{h}_i^2 - 2\pi i\mathbf{m}_i\cdot\mathbf{h}_i + \frac{\epsilon_0}{2}\mathbf{m}_i^2\right). \tag{64}$$

Using Eq. (55) and the integral representation of the Kronecker delta

$$\delta_{\boldsymbol{\nabla}\cdot\mathbf{m}_i,0} = \int_{-\pi}^{\pi}\frac{\mathrm{d}\theta_i}{2\pi}e^{i\theta_i(\boldsymbol{\nabla}\cdot\mathbf{m}_i)}, \tag{65}$$

we obtain

$$H'_{\text{dual}} = \sum_i \left(\frac{1}{2\beta}(\boldsymbol{\nabla}\times\mathbf{h}_i)^2 + \frac{e^2}{2}\mathbf{h}^2\right) + \sum_{i,\mu}\frac{1}{2\epsilon_c}(\nabla_\mu\theta_i - 2\pi i n_{i\mu} - 2\pi h_{i\mu})^2. \tag{66}$$

The Hamiltonian in Eq. (66) has the same form as the lattice GL Hamiltonian in the Villain approximation, except that in Eq. (66) the vector field is massive. Thus, we see that there is almost a self-duality between them. When $e = 0$ the Hamiltonian (66) is the dual of the (Villain) lattice XY Hamiltonian. Note that in this duality transformation a locally gauge invariant model is mapped on a globally invariant one.

Let us set $e = 0$ in Eq. (64) and look for the phase diagram in the β–ϵ_0 plane. In such a phase diagram the point $(\beta_c, 0)$ corresponds to the XY

critical point. Integrating out $\mathbf{h}_i$ we obtain the partition function

$$Z'|_{e=0} = \sum_{\{\mathbf{m}_i\}} (\delta_{\boldsymbol{\nabla}\cdot\mathbf{m}_i,0}) \exp\left(-2\pi^2\beta \sum_{i,j,\mu} m_{i\mu}\bar{G}(\mathbf{r}_i - \mathbf{r}_j)m_{j\mu} - \frac{\epsilon_0}{2}\mathbf{m}_i^2\right), \tag{67}$$

where $\bar{G}$ behaves at large distances as

$$\bar{G}(\mathbf{r}_i - \mathbf{r}_j) \sim \frac{1}{4\pi|\mathbf{r}_i - \mathbf{r}_j|}. \tag{68}$$

From Eqs. (57) and (67) we see that the point $(0, 1/2\beta_c)$ in the β–ϵ_0 plane corresponds to an "inverted" XY (IXY) transition.[10] By performing the $\mathbf{A}_i$ integration in Eq. (56) we obtain

$$Z = \sum_{\{\mathbf{m}_i\}} (\delta_{\boldsymbol{\nabla}\cdot\mathbf{m}_i,0}) \exp\left(-\frac{e^2}{2} \sum_{i,j,\mu} m_{i\mu}\bar{G}(\mathbf{r}_i - \mathbf{r}_j)m_{j\mu} - \frac{1}{2\beta}\mathbf{m}_i^2\right), \tag{69}$$

and we see that the IXY critical point corresponds to $e_c^2 = 4\pi^2\beta_c$.[10]

Clearly the IXY transition is a second-order phase transition. Note that this transition arises in a lattice GL model where the amplitude fluctuations are frozen (London limit). Therefore, we should not expect to find a first-order phase transition in this case. This London limit is appropriate when magnetic fluctuations are relevant in the type II regime. In Fig. 4 we show the approximate phase diagram.[11]

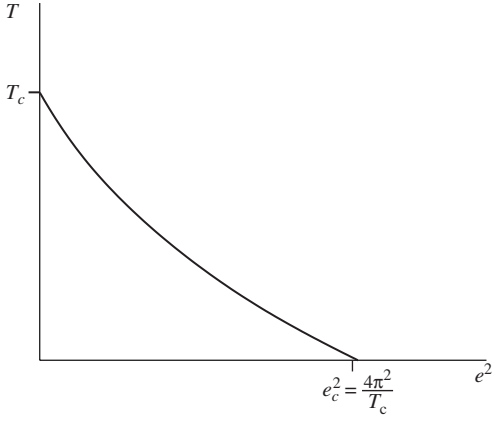

Fig. 4. Schematic phase diagram showing the critical points on the e^2- and T-axis. Here $T_c \approx 3$. The ordered superconducting phase corresponds to $0 < e^2 < e_c^2$.

3.2.2. *The Disorder Field Theory*

The IXY universality class must have the same thermodynamic exponents as the XY model. For instance, we expect $\nu \simeq 0.67$ and, from the scaling analysis of Section 3.1, $\nu' = \nu$. This last scaling relation has been confirmed in Monte Carlo simulations of the lattice model (51).[42] Although the thermodynamic exponents are the same as in the XY universality class, critical exponents like η and η_A are not the same. We have seen in Section 3.1 that $\eta_A = 4 - d$ near the charged fixed point. The $d = 3$ value, $\eta_A = 1$, corresponds to the IXY universality class discussed in the preceding subsection. The XY universality class, on the other hand, has $\eta_A = 0$. Also, we have $-1 < \eta < 0$ in the IXY universality class, while $\eta > 0$ in the XY one.

Useful information from different universality classes and crossovers in superconductors can be obtained from the DFT. The DFT is constructed out of the dual lattice Hamiltonians discussed in this section. The *bare* DFT associated to the lattice Hamiltonian (66) is given by[14,43]

$$\mathcal{H}_{\rm DFT} = \frac{1}{2}(\boldsymbol{\nabla}\times\mathbf{h}_0)^2 + \frac{m_{A,0}^2}{2}\mathbf{h}_0^2 + |(\boldsymbol{\nabla} - i\tilde{e}_0\mathbf{h}_0)\phi_0|^2 + \tilde{m}_0^2|\phi_0|^2 + \frac{\tilde{u}_0}{2}|\phi_0|^4, \quad (70)$$

where the bare *dual charge* $\tilde{e}_0 \equiv 2\pi m_{A,0}/e_0$. $m_{A,0}$ is the bare mass of the vector potential in the original theory. We see that the disordered phase of the DFT corresponds to the ordered phase of the GL model. This is a general feature of all duality transformations: the low temperature phase is mapped in the high temperature phase. This justifies the denomination "disorder field theory" for the continuum limit of the lattice dual model. The field ϕ_0 is the bare *disorder parameter field*. In the superconducting phase $\langle\phi_0\rangle = 0$, while the *order parameter* in the original GL model $\langle\psi_0\rangle \neq 0$. Conversely, the normal phase corresponds to $\langle\phi_0\rangle \neq 0$ and $\langle\psi_0\rangle = 0$.

It should be noted that the Hamiltonian (70) is a generalization of the London model. The field $\mathbf{h}_0$ is in fact the magnetic induction, while $|\phi_0|^2$ gives the vortex loop density.

The renormalization of the Hamiltonian (70) is similar to the one of the GL model, up to the following subtlety. From the Ward identities we obtain that the mass term for the vector field is not renormalized, that is, $m_{A,0}^2\mathbf{h}_0^2/2 = m_A^2\mathbf{h}^2/2$, where the absence of the zero subindices indicates renormalized quantities. Since the renormalized induction field is given by $\mathbf{h} = Z_h^{-1/2}\mathbf{h}_0$, we obtain

$$m_A^2 = Z_h m_{A,0}^2. \quad (71)$$

The dual charge renormalizes in a similar way:

$$\tilde{e}^2 = Z_h \tilde{e}_0^2. \tag{72}$$

Since $\tilde{e}_0^2 = 4\pi^2 m_{A,0}^2/e_0^2$, it follows from Eqs. (71) and (72) that the Cooper pair charge e_0 is not renormalized in the DFT, $e = e_0$.

It is important to remark that the vector potential mass renormalization in the DFT involves only one renormalization constant, while the same is not true in the GL model.[18]

Due to the presence of a massive vector field, the DFT has an ambiguous scaling.[23] This ambiguity has recently been a matter of debate.[37–39] Let us see how it works. In Ref. 14 the scaling chosen was in principle very natural, with the bare masses behaving in the same way with mean field exponents: $\tilde{m}_0^2 \sim |t|$ and $m_{A,0}^2 \sim |t|$. Renormalization is employed as usual. We have

$$\tilde{m}_0^2 = Z_{\tilde{m}} Z_\phi^{-1} \tilde{m}^2, \tag{73}$$

and therefore

$$\tilde{m} \frac{\partial \tilde{m}_0^2}{\partial \tilde{m}} = (2 + \gamma_{\tilde{m}}) \tilde{m}_0^2, \tag{74}$$

where $\gamma_{\tilde{m}}$ is defined in a way similar to γ_m in Eq. (28). Since $\tilde{m}_0^2/m_{A,0}^2 =$ const, we obtain

$$\tilde{m} \frac{\partial m_{A,0}^2}{\partial \tilde{m}} = (2 + \gamma_{\tilde{m}}) m_{A,0}^2. \tag{75}$$

Let us define the dimensionless renormalized dual coupling by $\tilde{f} = \tilde{e}^2/\tilde{m}$. From Eqs. (72) and (75), we obtain the β-function

$$\beta_{\tilde{f}} \equiv \tilde{m} \frac{\partial \tilde{f}}{\partial \tilde{m}} = (\gamma_h + \gamma_{\tilde{m}} + 1) \tilde{f}, \tag{76}$$

$$\gamma_h \equiv \tilde{m} \frac{\partial \ln Z_h}{\partial \tilde{m}}. \tag{77}$$

Now, we can easily obtain the bound

$$\gamma_{\tilde{m}} + 1 \leq (1/\nu) - 1 \leq 1. \tag{78}$$

It is also straightforward to show that $\gamma_h \geq 0$. Therefore, the infrared stable fixed point to (76) is at $\tilde{f}_* = 0$. This implies that the critical exponent ν has an XY value and that $\eta_h \equiv \gamma_h^* = 0$.

From Eqs. (71) and (75) we obtain

$$\tilde{m}\frac{\partial m_A^2}{\partial \tilde{m}} = (\gamma_h + \gamma_{\tilde{m}} + 2)m_A^2. \tag{79}$$

Near the fixed point the above equation becomes

$$\tilde{m}\frac{\partial m_A^2}{\partial \tilde{m}} \approx \frac{1}{\nu}m_A^2, \tag{80}$$

which implies the scaling

$$m_A^2 \sim \tilde{m}^{1/\nu}. \tag{81}$$

Since $\tilde{m} \sim |t|^{\nu}$, the above scaling implies that the penetration depth exponent is given exactly by $\nu' = \frac{1}{2}$.

Another possible scaling is the one considered by Herbut[37] where it is assumed that $m_{A,0}^2 = \text{const}$. Within this scaling we obtain instead of Eq. (76) the β-function

$$\beta_{\tilde{f}} = (\gamma_h - 1)\tilde{f}, \tag{82}$$

which is similar to the β-function of the coupling f in the GL model at $d = 3$. From Eq. (71) we obtain

$$\tilde{m}\frac{\partial m_A^2}{\partial \tilde{m}} = \gamma_h m_A^2. \tag{83}$$

The β-function for the coupling $\tilde{g} = \tilde{u}/\tilde{m}$ contains functions of the ratio $\tilde{m}/m_A$ multiplying every power of $\tilde{f}$.[37] Due to the evolution equation (83), we see that $m_A^2 \sim \tilde{m}^{\gamma_h^*} \sim \tilde{m}$. Therefore, $\tilde{m}/m_A \to 0$ as the critical point is approached. Thus, the fixed point $\tilde{g}_*$ is the same as in the XY model and once more the critical exponent ν has an XY value.[37] However, from the exact scaling behavior $m_A^2 \sim \tilde{m}$ we see that the penetration depth exponent is given by $\nu' = \nu/2$, which corresponds to the same value as in the 3D XY superconducting universality class. Therefore, the scaling considered in Ref. 37 does not give the expected value for the IXY universality class, which should be $\nu' = \nu \approx \frac{2}{3}$.[17] It was shown in Ref. 23 that the IXY universality class can only be obtained if the bare mass $m_{A,0}^2 \sim |t|^{\zeta}$, where $\zeta = 2\nu \approx \frac{4}{3}$, i.e., $m_{A,0}^2$ should scale as m^2 of the original GL model. It seems that if we want the dual model to imply the result $\nu' = \nu$, we have to make this assumption.

An alternative scenario for the scaling behavior in the DFT is the following. We have shown that the XY model dualizes in a GL model. The GL model, on the other hand, dualizes on the DFT whose Hamiltonian is given in Eq. (70). Now, the dual of the dual must be of course the original

model. This means that the GL model should dualize in an XY model and therefore the DFT Hamiltonian should be equivalent to it. On the basis of this argument we should expect a scaling consistent with the XY universality class, instead of IXY. If we accept this argument, we are led to the conclusion that the correct scaling behavior should assume $m_{A,0}^2 = \text{const}$ as in Ref. 37 to obtain the XY scaling of the penetration depth, $\nu' = \nu/2$.

4. The Physical Meaning of the Critical Exponent η

In the superconducting phase transition only the exponents ν, ν', and α are measured. Here α is the specific heat exponent, which is related to ν by the hyperscaling relation $d\nu = 2 - \alpha$. At present the critical exponent η is not measured and we can even doubt its physical significance. We can argue that the superconducting order parameter cannot be considered to be a physical measurable quantity because its conjugate field has no physical meaning. In a ferromagnet the field conjugate to the magnetization is just the external magnetic field, which can be controlled by experiments. Another problem is that the order parameter $\langle\psi\rangle$ is not gauge invariant. Thus, a calculation of $\langle\psi(\mathbf{r})\psi^\dagger(\mathbf{r}')\rangle$ will depend on the gauge choice and, as a consequence, η will also be gauge dependent.

In this section we shall show that it is possible to define a gauge-independent η exponent and discuss its physical significance. The physical meaning of η arises due to a special feature which at first glance looks very much like a pathology: *it has a negative sign*. Indeed, we would expect from very general non-perturbative arguments that η should be positive. In the case of a pure $|\psi|^4$ theory we can prove that $\eta \geq 0$ in the following way. In momentum space the correlation function $G(\mathbf{r} - \mathbf{r}') \equiv \langle\psi(\mathbf{r})\psi^\dagger(\mathbf{r}')\rangle$ has the spectral representation[45]

$$\hat{G}(\mathbf{p}) = \int_0^\infty d\mu \, \frac{\rho(\mu)}{\mathbf{p}^2 + \mu^2}, \tag{84}$$

where the spectral weight $\rho(\mu)$ satisfies the sum rule

$$\int_0^\infty d\mu \, \rho(\mu) = 1. \tag{85}$$

The above representation is well known in quantum field theory and is called the Källen–Lehmann spectral representation.[45] Now, because of the

condition (85) on the spectral weight, we have the inequality

$$\hat{G}(\mathbf{p}) \leq 1/\mathbf{p}^2. \tag{86}$$

If one assumes the low momentum behavior at the critical point $\hat{G}(\mathbf{p}) \sim 1/|\mathbf{p}|^{2-\eta}$, we obtain from the inequality (86) that $\eta \geq 0$.

In the case of the GL model, all calculations of η give a negative value in the interval $-1 < \eta < 0$ for $d = 3$.[9,15–18,46–48] In general it is argued that since $\hat{G}(\mathbf{p}) \sim 1/|\mathbf{p}|^{2-\eta}$, we have in real space the large distance behavior at the critical point,

$$G(\mathbf{r} - \mathbf{r}') \sim \frac{1}{|\mathbf{r} - \mathbf{r}'|^{d-2+\eta}}. \tag{87}$$

The above will not diverge as $|\mathbf{r} - \mathbf{r}'| \to \infty$ provided $\eta > 2 - d$ and for this reason we could have in principle a negative η exponent. Such an argument is certainly not correct in the case of pure $|\psi|^4$ theory where the Källen–Lehmann representation holds which implies $\eta \geq 0$. In the case of the GL model the situation is much more subtle and the Källen–Lehmann representation does not apply, at least not in the above form.[28,49]

In order to give a physical interpretation to the negative sign of η in superconductors, let us consider a one-loop approximation at the critical point and fixed dimensionality $d = 3$. The calculation is uncontrolled but serves to illustrate the main point. Assuming $N = 2$, the vector potential propagator is then given by

$$D_{\mu\nu}(\mathbf{p}) = \frac{1}{\mathbf{p}^2 + e^2|\mathbf{p}|/16}\left(\delta_{\mu\nu} - \frac{p_\mu p_\nu}{\mathbf{p}^2}\right), \tag{88}$$

while the order parameter two-point correlation function is

$$G(\mathbf{p}) = \frac{1}{\mathbf{p}^2 - e^2|\mathbf{p}|/4}. \tag{89}$$

Now, we see from Eq. (88) that as $|\mathbf{p}| \to 0$ the second term in the denominator dominates, implying $\eta_A = 1$. However, the same argument does not apply to Eq. (89) because the second term in the denominator has a negative sign in front of it and therefore the $\mathbf{p}^2$ term is still relevant. Thus, there is a momentum space instability in the problem similar to the one encountered in theories of magnetic systems exhibiting a Lifshitz point.[50] There the Hamiltonian already contains the momentum space instability from the very beginning due to the presence of higher order derivatives.[50] Due to this, the susceptibility in those magnetic systems has a maximum at a nonzero value of $\mathbf{p}$. This leads to the appearance of a modulated regime in

the phase diagram, which is plotted in the P–T-plane, where P is the ratio between two competing interactions. It was conjectured in Ref. 28 that a similar behavior occurs in the superconductor. The modulated regime would be associated to the type II behavior, which would be in this way analogous to the helical phase in magnetic systems exhibiting a Lifshitz point. In the case of magnetic systems, the Lifshitz point is the point in the phase diagram where the paramagnetic, ferromagnetic and helical phases coexist. In the case of the superconductor it corresponds to the point where the type I, type II, and normal phases coexist. In complete analogy with magnetic systems, the phase diagram is plotted in the κ^2–T-plane. Note that in the case of the GL model the Lifshitz point-like behavior would be generated by thermal fluctuations.

Further insight in this problem can be obtained by looking at the propagator in the $1/N$ expansion already discussed in this review. The self-energy at the critical point and $\mathcal{O}(1/N)$ is given by

$$\Sigma(\mathbf{p}) = \frac{40}{\pi^2 N}\mathbf{p}^2 \ln\left(\frac{|\mathbf{p}|}{Ne^2}\right). \tag{90}$$

Thus, besides the pole at $\mathbf{p} = \mathbf{0}$, we have also a pole at

$$|\mathbf{p}_0| = Ne^2 \exp\left(-\frac{\pi^2 N}{40}\right). \tag{91}$$

This instability is similar to the one leading to chiral symmetry breaking in three-dimensional QED (QED3).[51] The difference is that in QED3 the instability occurs with respect to the mass, which is dynamically generated by spontaneous chiral symmetry breaking. Thus, if M is the generated fermion mass, the pole of the propagator occurs at[51]

$$M = Ne^2 \exp\left(\frac{-\pi^2 N}{8}\right). \tag{92}$$

We have not yet discussed how to cure the disease which results from the lack of gauge invariance of the order parameter correlation function $G(\mathbf{r}-\mathbf{r}')$. Our physical interpretation of the critical exponent η given above has no value if η is a gauge-dependent quantity. The best thing to do is to define a gauge-invariant correlation function for the order parameter. The choice of such a gauge-invariant correlation function is not unique but as we shall show, there is one whose value of η coincides with the one which is obtained by computing it in the Coulomb gauge, which is the gauge we are using in this review.

A popular gauge-invariant correlation function which is often used in the literature is

$$\mathcal{G}(\mathbf{r}-\mathbf{r}') = \left\langle \psi(\mathbf{r}) \exp\left(-ie \int_{\mathbf{r}}^{\mathbf{r}'} d\mathbf{r}'' \cdot \mathbf{A}(\mathbf{r}'') \right) \psi^\dagger(\mathbf{r}') \right\rangle. \tag{93}$$

A calculation of η using the above correlation function was carried out recently by Kleinert and Schakel.[52] They calculated this exponent using both the ϵ-expansion and the $1/N$-expansion. In the former case the result is

$$\eta = -\frac{36}{N}\epsilon, \tag{94}$$

while in the latter case η was computed for arbitrary dimensionality $d \in (2,4)$ and up to order $1/N$[52]

$$\eta = -\frac{1}{N}\frac{(d^2+2d-6)\Gamma(d-2)}{\Gamma(2-d/2)\Gamma^2(d/2-1)\Gamma(d/2)}. \tag{95}$$

By setting $d = 4-\epsilon$ in Eq. (95) and expanding to order ϵ we obtain Eq. (94). In a GL Hamiltonian with a gauge-fixing term

$$\mathcal{H}_{\rm gf} = \frac{1}{2\alpha}(\nabla \cdot \mathbf{A})^2, \tag{96}$$

the above expression of η corresponds to values that would have been obtained by fixing the gauge $\alpha = -3$ in the ϵ-expansion case and $\alpha = 1-d$ in the case of the $1/N$-expansion. Thus, in each case the value of η does not agree with the one that is obtained by fixing the Coulomb gauge, which corresponds to $\alpha = 0$. Note, however, that the above gauge-independent results both confirm that η is indeed negative.

A different point of view discussed in Ref. 53 focuses instead in the flow of the gauge-fixing parameter α. From the Ward identities it follows that the gauge-fixing parameter renormalizes as

$$\alpha = Z_A^{-1}\alpha_0, \tag{97}$$

which implies the β-function

$$\beta_\alpha = -\gamma_A \alpha. \tag{98}$$

Since at the charge fixed point we have $\gamma_A(f_*, g_*) = 4-d$, the only way to get a fixed point to Eq. (98) when $d \in (2,4)$ is to set $\alpha = 0$. Due to the negative sign in Eq. (98), the flow is unstable for arbitrary nonzero α. Thus, it is clear that stable charged fixed points can be obtained only if the Coulomb gauge corresponds to the fixed point of the theory in $2 < d < 4$. For $d = 4$, which is the case of interest for particle physicists, any value

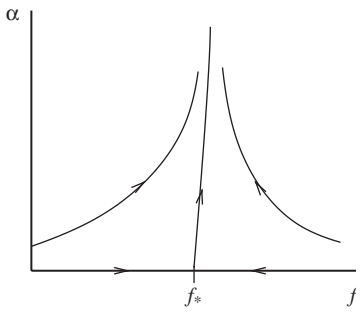

Fig. 5. Schematic flow diagram in the f–α-plane.

of α can be chosen, since in this case $\gamma_A(f_*, g_*) = 0$. In Fig. 5 we show a schematic flow diagram in the f–α-plane for the case where $d \in (2, 4)$. Based on this scenario, we are led to conclude that the above gauge-independent results for η do not correspond to the infrared stable fixed point. This means that the correlation function (93) is not a good choice of gauge-invariant correlation function giving a gauge-independent value of the η exponent. In fact, the correlation function (93) even fails to lead to long-range order. It can be rigorously shown that in the dimensions of interest the correlation function (93) always decays to zero.[54] A better gauge-invariant correlation function is[55]

$$\mathcal{G}(\mathbf{r} - \mathbf{r}') = \left\langle \psi(\mathbf{r}) \exp\left(-ie \int d^d\mathbf{r}'' \mathbf{A}(\mathbf{r}'') \cdot \mathbf{b}(\mathbf{r}'')\right) \psi^\dagger(\mathbf{r}') \right\rangle, \tag{99}$$

$$\mathbf{b}(\mathbf{r}'') = \boldsymbol{\nabla} V(\mathbf{r}'' - \mathbf{r}) - \boldsymbol{\nabla} V(\mathbf{r}'' - \mathbf{r}'), \tag{100}$$

$$-\nabla^2 V(\mathbf{r}) = \delta^d(\mathbf{r}). \tag{101}$$

Since the above correlation function is gauge-invariant, any gauge can be fixed to calculate it. The end result will be always gauge-independent. It is easy to see that in the Coulomb gauge

$$\mathcal{G}(\mathbf{r} - \mathbf{r}')|_{\text{Coulomb}} = \langle \psi(\mathbf{r}) \psi^\dagger(\mathbf{r}') \rangle|_{\alpha=0}. \tag{102}$$

Therefore in such a scenario the η exponent corresponds precisely to the one we calculated previously in the Coulomb gauge. Furthermore, it can be shown that the correlation function (99) exhibits long-range order,[55] in contrast to the one given in Eq. (93).

5. Renormalization Group Calculation at Fixed Dimension and below T_c

In the ϵ-expansion RG approach the same RG functions are obtained regardless of whether the calculation is carried out below or above T_c. As dictated by the Ward identities, the singular behavior is exactly the same above and below T_c.[7] However, if the calculation is done in fixed dimension $d = 3$ and below T_c the situation is different and the RG functions depend explicitly on the Ginzburg parameter κ. We shall not give the details of this approach here. Instead, we shall concentrate on the physical aspects of this new approach which allows one to obtain a charge fixed point at one-loop order. The interested reader is referred to Ref. 18 for the technical details.

The approach we are going to discuss is not really perturbative. Actually, only the powers of f are being effectively counted and the powers of g are counted only partially. Thus, by one-loop we mean first-order in f. The point is that κ arises in the calculations in two different ways: as the ratio between the masses $\kappa = m/m_A$ and as the ratio between coupling constants, $\kappa^2 = g/2f$. The coupling g, when it appears, is eliminated in favor of κ and the RG flow is in this way parametrized in terms of κ and f. This way of working is of course more complicated than more usual RG approaches but it has the advantage of being physically more appealing due to the explicit presence of κ in the RG functions. In the classical Abrikosov solution of the GL model in an external magnetic field κ appears explicitly and the existence of two types of superconductivity is made evident.[56] For instance, the slope of the magnetization curve near H_{c2} is given by

$$\frac{dM}{dH} = \frac{1}{4\pi\beta_A(2\kappa^2 - 1)}, \tag{103}$$

where β_A is the Abrikosov parameter. The above expression is singular at $\kappa = \frac{1}{\sqrt{2}}$, which corresponds to the point separating type I from type II superconductivity. Such a singular behavior at $\kappa = \frac{1}{\sqrt{2}}$ should be also visible in the GL model with a thermally fluctuating vector potential. The new approach introduced in Ref. 18 makes this feature explicit in a RG context. As we shall see, this aspect of this new approach is crucial to obtain the charged fixed point at $d = 3$ and $N = 2$.

The only RG function that is singular at $\kappa = \frac{1}{\sqrt{2}}$ is γ_A,

$$\gamma_A = \frac{\sqrt{2}C(\kappa)f}{24\pi(2\kappa^2 - 1)^3}, \tag{104}$$

$$C(\kappa) = 4\kappa^6 + 10\kappa^4 - 24\sqrt{2}\kappa^3 + 27\kappa^2 + 4\sqrt{2}\kappa - \frac{1}{2}. \tag{105}$$

The β-function for κ^2 is given by

$$\beta_{\kappa^2} = (2\gamma_\pi - \gamma_A - \zeta_\pi)\kappa^2, \tag{106}$$

where

$$\gamma_\pi = \frac{\kappa f}{12\pi}\frac{2\kappa^2 + \sqrt{2}\kappa - 8}{\sqrt{2}\kappa + 1}, \tag{107}$$

$$\zeta_\pi = -\frac{\sqrt{2}}{4\pi} f \left(\frac{3\kappa^2}{2} + \frac{1}{\sqrt{2}\kappa}\right). \tag{108}$$

As before, the charged fixed point at $d = 3$ is determined by the condition $\gamma_A(f_*, \kappa_*) = 1$. This leads to the fixed points

$$f_* \approx 0.3, \quad \kappa_* \approx \frac{1.17}{\sqrt{2}}. \tag{109}$$

Note that κ_* is slightly above the value $\frac{1}{\sqrt{2}}$ and therefore the charged fixed point occurs in the type II regime.

The reason why a charged fixed point is obtained in the above analysis is similar to the reason why the $1/N$-expansion leads to a charged fixed point already at order $1/N$. The fixed point coupling f_* is small enough such that an f_*^2-term is strongly suppressed in the other RG functions. It is a large f^2-term in β_g that spoils at $N = 2$. The charged fixed point in the HLM theory. In order to explain why this new method is so successful, let us define an effective coupling $\bar{f}$ by

$$\gamma_A(\bar{f}, \kappa) = 1. \tag{110}$$

The above equation defines a critical line in the sense that the β_f vanishes on this line. Note, however, that β_{κ^2} does not vanish in general. From Eq. (110) we obtain

$$\bar{f}(\kappa) = \frac{24\pi(2\kappa^2 - 1)^3}{\sqrt{2}C(\kappa)}. \tag{111}$$

From the above equation we see that $\bar{f}(\kappa)$ becomes very small when κ approaches $\frac{1}{\sqrt{2}}$ from the right. Precisely at $\kappa = \frac{1}{\sqrt{2}}$ we have $\bar{f} = 0$. This behavior suggests that the best approximation scheme should be one where the small parameter is given by $\Delta\kappa \equiv \kappa - \frac{1}{\sqrt{2}}$. Now it is easy to see that the ϵ-expansion based on RG fails because it effectively expands around $\kappa = 0$ and therefore it corresponds to the deep type I regime where the transition is clearly first-order. Furthermore, $C(\kappa)$ vanishes at $\kappa = \frac{0.096}{\sqrt{2}}$ and $\bar{f}$ becomes very large as this value of κ is approached from the left.

Thus, a perturbation expansion around $\kappa = 0$ breaks down at $\kappa = \frac{0.096}{\sqrt{2}}$. There is an "infinite barrier" separating the deep type I from the type II regime. In the interval $\frac{0.096}{\sqrt{2}} < \kappa < \frac{1}{\sqrt{2}}$ the effective coupling $\bar{f}$ is negative and thus unphysical. The coupling $\bar{f}$ can be really small only for $\kappa > \frac{1}{\sqrt{2}}$, i.e., in the type II regime.

Note that our one-loop approximation gives only one charged fixed point. The tricritical fixed point is absent in this approximation. This behavior also occurs in the $1/N$-expansion where only one charged fixed point is found. A higher order calculation is necessary to obtain the tricritical fixed point. At two loops the singular behavior in κ is expected to change. Thus, instead of finding a singularity at $\kappa = \frac{1}{\sqrt{2}}$, which is the same as in the mean-field solution, we expect to find a singular behavior at $\kappa_t \approx \frac{0.8}{\sqrt{2}}$, in agreement with Refs. 11 and 13.

6. Concluding remarks

In this chapter we have reviewed several modern field-theoretic approaches in the superconducting phase transition. We have emphasized some special topics which are not extensively discussed in the literature. In particular, the scaling behavior of the continuum dual model was analysed in more detail than in the original publications. The duality scenario is physically and conceptually very important, but its scaling behavior is not yet fully understood. Another topic that deserves further attention is the recently conjectured Lifshitz point-like behavior in the GL model.[18,28] Such a scenario provides an interesting possibility to understand physically the negative value of the critical exponent η.

Acknowledgements

This review is based on lectures delivered by F.S.N. at the "Ising Lectures 2002" at the Institute for Condensed Matter Physics (ICMP), Lviv, Ukraine. F.S.N. is grateful to Yurij Holovatch for the invitation to Lviv and the hospitality of the ICMP. F.S.N. also thanks the Alexander von Humboldt Foundation for the financial support.

References

1. V. L. Ginzburg and L. D. Landau, *Zh. Eksp. Teor. Fiz.* **20**, 1064 (1950).
2. J. Bardeen, L. N. Cooper and J. R. Schrieffer, *Phys. Rev.* **108**, 1175 (1957).
3. L. P. Gorkov, *Sov. Phys. JETP* **9**, 1364 (1959).

4. H. Kleinert, *Collective Quantum Fields,* Lectures presented at the First Erice Summer School on Low-Temperature Physics, 1977, *Fortschr. Phys.* **26**, 565–671 (1978) `http://www.physik.fu-berlin.de/~kleinert/55.`
5. P.-G. de Gennes, Solid State Commun. **10**, 753 (1972); B. I. Halperin and T. C. Lubensky, *ibid.* **14**, 997 (1974).
6. H. Kleinert, *On the Hadronization of Quark Theories,* Lectures presented at the Erice Summer Institute 1976, in *Understanding the Fundamental Constituents of Matter*, Plenum Press, New York, 1978, A. Zichichi ed. `http://www.physik.fu-berlin.de/~kleinert/5`.
7. J. Zinn-Justin, *Quantum Field Theory and Critical Phenomena* (Oxford, 1993).
8. S. Coleman and E. Weinberg, *Phys. Rev.* **D7**, 1888 (1983). For a comparison of the two theories see H. Kleinert, *Phys. Lett.* **B128**, 69 (1983).
9. B. I. Halperin, T. C. Lubensky and S.-K. Ma, *Phys. Rev. Lett.* **32**, 292 (1974); J.-H. Chen, T. C. Lubensky and D. R. Nelson, *Phys. Rev.* **B17**, 4274 (1978).
10. C. Dasgupta and B. I. Halperin, *Phys. Rev. Lett.* **47**, 1556 (1981).
11. H. Kleinert, *Lett. Nuovo Cimento* **35**, 405 (1982).
12. H. Kleinert, *Gauge Fields in Condensed Matter*, Vol. I Superflow and Vortex Lines, (World Scientific, Singapore 1989), pp. 1–744. `http://www.physik.fu-berlin.de/~kleinert/b1.`
13. S. Mo, J. Hove and A. Sudbø, *Phys. Rev.* **B65**, 104501 (2001).
14. M. Kiometzis, H. Kleinert and A. M. J. Schakel, *Phys. Rev. Lett.* **73**, 1975 (1994); *Fortschr. Phys.* **43**, 697 (1995).
15. R. Folk and Y. Holovatch, *J. Phys.* **A29**, 3409 (1996).
16. B. Bergerhoff, F. Freire, D. F. Litim, S. Lola and C. Wetterich, *Phys. Rev.* **B53**, 5734 (1996).
17. I. F. Herbut and Z. Tešanović, *Phys. Rev. Lett.* **76**, 4588 (1996).
18. H. Kleinert and F. S. Nogueira, *Nucl. Phys.* **B651**, 361 (2003).
19. R. Folk and Y. Holovatch, *Critical fluctuations in normal-to-superconducting transition*, in: *Correlations, Coherence, and Order*, ed. by D. V. Shopova and D. I. Uzunov, Kluwer Academic/Plenum Publishers, N.Y., London, pp. 83–116 (1999).
20. H. Kleinert, *Theory of Fluctuating Nonholonomic Fields and Applications: Statistical Mechanics of Vortices and Defects and New Physical Laws in Spaces with Curvature and Torsion*, in: Proceedings of NATO Advanced Study Institute on Formation and Interaction of Topological Defects at the University of Cambridge, Plenum Press, New York, 1995, S. 201–232 (cond-mat/9503030).
21. K. G. Wilson and Kogut, *Phys. Rep.* **12**, 75 (1974).
22. H. Kleinert and V. Schulte-Frohlinde, *Critical Properties of* Φ^4*-theory* (World Scientific, Singapore, 2001).
23. C. de Calan and F. S. Nogueira, *Phys. Rev.* **B60**, 4255 (1999).
24. B. W. Lee, *Phys. Rev.* **D5**, 823 (1972).
25. D. S. Fisher, M. P. A. Fisher and D. A. Huse, *Phys. Rev.* **B43**, 130 (1991).
26. B. D. Josephson, *Phys. Lett.* **21**, 608 (1966).

27. S. Kamal, D. A. Bonn, N. Goldenfeld, P. J. Hirschfeld, R. Liang and W. N. Hardy, *Phys. Rev. Lett.* **73**, 1845 (1994); S. Kamal, R. Liang, A. Hosseini, D. A. Bonn and W. N. Hardy, *Phys. Rev.* **B58**, R8933 (1998).
28. F. S. Nogueira, *Phys. Rev.* **B62**, 14559 (2000).
29. C.-Y. Mou, *Phys. Rev.* **B55**, R3378 (1997).
30. A detailed discussion on duality can be found in the textbook Ref. 12.
31. H. A. Kramers and G. H. Wannier, *Phys. Rev.* **60**, 252 (1941).
32. L. Onsager, *Phys. Rev.* **65**, 117 (1944).
33. J. Bartholomew, *Phys. Rev.* **B28**, 5378 (1983).
34. J. Villain, *J. Phys. (Paris)* **36**, 581 (1975).
35. W. Janke and H. Kleinert, *Nucl. Phys.* **B270**, 135 (1986).
36. M. Peskin, *Ann. Phys. (N.Y.)* **113**, 122 (1978).
37. I. F. Herbut, *J. Phys.* **A30**, 423 (1997).
38. I. F. Herbut, cond-mat/9702167.
39. H. Kleinert and A. M. J. Schakel, cond-mat/9702159.
40. A. M. J. Schakel, cond-mat/9805152.
41. S. Kolnberger and R. Folk, *Phys. Rev.* **B41**, 4083 (1990).
42. P. Olsson and S. Teitel, *Phys. Rev. Lett.* **80**, 1964 (1998).
43. See Eq. (13.30) in the textbook Ref. 12.
44. I. D. Lawrie, *Nucl. Phys.* **B200**, [FS 14], 1 (1982).
45. J. Glimm and A. Jaffee, *Quantum Physics – A Functional Integral Point of View*, 2nd ed. (Springer-Verlag, Berlin, 1987).
46. J. Hove and A. Sudbø, *Phys. Rev. Lett.* **84**, 3426 (2000).
47. P. Olsson, *Europhys. Lett.* **58**, 705 (2002).
48. L. Radzihovsky, *Europhys. Lett.* **29**, 227 (1995).
49. J. Hove, S. Mo, and A. Sudbø, *Phys. Rev. Lett.* **85**, 2368 (2000).
50. H. W. Diehl, *Acta Phys. Slovaca* **52**, 271 (2002), and references therein.
51. R. Pisarski, *Phys. Rev.* **D29**, 2423 (1984); T. Appelquist, J. Terning and L. C. R. Wijewardhana, *Phys. Rev. Lett.* **75**, 2081 (1995); T. W. Appelquist, M. Bowick, D. Karabali and L. C. R. Wijewardhana, *Phys. Rev.* **D33**, 3704 (1986).
52. H. Kleinert and A. M. J. Schakel, *Phys. Rev. Lett.* **90** 097001 (2003).
53. C. de Calan and F. S. Nogueira, *Phys. Rev.* **B60**, 11929 (1999).
54. J. Fröhlich, G. Morchio, and F. Strocchi, *Nucl. Phys.* **B190**, 553 (1981).
55. T. Kennedy and C. King, *Phys. Rev. Lett.* **55**, 776 (1985); *Commun. Math. Phys.* **104**, 327 (1986); Borgs and Nill, *ibid.*, 349 (1986).
56. A. L. Fetter and P. C. Hohenberg, in: *Superconductivity* Vol. 2, p. 817, edited by R. D. Parks (Marcel Dekker, Inc. New York, 1969).

This page intentionally left blank

INDEX